

New frontiers in diagnosis and treatment for skin diseases

Edited by

Stefania Guida, Claudio Conforti, Roberta Giuffrida and Paolo Romita

Published in

Frontiers in Medicine



FRONTIERS EBOOK COPYRIGHT STATEMENT

The copyright in the text of individual articles in this ebook is the property of their respective authors or their respective institutions or funders. The copyright in graphics and images within each article may be subject to copyright of other parties. In both cases this is subject to a license granted to Frontiers.

The compilation of articles constituting this ebook is the property of Frontiers.

Each article within this ebook, and the ebook itself, are published under the most recent version of the Creative Commons CC-BY licence. The version current at the date of publication of this ebook is CC-BY 4.0. If the CC-BY licence is updated, the licence granted by Frontiers is automatically updated to the new version.

When exercising any right under the CC-BY licence, Frontiers must be attributed as the original publisher of the article or ebook, as applicable.

Authors have the responsibility of ensuring that any graphics or other materials which are the property of others may be included in the CC-BY licence, but this should be checked before relying on the CC-BY licence to reproduce those materials. Any copyright notices relating to those materials must be complied with.

Copyright and source acknowledgement notices may not be removed and must be displayed in any copy, derivative work or partial copy which includes the elements in question.

All copyright, and all rights therein, are protected by national and international copyright laws. The above represents a summary only. For further information please read Frontiers' Conditions for Website Use and Copyright Statement, and the applicable CC-BY licence.

ISSN 1664-8714
ISBN 978-2-8325-2415-2
DOI 10.3389/978-2-8325-2415-2

About Frontiers

Frontiers is more than just an open access publisher of scholarly articles: it is a pioneering approach to the world of academia, radically improving the way scholarly research is managed. The grand vision of Frontiers is a world where all people have an equal opportunity to seek, share and generate knowledge. Frontiers provides immediate and permanent online open access to all its publications, but this alone is not enough to realize our grand goals.

Frontiers journal series

The Frontiers journal series is a multi-tier and interdisciplinary set of open-access, online journals, promising a paradigm shift from the current review, selection and dissemination processes in academic publishing. All Frontiers journals are driven by researchers for researchers; therefore, they constitute a service to the scholarly community. At the same time, the *Frontiers journal series* operates on a revolutionary invention, the tiered publishing system, initially addressing specific communities of scholars, and gradually climbing up to broader public understanding, thus serving the interests of the lay society, too.

Dedication to quality

Each Frontiers article is a landmark of the highest quality, thanks to genuinely collaborative interactions between authors and review editors, who include some of the world's best academicians. Research must be certified by peers before entering a stream of knowledge that may eventually reach the public - and shape society; therefore, Frontiers only applies the most rigorous and unbiased reviews. Frontiers revolutionizes research publishing by freely delivering the most outstanding research, evaluated with no bias from both the academic and social point of view. By applying the most advanced information technologies, Frontiers is catapulting scholarly publishing into a new generation.

What are Frontiers Research Topics?

Frontiers Research Topics are very popular trademarks of the *Frontiers journals series*: they are collections of at least ten articles, all centered on a particular subject. With their unique mix of varied contributions from Original Research to Review Articles, Frontiers Research Topics unify the most influential researchers, the latest key findings and historical advances in a hot research area.

Find out more on how to host your own Frontiers Research Topic or contribute to one as an author by contacting the Frontiers editorial office: frontiersin.org/about/contact

New frontiers in diagnosis and treatment for skin diseases

Topic editors

Stefania Guida — Vita-Salute San Raffaele University, Italy

Claudio Conforti — University of Trieste, Italy

Roberta Giuffrida — University of Messina, Italy

Paolo Romita — University of Bari Aldo Moro, Italy

Citation

Guida, S., Conforti, C., Giuffrida, R., Romita, P., eds. (2023). *New frontiers in diagnosis and treatment for skin diseases*. Lausanne: Frontiers Media SA.
doi: 10.3389/978-2-8325-2415-2

Table of contents

- 05 **Effective Intense Pulsed Light Protocol in the Treatment of Moderate to Severe Acne Vulgaris**
Piccolo Domenico, Kostaki Dimitra, Crisman Giuliana, Dianzani Caterina, Avallone Gianluca, Giuffrida Roberta, Guarneri Fabrizio, Guida Stefania, Zalaudek Iris, Fusco Irene and Conforti Claudio
- 08 **Psychologic interventions in patients with the chronic dermatologic itch in atopic dermatitis and psoriasis: A step forward with family constellations seminars**
Szergej Capek, Martin Petrek, Gabriella Capek, Roman Yaremkevych and Yuriy Andrashko
- 16 **Dupilumab modulates specific IgE mite responses at the molecular level in severe T2-high atopic dermatitis: A real-world experience**
Ruperto González-Pérez, Paloma Poza-Guedes, Elena Mederos-Luis and Inmaculada Sánchez-Machín
- 23 **Role of teledermatology in the management of dermatological diseases among marine workers: A cross-sectional study comparing general practitioners and dermatological diagnoses**
Marzio Di Canio, Lorenza Burzi, Simone Ribero, Francesco Amenta and Pietro Quaglinò
- 28 **Nail changes in pemphigus and bullous pemphigoid: A single-center study in China**
Shan Cao, Xiaochen Cui, Jianke Li, Futang Pan, Xiaoxiao Yan, Qing Yang, Mingfei Chen, Shengji Zhou, Donghong Du, Weiwei Wang, Yuanhang Sun, Zhongxiang Shi, Mei Wu, Baoqi Yang and Furen Zhang
- 34 **1540-nm fractional laser treatment modulates proliferation and neocollagenesis in cultured human dermal fibroblasts**
Giada Magni, Domenico Piccolo, Paolo Bonan, Claudio Conforti, Giuliana Crisman, Laura Pieri, Irene Fusco and Francesca Rossi
- 40 **Single-cell RNA-seq reveals the communications between extracellular matrix-related components and Schwann cells contributing to the earlobe keloid formation**
Taogen Gong, Yayu Wang, Shaowei Dong, Xiaoshi Ma, Danfeng Du, Chang Zou, Qijun Zheng and Zhong Wen
- 54 **A deep learning-based approach toward differentiating scalp psoriasis and seborrheic dermatitis from dermoscopic images**
Zhang Yu, Shen Kaizhi, Han Jianwen, Yu Guanyu and Wang Yonggang
- 63 **Lipoma management with a minimally invasive 1,444 nm Nd:YAG laser technique**
Domenico Piccolo, Mohammed Hussein Mutlag, Laura Pieri, Irene Fusco, Claudio Conforti, Giuliana Crisman and Paolo Bonan

- 71 **Reduced blood-brain barrier penetration of acne vulgaris antibiotic sarecycline compared to minocycline corresponds with lower lipophilicity**
Ayman Grada, James Q. Del Rosso, Angela Y. Moore, Linda Stein Gold, Julie Harper, Giovanni Damiani, Katharina Shaw, Sabine Obagi, Raidah J. Salem, S. Ken Tanaka and Christopher G. Bunick
- 79 **Exploration of and insights into advanced topical nanocarrier systems for the treatment of psoriasis**
Miao Zhang, Seokgyeong Hong, Xiaoying Sun, Yaqiong Zhou, Ying Luo, Liu Liu, Jiao Wang, Chunxiao Wang, Naixuan Lin and Xin Li
- 93 **Minimally invasive 1,444-nm Nd:YAG laser treatment for axillary bromhidrosis**
Domenico Piccolo, Mohammed Hussein Mutlag, Laura Pieri, Irene Fusco, Claudio Conforti, Giuliana Crisman and Paolo Bonan
- 99 **Clinicopathological features, therapeutic options, and significance of CD103 expression in 15 patients with follicular mucinosis**
Jiaqi Wang, Yanqing Wang, Hongyu Zhou, Ping Wang, Mengyan Zhu, Liuyu Li and Hong Shen



Effective Intense Pulsed Light Protocol in the Treatment of Moderate to Severe Acne Vulgaris

Piccolo Domenico¹, Kostaki Dimitra¹, Crisman Giuliana¹, Dianzani Caterina², Avallone Gianluca³, Giuffrida Roberta⁴, Guarneri Fabrizio⁴, Guida Stefania⁵, Zalaudek Iris⁶, Fusco Irene^{7*} and Conforti Claudio⁶

¹ Skin Centers, Avezzano, Italy, ² Plastic and Reconstructive Surgery Department, Campus Biomedico University, Rome, Italy, ³ Dermatology Clinic, Department of Medical Sciences, University of Turin, Turin, Italy, ⁴ Department of Clinical and Experimental Medicine, Dermatology Section, University of Messina, Messina, Italy, ⁵ Dermatology Unit, Department of Surgical, Medical, Dental and Morphological Science With Interest Transplant, Oncological and Regenerative Medicine, University of Modena and Reggio Emilia, Modena, Italy, ⁶ Dermatology Clinic, Hospital Maggiore, University of Trieste, Trieste, Italy, ⁷ Department of Pharmacology, University of Florence, Florence, Italy

Keywords: acne, lasers, IPL, papulo-pustulous acne vulgaris, young adults

OPEN ACCESS

Edited by:

Jolanta Idkowiak-Baldys,
Avon, United States

Reviewed by:

Karolina Chilicka,
Opole University, Poland

*Correspondence:

Fusco Irene
irene-fusco@libero.it
orcid.org/0000-0001-7264-8808

Specialty section:

This article was submitted to
Dermatology,
a section of the journal
Frontiers in Medicine

Received: 17 May 2022

Accepted: 07 June 2022

Published: 01 July 2022

Citation:

Domenico P, Dimitra K, Giuliana C, Caterina D, Gianluca A, Roberta G, Fabrizio G, Stefania G, Iris Z, Irene F and Claudio C (2022) Effective Intense Pulsed Light Protocol in the Treatment of Moderate to Severe Acne Vulgaris. *Front. Med.* 9:946405. doi: 10.3389/fmed.2022.946405

Acne is defined as a chronic inflammatory-infectious disease of the pilosebaceous units, mainly affecting the face of young adults. Oral antibiotics, topical retinoids, azelaic acid, benzoyl peroxide, and isotretinoin represent the most common treatments, even though several adverse effects and a lack of durable remission, with a subsequent poor compliance by the patients, have been reported so far (1). On the other side, lasers have been proved to be effective and safe to treat acne; Intense Pulsed Light (IPL), particularly, demonstrates high efficacy rates, minimal discomfort, rapid recovery times, and excellent cosmetic and therapeutic outcomes (2).

We herein report our clinical experience with IPL for the treatment of moderate papulo-pustulous acne of the face. We used an IPL handpiece (Luxea Lazur handpiece, DEKA MELA srl, Calenzano, Italy) with the following parameters: wavelength 400 nm, fluence 8–9 J/cm² and single-pulse mode of 30 ms duration. The protocol used was at least one session and at most 5 sessions separated by 2 weeks intervals.

The study included 62 patients (11 males and 51 females) with moderate to severe facial acne, not responsive to conventional therapies; patients suffering from mild acne were not enrolled in this study. The mean age was 20.95 ± 3.52 (minimum 18, maximum 39), with Fitzpatrick phototype I-II ($n = 45$, 72.58%), III ($n = 13$, 20.97%) and IV-VI ($n = 4$, 6.45%).

Majority of the patients had papulopustular acne ($n = 50$, 80.65%), whereas nodulocystic and comedonal acne were less common ($n = 10$, i.e., 16.13%, and $n = 2$, i.e., 3.23%, respectively).

Fifty-two (83.87%) patients were not on other anti-acne treatments. Concomitant medications were used in 10 patients (oral tetracycline in 6 cases, adapalene and benzoyl peroxide in 2 cases each).

According to the Hayashi score system (3), 20.97% ($n = 13$) of the participants had moderate acne, 48.39% ($n = 30$) severe and 30.65% ($n = 19$) very severe at baseline (**Figure 1**).

There was a significant ($p = 2.84 \times 10^{-20}$) improvement of Hayashi score after IPL at the final compared to before the treatment, with 48 patients (77.42%) with mild acne, 13 (20.97%) patients with moderate and only one (1.61%) with severe acne.

One patient (1.61%) received only one session of IPL, 37 (59.68%) two sessions, 17 (27.42%) three sessions, 5 (8.06%) four sessions and 2 (3.23%) five sessions.

No serious side effects occurring during or after the procedure were noted.



FIGURE 1 | Nodulocystic acne before **(A)** and after **(B)** 4 sessions of IPL treatment (wavelength 400 nm) (top panel); Papulo-pustulous acne before **(A)** and after **(B)** 5 sessions of IPL treatment with notable improving of active acne lesions and acne scars (middle and bottom panel).

At the time of final assessment, 6 weeks after the last IPL session, the response to IPL treatment was considered excellent in 58.06% ($n = 36$) of patients, with complete regression of inflammatory lesions. Eighteen patients (29.03%) presented a good response, with few inflammatory lesions. Seven participants (11.29%) showed a moderate response to IPL, while only one (1.61%) presented a poor response.

There was no relationship between the response to treatment and any age, sex, phototype and type of acne lesions.

At 6 weeks follow-up, residual nodules were present in 13 patients (20.97%), brown macules in 3 (4.84%), papules and pustules in 13 patients (20.97%), papules, pustules and brown macules in 20 (32.26%) patients. No residual lesions were observed in 13 patients (20.97%).

Our study shows efficacy and safety of IPL in the treatment of acne vulgaris, as demonstrated by the statistically significant

reduction of Hayashi score and by the absence of side effects; its validity is promising either as a complementary therapy during systemic or topical therapies (with the only exception of isotretinoin) or as a first therapeutic choice in patients with contraindications to normal therapies. The major limitations of this study are the limited number of the patients and concomitant medications in some of them. Future larger prospective studies are needed to evaluate the maintenance of long-term response.

AUTHOR CONTRIBUTIONS

PD, KD, CG, DC, AG, GR, GE, GS, ZI, and CC contributed to conception and design of the study. FI revised and submitted the manuscript. All authors contributed to manuscript revision, read, and approved the submitted version.

REFERENCES

1. Conforti C, Chello C, Giuffrida R, di Meo N, Zalaudek I, Dianzani C. An overview of treatment options for mild-to-moderate acne based on American academy of dermatology, European academy of dermatology and venereology, and Italian society of dermatology and venereology guidelines. *Dermatol Ther.* (2020) 4:e13548. doi: 10.1111/dth.13548
2. In Ryu S, Suh DH, Lee SJ, Kim KE, Jeong JY, Ryu HJ. Efficacy and safety of intense pulsed light using a dual-band filter for the treatment of facial acne vulgaris. *Lasers Med Sci.* (2021) 37:531–6. doi: 10.1007/s10103-021-03292-3
3. Hayashi N, Kawashima M. Efficacy of oral antibiotics on acne vulgaris and their effects on quality of life: a multicenter randomized controlled trial using minocycline, roxithromycin and faropenem. *J Dermatol.* (2011) 38:111–9. doi: 10.1111/j.1346-8138.2010.00969.x

Conflict of Interest: The authors declare that the research was conducted in the absence of any commercial or financial relationships that could be construed as a potential conflict of interest.

Publisher's Note: All claims expressed in this article are solely those of the authors and do not necessarily represent those of their affiliated organizations, or those of the publisher, the editors and the reviewers. Any product that may be evaluated in this article, or claim that may be made by its manufacturer, is not guaranteed or endorsed by the publisher.

Copyright © 2022 Domenico, Dimitra, Giuliana, Caterina, Gianluca, Roberta, Fabrizio, Stefania, Iris, Irene and Claudio. This is an open-access article distributed under the terms of the Creative Commons Attribution License (CC BY). The use, distribution or reproduction in other forums is permitted, provided the original author(s) and the copyright owner(s) are credited and that the original publication in this journal is cited, in accordance with accepted academic practice. No use, distribution or reproduction is permitted which does not comply with these terms.



OPEN ACCESS

EDITED BY
Roberta Giuffrida,
University of Messina, Italy

REVIEWED BY
Claudia Zeidler,
University Hospital Münster, Germany

*CORRESPONDENCE
Szergej Capec
szergej.capec@upol.cz

SPECIALTY SECTION
This article was submitted to
Dermatology,
a section of the journal
Frontiers in Medicine

RECEIVED 09 June 2022
ACCEPTED 29 July 2022
PUBLISHED 12 August 2022

CITATION
Capec S, Petrek M, Capec G,
Yaremkevych R and Andrashko Y
(2022) Psychologic interventions
in patients with the chronic
dermatologic itch in atopic dermatitis
and psoriasis: A step forward with
family constellations seminars.
Front. Med. 9:965133.
doi: 10.3389/fmed.2022.965133

COPYRIGHT
© 2022 Capec, Petrek, Capec,
Yaremkevych and Andrashko. This is an
open-access article distributed under
the terms of the [Creative Commons
Attribution License \(CC BY\)](#). The use,
distribution or reproduction in other
forums is permitted, provided the
original author(s) and the copyright
owner(s) are credited and that the
original publication in this journal is
cited, in accordance with accepted
academic practice. No use, distribution
or reproduction is permitted which
does not comply with these terms.

Psychologic interventions in patients with the chronic dermatologic itch in atopic dermatitis and psoriasis: A step forward with family constellations seminars

Szergej Capec^{1*}, Martin Petrek¹, Gabriella Capec¹,
Roman Yaremkevych² and Yuriy Andrashko²

¹Department of Pathological Physiology, Faculty of Medicine and Dentistry, Palacký University, Olomouc, Czechia, ²Department of Skin and Venereal Diseases, Faculty of Medicine, Uzhhorod National University, Uzhhorod, Ukraine

Chronic itch is a complex psychophysiological sensation, which can severely affect the quality of life in patients with atopic dermatitis and psoriasis. Itch depends on the irritation of receptors in the skin and the processing of sensory information in the central nervous system. Severe itch leads to activation and later on to disruption of the stress response, resulting in disorders of skin repair, functional and microstructural changes in the areas of the central nervous system that are responsible for the perception of itch. Psychosocial stress can be an essential factor, activating neurohumoral mechanisms which lead to increased itch and scratch, exacerbating skin damage. Patients with chronic itch often have sleep disorders, increased irritability, and depletion of the nervous system. They are characterized by disrupting social relationships, high incidence of anxiety, depressive disorders, and suicidal tendencies. Psychological methods of intervention can effectively influence various mechanisms in the pathogenesis of itch and scratch and improve social functioning in patients with chronic dermatological itch. In this mini-review, we discuss family constellation seminars as an effective method of psychological intervention that can reduce the intensity of itch, and improve sleep and performance in patients with atopic dermatitis and psoriasis. This method is insufficiently described in previous reviews of psychological interventions in atopic dermatitis and psoriasis patients. The positive impact of family constellations seminars in patients with chronic dermatological itch may be related to reducing stress by improving understanding of the family situation, appropriate management of family secrets, and enhancing interactions with the social environment.

KEYWORDS

psychological distress, atopic dermatitis, psoriasis, chronic itch, family constellations

Introduction

Itch is an unpleasant sensation leading to a desire to scratch. Normally, itch and scratch help get rid of parasites or dirt and prevent additional skin damage. In atopic dermatitis (AD) and psoriasis, itch is chronic and can be severe and exhausting. Patients often develop a vicious circle: skin damage (sometimes even minor) leads to stimulation and sensitization of sensory fibers, itch, and scratching, provoking further skin damage, thus significantly reducing the chances of appropriate skin healing and prolonging itch (1).

There are bi-directional relationships between itch and stress:

1. Itch can initiate stress response (2–4).
2. Stress response through endocrine, immune, nervous, and behavioral mechanisms can exacerbate itch (5–7).

Patients with chronic itch differ from healthy individuals: they experience more stress, mental and sleep disorders, more frequent and severe problems in family relationships (8, 9). The current mini-review discusses central psychophysiological mechanisms of itch-scratch-stress interaction and the possible benefits of psychologic intervention in patients with chronic dermatologic itch with family constellation seminars (FCS).

Association of dermatological itch, stress, and mental disorders

Itch is an important factor in worsening health-related quality of life (2, 10–12). Patients with dermatoses with itch are more stressed than healthy people or patients with dermatologic disorders without itch (11–15). The more intense itch and skin injury, the higher risk of stress and mental disorders (16, 17). Outpatients of dermatology clinics with moderate or severe itch are 10 times more likely to have depression than patients with the mild itch, regardless of the dermatological cause (18).

Atopic dermatitis and psoriasis are the most common dermatological diseases accompanied by itch. Over 80% of patients in dermatology clinics with AD and psoriasis suffer from chronic itch (19, 20). About half of patients in dermatological clinics with AD have a high level of depressive disorders, which is more than 3.5 times higher than in the general population (5, 21, 22). The level of anxiety in adult patients with AD is positively correlated with the intensity of itch (23). In late adolescence, AD with the itch is associated with suicidal ideation (odds ratio, OR > 3.5), mental stress (OR > 2.5), and mental health problems (OR > 2.5) (24). Psoriasis patients are 1.5–3 times more

likely to show depressive symptoms and experience a several times higher prevalence of anxiety symptoms, schizophrenia (OR > 2.5), and suicidal ideation than individuals without psoriasis (25, 26).

Pathophysiological mechanism of itch

Peripheral mechanisms

The itch sensation depends on the peripheral stimulation of unmyelinated C-type nerve endings (both nociceptors and specialized itch fibers) and the processing of these impulses in the central nervous system. The main substances that stimulate the activation or modulation of these nerve endings are histamine (*via* H1 receptors in acute pruritus and H4 receptors in chronic pruritus), interleukins (IL) IL-1 β , IL-4, IL-6, IL-13, IL-17A, IL-31, IL-33, IL-35, tumor necrosis factor alpha (TNF- α) (27, 28). Most of these molecules are produced by keratinocytes, T-helper cells, mast cells, macrophages, and neutrophils. Activation of sensory nerve endings leads to the release of substance P and calcitonin-gene-related peptide (CGRP), which can enhance the production of the abovementioned cytokines by mast cells and mononuclear cells leading to a vicious circle of increasing itch.

Central mechanisms of itch and scratch

Information from the sensory nerve endings enters the spinal ganglion and spinal cord and follows the spinothalamic pathway. This information is then processed in the thalamus, somatosensory cortex, cingulate cortex, medial parietal cortex, insular cortex (IC), motor cortex (29), and basal ganglia (30, 31).

Different areas of the brain have different functions in perceiving and processing information about itch. The somatosensory cortex is mainly responsible for the topical perception of itch and its intensity. Activations of the cingulate cortex are likely associated with cognition/evaluation of itch stimuli and/or the urge to scratch. The medial parietal cortex is associated with memory and attention, and at the same time, it may be partially responsible for the subjective sensations of itch and pain. The posterior insular cortex is associated with awareness of affective body feelings (e.g., pain, cold, thirst) and its activity significantly correlates with the intensity of itch stimuli. Activation of the anterior insular cortex correlates with subjective sensation and unpleasantness of itch. Usually, this part of the brain is considered responsible for awareness of emotions and subjective feelings (29).

Peculiarities of itch perception in patients with chronic dermatologic itch

Chronic itch patients' minds are often occupied by negative thoughts due to their itch, including their past unpleasant itch episodes (17). Many of the abovementioned brain areas are activated more intensely in patients with AD than in healthy controls, both with the physical induction of itch on the skin and when watching someone scratch (32). In patients with AD, there is greater activation of the basal ganglia (which are among other functions responsible for motivation and craving) when exposed to histamine on the affected areas of the skin, resulting in excessive itch. In patients with psoriasis, brain structures related to the perception and response to itch demonstrate both functional and microstructural changes (31).

Activity in the right medial prefrontal cortex, posterior cingulate cortex/precuneus, and angular gyrus correlates with the severity of chronic itch (33). These structures are essential in autobiographical memory retrieval, envisioning the future, conceiving the perspectives of others, participate in using past experiences to plan for the future, navigate social interactions (34), and it is important to research if psychological interventions in patients with chronic itch can influence the activity of these structures.

Basic mechanisms of the stress response

In modern society, most stress reactions are related to the social environment: family, partners, colleagues, and friends. If a person does not have efficient strategies to adapt, general adaptation syndrome (stress) mechanisms are triggered (Figure 1). These mechanisms include activation of the nervous system (autonomous nervous system, cortical and subcortical structures), the endocrine system (primarily the hypothalamus-pituitary-adrenal axis), behavioral mechanisms (fight-flight-freeze reactions), and the immune system (35). The response by scratching can be one of the equivalents of the desire to get rid of an unpleasant stimulus, not only from a physical one but also in symbolic form, from a mental trigger.

Itch and stress interactions in dermatologic patients

Itch as a stressor

Intensive itch is an independent factor that triggers a stress response (4). Patients with chronic itch experience

neurophysiologic irritation, which can be an additional factor in the emergence of conflicts, stresses, mental disorders, and finally in depletion of endocrine mechanisms of the stress response (36). Peak levels of daily stressors are associated with an increase in psoriasis severity a month later and a lower cortisol level (37).

Skin changes under acute and chronic stress

Acute and chronic mental stress affects the skin in many ways (7). Keratinocytes have receptors for catecholamines, histamine, acetylcholine, neurotrophic factors, glucocorticoids, and neuropeptides (e.g., substance P and nerve growth factor) (6). Keratinocytes and fibroblasts locally produce hormones that are traditionally attributed to the hypothalamic-pituitary system, namely, corticotropin-releasing hormone, proopiomelanocortin, and molecules that occur during its degradation: ACTH, opioid hormones, alpha-melanocyte-stimulating hormone (7, 38). In moderate acute stress, the barrier function of the skin and its regeneration may improve (4). However, under severe acute psychosocial stress inflammatory processes in the skin of patients with psoriasis are activated. TNF- α , sympathetic nervous system, and neuropeptide system are essential players in this activation. Mental stress increases the production of IL-6 by keratinocytes, changes the composition of the secretion of sebaceous glands, and as a consequence, leads to damage of the barrier function of the skin (38). The effects of chronic stress include a long-term increase in endogenous glucocorticoids associated with impaired skin regeneration and permeability, leading to exacerbation of itch. However, a significant proportion of patients with AD have an insufficient systemic hormonal response to acute stress, which may be a sign of the depletion of adaptive mechanisms (36).

Role of itch and stress in the development of sleep disorders

Both itch and psychosocial conflicts can disrupt patients' sleep (39). Multidirectional relationships exist between pruritus intensity and psychological distress, psychological distress and sleep disturbances, and pruritus intensity and sleep disturbances (3, 40). Sleep disorders can result in additional irritability, impaired social functioning, and a higher risk of mental disorders in patients with chronic pruritus. Even one night of sleep deprivation leads to increased levels of glucocorticoids, and along with acute stress, impairs the barrier function of the skin, increases skin dryness, itch, and worsens the course of AD (4).

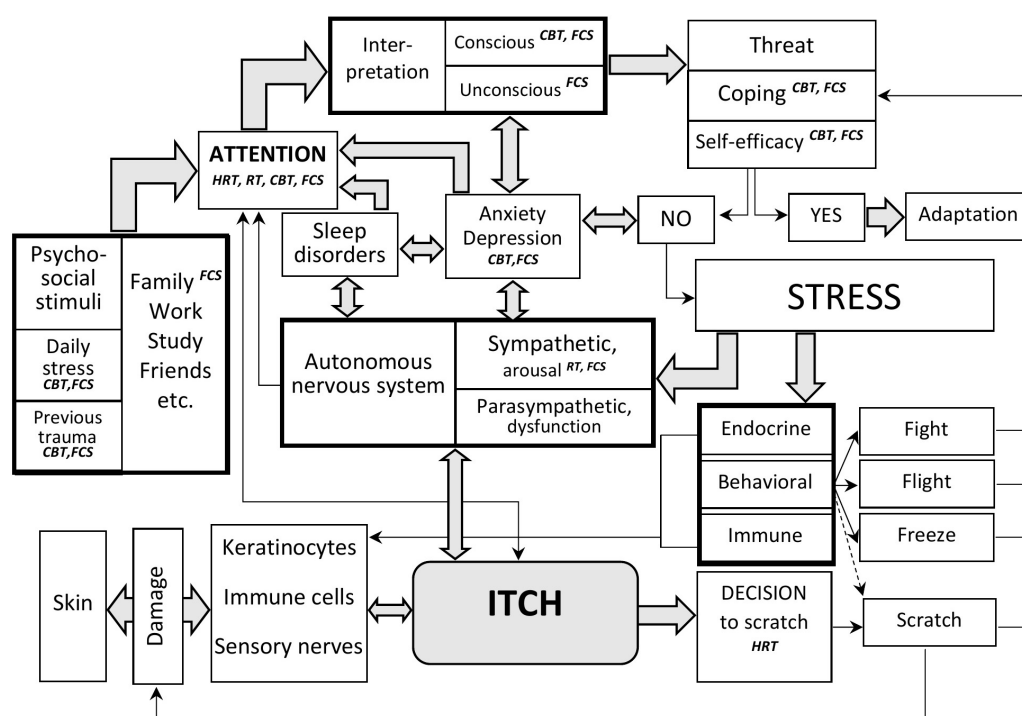


FIGURE 1

Interaction of stress and itch, key points of psychologic interventions in patients with itch. The perception of itch and the reaction to it depend on the interaction of sensory impulses from the skin, attention to these stimuli, and the state of the autonomic nervous system. Attention is modified under the influence of other external stimuli, including psychosocial, sleep, state of mental functions, etc. After the attention filter, sensory information is processed, and the general adaptation syndrome (stress reaction) is triggered in the case of a threat to survival. The stress reaction modifies endocrine, behavioral, and immune reactions. It can lead to changes in the function of keratinocytes, immune cells, and nerve structures, worsening the skin condition and increasing itching. With the help of psychological methods, it is possible to influence attention, interpretation of stimuli, methods of behavioral reactions, and improve the psychosocial adaptation of patients with chronic pruritus. The psychological techniques discussed in the article and the key points of their influence are indicated in italics. *HRT*, habit reversal training; *RT*, relaxation training; *CBT*, cognitive behavioral therapy; *FCS*, family constellations seminars.

Social interactions are important causes of stress in patients with chronic dermatologic itch

Leading sources of stress in patients with AD and psoriasis include social interactions and itch itself (2, 8, 41). Patients with AD and psoriasis are often characterized by a high level of childhood traumatic events, physical neglect in childhood (42), stressful life events, higher anxiety and depression scores (12, 43), long-lasting family distress (9, 44), family secrets, emotional abuse, alcohol and drug abuse (8), insecure attachment styles (45, 46) inability to perceive safety environment (14) and helplessness (2). Many dermatologic patients with chronic itch feel a pleasurable sensation after scratching even in the absence of itch (29), so they may use scratching as a way to soothe themselves to decrease stress. Both adults and adolescents with atopic dermatitis point to the importance of psycho-emotional factors in triggering the subjective feeling of itch, followed by scratching (47).

Social loyalty, agreeableness, and alexithymia may be associated with impaired social functioning in patients with chronic itch

Atopic dermatitis and psoriasis can be perceived as a disorder of communication between an individual and the environment (48). Many psoriatic and AD patients cannot reach personal goals in social situations. They refuse to acknowledge the presence of the high family strain even when there are objective signs and causes of family stress (14, 20). Among possible causes of this phenomenon can be high family loyalty (20). Psoriasis patients describe themselves as more cooperative and agreeable than healthy controls. In psoriasis patients, public self-consciousness is significantly positively associated with induced itch, and agreeableness is significantly negatively associated with induced scratching (49). High levels of alexithymia may be another essential mechanism explaining misinterpretation of social situations and emotional distress by patients with AD. More than 56% of patients

with AD have alexithymia, compared with 21% of healthy individuals in the control group (21). Alexithymia, in turn, can develop as a reaction of "fading" to reduce maladaptation and exhaustion with a large number of stresses. Patients with pruritus also tend to develop dissociative states (in which the psyche is detached from bodily sensations), which are typical for psychological trauma (2). In patients with chronic itch, dissociative states may be one of the ways to reduce subjective discomfort.

Psychological interventions in patients with itch

Medications, biological therapy, and psychological interventions are essential to control itch (27, 50). In our own work, we focus on the psychological mechanisms of influence on itch, and describe the possible mechanisms of influence of the method of FCS (51) in detail, and compare this method with other forms of psychological interventions.

Several types of psychological interventions were effective in the reduction of itch and scratch in patients with psoriasis and AD (52–55). According to an older meta-analysis (56), autogenous training (AT), cognitive behavioral therapy (CBT), dermatological education and CBT, and stress management program significantly decreased itch in these patients. AT, CBT, dermatological education and CBT, and habit reversal training (HRT) effectively decreased scratching intensity and eczema severity, though HRT did not decrease the feeling of itch. After a one-month course of relaxation therapy (RT), patients with AD demonstrated reduced itch and improved sleep quality compared with the control group (23). Objectively, the skin condition in patients of the RT group on the background of basic therapy improved in the same way as in the control group, but the level of biomarkers did not change (23).

Atopic dermatitis and habit reversal training do not address family problems as an essential source of stress. They are based on targeting attention, arousal, and scratching behavior, which is a relatively late stage in the itch-scratch process (Figure 1). At the same time, proper understanding of the social situation, successful coping strategies (57), acting with awareness (58), feeling of self-efficacy, and appropriate attachment orientation (46) may be critical in the reduction of stress by CBT and FCS interventions.

Family constellation seminars as a candidate method for patients with chronic itch

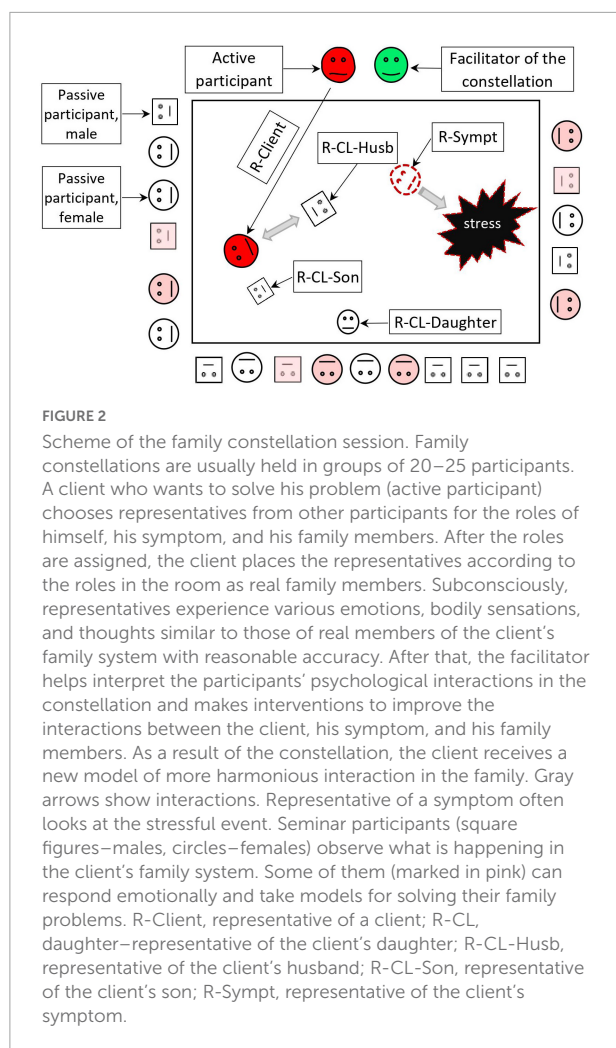
Family constellation seminars are becoming increasingly popular in solving various problems related to relationships

and health (59). The number of English literature publications explaining the basics of this method and the peculiarities of use in different groups of patients is limited (59, 60). Recent randomized control clinical trials (61, 62) have shown that FCS effectively help people manage family-related psychological issues especially connected with implicit interactions and family secrets. Participants of FCS reported significant improvement in psychological functioning, psychological distress, decreased motivational incongruence, better experience in their personal social systems, and overall goal attainment after FCS and in 4- and 12- follow-up periods after FCS (62, 63).

Family constellation seminars method was not discussed in several reviews about psychological interventions in the patients with itch (52–56), but we reported its effectiveness in decreasing itch, scratch, and improving skin condition (51). After a series of FCS, along with reduced itch severity and duration, patients with AD and psoriasis improved attentiveness, working capacity, productivity, quality of sleep and daily activities, and felt less emotional depletion due to itch (51).

Family constellation seminars are usually held in group sessions with about 20–25 participants and are led by a trained facilitator, usually a psychotherapist or clinical psychologist (63). The facilitator often uses the genogram to diagnose implicit family stresses and relationships, and that is of particular importance in patients with chronic itch (8, 20). With the help of the facilitator, one of the participants (the client, the so-called "active participant") describes essential facts about his family and his problem. After that client asks other participants to act as representatives (or so-called "stand-ins") for him/herself and his/her family members to depict the actual family interactions. Active participant places representatives in the room according to his/her own image of the stressful situation (Figure 2). Under the supervision of the facilitator, representatives subconsciously interact as if they were real people from the client's life. The difference between the FCS method and other group interaction methods is that after the placement in the specific places, representatives act according to their subconscious impulses depicting the behavior and emotions of family members with reliable accuracy. The facilitator makes phenomenological interpretations of the active participant's and representatives' cognitive, emotional and bodily reactions, and implements psychological interventions, helping the active client understand additional information about the family situation, developing more balanced interactions. After interventions, representatives change their places, and finally, the optimal "solution constellation" should provide a new, more comfortable pattern of the family relationships for the client. In the "solution constellation," the client is able to communicate and behave more efficiently in his/her personal social system (59).

Family constellation seminars postulates that a symptom (e.g., itch) may often play an adaptive role in the functioning



of the individual and his/her family as a social unit, so the active participant often assigns a representative to depict his symptom or disease in the constellation (64). The representative in the role of a symptom often helps to reveal important information about the specific psychological trauma or pattern of stressful relationships in the family. In “solution constellation,” the representative of the symptom usually feels that he/she is no longer needed to balance a client's system. By acquiring the new information and the new models of behavior, not only do active participant feels more resourceful, but all the participants of FCS use the new experience to improve real interactions with their family members (64).

The family constellations approach can also be used in individual (private, face-to-face) form and videoconferencing. Private setting differs from the group context, particularly with regard to the representatives: in groups, the participants themselves are used, while in an individual session, the constellation is done with specifically designed figurines, objects, or pictures (60).

Possible benefits of the family constellation seminars method for patients with chronic itch

1. Family constellation seminars addresses both conscious and unconscious family communication issues, helping reveal family secrets (especially connected with severe psychologic trauma) and making sense of implicit interactions between family members.
2. Usage of representatives and observation of their interactions from the third person point of view (in dissociated mode) may help the patient decrease stress from traumatic events revealed during the constellation. Considering the tendency of dermatologic patients to avoid speaking about family problems (20), this feature of FCS can be of essential importance.
3. Participation both as active participants and as representatives in the process of a constellation of the other participants of the seminar helps clients learn adaptive and safe models of behavior in their stressful situations, improving self-efficacy and coping skills (61, 62), especially important for patients with helplessness and worrying (2). Considering that patients with itch have difficulties with consciously admitting family problems (20), FCS might decrease stress in patients by offering a new solution to the problem without placing extra responsibility on the clients.
4. Family constellation seminars is traditionally held in groups of approximately 25 people, helping to establish a safe microenvironment (61) and possibly improve the attachment style of dermatologic patients.
5. Family constellation seminars is economically efficient due to the group format and the possibility of the weekend and online settings (61, 62).
6. From 66 to 92% of FCS participants reported increased happiness, courage, optimism, higher coping abilities, and improved interpersonal relationships due to the intervention (59). It is essential for patients with chronic itch, who are at an increased risk of depression and anxiety.
7. Family constellation seminars has a long-lasting effect, which may be of special importance in patients with chronic dermatoses (51, 62).

In conclusion, this review provides evidence for the effective use of FCS for stress coping in a general population sample and in patients with a variety of mental health disorders. Based on pathophysiological and social aspects of chronic itch and our own experience, we suggest implementing this method in the dermatological clinical setting. However, prior to its wider implementation, data from further research on the applications of FCS and other forms of family-centered

psychologic interventions in patients with chronic itch are required.

Author contributions

SC, MP, and GC performed the literature review, designed the figures, and wrote the manuscript. RY and YA added intellectual content and critically revised the manuscript. All authors approved the final manuscript for publication.

Funding

This study was supported by a grant from the Faculty of Medicine and Dentistry, Palacký University, Olomouc, IGA UP: LF_2022_005 and RVO: 61989592.

References

- Tominaga M, Takamori K. Peripheral itch sensitization in atopic dermatitis. *Allerg Int.* (2022) 71:265–77. doi: 10.1016/j.alit.2022.04.003
- Verhoeven E, De Klerk S, Kraaimaat F, Van de Kerkhof P, De Jong E, Evers A. Biopsychosocial mechanisms of chronic itch in patients with skin diseases: A review. *Acta Derm Venereol.* (2008) 88:211–8. doi: 10.2340/00015555-0452
- Spindler M, Przybyłowicz K, Hawro M, Weller K, Reidel U, Metz M, et al. Sleep disturbance in adult dermatologic patients: A cross-sectional study on prevalence, burden, and associated factors. *J Am Acad Dermatol.* (2021) 85:910–22. doi: 10.1016/j.jaad.2021.04.015
- Passeron T, Zouboulis C, Tan J, Andersen M, Katta R, Lyu X, et al. Adult skin acute stress responses to short-term environmental and internal aggression from exosome factors. *J Eur Acad Dermatol Venereol.* (2021) 35:1963–75. doi: 10.1111/jdv.17432
- Chrostowska-Plak D, Reich A, Szepietowski J. Relationship between itch and psychological status of patients with atopic dermatitis. *J Eur Acad Dermatol Venereol.* (2013) 27:e239–42. doi: 10.1111/j.1468-3083.2012.04578.x
- Grandgeorge M, Misery L. Mediators of the relationship between stress and itch. *Exp Dermatol.* (2015) 24:334–5. doi: 10.1111/exd.12653
- Golpanian R, Kim H, Yosipovich G. Effects of stress on itch. *Clin Ther.* (2020) 42:745–56. doi: 10.1016/j.clinthera.2020.01.025
- Poot F, Antoine E, Gravelier M, Hirtt J, Alfani S, Forchetti G, et al. A case-control study on family dysfunction in patients with alopecia areata, psoriasis and atopic dermatitis. *Acta Derm Venereol.* (2011) 91:415–21. doi: 10.2340/00015555-1074
- Snyder A, Brandenberger A, Taliere V, Rich B, Webber L, Beshay A, et al. Quality of life among family of patients with atopic dermatitis and psoriasis. *Int J Behav Med.* (2022): [Online ahead of print]. doi: 10.1007/s12529-022-10104-7
- Huang J, Choo Y, Smith H, Apfelbacher C. Quality of life in atopic dermatitis in Asian countries: A systematic review. *Arch Dermatol Res.* (2022) 314:445–62. doi: 10.1007/s00403-021-02246-7
- Dalgard F, Stern R, Lien L, Hauser S. Itch, stress and self-efficacy among 18-year-old boys and girls: A Norwegian population-based cross-sectional study. *Acta Derm Venereol.* (2012) 92:547–52. doi: 10.2340/00015555-1309
- Matterne U, Apfelbacher C, Vogelgsang L, Loerbroks A, Weisshaar E. Incidence and determinants of chronic pruritus: A population-based cohort study. *Acta Derm Venereol.* (2013) 93:532–7. doi: 10.2340/00015555-1572
- Dalgard F, Lien L, Dalen I. Itch in the community: Associations with psychosocial factors among adults. *J Eur Acad Dermatol Venereol.* (2007) 21:1215–9.
- Simonić E, Kaštelan M, Peternel S, Pernar M, Brajac I, Rončević-Gržeta I, et al. Childhood and adulthood traumatic experiences in patients with psoriasis. *J Dermatol.* (2010) 37:793–800. doi: 10.1111/j.1346-8138.2010.00870.x
- Lee S, Lee B, Park Y. Psychological health status and health-related quality of life in adults with atopic dermatitis: A nationwide cross-sectional study in South Korea. *Acta Derm Venereol.* (2018) 98:89–97. doi: 10.2340/00015555-2797
- Kowalewska B, Krajewska-Kulak E, Sobolewski M. The impact of stress-coping strategies and the severity of psoriasis on self-esteem, illness acceptance and life satisfaction. *Dermatol Ther (Heidelb).* (2022) 12:529–43. doi: 10.1007/s13555-021-00669-8
- Erturk I, Arican O, Omurlu I, Sut N. Effect of the pruritus on the quality of life: A preliminary study. *Ann Dermatol.* (2012) 24:406–12. doi: 10.5021/ad.2012.24.4.406
- Lee J, Suh H, Jung H, Park M, Ahn J. Association between chronic pruritus, depression, and insomnia: A cross-sectional study. *JAAD Int.* (2021) 3:54–60. doi: 10.1016/j.jdin.2021.02.004
- Ständer S, Weisshaar E, Mettang T, Szepietowski J, Carstens E, Ikoma A, et al. Clinical classification of itch: A position paper of the International Forum for the Study of Itch. *Acta Derm Venereol.* (2007) 87:291–4. doi: 10.2340/00015555-0305
- Marron S, Tomas-Aragones L, Boira S, Campos-Rodenas R. Quality of life, emotional wellbeing and family repercussions in dermatological patients experiencing chronic itching: A pilot study. *Acta Derm Venereol.* (2016) 96:331–5. doi: 10.2340/00015555-2263
- Talamonti M, Galluzzo M, Silvaggio D, Lombardo P, Tartaglia C, Bianchi L. Quality of life and psychological impact in patients with atopic dermatitis. *J Clin Med.* (2021) 10:1298. doi: 10.3390/jcm10061298
- Ferrucci S, Tavecchio S, Angileri L, Surace T, Berti E, Buoli M. Factors associated with affective symptoms and quality of life in patients with atopic dermatitis. *Acta Derm Venereol.* (2021) 101:adv00590. doi: 10.2340/00015555-3922
- Lee K, Bae B, Oh S, Park C, Noh S, Noh J, et al. Progressive muscle relaxation therapy for atopic dermatitis: Objective assessment of efficacy. *Acta Derm Venereol.* (2012) 92:57–61. doi: 10.2340/00015555-1189
- Halvorsen J, Lien L, Dalgard F, Bjertness E, Stern R. Suicidal ideation, mental health problems, and social function in adolescents with eczema: A population-based study. *J Invest Dermatol.* (2014) 134:1847–54. doi: 10.1038/jid.2014.70
- Hedemann T, Liu X, Kang C, Husain M. Associations between psoriasis and mental illness: An update for clinicians. *Gen Hosp Psychiatry.* (2022) 75:30–7. doi: 10.1016/j.genhosppsych.2022.01.006
- Esposito M, Saraceno R, Giunta A, Maccarone M, Chimenti S. An Italian study on psoriasis and depression. *Dermatology (Basel).* (2006) 212:123–7. doi: 10.1159/000090652
- Misery L, Belloni Fortina A, El Hachem M, Chernyshov P, Kobyletzki L, Heratizadeh A, et al. A position paper on the management of itch and pain in atopic dermatitis from the International Society of Atopic Dermatitis (ISAD)/Oriented

Conflict of interest

The authors declare that the research was conducted in the absence of any commercial or financial relationships that could be construed as a potential conflict of interest.

Publisher's note

All claims expressed in this article are solely those of the authors and do not necessarily represent those of their affiliated organizations, or those of the publisher, the editors and the reviewers. Any product that may be evaluated in this article, or claim that may be made by its manufacturer, is not guaranteed or endorsed by the publisher.

Patient-Education Network in Dermatology (OPENED) task force. *J Eur Acad Dermatol Venereol.* (2021) 35:787–96. doi: 10.1111/jdv.16916

28. Borgia F, Custurone P, Peterle L, Pioggia G, Gangemi S. Role of epithelium-derived cytokines in atopic dermatitis and psoriasis: Evidence and therapeutic perspectives. *Biomolecules.* (2021) 11:1843. doi: 10.3390/biom11121843

29. Mochizuki H, Schut C, Nattkemper L, Yosipovitch G. Brain mechanism of itch in atopic dermatitis and its possible alteration through non-invasive treatments. *Allerg Int.* (2017) 66:14–21. doi: 10.1016/j.alit.2016.08.013

30. Mochizuki H, Hernandez L, Yosipovitch G, Sadato N, Kakigi R. The amygdala network for processing itch in human brains. *Acta Derm Venereol.* (2020) 100:adv00345. doi: 10.2340/00015555-3703

31. Najafi P, Ben Salem D, Carré J, Misery L, Dufoir O. Functional and anatomical brain connectivity in psoriasis patients and healthy controls: A pilot brain imaging study after exposure to mentally induced itch. *J Eur Acad Dermatol Venereol.* (2020) 34:2557–65. doi: 10.1111/jdv.16441

32. Papoiu A, Wang H, Coghill R, Chan Y, Yosipovitch G. Contagious itch in humans: A study of visual ‘transmission’ of itch in atopic dermatitis and healthy subjects. *Br J Dermatol.* (2011) 164:1299–303. doi: 10.1111/j.1365-2133.2011.10318.x

33. Mochizuki H, Kursewicz C, Nomi J, Yosipovitch G. The right default mode network is associated with the severity of chronic itch. *J Eur Acad Dermatol Venereol.* (2021) 35:e819–21. doi: 10.1111/jdv.17510

34. Buckner R, Andrews-Hanna J, Schacter D. The brain’s default network. *Ann N Y Acad Sci.* (2008) 1124:1–38. doi: 10.1196/annals.1440.011

35. Buske-Kirschbaum A, Kern S, Ebrecht M, Hellhammer D. Altered distribution of leukocyte subsets and cytokine production in response to acute psychosocial stress in patients with psoriasis vulgaris. *Brain Behav Immun.* (2007) 21:92–9. doi: 10.1016/j.bbi.2006.03.006

36. Buske-Kirschbaum A, Ebrecht M, Hellhammer D. Blunted HPA axis responsiveness to stress in atopic patients is associated with the acuity and severeness of allergic inflammation. *Brain Behav Immun.* (2010) 24:1347–53. doi: 10.1016/j.bbi.2010.06.013

37. Evers A, Verhoeven E, Kraaijaat F, de Jong E, de Brouwer S, Schalkwijk J, et al. How stress gets under the skin: Cortisol and stress reactivity in psoriasis. *Br J Dermatol.* (2010) 163:986–91. doi: 10.1111/j.1365-2133.2010.09984.x

38. Pondeljak N, Lugović-Mihic L. Stress-induced interaction of skin immune cells, hormones, and neurotransmitters. *Clin Ther.* (2020) 42:757–70. doi: 10.1016/j.clinthera.2020.03.008

39. Sahin E, Hawro M, Weller K, Sabat R, Philipp S, Kokolakis G, et al. Prevalence and factors associated with sleep disturbance in adult patients with psoriasis. *J Eur Acad Dermatol Venereol.* (2022) 36:688–97. doi: 10.1111/jdv.17917

40. Xerfan E, Tomimori J, Andersen M, Tufik S, Facina A. Sleep disturbance and atopic dermatitis: A bidirectional relationship? *Med Hypotheses.* (2020) 140:109637. doi: 10.1016/j.mehy.2020.109637

41. Hunter H, Griffiths C, Kleyn C. Does psychosocial stress play a role in the exacerbation of psoriasis? *Br J Dermatol.* (2013) 169:965–74. doi: 10.1111/bjd.12478

42. Wintermann G, Bierling A, Peters E, Abraham S, Beissert S, Weidner K. Childhood trauma and psychosocial stress affect treatment outcome in patients with psoriasis starting a new treatment episode. *Front Psychiatry.* (2022) 13:848708. doi: 10.3389/fpsy.2022.848708

43. Şahiner I, Taskintuna N, Sevik A, Kose O, Atas H, Sahiner S, et al. The impact role of childhood traumas and life events in patients with alopecia areata and psoriasis. *Afr J Psychiatry.* (2014) 17:1–6.

44. Malhotra S, Mehta V. Role of stressful life events in induction or exacerbation of psoriasis and chronic urticaria. *Indian J Dermatol Venereol Leprol.* (2008) 74:594–9.

45. Szabó C, Altmayer A, Lien L, Poot F, Gieler U, Tomas-Aragones L, et al. Attachment styles of dermatological patients in Europe: A multi-centre study in 13 Countries. *Acta Derm Venereol.* (2017) 97:813–8. doi: 10.2340/00015555-2619

46. Krasuska M, Lavda A, Thompson A, Millings A. The role of adult attachment orientation and coping in psychological adjustment to living with skin conditions. *Br J Dermatol.* (2018) 178:1396–403. doi: 10.1111/bjd.16268

47. Fang M, Nowinski C, Lai J, Shaunfield S, Silverberg J, Rangel S, et al. Characteristics and impacts of itch in children with inflammatory skin disorders. *Br J Dermatol.* (2021) 184:896–904. doi: 10.1111/bjd.19541

48. Ferreira B, Pio-Abreu J, Figueiredo A, Misery L. Pruritus, allergy and autoimmunity: Paving the way for an integrated understanding of psychodermatological diseases? *Front Allergy.* (2021) 2:688999. doi: 10.3389/falgy.2021.688999

49. Schut C, Muhl S, Reinisch K, Claßen A, Jäger R, Gieler U, et al. Agreeableness and self-consciousness as predictors of induced scratching and itch in patients with psoriasis. *Int J Behav Med.* (2015) 22:726–34. doi: 10.1007/s12529-015-9471-5

50. Gupta M, Gupta A. Psychiatric and psychological co-morbidity in patients with dermatologic disorders. *Am J Clin Dermatol.* (2003) 4:833–42. doi: 10.2165/00128071-200304120-00003

51. Jafferany M, Capec S, Yaremkevych R, Andrashko Y, Capec G, Petrek M. Effects of family constellation seminars on itch in patients with atopic dermatitis and psoriasis: A patient preference controlled trial. *Dermatol Ther.* (2019) 32:e13100. doi: 10.1111/dth.13100

52. Schut C, Mollanazar N, Kupfer J, Gieler U, Yosipovitch G. Psychological interventions in the treatment of chronic itch. *Acta Derm Venereol.* (2016) 96:157–63. doi: 10.2340/00015555-2177

53. Lavda A, Webb T, Thompson A. A meta-analysis of the effectiveness of psychological interventions for adults with skin conditions. *Br J Dermatol.* (2012) 167:970–9. doi: 10.1111/j.1365-2133.2012.11183.x

54. Jafferany M, Davari M. Itch and psyche: Psychiatric aspects of pruritus. *Int J Dermatol.* (2018) 58:3–23. doi: 10.1111/ijd.14081

55. Hedman-Lagerlöf E, Fust J, Axelsson E, Bonnert M, Lalouni M, Molander O, et al. Internet-delivered cognitive behavior therapy for atopic dermatitis. *JAMA Dermatol.* (2021) 157:796–804. doi: 10.1001/jamadermatol.2021.1450

56. Chida Y, Steptoe A, Hatakawa N, Sudo N, Kubo C. The effects of psychological intervention on atopic dermatitis. *Int Arch Allergy Immunol.* (2007) 144:1–9. doi: 10.1159/000101940

57. Schut C, Weik U, Tews N, Gieler U, Deinzer R, Kupfer J. Coping as mediator of the relationship between stress and itch in patients with atopic dermatitis: A regression and mediation analysis. *Exp Dermatol.* (2015) 24:148–50. doi: 10.1111/exd.12578

58. Lüßmann K, Montgomery K, Thompson A, Gieler U, Zick C, Kupfer J, et al. Mindfulness as predictor of itch catastrophizing in patients with atopic dermatitis: Results of a cross-sectional questionnaire study. *Front Med (Lausanne).* (2021) 8:627611. doi: 10.3389/fmed.2021.627611

59. Konkoly Thege B, Petroll C, Rivas C, Scholtens S. The effectiveness of family constellation therapy in improving mental health: A systematic review. *Fam Process.* (2021) 60:409–23. doi: 10.1111/famp.12636

60. Ramos S, Ramos J. Process of change and effectiveness of family constellations: A mixed methods single case study on depression. *Fam J Alex Va.* (2019) 27:418–28. doi: 10.1177/1066480719868706

61. Hunger C, Bornhäuser A, Link L, Schweitzer J, Weinhold J. Improving experience in personal social systems through family constellation seminars: Results of a randomized controlled trial. *Fam Process.* (2014) 53:288–306. doi: 10.1111/famp.12051

62. Hunger C, Weinhold J, Bornhäuser A, Link L, Schweitzer J. Mid- and long-term effects of family constellation seminars in a general population sample: 8- and 12-month follow-up. *Fam Process.* (2015) 54:344–58. doi: 10.1111/famp.12102

63. Weinhold J, Hunger C, Bornhäuser A, Link L, Rochon J, Wild B, et al. Family constellation seminars improve psychological functioning in a general population sample: Results of a randomized controlled trial. *J Couns Psychol.* (2013) 60:601–9. doi: 10.1037/a0033539

64. Kutschera I, Brugger C. *What's out of order here? Illness and family constellations.* Heidelberg: Carl-Auer Verlag (2006).



OPEN ACCESS

EDITED BY

Stefania Guida,
University of Modena and Reggio
Emilia, Italy

REVIEWED BY

Wayne Robert Thomas,
University of Western
Australia, Australia
Ryoji Tanei,
Tokyo Metropolitan Geriatric Hospital
and Institute of Gerontology
(TMGH-IG), Japan

*CORRESPONDENCE

Ruperto González-Pérez
glezruperto@gmail.com

SPECIALTY SECTION

This article was submitted to
Dermatology,
a section of the journal
Frontiers in Medicine

RECEIVED 09 May 2022

ACCEPTED 25 July 2022

PUBLISHED 12 August 2022

CITATION

González-Pérez R, Poza-Guedes P,
Mederos-Luis E and Sánchez-Machín I
(2022) Dupilumab modulates specific
IgE mite responses at the molecular
level in severe T2-high atopic
dermatitis: A real-world experience.
Front. Med. 9:939598.
doi: 10.3389/fmed.2022.939598

COPYRIGHT

© 2022 González-Pérez,
Poza-Guedes, Mederos-Luis and
Sánchez-Machín. This is an
open-access article distributed under
the terms of the [Creative Commons
Attribution License \(CC BY\)](#). The use,
distribution or reproduction in other
forums is permitted, provided the
original author(s) and the copyright
owner(s) are credited and that the
original publication in this journal is
cited, in accordance with accepted
academic practice. No use, distribution
or reproduction is permitted which
does not comply with these terms.

Dupilumab modulates specific IgE mite responses at the molecular level in severe T2-high atopic dermatitis: A real-world experience

Ruperto González-Pérez ^{1,2*}, Paloma Poza-Guedes ^{1,2},
Elena Mederos-Luis¹ and Inmaculada Sánchez-Machín ¹

¹Allergy Department, Hospital Universitario de Canarias, Santa Cruz de Tenerife, Spain, ²Severe Asthma Unit, Hospital Universitario de Canarias, Santa Cruz de Tenerife, Spain

Background: Atopic dermatitis (AD) is regarded as a chronic systemic disease which is characterized by a robust overexpression of type 2 related cytokines, with increased total IgE levels and a concomitant sensitization to common allergens. Dupilumab, a fully human monoclonal antibody (mAb) to IL-4R α that inhibits both IL-4 and IL-13 signaling, has previously shown a marked and rapid improvement when treating the moderate-to-severe forms of AD. We sought to evaluate the real-world evidence (RWE) of dupilumab in the modulation of total and specific IgE (sIgE) serum levels to a panel of molecular house dust mites (HDM) and storage mites (SM) allergens in patients with severe AD.

Methods: Demographic and clinical data for severe AD adult patients receiving dupilumab treatment (300 mg every 2 weeks) were reviewed. Mean (standard deviations SD) values and percent changes from baseline in total and sIgE to the complete HDM and SM extracts, and 14 individual molecular allergens were measured over 52 weeks.

Results: Significant ($p < 0.05$) changes in mean total IgE levels were observed from baseline to week-52 after treatment with dupilumab. Despite no changes were found in sIgE against the extract of HDM during the 52-week treatment with dupilumab, baseline mean levels from 7 out of 14 individual molecular mite allergens -Der p 1, Der p 2, Der p 5, Der p 7, Der p 21, Der p 23, and Lep d 2- were significantly ($p < 0.05$) decreased—after 52 weeks of treatment with dupilumab.

Conclusions: Dupilumab therapy for 52 weeks resulted in a profound reduction in blood levels of total IgE and allergen-specific IgE to both HDM and SM at the molecular level in adults with severe AD under RWE conditions. The potential benefits of these concomitant immunomodulatory effects after treatment with dupilumab should be explored to a greater extent.

KEYWORDS

atopic dermatitis, dupilumab, specific IgE, mites, personalized allergy molecular diagnosis

Introduction

Atopic dermatitis (AD), an inflammatory, chronically relapsing and intensely pruritic skin disease, is nowadays considered a systemic Type 2 inflammation driven disease, enclosing a specific CD4+ T helper type (Th) 2 cell response and the activation of several T-cell lineages, such as Th1, Th17/interleukin (IL)-23, and Th22 (1, 2). Former clinical and experimental studies indicate that house dust mites (HDM) can play a critical role in the pathogenesis of AD in sensitized and genetically predisposed subjects (3, 4). The introduction of Precision Allergy Molecular Diagnosis (PAMD@) has a major effect on analytic specificity and allergy diagnosis, to a comprehensive assessment of the patient's specific IgE (sIgE) binding to a panel of individual allergens (5).

Dupilumab, the first fully human monoclonal IgG4 antibody inhibiting the signaling of IL-4 and IL-13, significantly reduces type 2 biomarkers in circulating serum and lesional skin (6, 7). Nowadays, changes in allergen-specific IgE serum levels have only been described for allergen extracts in subjects with moderate-to-severe AD from clinical trials with dupilumab (8, 9). Herein, we aimed to investigate the real-world evidence (RWE) effects of after 52 weeks of treatment with dupilumab in total and mite-molecular IgE serum levels in a cohort of individuals afflicted with the severe extrinsic AD phenotype subjected to a high local environmental mite exposure (10, 11).

Materials and methods

Subjects

We consecutively recruited patients from May 2020 to November 2021 from the Outpatient Allergy Clinic & Severe Asthma Unit at Hospital Universitario de Canarias (Tenerife, Spain). Eligibility criteria included subjects in treatment with dupilumab 300 mg every 2 weeks (300 mg-q2w) for 52 weeks with a clinician confirmed diagnosis of severe AD with the T2-high endotype (extrinsic subtype) according to current guidelines (12).

Clinical data -including Scoring Atopic Dermatitis (SCORAD), Eczema Area and Severity Index (EASI) score, Investigator's Global Assessment (IGA) and peak pruritus numerical rating scale (PNRS)- were retrieved from the patients' medical records 4 weeks before treatment with dupilumab 300 mg-q2w (Time 0, T0), 26 weeks after starting therapy with dupilumab (Time 1, T1), 32 weeks after dupilumab (Time 2, T2) and finally after completing 52 weeks with dupilumab (Time 3, T3). The study was conducted according to the guidelines of

the Declaration of Helsinki and approved by the Institutional Ethics Committee of CEIC Hospital Universitario de Canarias, Tenerife, Spain with the reference number P.I.-2017/72 on 30 October 2017.

Pregnant and breast-feeding women and patients receiving allergen immunotherapy (AIT), and/or other biologics apart from dupilumab were excluded from the investigation. Blood specimens were collected for all subjects, identified with a code label, stored at -40°C and immediately thawed in preparation for *in vitro* analysis to evaluate median values and percent changes from baseline in total and allergen-specific IgE over the 52 weeks follow up.

Skin prick test and mite allergenic extracts

Percutaneous tests were performed according to European standards (13) with standardized allergenic extracts of *Dermatophagoides pteronyssinus*, *Blomia tropicalis*, *Lepidoglyphus destructor*, and *Tyrophagus putrescentiae* (Diater, Madrid, Spain). Saline (0.9%) and histamine (10 mg/ml) were respectively included as negative and positive controls. Antihistamines were drop back seven days in advance to each SPT, with wheal diameters >3 mm considered positive after a 20 min immediate reading.

Serological workup

Total IgE levels, sIgE to the whole *D. pteronyssinus* and *B. tropicalis* extract, and 14 individual molecular allergens -Der p 1, Der p 2, Der p 5, Der p 7, Der p 10, Der p 11, Der p 20, Der p 21, Der p 23, Blo t 5, Blo t 10, Blo t 21, Lep d 2, and Tyr p 2- were measured by a MedTech company (MacroArray Diagnostics, Viena, Austria), according to the manufacturer's instructions. In brief, the Allergy Explorer (ALEX[®]) test is a multiplex array containing 282 reagents (157 extractive allergens and 125 molecular components). The different allergens and components are coupled onto polystyrene nano-beads, and then the allergen beads are deposited on a nitrocellulose membrane, as previously published (14). Total IgE levels were expressed in international units per unit volume (IU/mL), sIgE levels were expressed in $\text{kU}_\text{A}/\text{L}$. Values $\geq 0.35 \text{ kU}_\text{A}/\text{L}$ were regarded as positive.

Statistical data

Demographic features were summarized by means and standard deviations for continuous variables and percentages for categorical variables. To compare differences analysis of variance, Kruskal-Wallis, Mann-Whitney U and Chi-square tests are required for parametric continuous, non-parametric

Abbreviations: AD, Atopic Dermatitis; HDM, House Dust Mite; PAMD@, Personalized Allergy Molecular Diagnosis; *D. pteronyssinus*, *Dermatophagoides pteronyssinus*; *B. tropicalis*, *Blomia tropicalis*; SPT, Skin Prick Test; RWE, Real World Evidence.

TABLE 1 Descriptive statistics at baseline.

Study population (N = 12)	Severe atopic dermatitis
Age (y.o.) median (range)	27.0 (19–57)
Sex (M/F)	(10/2)
SCORAD index >40 N (%)	12 (100)
EASI score >21 N (%)	12 (100)
IGA = 4 N (%)	12 (100)
PNRS median (range)	8 (7–9)
Systemic cyclosporin/steroids N (%)	12 (100)
Rhinitis and/or Asthma N (%)	11 (91.66)
Food Allergy N (%)	3 (25.0)
Family History of Atopy N (%)	10 (83.3)
Total IgE (UI/ml) median (range)	4,246 (221–19,370)
sIgE <i>D. pteronyssinus</i> (kU/L) > 100 N (%)	12 (100)
sIgE <i>B. tropicalis</i> (kU/L) median (range)	64 (8.11–>100)
Blood Eosinophils/mm ³ median (range)	390 (40–1,800)

SCORAD, Scoring Atopic Dermatitis; EASI, Eczema Area and Severity Index; IGA, Investigator's Global Assessment; PNRS, Pruritus Numerical Rating Scale. *D. pteronyssinus*: Dermatophagoides pteronyssinus. *B. tropicalis*: Blomia tropicalis. Median values are shown.

continuous, and categorical variables respectively. A *P*-value of <0.05 was considered statistically significant. All statistical data were analyzed using GraphPad Prism version 8.0.0 for Windows, GraphPad Software, La Jolla, California, USA.

Results

Demographic characteristics of patients

We finally selected 12 (out of 22) European-American ethnicity subjects from the outpatient allergy office –10 males and 2 females, median age 27.0 (19–57) years of age– who met the inclusion criteria and a previous clinician-confirmed diagnosis of AD ongoing for more than 15 years. Considering SCORAD >40 and EASI >21 as markers for the severe forms of (15), all selected subjects showed upon inclusion a median SCORAD and EASI of 84.5 (54.0–96.4) and 62.40 (27.0–70.0), respectively. A median Investigator's Global Assessment (IGA) score of 4 (severe on a scale of 0–4) and a median peak pruritus numerical rating scale (NRS) of 8 (severe on a scale of 0–10) was also quantified for all subjects at baseline.

More than 80% (10 out 12 subjects) had a former family history of atopy and regarding comorbidities, 91.66% patients were afflicted with allergic rhinitis and/or asthma, and 25.0% had a clinically confirmed food allergy (milk, seafood and/or tree nuts) associated (Table 1).

Concerning the need of systemic medication for AD at baseline, patients were in treatment with either cyclosporin (75%

of subjects with a median dose of 75 mg/day), steroids (16.6% with a median dose of prednisone 15 mg/day) or azathioprine (50 mg/day in 1 individual).

Quantification of basal total IgE, SPT, and sIgE to the extract of *D. pteronyssinus* and *Blomia tropicalis* and mite molecular profile

All patients confirming their eligibility for the study showed a marked Th2-high endotype –featuring elevated peripheral eosinophil count, total IgE and aeroallergen-specific IgE levels. Basal total IgE (before treatment with dupilumab) ranged from 221.0 to 19,370.0 IU/mL, with a median value of 3765.0 IU/mL. Basal median blood eosinophils showed a value of 390 (40–1,800) eosinophils/μL. All enrolled individuals had a positive SPT and serum sIgE (≥ 0.35 kU/l) against both *D. pteronyssinus* and *B. tropicalis* (crude extract), with median values of >100 and 64 (8.11 to >100) kU/L, respectively (Table 1).

Globally, all patients were simultaneously sensitized to 3 or more of the 14 mite allergens included in the customized molecular panel. Regarding the frequency of sIgE-binding to individual molecular allergens, Der p 2, Der p 21, and Der p 23 led the sIgE immunoresponse in all individuals (100%), followed by Der p 1 and Der p 5 (83.33%) subjects, while 75.0% individuals were sensitized to Der p 7. Minor allergens as Der p 10 were only present in 8.33%, while Der p 11 and Der p 20 were found in 16.66% of the investigated serum samples. Considering storage mites, Lep d 2 (58.8%) and Blo t 5 (50.0%) were the most frequently identified allergens in the current cohort.

In relation to the aggregation of allergens, despite the repertoire of IgE-recognized molecules was highly polyclonal, a preponderant specific pattern could not be found (Table 2). The quantitative basal mean values of sIgE (kU/L) were the highest for Der p 2 (52.64 ± 5.28), followed by Der p 23 (45.0 ± 12.06), Der p 21 (43.71 ± 22.79), Der p 5 (42.25 ± 16.64), Der p 1 (24.6 ± 17.87), Blo t5 22.32 ± 13.62 Der p 7 (20.05 ± 20.44), and Lep d 2 (13.95 ± 11.56).

Evolution of clinical severity and pruritus after therapy with dupilumab 300 mg-Q2w for 52 weeks

A significant improvement in both SCORAD index and EASI score was reported at weeks 26 and 52 in all subjects compared to their baseline scores (Table 3). In addition, at weeks 26 and 52, 83.33% patients receiving dupilumab had an IGA score of 0 or 1 and an improvement of 2 points or more on the IGA from the baseline score. Also, at weeks 26

TABLE 2 Specific IgE profiles to 14 allergen molecules from *Dermatophagoides pteronyssinus*, *Blomia tropicalis*, *Lepidoglyphus destructor*, and *Tyrophagus putrescentiae* in subjects afflicted with severe atopic dermatitis tested with microarray.

n = 12	Number of molecules	Der p 1	Der p 2	Der p 5	Der p 7	Der p 10	Der p 11	Der p 20	Der p 21	Der p 23	Blo t 5	Blo t 10	Blo t 21	Lep d 2	Tyr p 2
1	3	*	*							*					
1	5	*	*						*	*				*	
1	6	*	*	*	*				*	*				*	
2	7	*	*	*	*				*	*	*			*	
2	8	*	*	*	*				*	*	*			*	
1	8	*	*	*	*				*	*	*		*	*	*
1	10	*	*	*	*	*			*	*	*	*	*	*	*
1	10	*	*	*	*	*			*	*	*	*	*	*	*
2	12	*	*	*	*	*	*	*	*	*	*	*	*	*	*

Profiles are ordered by the increasing number of recognized molecules.
Asterisk (*) indicates specific IgE sensitization to single molecular allergens.

and 52, a reduction of at least 5 points in the peak score on the PNRS was found in all patients after treatment with dupilumab in contrast to their baseline scores ($P < 0.05$ for all comparisons). Concomitant systemic medication was discontinued (ciclosporin, steroids and/or azathioprine) in all subjects at week 52 after treatment with dupilumab.

Total serum IgE and mite molecular responses after treatment with dupilumab 300 mg every 2 weeks for 52 weeks

Significant ($p < 0.05$) changes in mean total IgE levels were observed from baseline ($6,751.88 \pm 7,626.39$ IU/mL) to week-26 ($3,040.5 \pm 2,546.61$ IU/mL) and week-52 ($3,149.33 \pm 2,513.24$ IU/mL) after treatment with dupilumab. No changes were found in sIgE against the extract of *D. pteronyssinus* - as mean values remained >100 kU/L- during the 52-week treatment with dupilumab. Mean sIgE levels against the extract of *B. tropicalis* were significantly reduced from baseline (75.02 ± 39.61 kU/L) to (19.92 ± 26.03 kU/L) by week 52.

Interestingly, baseline mean levels (kU/L) from 7 out of 14 (50%) individual molecular mite allergens -Der p 1 (24.6 ± 17.87), Der p 2 (52.64 ± 5.28), Der p 5 (42.25 ± 16.64), Der p 7 (20.05 ± 20.44), Der p 21 (43.71 ± 22.79), Der p 23 (45.0 ± 12.06) and Lep d 2 (13.95 ± 11.56)- were significantly ($p < 0.05$) decreased -Der p 1 (11.82 ± 11.5), Der p 2 (28.63 ± 15.64), Der p 5 (25.74 ± 18.02), Der p 7 (14.78 ± 16.08), Der p 21 (29.31 ± 23.31), Der p 23 (27.0 ± 11.99), and Lep d 2 (3.72 ± 4.35)- after 52 weeks of treatment with dupilumab. In addition, despite no statistical significance was reached, even a decreased in the mean sIgE levels was confirmed for Der p 10, Der p 11 and Der p 20 (regarded as minor allergens from *D. pteronyssinus*), and also for the major allergens (Blo t 5 and Blo t 21) from *B. tropicalis* and *T. putrescentiae* (Tyr p 2), respectively, after 52 weeks of treatment with dupilumab (Figure 1).

Safety and adverse events

Two subjects (16.66%) had adverse events developing mild conjunctivitis after 16-weeks of treatment with dupilumab. Conjunctivitis was controlled after using moisturizing sodium hyaluronate eye drops. None of the patients had to discontinue therapy with dupilumab during the study period.

Discussion

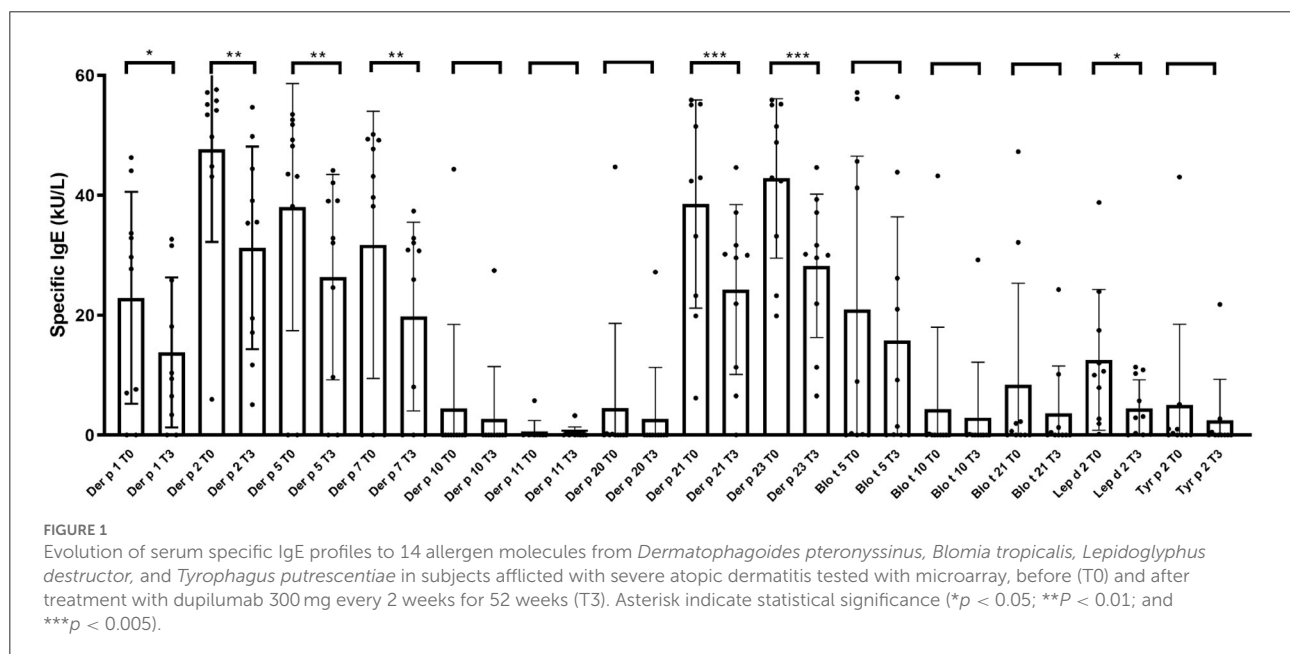
The identification of *in vitro* biomarkers -including the reduction of sIgE- and their direct association with disease severity and the potential prediction of severe disease are of great

TABLE 3 Scoring features and routine laboratory testing in patients ($n = 12$) with severe atopic dermatitis at baseline and follow-up after 26 and 52 weeks of treatment with dupilumab 300 mg every 2 weeks for 52 weeks.

	Baseline	Week 26	Week 52
SCORAD index	74.93 \pm 15.89	25.12 \pm 12.75*	15.07 \pm 7.97*
EASI score	50.75 \pm 17.83	5.94 \pm 2.68*	2.24 \pm 2.17*
IGA	4 \pm 0.0	1.33 \pm 0.7*	1.0 \pm 0.81*
PNRS	7.91 \pm 0.66	1.75 \pm 1.38*	1.26 \pm 0.76*
BSA (%)	70.69 \pm 16.07	14.0 \pm 7.19*	11.9 \pm 8.65*
POEM score	24.79 \pm 3.41	13.24 \pm 4.68*	9.39 \pm 5.23*
Eosinophils/mm ³ (blood)	562.5 \pm 563.47	1,113.42 \pm 1,005.94	778.12 \pm 691.16
sIgE <i>D. pteronyssinus</i> (kU/L)	100 \pm 0.0	100 \pm 0.0	100 \pm 0.0
sIgE <i>B. tropicalis</i> (kU/L)	75.02 \pm 39.61	64.0 \pm 29.48	19.92 \pm 26.03*
Serum Total IgE (UI/mL)	6,751.88 \pm 7,626.39	3,040.5 \pm 2,546.61*	3,149.33 \pm 2,513.24*

Mean values and standard deviations are shown.

Asterisk (*) indicates statistical significance ($p < 0.05$). *D. pteronyssinus*: Dermatophagoides pteronyssinus. *B. tropicalis*: Blomia tropicalis.



clinical interest in monitoring the effects of targeted therapy for different allergic conditions (16–20).

Previous studies provide evidence that AD and allergic asthma might share related drivers -i.e., IL-4 and IL-13- and that both conditions may benefit from a common therapeutic inhibition of these Th2 cytokines with dupilumab (21).

The contributing role of mites and a high prevailing capacity for sIgE sensitization -based on the frequency of IgE-binding- has been previously described in the pathogenesis and severity of AD in populations from diverse geographical areas and ethnicities (22, 23). In the present investigation, and in addition to the supporting clinical outcomes after therapy with dupilumab, a significant immunomodulation in the sIgE molecular profile to major and mid-tier mite allergens has been

found in a RWE subset of patients afflicted with severe AD. The current discernment of B cell activation and differentiation during development and later persistence or resolution of human IgE-mediated allergic diseases is still limited. The lifespan of IgE plasma cells and the conditions in which new IgE plasma cells are generated are essential questions in the recognition of potential pathways for therapeutic intervention in allergic disease (24). In respect to perennial allergens (i.e., mites), persistent IgE could be attributed to long-lived IgE plasma cells or short-lived IgE plasma cells continuously generated from a memory reservoir. As plasmablasts originate from non-IgE memory cells, it has been speculated that dupilumab resulted in a marked reduction of serum allergen-specific IgE -an IL-4 and IL-13-dependent process- as a large portion of circulating IgE in

AD patients derives from short-lived IgE plasma cells elicited in recent class-switching events (25).

The disease-modifying effects of AIT are also associated with immune modulation of the innate and adaptive immune responses. In fact, successful AIT has been related to the induction of allergen-specific blocking IgG antibodies, inhibiting allergen-induced mast cell and basophil degranulation and IgE-facilitated allergen presentation to T cells (26–28). In addition to AIT, it has been shown that circulating IgE can be effectively reduced by the binding of omalizumab –a recombinant humanized monoclonal anti-IgE-antibody– to the binding site of the high affinity FcεRI receptor on the IgE antibody priming the downregulation of the FcεRI receptor on basophils and mast cells (29). Interestingly, despite both AIT and omalizumab have confirmed a clinical benefit in a variety of IgE-mediated allergic diseases -i.e., allergic rhinitis and/or asthma and chronic spontaneous urticaria- their role in AD is still controversial (30–32). In the present report, the significant reduction in the molecular sIgE to mite allergens may be only speculated as a part in the mechanistic puzzle to a favored outcome after dupilumab therapy in severe AD individuals. Furthermore, although no changes in the *in vitro* sIgE to the extract of *D. pteronyssinus* were identified -as median sIgE values remained >100 kU/L during the 52 weeks of treatment with dupilumab-, PAMD@ unveiled a significant decrease in major and mid-tier molecular allergens from *D. pteronyssinus*. These observations would suggest that only sIgE antibody responses to the serodominant -but not those molecules with the lowest prevalence- are being continually stimulated by Th2 dependent immune responses. The current research has potential bias as the study was performed in a single center, with a limited number of subjects, and data from T2 could not be retrieved in 5 subjects due to local COVID-19 pandemic restrictions. Also, the identification of minor molecules as Der p 18, Der f 13, Der f 14, Der f 32, and Der f Alt a 10, regarded as mite immunologic markers for AD, was neither assessed in the intended population (33, 34).

Despite previous trials with dupilumab treatment resulted in a prompt decrease of total and allergen serum sIgE in moderate-to-severe AD (35), this is to our knowledge the first RWE report to confirm a significant and sustained reduction in blood levels of mite sIgE at the molecular level after 52 weeks of treatment with dupilumab in a selected cohort of adult patients with severe AD. In line with recent reports, (36–38), our data suggest that a long-term clinical benefit could be sustained even after discontinuing dupilumab therapy in adult patients with AD, similar to the sustained decreases in serum sIgE levels and long-term clinical improvements observed in subjects with allergic rhinitis and/or asthma during and after AIT. Either these results may extend the potential benefit of dupilumab, not only from severe AD to other coexisting atopic conditions but also in the

so-called atopic march, it is an issue that certainly deserves further research.

Data availability statement

The raw data supporting the conclusions of this article will be made available by the authors, without undue reservation.

Ethics statement

The studies involving human participants were reviewed and approved by Institutional Ethics Committee of CEIC Hospital Universitario de Canarias, Tenerife, Spain with the reference number P.I.-2017/72 on October 30, 2017. The Ethics Committee waived the requirement of written informed consent for participation.

Author contributions

RG-P and PP-G: conceptualization, data curation, writing—original draft preparation, and funding acquisition. RG-P, PP-G, and EM-L: methodology. PP-G: software. PP-G and IS-M: validation and formal analysis. IS-M, RG-P, PP-G, and EM-L: investigation and writing—review and editing. IS-M: resources. RG-P, PP-G, and IS-M: project administration. All authors have read and agreed to the published version of the manuscript.

Funding

This research was funded by Fundación Canaria Instituto de Investigación Sanitaria de Canarias (FIISC), Servicio Canario de Salud, grant number OA17/042.

Conflict of interest

The authors declare that the research was conducted in the absence of any commercial or financial relationships that could be construed as a potential conflict of interest.

Publisher's note

All claims expressed in this article are solely those of the authors and do not necessarily represent those of their affiliated organizations, or those of the publisher, the editors and the reviewers. Any product that may be evaluated in this article, or claim that may be made by its manufacturer, is not guaranteed or endorsed by the publisher.

References

- Bakker DS, van der Wal MM, Heeb LEM, Giovannone B, Asamoah M, Delemarre EM, et al. Early and long-term effects of dupilumab treatment on circulating T-cell functions in patients with moderate-to-severe atopic dermatitis. *J Invest Dermatol*. (2021) 141:1943–53.e13. doi: 10.1016/j.jid.2021.01.022
- Czarnowicki T, He H, Krueger JG, Guttman-Yassky E. Atopic dermatitis endotypes and implications for targeted therapeutics. *J Allergy Clin Immunol*. (2019) 143:1–11. doi: 10.1016/j.jaci.2018.10.032
- Tamagawa-Mineoka R, Katoh N. Atopic dermatitis: identification and management of complicating factors. *Int J Mol Sci*. (2020) 21:2671. doi: 10.3390/ijms21082671
- González-Pérez R, Poza-Guedes P, Pineda F, Castillo M, Sánchez-Machín I. House dust mite precision allergy molecular diagnosis (PAMD®) in the Th2-prone atopic dermatitis endotype. *Life*. (2021) 11:1418. doi: 10.3390/life11121418
- Valenta R, Lidholm J, Niederberger V, Hayek B, Kraft D, Grönlund H. The recombinant allergen-based concept of component-resolved diagnostics and immunotherapy (CRD and CRIT). *Clin Exp Allergy*. (1999) 29:896–904.
- Hamilton JD, Suarez-Fariñas M, Dhingra N, Cardinale I, Li X, Kostic A, et al. Dupilumab improves the molecular signature in skin of patients with moderate-to-severe atopic dermatitis. *J Allergy Clin Immunol*. (2014) 134:1293e300. doi: 10.1016/j.jaci.2014.10.013
- Sastre J, Dávila I. Dupilumab: a new paradigm for the treatment of allergic diseases. *J Invest Allergol Clin Immunol*. (2018) 28:139–50. doi: 10.18176/jiaci.0254
- Guttman-Yassky E, Bissonnette R, Ungar B, Suárez-Fariñas M, Ardeleanu M, Esaki H, et al. Dupilumab progressively improves systemic and cutaneous abnormalities in patients with atopic dermatitis. *J Allergy Clin Immunol*. (2019) 143:155–72. doi: 10.1016/j.jaci.2018.08.022
- Simpson E, Cork M, Arkwright P, Deleuran M, Chen Z, Rodriguez Marco A, et al. Dupilumab decreases total and allergen-specific IgE in adolescents with moderate-to-severe atopic dermatitis. *Ann Allergy Asthma Immunol*. (2021) 127 (Suppl. 5):S54–5. doi: 10.1016/j.anai.2021.08.164
- Sanchez-Covisa A, Rodriguez-Rodriguez JA, De la Torre F, Garcia-Robaina JC. Mite fauna of house dust of the island of Tenerife. *Acarologica*. (1999) 1:55–8.
- González-Pérez R, Pineda F, Poza-Guedes P, Castillo M, Matheu V, Sánchez-Machín I. Molecular allergen profiling of dual mite sensitization in severe allergic rhinitis. *J Invest Allergol Clin Immunol*. (2020) 30:421–29. doi: 10.18176/jiaci.0439
- Saeki H, Nakahara T, Tanaka A, Kabashima K, Sugaya M, Murota H, et al. Clinical practice guidelines for the management of atopic dermatitis. *J Dermatol*. (2016) 43:1117–45. doi: 10.1111/1346-8138.13392
- Heinzerling L, Mari A, Bergmann K-C, Bresciani M, Burbach G, Darsow U, et al. The skin prick test—European standards. *Clin Transl Allergy*. (2013) 3:3. doi: 10.1186/2045-7022-3-3
- Bojcukova, J.; Vlas, T.; Forstenlechner, P.; Panzner, P. Comparison of two multiplex arrays in the diagnostics of allergy. *Clin Transl Allergy*. (2019) 9:31. doi: 10.1186/s13601-019-0270-y
- Wollenberg A, Christen-Zäch S, Taieb A, Paul C, Thyssen JB, de Bruin-Weller M, et al. European task force on atopic dermatitis/EADV Eczema Task Force. ETFAD/EADV Eczema task force 2020 position paper on diagnosis and treatment of atopic dermatitis in adults and children. *J Eur Acad Dermatol Venereol*. (2020) 34:2717–44. doi: 10.1111/jdv.16892
- Thijs JL, Strickland I, Bruijnzeel-Koomen CA, Nierkens S, Giovannone B, Csomor E, et al. Moving toward endotypes in atopic dermatitis: identification of patient clusters based on serum biomarker analysis. *J Allergy Clin Immunol*. (2017) 140:730–7. doi: 10.1016/j.jaci.2017.03.023
- Czarnowicki T, Gonzalez J, Shemer A, Malajian D, Xu H, Zheng X, et al. Severe atopic dermatitis is characterized by selective expansion of circulating TH2/TC2 and TH22/TC22, but not TH17/TC17, cells within the skin-homing T-cell population. *J Allergy Clin Immunol*. (2015) 136:104–15.e7. doi: 10.1016/j.jaci.2015.01.020
- Wollmann E, Lupinek C, Kundi M, Selb R, Niederberger V, Valenta R. Reduction in allergen-specific IgE binding as measured by microarray: a possible surrogate marker for effects of specific immunotherapy. *J Allergy Clin Immunol*. (2015) 136:806–9.e7. doi: 10.1016/j.jaci.2015.02.034
- Mikus M, Zandian A, Sjöberg R, Hamsten C, Forsström B, Andersson M, et al. Allergome-wide peptide microarrays enable epitope deconvolution in allergen-specific immunotherapy. *J Allergy Clin Immunol*. (2021) 147:1077–86. doi: 10.1016/j.jaci.2020.08.002
- Feng M, Su Q, Lai X, Xian M, Shi X, Wurtzen PA, et al. Functional and immunoreactive levels of IgG4 correlate with clinical responses during the maintenance phase of house dust mite immunotherapy. *J Immunol*. (2018) 200:3897–904. doi: 10.4049/jimmunol.1701690
- Beck LA, Thaci D, Hamilton JD, Graham NM, Bieber T, Rocklin, et al. Dupilumab treatment in adults with moderate-to-severe atopic dermatitis. *N Engl J Med*. (2014) 371:130–9. doi: 10.1056/NEJMoa1314768
- Jeong KY, Lee JY, Son M, Yi MH, Yong TS, Shin JU, et al. Profiles of IgE sensitization to Der f 1, Der f 2, Der f 6, Der f 8, Der f 10, and Der f 20 in Korean house dust mite allergy patients. *Allergy Asthma Immunol Res*. (2015) 7:483–8. doi: 10.4168/aaair.2015.7.5.483
- Mittermann I, Wikberg G, Johansson C, Lupinek C, Lundeberg L, Cramer R, et al. IgE sensitization profiles differ between adult patients with severe and moderate atopic dermatitis. *PLoS ONE*. (2016) 11:e0156077. doi: 10.1371/journal.pone.0156077
- Aranda CJ, Curotto de Lafaille MA. The secret life of IgE-producing cells. *Immunity*. (2019) 50:285–7. doi: 10.1016/j.immuni.2019.01.018
- Croote D, Darmanis S, Nadeau KC, Quake SR. High-affinity allergen-specific human antibodies cloned from single IgE B cell transcriptomes. *Science*. (2018) 362:1306–9. doi: 10.1126/science.aau2599
- Varga EM, Francis JN, Zach MS, Klunker S, Aberer W, Durham SR. Time course of serum inhibitory activity for facilitated allergen-IgE binding during bee venom immunotherapy in children. *Clin Exp Allergy*. (2009) 39:1353–7. doi: 10.1111/j.1365-2222.2009.03303.x
- Till SJ, Francis JN, Nouri-Aria K, Durham SR. Mechanisms of immunotherapy. *J Allergy Clin Immunol*. (2004) 113:1025–34. doi: 10.1016/j.jaci.2004.03.024
- Dreborg S, Lee TH, Kay AB, Durham SR. Immunotherapy is allergen-specific: a double-blind trial of mite or timothy extract in mite and grass dual-allergic patients. *Int Arch Allergy Immunol*. (2012) 158:63–70. doi: 10.1159/000330649
- Zielen S, Lieb A, De La Motte S, Wagner F, de Monchy J, Fuhr R, et al. Omalizumab protects against allergen-induced bronchoconstriction in allergic (immunoglobulin E-mediated) asthma. *Int Arch Allergy Immunol*. (2013) 160:102–10. doi: 10.1159/000339243
- Nikolov G, Todordova Y, Emilova R, Hristova D, Nikolova M, Petrunov B. Allergen-specific IgE and IgG4 as biomarkers for immunologic changes during subcutaneous allergen immunotherapy. *Antibodies*. (2021) 10:49. doi: 10.3390/antib10040049
- Cox L, Calderon MA. Allergen immunotherapy for atopic dermatitis: is there room for debate? *J Allergy Clin Immunol Pract*. (2016) 4:435–44. doi: 10.1016/j.jaip.2015.12.018
- Makris MP, Papadavid E, Zuberbier T. The use of biologicals in cutaneous allergies—present and future. *Curr Opin Allergy Clin Immunol*. (2014) 14:409–16. doi: 10.1097/ACI.0000000000000096
- Resch Y, Blatt K, Malkus U, Fercher C, Swoboda I, Focke-Tejkl M, et al. Molecular, structural and immunological characterization of Der p 18, a chitinase-like house dust mite allergen. *PLoS ONE*. (2016) 11:e0160641. doi: 10.1371/journal.pone.0160641
- Park KH, Lee J-H, Lee SC, Sim DW, Shin JU, Park CO, et al. Sensitization to various minor house dust mite allergens is greater in patients with atopic dermatitis than in those with respiratory allergic disease. *Clin Exp Allergy*. (2018) 48:1050–8. doi: 10.1111/cea.13164
- Simpson EL, Paller AS, Siegfried EC, Boguniewicz M, Sher L, Gooderham MJ, et al. Efficacy and safety of dupilumab in adolescents with uncontrolled moderate to severe atopic dermatitis: a phase 3 randomized clinical trial. *JAMA Dermatol*. (2020) 156:44–56. doi: 10.1001/jamadermatol.2019.3336
- Lee Y, Kim ME, Nahm DH. Real clinical practice data of monthly dupilumab therapy in adult patients with moderate-to-severe atopic dermatitis: clinical efficacy and predictive markers for a favorable clinical response. *Allergy Asthma Immunol Res*. (2021) 13:733–45. doi: 10.4168/aaair.2021.13.5.733
- Shamji MH, Durham SR. Mechanisms of allergen immunotherapy for inhaled allergens and predictive biomarkers. *J Allergy Clin Immunol*. (2017) 140:1485–98. doi: 10.1016/j.jaci.2017.10.010
- Bangert C, Rindler K, Krausgruber T, Alkon N, Thaler FM, Kurz H, et al. Persistence of mature dendritic cells, T_H2A, and Tc2 cells characterizes clinically resolved atopic dermatitis under IL-4Rα blockade. *Sci Immunol*. (2021) 6:eabe2749. doi: 10.1126/sciimmunol.abe2749



OPEN ACCESS

EDITED BY
Claudio Conforti,
University of Trieste, Italy

REVIEWED BY
Francesco Lacarrubba,
University of Catania, Italy
Andrea De Berardinis,
University of L'Aquila, Italy
Paola Pasquali,
Pius Hospital de Valls, Spain

*CORRESPONDENCE
Pietro Quaglinò
pietro.quaglinò@unito.it

†These authors share senior authorship

SPECIALTY SECTION
This article was submitted to
Dermatology,
a section of the journal
Frontiers in Medicine

RECEIVED 28 May 2022
ACCEPTED 20 July 2022
PUBLISHED 12 August 2022

CITATION
Di Canio M, Burzi L, Ribero S, Amenta F
and Quaglinò P (2022) Role of
tele dermatology in the management
of dermatological diseases among
marine workers: A cross-sectional
study comparing general practitioners
and dermatological diagnoses.
Front. Med. 9:955311.
doi: 10.3389/fmed.2022.955311

COPYRIGHT
© 2022 Di Canio, Burzi, Ribero,
Amenta and Quaglinò. This is an
open-access article distributed under
the terms of the [Creative Commons
Attribution License \(CC BY\)](#). The use,
distribution or reproduction in other
forums is permitted, provided the
original author(s) and the copyright
owner(s) are credited and that the
original publication in this journal is
cited, in accordance with accepted
academic practice. No use, distribution
or reproduction is permitted which
does not comply with these terms.

Role of tele dermatology in the management of dermatological diseases among marine workers: A cross-sectional study comparing general practitioners and dermatological diagnoses

Marzio Di Canio¹, Lorenza Burzi², Simone Ribero²,
Francesco Amenta^{1,3†} and Pietro Quaglinò^{2*†}

¹Research Department, International Radio Medical Centre (C.I.R.M.), Rome, Italy, ²Department of Medical Sciences, Dermatology Clinic, University of Turin, Turin, Italy, ³Telemedicine and Telepharmacy Centre, University of Camerino, Camerino, Italy

Background: Diagnosis and treatment of skin disease in sea workers is an unmet need. The purpose of this study is to highlight how remote management of dermatological conditions appears inadequate in this scenario.

Objective: This study aimed to identify the best epidemiology for seafarers' diseases and analyze the adequacy of medical assistance in the diagnosis of dermatological maritime diseases.

Material and methods: A total of 420 cases of requests for dermatological diseases received by the Telemedical Maritime Assistance Service of the International Medical Radio Center (C.I.R.M.) in a referral year were included in this cross-sectional study. All pictures of cutaneous lesions had been submitted to both C.I.R.M. doctors and an expert dermatologist who provided their diagnosis.

Results: The most frequent diagnosis in both groups was infectious or inflammatory skin diseases. The main differences are represented by the amount of "unclassified dermatitis" or descriptive diagnosis, such as "cutaneous eruption" which were the most frequent diagnosis of C.I.R.M. doctors ($p < 0.05$ and $p > 0.0001$). In these cases, Cohen's K was < 0.5 consistent with low concordance between dermatologic diagnosis and C.I.R.M. diagnosis.

Conclusion and relevance: Our study emphasizes the magnitude of dermatological diseases in the maritime sector, although often underestimated, and highlights the difficulty in their diagnosis for doctors on call that need more training on specific dermatological issues.

KEYWORDS

maritime dermatology, tele dermatology, seaway, occupational disease, diagnosis

Introduction

Dermatological diseases represent a primary cause of morbidity among fishermen and seafarers on board merchant ships (1, 2). Marine workers are exposed to conditions such as humidity, seawater contact, and chemicals, which are known risk factors for the development of hyperkeratosis, contact dermatitis, and injuries (3). Furthermore, UV exposure is 20% higher than that of land-based workers (4), increasing the risk of skin cancers (5). The most frequent professional skin diseases are contact dermatitis (6), mechanical injuries, infections, and stings from marine animals (3). However, the coverage of this topic in literature is limited with only a few small collections reported, mainly with small patient numbers and without dermatological evaluation (3, 7, 8).

The objective of this study is to identify the most frequent dermatological diseases encountered onboard, the epidemiology of sea workers affected, and the possible role and implications of teledermatology in dermatological diagnosis among marine workers.

Materials and methods

Dermatological diseases for which medical assistance was requested from the International Medical Radio Center (C.I.R.M.) in the years 2013–2017 were collected from the C.I.R.M. database and dermatological cases were identified. Cases from 1 January to 31 December 2017 were extracted and analyzed. They accounted for 5,095 assistance requests among which 512 were dermatological consultations. Photographic images or symptoms description were not available in 92 cases, which were excluded. C.I.R.M. Telemedicine platform accepts images with a resolution of at least $1,024 \times 768$ pixels, consistent with the American Telemedicine Association (ATA) guidelines; images with the lowest resolutions are automatically rejected. A total of 420 cases were included in the study; each patient received a diagnosis by a C.I.R.M. doctor who is not a dermatologist and one by an expert dermatologist (PQ) after pictures and case description had been sent to him through an email-telemedicine system.

The Pearson X² test with Yates correction was performed to compare the frequency of diagnoses between the two groups. Cohen's kappa coefficient (κ) was used to measure the inter-rater reliability. Statistical analysis was conducted by using STATA 16 software.

Results

Between 2013 and 2017, the C.I.R.M. has assisted a mean of $4,363.4 \pm 611.5$ patients per year. Each year, the number of patients treated increases on average by 9.77%, while requests for medical care of dermatological interest increase on average

by +17.99% every year. Dermatological consultations were on average 403.6 ± 108.1 per year, representing 10% of total cases.

The median age of patients with dermatological manifestations was 37 ± 10 years, the majority were part of the deck (35.4%) or engine crew (19.7%) and came from India or the Philippines.

Based on the diagnosis of the dermatologist, the most common diseases encountered on board were psoriasis (4.1%), herpes virus (3.52%), entomodermatosis (3.13%), pityriasis rosea (2.73%), cysts (2.40%), tinea (2.34%), pyodermitis (2.15%), and folliculitis (2.15%); while according to C.I.R.M. doctors, the most common were dermatitis (36.91%), mycosis (5.27%), skin infections (3.13%), and pimples (3.32%). The highest level of concordance between dermatologists and C.I.R.M. doctors concerned the diagnosis of abscesses (11.33 and 7.81%, respectively, κ 0.79), whitlows (5.66 and 3.52%, respectively, κ 0.79), and eczema (3.52 and 8.4% cases, respectively, κ 0.52).

Table 1 summarizes the diagnoses made by C.I.R.M. doctors and dermatologists. The most relevant differences are represented by the amount of “unclassified dermatitis” which was the most frequent diagnosis of C.I.R.M. doctors (36.91%), while rarely made by the dermatologist (only 3 cases) (chi-square: 151.08 $p < 0.05$). Similarly, C.I.R.M. doctors reported a descriptive diagnosis (“dermatitis/cutaneous eruption,” “erythema” or “wound”) in 197 cases while this happened in only 10 cases by the dermatologist (chi-square: 2,209.48, $p > 0.0001$).

The dermatologist made a significantly more frequent diagnosis of psoriasis, perionyxis, entomodermatosis, granulomas, angiomas, lichen planus, and tinea. No significant differences between C.I.R.M. and dermatologist diagnoses were found for other diagnoses (warts, whitlows, urticaria, abscess, herpes virus, and alopecia areata).

Cohen's Kappa test showed a moderate/high level of concordance ($0.6 < K\text{-coefficient} < 1$) between C.I.R.M. doctors and dermatologists regarding the diagnosis resulted in not statistically significant at previous tests and low/null level of concordance ($K\text{-coefficient} < 0.5$) for those statistically significant.

Discussion

Dermatological diseases represent common frequent pathologies aboard ships. According to the C.I.R.M. database, requests for dermatological medical assistance increased from 2.45% of total requests in 1994 to 8.3% in the years 2012–2014 (1), up to 10% in this report. In fact, in the last 5 years, requests for C.I.R.M. dermatological assistance have increased by 17.99% every year, against the average increase of 9.77% for medical assistance in general.

This case series of 420 cases represent, as far as we are concerned, the first cohort of sea workers analyzed by

TABLE 1 Comparison between C.I.R.M. doctors' and dermatologist's diagnoses, χ^2 test ($p > 0.05$) and Cohen's K-coefficient (<0.01 : null; $0.01-0.2$ low; $0.21-0.4$ modest; $0.41-0.6$ moderate; $0.61-0.8$ good; $0.81-1$ excellent).

Diagnosis	C.I.R.M. doctor		Dermatologist		chi ² test		Cohen's kappa coefficient (κ)				
	Nr.	%	Nr.	%	chi ²	p-value	Both positive	Dermatologist positive and guard doctor negative	Dermatologist negative and guard doctor positive	Cohen's Kappa (Concordance)*	
Intertrigo	2	0.39%	18	3.52%	13.19*	0.0001	2	16	1	0.180	
Pityriasis	3	0.59%	14	2.73%	11.47*	0.0007	3	11	3	0.286	
Mycosis	27	5.27%	7	1.37%	12.261*	0.0004	7	6	26	0.273	
Unclassified dermatitis/skin eruption/skin rash	189	36.91%	3	0.59%	151.08*	0.0001	3	1	186	0.013	
Wart	4	0.78%	7	1.37%	0.82	0.36	4	3	0	0.724	
Pimple	17	3.32%	5	0.98%	6.72*	0.009	5	10	2	0.442	
Urticaria	9	1.76%	19	3.71%	3.69	0.054	9	0	10	0.632	
Abscess	58	11.33%	40	7.81%	3.74	0.0530	40	0	18	0.793	
Perionyxis	2	0.39%	13	2.54%	8.19*	0.0008	2	11	0	0.261	
Skin infection	16	3.13%	2	0.39%	11.08*	0.0009	2	1	14	0.201	
Pyodermitis	1	0.20%	11	2.15%	8.43*	0.0037	1	10	0	0.163	
Eczema	18	3.52%	43	8.40%	10.89*	0.0010	18	25	4	0.521	
Entomodermatosis	5	0.59%	17	3.13%	6.72*	0.009	5	12	1	0.423	
Granuloma	2	0.39%	10	1.95%	5.40*	0.0202	2	8	0	0.328	
Detritive dermatitis	1	0.20%	8	1.56%	5.49*	0.0191	1	7	1	0.194	
Seborrheic dermatitis	1	0.20%	8	1.56%	5.49*	0.0191	1	7	0	0.219	
Psoriasis	5	0.98%	21	4.10%	10.01*	0.0001	5	16	2	0.341	
Angioma	1	0.20%	8	1.56%	5.49*	0.0191	1	1	7	0.194	
Erysipela	4	0.20%	14	1.56%	5.65*	0.017	4	10	1	0.411	
Lichen planus	1	0.20%	8	1.56%	5.49*	0.0191	1	7	0	0.194	
Actinic Keratosis	1	0.20%	8	1.17%	5.49*	0.0191	1	7	1	0.194	
Whitlow	29	5.66%	18	3.52%	2.70	0.1005	18	9	0	0.789	
Tinea	2	0.39%	12	2.34%	7.24*	0.0071	2	10	0	0.280	
Folliculitis	6	1.17%	11	2.15%	1.5	0.2	6	5	1	0.660	
Alopecia areata	4	0.78%	6	1.17%	0.4	0.5	4	2	0	0.798	
Herpes virus infection	9	1.76%	18	3.52%	3	0.07	9	9	0	0.657	
Cysts	4	0.79%	10	2.40%	2.6	0.1	4	6	0	0.566	

*refers to the concordance (Cohen's Kappa).

comparing the diagnoses made by the doctor on call and an expert dermatologist.

The two main groups of dermatological diseases can be singled out: infectious dermatitis (abscesses 7.81%, herpes virus skin infections 3.52%, pyodermitis 2.15%, whitlows 3.52%, tinea 2.34%, warts 1.37%) and diseases related to environmental and working conditions (folliculitis 2.15%; intertrigo 3.52%, and detritive dermatitis 1.56%). Moreover, cases of eczema (8.4%) and urticaria (3.71%) could be

attributed to contact with allergens or irritants due to working conditions.

A survey (3) involving 1,102 Moroccan fishermen based on legal medical consultation and not on requests for dermatological diseases, showed a high prevalence of palmo-plantar hyperkeratosis (67%), skin infections (59.2%), and entomodermatosis (11.2%). Lucas et al. (8) reported dermatological diseases in 183 sea-workers through a telemedicine service without a dermatological review. Among

them, 68% had infections, 14% had inflammatory diseases, 7% had environmental conditions, and 11% had non-specific rashes. Another study reported data collection through self-completed questionnaires revealing that contact and allergic dermatitis followed by eczema were the most frequent diseases of seafarers' lower limbs (10).

In our series, psoriasis accounted for 4.1% of cases, a quite high figure as the majority of sea-workers came from India and the Philippines, where its prevalence is lower (1.49%) (9). On the other hand, diseases related to UV exposure (1.17% actinic keratosis) were not so common. This could be due to the young age of patients (median 37 years); moreover, effective UV exposure for these people was not available. Oldenburg et al. (7) reported higher percentages with actinic keratosis in 18.3% of patients and skin cancer suspected in 9.3% of patients. However, in this study, all the patients received a full body examination by a dermatologist, and not only through telemedicine, and the patient age was higher (median more than 50 years).

In contrast with the frequency of dermatological manifestations in sea workers and the increase in dermatological medical assistance, our study highlights the difficulty in their diagnosis for doctors on call, not supported by a dermatologist. Indeed, significant differences were found between the diagnoses made by the two doctors. The dermatologist made a disease diagnosis in a significant percentage of patients (97.6%) and thus supporting the cornerstone role of teledermatology in this field; the fact that a dermatologist was able to make a disease diagnosis in the large majority of cases argues in favor of the good quality of clinical pictures sent to the C.I.R.M. On the other hand, the diagnosis of the doctor on call was descriptive in nearly half of the cases (46.9%) and only some pathologies were identified correctly (abscesses, whitlows, warts, urticaria, and herpes virus) probably due to the signs and symptoms easily identifiable. Based on these data, doctors on call should be trained to acquire a more comprehensive knowledge of dermatological diseases or could be assisted by an expert dermatologist.

Data availability statement

The raw data supporting the conclusions of this article will be made available by the authors, without undue reservation.

References

1. Mahdi SS, Amenta F. Eighty years of CIRM. A journey of commitment and dedication in providing maritime medical assistance. *Int Marit Health*. (2016) 67:187–95. doi: 10.5603/IMH.2016.0036
2. Tomaszunas S, Weclawik Z, Lewiński M. Morbidity, injuries and sick absence in fishermen and seafarers—a prospective study. *Bull Inst Marit Trop Med Gdynia*. (1988) 39:125–35.
3. Laraqui O, Manar N, Laraqui S, Ghailan T, Deschamps F, Hammouda R, et al. Prevalence of skin diseases amongst Moroccan fishermen. *Int Marit Health*. (2018) 69:22–7. doi: 10.5603/IMH.2018.0004
4. Caruso G. Do seafarers have sunshine? In: *8th International Symposium on Maritime Health (ISMH) Book of abstracts Rijeka-Croatia* (2005).
5. ICNIRP. ICNIRP statement—Protection of workers against ultraviolet radiation. *Health Phys*. (2010) 99:66–87. doi: 10.1097/HP.0b013e3181d85908

Ethics statement

Ethical review and approval was not required for the study on human participants in accordance with the local legislation and institutional requirements. Written informed consent for participation was not required for this study in accordance with the national legislation and the institutional requirements.

Author contributions

PQ and FA planned the work. MD collected data. LB and SR make specialist diagnoses and statistical analysis. MD, LB, SR, FA, and PQ have discussed data. All authors contributed to the article and approved the submitted version.

Funding

This work was supported by the grant No. 1624/2021 of the ITF Trust, London, United Kingdom and by the grant No. J59J21011210001 of the Italian Ministry of Health - Development of the Epidemiological Observatory of Seafarers Pathologies and Injuries.

Conflict of interest

The authors declare that the research was conducted in the absence of any commercial or financial relationships that could be construed as a potential conflict of interest.

Publisher's note

All claims expressed in this article are solely those of the authors and do not necessarily represent those of their affiliated organizations, or those of the publisher, the editors and the reviewers. Any product that may be evaluated in this article, or claim that may be made by its manufacturer, is not guaranteed or endorsed by the publisher.

6. Clark SC, Zirwas MJ. Management of occupational dermatitis. *Dermatol Clin.* (2009) 27:365–83, vii–viii. doi: 10.1016/j.det.2009.05.002
7. Oldenburg M, Kuechmeister B, Ohnemus U, Baur X, Moll I. Actinic keratosis among seafarers. *Arch Dermatol Res.* (2013) 305:787–96. doi: 10.1007/s00403-013-1384-z
8. Lucas R, Boniface K, Hite M. Skin disorders at sea. *Int Marit Health.* (2010) 61:9–12.
9. Michalek IM, Loring B, John SM. A systematic review of worldwide epidemiology of psoriasis. *J Eur Acad Dermatol Venereol.* (2017) 31:205–12. doi: 10.1111/jdv.13854
10. Rego-Pena V, Bouza-Prego MÁ, Gómez-Muniz F, Veiga-Seijo R. Dermatological diseases in seamen's lower extremity: a prevalence study. *Int Marit Health.* (2021) 72:18–25. doi: 10.5603/IMH.2021.0003



OPEN ACCESS

EDITED BY

Paolo Romita,
University of Bari Aldo Moro, Italy

REVIEWED BY

Artem Vorobyev,
University Medical Center
Schleswig-Holstein, Germany
Gianluca Caliano,
University of Bari Aldo Moro, Italy

*CORRESPONDENCE

Baoqi Yang
baoqiyang@126.com

SPECIALTY SECTION

This article was submitted to
Dermatology,
a section of the journal
Frontiers in Medicine

RECEIVED 01 May 2022

ACCEPTED 06 July 2022

PUBLISHED 20 September 2022

CITATION

Cao S, Cui X, Li J, Pan F, Yan X, Yang Q,
Chen M, Zhou S, Du D, Wang W, Sun Y,
Shi Z, Wu M, Yang B and Zhang F
(2022) Nail changes in pemphigus and
bullous pemphigoid: A single-center
study in China. *Front. Med.* 9:933608.
doi: 10.3389/fmed.2022.933608

COPYRIGHT

© 2022 Cao, Cui, Li, Pan, Yan, Yang,
Chen, Zhou, Du, Wang, Sun, Shi, Wu,
Yang and Zhang. This is an
open-access article distributed under
the terms of the [Creative Commons
Attribution License \(CC BY\)](#). The use,
distribution or reproduction in other
forums is permitted, provided the
original author(s) and the copyright
owner(s) are credited and that the
original publication in this journal is
cited, in accordance with accepted
academic practice. No use, distribution
or reproduction is permitted which
does not comply with these terms.

Nail changes in pemphigus and bullous pemphigoid: A single-center study in China

Shan Cao, Xiaochen Cui, Jianke Li, Futang Pan, Xiaoxiao Yan, Qing Yang, Mingfei Chen, Shengji Zhou, Donghong Du, Weiwei Wang, Yuanhang Sun, Zhongxiang Shi, Mei Wu, Baoqi Yang* and Furen Zhang

Department of Dermatology, Shandong Provincial Hospital for Skin Diseases & Shandong Provincial Institute of Dermatology and Venereology, Shandong First Medical University & Shandong Academy of Medical Sciences, Jinan, China

Common autoimmune bullous diseases (AIBDs) include pemphigus and bullous pemphigoid (BP), which are primarily caused by IgG autoantibodies against the structural proteins of desmosomes at the cell–cell junction and hemidesmosomes at the epidermal–dermal junction. Few studies have assessed nail changes in patients with pemphigus or BP. In the present study, we collected the clinical data of 191 patients with AIBDs (108 patients with pemphigus and 83 patients with BP) and 200 control subjects. Nail changes were observed in 77.0% (147/191), 77.8% (84/108), and 75.9% (63/83) of patients with AIBDs, pemphigus, and BP, respectively, and 14.5% (29/200) of control subjects. Beau's lines and paronychia were the most common nail involvement, observed in 22.5% (43/191) and 22.5% (43/191) of patients with AIBDs, 25.0% (27/108) and 25.9% (28/108) of patients with pemphigus, 19.3% (16/83) and 18.1% (15/83) of patients with BP, respectively. The autoimmune bullous skin disorder intensity score (ABSIS) and the onset time of patients with pemphigus or BP with nail changes were different. Onychomycosis accounted for 21.5% (41/191) of all patients with AIBDs. The ABSIS was correlated with nail involvement in patients with BP ($r = 0.46$, $p < 0.001$), and weakly correlated with nail involvement in patients with AIBDs ($r = 0.37$, $p < 0.001$), pemphigus ($r = 0.29$, $p = 0.009$), and pemphigus vulgaris (PV; $r = 0.35$, $p = 0.008$). No correlation was observed between nail involvement and disease antibody titers. In conclusion, nail changes are frequently observed in patients with pemphigus and BP. The type and onset time of nail changes may indicate the severity of pemphigus and BP, which warrants the attention of dermatologists.

KEYWORDS

autoimmune bullous diseases, pemphigus, bullous pemphigoid, nail, disease severity, antibodies

Introduction

Autoimmune bullous diseases (AIBDs) are a heterogeneous group of diseases characterized by the development of cutaneous and mucosal vesicles, blisters, and erosions. Pemphigus and bullous pemphigoid (BP) represent the two major types of AIBDs caused by circulating autoantibodies against the desmosomal antigens desmoglein (Dsg) 1 and Dsg3 and hemidesmosomal antigens BP180 and BP230, respectively. Pemphigus vulgaris (PV) and pemphigus foliaceus (PF) are the most common forms of pemphigus (1). These dermatoses are characterized by the production of pathogenic autoantibodies that react with desmosomal proteins or hemidesmosomal antigens (2).

Autoimmune bullous diseases may cause nail changes (i.e., Beau's lines and paronychia) when target antigens are expressed in the hyponychium, nail matrix, and proximal nail fold, except for skin and mucosal lesions (3, 4). The incidence of nail involvement in patients with AIBDs is different in different studies (4–6). Previous studies have reported nail involvement in 13.4–47.0% of patients with PV (6, 7) and 71.4% of patients with BP (8). One study suggested that hemorrhagic nail abnormalities might be associated with a poor prognosis in patients with PV (9). The above findings indicate that nail involvement may be a clinical sign correlated with the severity of pemphigus and BP (4, 8–12).

In this study, we aimed to investigate the clinical characteristics of nail changes and their relationships with disease severity in Chinese patients with pemphigus and BP.

Methods

We retrospectively analyzed the clinical nail data of patients diagnosed with pemphigus or BP at Shandong Provincial Hospital for Skin Diseases from January 2019 to December 2020. The diagnosis of pemphigus and BP was made on the basis of clinical manifestations and the results of histological and immunological examinations [i.e., direct immunofluorescence, indirect immunofluorescence, and enzyme-linked immunosorbent assay (ELISA)]. Age- and sex-matched healthy subjects were recruited as control subjects. The study was conducted according to the guidelines of the Declaration of Helsinki, and all patients provided written informed consent. This study was approved by the Ethics Committee of the Shandong Provincial Hospital for Skin Diseases (Approval no. 20181225KYKT024).

Nail characteristics were classified according to each type of nail change (4, 8, 11, 13). Disease severity was evaluated by the autoimmune bullous skin disorder intensity score (ABSIS) and antibody titers. The ABSIS, ranging from 0 to 206, was obtained by scoring the quality of skin lesions, indicating both disease activity and damage (14). The score of nail changes was

calculated based on the type and location of nail changes: one type of nail change = 1 point; one location of nail change = 1 point. The total score is the sum of the scores of nail change types and nail change locations. Spearman's correlation coefficient (r) was used for the correlation analysis. A $p < 0.05$ was considered statistically significant.

Results

A total of 191 patients with AIBDs, including 108 patients with pemphigus and 83 patients with BP, and 200 control subjects were collected in this study. Patients with pemphigus and BP had a mean age of 56.5 ± 9.2 and 64.8 ± 12.2 years, respectively. Patients with pemphigus and BP had a male to female ratio of 1.3:1 and 1.5:1, respectively. Overall, 77.8% (84/108) of patients with pemphigus and 75.9% (63/83) of patients with BP exhibited nail involvement, compared to 14.5% (29/200) of control subjects (Table 1). The duration between disease onset and nail changes varied between 0.5–12.8 and 2.0–6.6 months, respectively. Nail involvement occurred in 77.0% (147/191) of patients with AIBDs (Figure 1). Among them, 96.6% (142/147) had nail changes after the onset of skin or mucosal lesions.

Beau's lines [22.5% (43/192)] and paronychia [22.5% (43/192)] were the most common types of nail changes in patients with AIBDs, followed by onycholysis [21.5% (41/191)]. Beau's lines, paronychia, and onychomycosis were observed in 0, 0, and 7.0% (14/200) of control subjects, respectively. Paronychia was the most common nail involvement in patients with pemphigus [25.9% (28/108)]. Onychomycosis was observed in 22.2% (24/108) of patients with pemphigus and 20.5% (17/83) of patients with BP, which was higher than the control group [7.0% (14/200)]. Pterygium was observed in one patient with BP. Muehrcke's lines (transverse leukonychia) were observed in one patient with relapsed PV. However, no nail changes were observed at the first onset of pemphigus. All other types of nail involvement occurred in patients with pemphigus and BP (Table 2). The highest ABSIS was observed in patients with onychomycosis, which accounted for 21.5% (41/191) of all patients with AIBDs. Various types and onset time of nail changes with different ABSIS of patients with pemphigus and BP. Paronychia, Beau's lines, subungual hemorrhage, and onycholysis of the nails usually represent a higher ABSIS.

The score of nail changes, ranging between 0 and 25, showed mild to severe nail changes in patients with pemphigus and BP. One patient with PV had the highest score of nail changes. This patient's fingernails and toenails showed different degrees of nail changes with Beau's lines, paronychia, onycholysis, subungual hemorrhage, and onychorrhexis.

Nail changes were correlated with the ABSIS in patients with BP ($r = 0.46$, $p < 0.001$). There was a weak correlation between ABSIS and the nail involvement score in patients with AIBDs

TABLE 1 General characteristics of patients with pemphigus or bullous pemphigoid.

Types	Number	Age (Mean±SE)	Male-to-female	Number of patients with nail changes (%)	ABSIS (Mean±SE)
PV	68	54.5 ± 14.0	1.1:1	57 (83.8)	69.9 ± 37.2
PF	40	54.5 ± 12.5	1.4:1	27 (67.5)	66.6 ± 39.3
Pemphigus	108	56.5 ± 9.2	1.3:1	84 (77.8)	67.3 ± 39.1
BP	83	64.8 ± 12.2	1.5:1	63 (75.9)	56.5 ± 24.4
AIBDs	191	65.4±12.4	1.4:1	147 (77.0)	63.0±33.9
Controls	200	52.5 ± 6.2	1.3:1	29 (14.5)	none

ABSIS, autoimmune bullous skin disorder intensity score; PV, pemphigus vulgaris; PF, pemphigus foliaceus; BP, bullous pemphigoid; AIBDs, autoimmune bullous diseases, including pemphigus and BP.



FIGURE 1

Various types of nail involvement in patients with autoimmune bullous disease (AIBDs). (A) Beau's lines, (B) paronychia, (C) onycholysis, (D) onychomycosis, (E) subungual hemorrhage, (F) onychorrhexis, (G) longitudinal ridging, (H) nail discoloration, (I) periungual bullae, (J) nail pitting, (K) pterygium, and (L) Muehrcke's lines (transverse leukonychia).

($r = 0.37$, $p < 0.001$), pemphigus ($r = 0.29$, $p = 0.009$), and PV ($r = 0.35$, $p = 0.008$), and no correlation in patients with PF ($r = 0.14$, $p = 0.48$). There was no significant correlation between nail involvement and anti-DSG1/DSG3 antibody titers in patients with pemphigus ($r = 0.14$, $p = 0.22$; $r = 0.09$, $p = 0.44$, respectively), PV ($r = 0.16$, $p = 0.24$; $r = 0.17$, $p = 0.23$, respectively), or PF ($r = 0.07$, $p = 0.73$; $r = -0.128$, $p = 0.53$, respectively). There was also no significant correlation between nail involvement and anti-BP180/BP230 antibody titers in patients with BP ($r = 0.18$, $p = 0.16$; $r = -0.10$, $p = 0.44$, respectively) (Table 3).

Discussion

Nail changes may be associated with skin lesions as an AIBDs diathesis (5, 8–11, 15, 16). The incidence of nail involvement in patients with PV was 47.0% and 31.6% in two retrospective studies ($n = 64$ and $n = 79$, respectively) (7, 12). A case-control study in India showed a significant association between the severity of AIBDs (29 cases with pemphigus and seven cases with BP) and nail changes ($p = 0.0021$) (8). Recently, a retrospective study of 448 patients with PV and 41 patients with PF found that

finger nail changes were common in PV and were associated with the ABSIS (10). Future studies need to validate these findings, which summarize the clinical characteristics of different types of nails and their relationships with disease severity, especially in patients with BP.

Nail involvement in AIBDs occurs either before or in conjunction with a flare of pre-existing disease, and is rarely a part of the initial presentation (8, 11, 12). It is consistent with our observation that 96.6% (142/147) of nail involvement in patients with AIBDs occurs after the onset of cutaneous or mucosae lesions.

In patients with pemphigus, paronychia was associated with a higher ABSIS than either Beau's lines or onycholysis, consistent with previous findings (10). Patients with paronychia had the second highest ABSIS, either at initial presentation or during disease exacerbation, with the prevalence of pemphigus. AIBD-associated paronychia may be distinguished from other similar clinical presentations of acute or chronic paronychia and bacterial infections (4), which are considered a sign of exacerbation and can be cured by systemic therapy, nor with topical therapy (6, 16–18). The prevalence of Beau's lines or onychomadesis (nail shedding) may be related to the formation of proximal nail fold and nail matrix, which are temporarily

TABLE 2 Clinical characteristics and frequency of nail involvement in patients with pemphigus or bullous pemphigoid.

Nail changes	AIBDs cases (%)	Pemphigus cases (%)	BP cases (%)	Controls (%)	AIBDs ABSIS (Mean±SE)	Onset days (Mean±SE)
Beau's lines	43 (22.5)	27 (24.8)	16 (19.3)	0	68.4 ± 38.6	53.2 ± 54.2
Paronychia	43 (22.5)	28 (25.7)	15 (18.1)	0	73.6 ± 40.1	52.5 ± 68.8
Onycholysis	41 (21.5)	27 (24.8)	14 (16.9)	5 (2.5)	62.6 ± 31.2	57.33 ± 70.71
Onychorrhexis	33 (17.3)	18 (16.5)	15 (18.1)	6 (3.0)	64.7 ± 37.2	78.1 ± 72.4
Subungual hemorrhage	32 (16.8)	23 (21.1)	9 (10.8)	1 (0.5)	71.2 ± 38.6	46.8 ± 49.2
Longitudinal ridging	30 (15.7)	21 (19.3)	9 (10.8)	1 (0.5)	66.0 ± 37.3	65.9 ± 81.1
Nail discoloration	21 (11.0)	9 (8.3)	12 (14.5)	2 (1.0)	57.9 ± 22.4	54.3 ± 36.9
Perungual bullae	11 (5.8)	4 (3.7)	7 (8.4)	0	55.0 ± 27.7	89.9 ± 96.3
Nail pitting	3 (1.6)	1 (0.9)	2 (2.4)	0	55.7 ± 22.8	110.0 ± 113.6
Pterygium	1 (0.5)	0	1 (1.2)	0	32.0	none
Muehrcke's lines	1 (0.5)	1 (0.9)	0	0	66.0	none

ABSIS, autoimmune bullous skin disorder intensity score; PV, pemphigus vulgaris; PF, pemphigus foliaceus; BP, bullous pemphigoid.

TABLE 3 Spearman's correlation coefficient (r) of disease severity with nail changes in patients with pemphigus or bullous pemphigoid.

AIBDs subtype	ABSIS	Anti-Dsg1/BP180 antibody	Anti-Dsg3/BP230 antibody
PV	$r = 0.35, P = 0.008$	$r = 0.16, P = 0.24$	$r = 0.17, P = 0.23$
PF	$r = 0.14, P = 0.48$	$r = 0.07, P = 0.73$	$r = -0.128, P = 0.53$
Pemphigus	$r = 0.29, P < 0.001$	$r = 0.14, P = 0.22$	$r = 0.09, P = 0.44$
BP	$r = 0.46, P < 0.001$	$r = 0.18, P = 0.16$	$r = -0.10, P = 0.44$
AIBDs	$r = 0.37, P < 0.001$	$r = 0.17, P = 0.05$	$r = 0.06, P = 0.46$

AIBDs, autoimmune bullous disease; ABSIS, autoimmune bullous skin disorder intensity score; Dsg, desmoglein; BP, bullous pemphigoid; PV, pemphigus vulgaris; PF, pemphigus foliaceus.

blocked by antigens to reduce the formation of nail board proteins (4, 8). Onychomycosis was observed in 22.2% (24/108) of patients with pemphigus, with an increased prevalence among patients undergoing immunosuppressive therapy. This is consistent with previous studies (4, 7, 18). Patients with pemphigus with nail pitting showed the longest onset than those with other types of nail changes, but had a moderate ABSIS. This data suggest that nail pitting may take a long time to develop and cause a mild damage to the nail. Nail pitting, periungual bullae, and nail discoloration occurred in patients with PV and BP, which was consistent with the findings that patients with PV and BP had a higher ABSIS than those with PF.

Muehrcke's lines (transverse leukonychia) occurred in one patient with PV when he relapsed. However, no nail changes were observed at the first onset. The ABSIS of the patient at relapse was higher than that at the first onset. Muehrcke's lines are usually associated with chronic hypoalbuminemia secondary to other diseases (13). However, our patient did not have hypoalbuminemia. Muehrcke's lines induce edema in the connective tissues in front of the lunula, just below the epidermis of the nail bed, altering the compact arrangement of the collagen in this area to one with a looser texture coinciding with hypoalbuminemia (13). The structure resembled the lunula, indicating a relationship with the severity of PV.

Onychomycosis is found in 20.5% (17/83) of patients with BP, probably because onychomycosis occurs following secondary nail changes, accompanied by paronychia, Beau's lines, onycholysis, onychorrhexis, nail discoloration, longitudinal ridging, subungual hemorrhage, and nail pitting, or as a result of immunosuppressive therapy (4, 7, 19). In our study, most patients with pemphigus or BP were treated with immunosuppressive therapy. Pterygium was found in only one patient with BP, with a relatively low ABSIS score. Fingernail pterygium has been reported in a few patients with cicatricial pemphigoid and paraneoplastic pemphigus (4, 8). Here, one patient developed pterygium when BP relapsed. We assumed that pterygium might be associated with chronic recurrent inflammatory conditions. Patients with subungual hemorrhage had the shortest onset time and higher ABSIS among all pemphigus and BP cases, suggesting that this type of nail change occurs rapidly and represents a more severe condition. Subungual hemorrhage may indicate overall disease severity in most cases of pemphigus and BP. A higher prevalence of onychorrhexis was observed in previous studies (30%) (8) than in our study (17.3%).

Generally occurring or specific nail changes (i.e., paronychia, Beau's lines, subungual hemorrhage, and onycholysis) in patients with pemphigus and BP are caused by the pathology and

not by drug cytotoxicity (11). The proximal nail fold, nail matrix, and hyponychium express all basement membrane zone (BMZ) antigens and components (4, 20). The type of nail changes may indicate the disease severity, onset time, and location of the nail involvement according to the pemphigus or BP antigen damage (4). Nail changes are determined by the location of blistering in the nail apparatus, and may include onychomadesis, paronychia, and pterygium (4).

The limitation of this study is that most of the patients are inpatients with a high level of disease severity and a high ABSIS. Also, we found no significant correlation between the different types of nail changes and pemphigus/BP antibody titers. These findings will be validated by future studies with a larger sample size.

In conclusion, the different types and onset times of nail changes represent different severities of pemphigus and BP. Paronychia, Beau's lines, subungual hemorrhage, and onycholysis are associated with a higher ABSIS score, which warrants the attention of dermatologists. The mechanisms of nail changes in pemphigus and BP require further investigation.

Data availability statement

The raw data supporting the conclusions of this article will be made available by the authors, without undue reservation.

Ethics statement

The studies involving human participants were reviewed and approved by Ethics Committee of the Shandong Provincial Hospital for Skin Diseases. Written informed consent to participate in this study was provided by the participants' legal

guardian/next of kin. Written informed consent was obtained from the individual(s) for the publication of any potentially identifiable images or data included in this article.

Author contributions

SC and BY contributed to the conception, design of the study, wrote the manuscript, analyzed, and interpreted the data set. SC, XC, JL, FP, XY, QY, MC, SZ, DD, WW, YS, ZS, MW, BY, and FZ organized the database. All authors contributed to manuscript revision, read, and approved the submitted version.

Acknowledgments

The signed consent form had been securely stored in the patient's case notes and the material was supported by Shandong Provincial Hospital for Skin Diseases.

Conflict of interest

The authors declare that the research was conducted in the absence of any commercial or financial relationships that could be construed as a potential conflict of interest.

Publisher's note

All claims expressed in this article are solely those of the authors and do not necessarily represent those of their affiliated organizations, or those of the publisher, the editors and the reviewers. Any product that may be evaluated in this article, or claim that may be made by its manufacturer, is not guaranteed or endorsed by the publisher.

References

1. Kershenovich R, Hodak E, Mimouni D. Diagnosis and classification of pemphigus and bullous pemphigoid. *Autoimmun Rev.* (2014) 13:477–81. doi: 10.1016/j.autrev.2014.01.011
2. Takahashi H, Iriki H, Mukai M, Kamata A, Nomura H, Yamagami J, et al. Autoimmunity and immunological tolerance in autoimmune bullous diseases. *Int Immunol.* (2019) 31:431–7. doi: 10.1093/intimm/dxz030
3. Schmidt E, Kasperkiewicz M, Joly P. Pemphigus. *Lancet.* (2019) 394:882–94. doi: 10.1016/S0140-6736(19)31778-7
4. Tosti A, André M, Murrell DF. Nail involvement in autoimmune bullous disorders. *Dermatol Clin.* (2011) 29:511–3. doi: 10.1016/j.det.2011.03.006
5. Wang H, Wang X, Yang B, Hong L, Zhang F. Image Gallery: onychomycosis in linear IgA bullous dermatosis. *Br J Dermatol.* (2020) 182:160. doi: 10.1111/bjd.18744
6. Pietkiewicz P, Bowszyc-Dmochowska M, Gornowicz-Porowska J, Dmochowski M. Involvement of nail apparatus in pemphigus vulgaris in ethnic poles is infrequent. *Front Med (Lausanne).* (2018) 5:227. doi: 10.3389/fmed.2018.00227
7. Schlesinger N, Katz M, Ingber A. Nail involvement in pemphigus vulgaris. *Br J Dermatol.* (2002) 146:836–9. doi: 10.1046/j.1365-2133.2002.04696.x
8. Gopal V, Shenoy MM, Bejai V, Nargis T. Nail changes in autoimmune blistering disorders: A case-control study. *Indian J Dermatol Venereol Leprol.* (2018) 84:373. doi: 10.4103/ijdv.IJDVL_19_17
9. Reich A, Wiśnicka B, Szepietowski JC. Haemorrhagic nails in pemphigus vulgaris. *Acta Derm Venereol.* (2008) 88:542. doi: 10.2340/00015555-0475
10. De D, Kumar S, Handa S, Mahajan R. Fingernail involvement in pemphigus and its correlation with disease severity and other clinicodemographic parameters. *Br J Dermatol.* (2019) 180:662–3. doi: 10.1111/bjd.17136
11. Baghdad B, Chiheb S. Nail Involvement during Pemphigus. *Skin Appendage Disord.* (2019) 5:362–5. doi: 10.1159/000501228
12. Habibi M, Mortazavi H, Shadianloo S, Balighi K, Ghodsi SZ, Daneshpazhooh M, et al. Nail changes in pemphigus vulgaris. *Int J Dermatol.* (2008) 47:1141–4. doi: 10.1111/j.1365-4632.2008.03796.x

13. Kozaru T, Fukumoto T, Shirai T, Takasawa N, Kameoka JI, Oka M. Muehrcke lines on fingers and toenails. *Eur J Dermatol.* (2019) 29:87–8. doi: 10.1684/ejd.2018.3439
14. Daniel BS, Hertl M, Werth VP, Eming R, Murrell DF. Severity score indexes for blistering diseases. *Clin Dermatol.* (2012) 30:108–13. doi: 10.1016/j.clindermatol.2011.03.017
15. Barth JH, Wojnarowska F, Millard PR, Dawber RP. Immunofluorescence of the nail bed in pemphigoid. *Am J Dermatopathol.* (1987) 9:349–50. doi: 10.1097/00000372-198708000-00010
16. Tomita M, Tanei R, Hamada Y, Fujimura T, Katsuoka K. A case of localized pemphigoid with loss of toenails. *Dermatology.* (2002) 204:155. doi: 10.1159/000051839
17. Kolivras A, Gheeraert P, André J. Nail destruction in pemphigus vulgaris. *Dermatology.* (2003) 206:351–2. doi: 10.1159/000069955
18. Serratos BD, Rashid RM. Nail disease in pemphigus vulgaris. *Dermatol Online J.* (2009) 15:2. doi: 10.5070/D34X05D6VH
19. Engineer L, Norton LA, Ahmed R. Nail involvement in pemphigus vulgaris. *J Am Acad Dermatol.* (2000) 43:529–35. doi: 10.1067/mjd.2000.106236
20. Sinclair RD, Wojnarowska F, Leigh IM, Dawber RP. The basement membrane zone of the nail. *Br J Dermatol.* (1994) 131:499–505. doi: 10.1111/j.1365-2133.1994.tb08550.x



OPEN ACCESS

EDITED BY
Giusto Trevisan,
University of Trieste, Italy

REVIEWED BY
Gianluca Avallone,
University of Turin, Italy
Antonio Caldarìa,
University of Ferrara, Italy

*CORRESPONDENCE
Irene Fusco
i.fusco@deka.it

SPECIALTY SECTION
This article was submitted to
Dermatology,
a section of the journal
Frontiers in Medicine

RECEIVED 03 August 2022
ACCEPTED 29 August 2022
PUBLISHED 18 October 2022

CITATION
Magni G, Piccolo D, Bonan P,
Conforti C, Crisman G, Pieri L, Fusco I
and Rossi F (2022) 1540-nm fractional
laser treatment modulates
proliferation and neocollagenesis in
cultured human dermal fibroblasts.
Front. Med. 9:1010878.
doi: 10.3389/fmed.2022.1010878

COPYRIGHT
© 2022 Magni, Piccolo, Bonan,
Conforti, Crisman, Pieri, Fusco and
Rossi. This is an open-access article
distributed under the terms of the
[Creative Commons Attribution License
\(CC BY\)](https://creativecommons.org/licenses/by/4.0/). The use, distribution or
reproduction in other forums is
permitted, provided the original
author(s) and the copyright owner(s)
are credited and that the original
publication in this journal is cited, in
accordance with accepted academic
practice. No use, distribution or
reproduction is permitted which does
not comply with these terms.

1540-nm fractional laser treatment modulates proliferation and neocollagenesis in cultured human dermal fibroblasts

Giada Magni¹, Domenico Piccolo², Paolo Bonan³,
Claudio Conforti⁴, Giuliana Crisman², Laura Pieri⁵,
Irene Fusco ^{5*} and Francesca Rossi¹

¹Istituto di Fisica Applicata "Nello Carrara", Consiglio Nazionale delle Ricerche (IFAC-CNR), Florence, Italy, ²Skin Centers, Avezzano, Italy, ³Laser Cutaneous Cosmetic and Plastic Surgery Unit, Villa Donatello Clinic, Florence, Italy, ⁴Department of Dermatology and Venereology, Dermatology Clinic, Maggiore Hospital, University of Trieste, Trieste, Italy, ⁵El.En Group, Calenzano, Italy

KEYWORDS

carbon dioxide laser, skin rejuvenation, collagen synthesis, human dermal fibroblasts, confocal microscopy

Introduction

Aging and sunlight exposure induce different changes in facial skin. Furthermore, collagen synthesis and the dermal lifespan of fibroblasts are reduced. As a result, an overall reduction of collagen and elastic fibers in the dermis leads to deep wrinkles, skin laxity, and post-inflammatory hyperpigmentation (PHI), characteristics typical of photoaged skin (1, 2). To date, several types of lasers for skin aging are marketed.

Manstein (3) was the first to introduce the concept of fractional photothermolysis or fractional resurfacing Carbon Dioxide (CO₂) laser. This new approach is based on the generation of microscopic columns of thermal damage (both in ablation and in coagulation) at the interface between epidermis and dermis, which stimulate a wound healing response (4, 5) and collagen synthesis (6, 7). Furthermore, *in vivo* experiments conducted by Cohen (8) showed that fractional treatments with 1,540 nm affect coagulation, collagen production, and dermal remodeling, leading to skin rejuvenation and benefits in acne scars and stretch marks.

It has also been observed that a solution of near-infrared (NIR) sources in which coagulation is not sought is a 1540 nm fractional erbium-glass laser system, which has many advantages over other lasers, including regulation of penetration depth (2–3 mm) (9). However, these conditions cannot induce tissue alterations but only reversible action, which has significant biological effects on biostimulation: it causes an increment in blood flow, cytokines, and growth factor changes. Generally speaking, changes in growth factors and cytokines might be essential in the pathogenesis of the 1540 nm fractional erbium-glass laser-induced wound healing, hair regrowth and cellular

metabolism (10). Fractional ablative lasers have a higher safety profile than traditional ones (5). However, only the fractional ablative CO₂ laser requires higher energies to reach different reticular depths, which could induce hyperpigmentation and energy-related prolonged bleeding. In addition, these post-treatment reactions should be associated with acute inflammatory responses to skin heat damage leading to increased side effects, such as persistent erythema, skin changes, PHI, scarring, and prolonged healing time (11, 12). On the other hand, the lower absorption coefficient of 1540 and 1550 nm devices results in a greater maximum depth of 1400 μm (13).

This different mode of delivering laser energy reduces the post-treatment erythema and recovery times (14). Furthermore, the thermal injury generated by non-ablative laser remains spatially confined to the dermis, while the surrounding skin enables fast recovery of damaged tissue. Complete re-epithelialization is usually observed within 24 to 48 h (5, 15).

Fractional CO₂ laser treatment stimulates a molecular cascade that can lead to wound healing, collagen remodeling and scar regression (10, 16–20). These molecular processes also evoke an increase in type III collagen synthesis (21), and histological analysis clearly shows neocollagenesis, epidermal thickening and an increase in elastic fibers (22).

It is well known that during the aging process, due to photoaging, the skin shows a reduction in type I and type III collagen (23). The synergistic combination of ablative and non-ablative laser sources could improve the effect on the tissue. The simultaneous emission of the CO₂ laser and the bipolar radiofrequency is a viable and possible alternative, which provides epidermal coagulation and tissue remodeling due to the production of new collagen in the dermis. This methodology can modulate the coagulation and ablative effects, affecting healing times compared to typical CO₂ laser stimulation (24, 25), reducing patient downtime and pain, and improving skin rejuvenation results (26, 27).

This dual wavelength system aims to couple the ablative aspect of CO₂ laser and the deep non-ablative and non-coagulative properties to enhance the effects of CO₂ laser while limiting the side effects. For this purpose, the DuoGlide system (DEKA Mela, Florence, Italy) was used in this study. This technology combines the two wavelengths (CO₂ and 1540 nm), but the possibility of excluding the CO₂ allowed us to perform an *in vitro* study of the non-coagulative thermal effect of 1540 nm.

The effect of the 1540 nm wavelength on cultured fibroblast is known to upregulate the expression of collagen-related synthesis genes and, at the same time, to downregulate matrix proteins production (28–30). On these bases, our research aimed to evaluate the photobiomodulation effect of the 1540 nm wavelength treatment on the proliferation of cultured fibroblast and their ability to express type I and III collagen.

Materials and methods

Laser device description

The DuoGlide system (DEKA Mela Srl, Florence, Italy) is a laser with a new design that incorporates a 10.6 μm Carbon Dioxide (CO₂) laser device (60 W) and a 1540 nm laser (10 W), which can be used with the fractional scanning units ($\mu\text{Scan DOT}$). This scanner can deliver one or both wavelengths (1540 nm and 10.6 μm) in a sequential emission mode on the same microthermal zone (DOT) separated by healthy tissue (DOT spacing) DOT; this allows for a tunable balance between ablation and coagulation depths and for delivery of new and more efficient treatments. Furthermore, the second wavelength of 1540 nm conveyed through the new miniaturized scanning systems can achieve homogeneous, continuous and non-coagulative heating of the entire scanning area, reaching further and deeper into the dermis (not gently reachable with the ablative laser alone), thanks to spots of the order of 1000 μm emitted on the same axis as the DOT and thanks to the use of the typical CO₂ spacing parameters ($\sim 500 \mu\text{m}$) used in the literature for dermatological applications (25).

Cell culture

Adult Human Dermal Fibroblast cells (HDFa, Lot# 2207322) were purchased from Thermo Fisher Scientific (Waltham, Massachusetts, USA) and used following the recommendation of the manufacturer. HDFa were cultivated in Dulbecco Modified Eagle Medium (DMEM, PAN-Biotech GmbH, Aidenbach, Germany) added with 10% of Fetal Bovine Serum (FBS), 1% of Glutamine and Streptomycin (PAN-Biotech GmbH, Aidenbach, Germany). Cells were kept under standard culture conditions (37 °C and 5% CO₂) and the DMEM was refreshed every 48 h.

Sample irradiation

To perform a colourimetric assay, HDFa cells were counted using a Neubauer chamber (Karl Hecht Assistant GmbH, Sondheim vor der Rhön, Germany), and 8×10^3 cells were seeded in 96-multiwell plates (Greiner Bio-One Italia, Milan, Italy). Before the experiments, cells were seeded in rows and columns for each multiwell in alternate wells to avoid double or partial irradiation. Next, each sample was maintained for 24 h in standard culture conditions in DMEM without FBS. Then, HDFa cells were subjected to irradiation.

Cytotoxicity and proliferation assay

Cellular viability was evaluated 24 and 48 h after the treatment using the Cell Counting Kit-8 (CCK-8) assay

(Sigma-Aldrich, Milan, Italy). The CCK-8 uses WST-8 reagent, which is bio-reduced by mitochondrial dehydrogenases and becomes WST-8 formazan with an orange color soluble in the tissue culture medium (31, 32). Proliferation was measured by Sulforhodamine B-based assay (SRB, Sigma-Aldrich, Milan, Italy) 24 and 48 h after irradiation. This test is based on the capability of the protein-dye sulforhodamine B to bind electrostatically and pH-dependent on basic amino acid residues on cells. The quantification of the bound dye can serve as an approximation of total cell biomass, thus cell proliferation (33–35). Absorbance at 450 nm and 570 nm for CCK-8 and SRB, respectively (reference wavelength at 630 nm), were read using an automatic microplate absorbance reader equipped with SkanIt software (Multiskan FC Micro-plate Photometer, Thermo Fisher Scientific, Milan, Italy). Each experiment was performed at least in triplicate.

Immunocytochemical staining and fluorescence quantification

HDFa cells were cultivated in 35 mm² dishes suitable for confocal acquisition (Ibidi GmbH, Martinsried, Germany). Cells were left homogeneously adhered to the bottom of the petri dish to avoid bias during the subsequent analysis steps. The immunocytochemical protocol was previously described (36). Briefly, a 3.6% paraformaldehyde solution was used to fix HDFa cells. After two washes in phosphate buffer saline (PBS), cells were permeabilised using Triton-X100 for 10 min at room temperature. The unspecific sites were blocked using 10% goat serum diluted in PBS and 0.1% Tween20 (PBST). Primary antibodies were diluted as follows: anti-type I collagen (1:400) and anti-type III collagen (1:200), both in PBST solution. Secondary antibodies AlexaFluor555 and AlexaFluor647 were diluted at 1:500 in PBST. All the antibodies were purchased from AbCam (Cambridge, UK) and used according to the manufacturer's instructions. Fixed cells were incubated with the secondary antibodies for control experiments to exclude non-specific binding. A mounting medium with DAPI (4',6-diamidino-2-phenylindole, Sigma-Aldrich, Milan, Italy) was used to stain cell nuclei and mount the coverslip. Immunocytochemical images were obtained by SP8 laser scanning confocal microscope (Leica Microsystems, Mannheim, Germany) using a 20x dry objective (NA 0.4). All the photos from treated and control samples were acquired keeping the same microscope parameters (gain, laser intensity, scan area and speed). The collected images obtained were analyzed with open-source software [ImageJ (37)]. Each image was separated into two channels corresponding to the fluorescence signal for a specific type of collagen (type I or type III). The fluorescence intensity analysis was performed over the entire image area (38).

Statistical analysis

The CCK-8 and SRB assay data were expressed as mean±SD. In addition, the Kruskal-Wallis test followed by Dunn's test for multiple comparisons were performed. The data obtained from immunofluorescence analysis were described as mean±SEM. The Mann-Whitney two-tailed test was selected. Statistical significance was set for all the experimental results at * $p < 0.05$. All the data were analyzed using the commercial software GraphPad Prism 8th edition (San Diego, CA, USA).

Results

Evaluation of cytotoxicity and cell proliferation after cell irradiation

Data obtained from the CCK-8 assay showed that all the tested fluences (J/cm²) (2.1, 2.8, 3.5, 4.2) did not affect cellular viability 24 and 48 h after treatment (Figure 1A). On the other hand, the SRB assay demonstrated that the application of 3.5 and 2.8 J/cm² induced a significant increase in cell proliferation compared to the untreated samples. This increase occurred 24 h after the treatment, but was not observed after 48 h (Figure 1B).

Confocal analysis of type I and type III collagen

Firstly, we evaluated the fluorescence intensity of the basal expression of collagen in HDFa cells not subjected to irradiation. Figure 1C shows that type I collagen is significantly higher than type III collagen. In Figure 1D, the application of 3.5 and 2.8 J/cm² induced a significant increase in fluorescence intensity related to type III collagen.

Discussion

The extracellular matrix (ECM) is responsible to the physiological properties of the skin and its architectural organization; the ECM consists of many elements, including collagen fibers. Fibroblasts synthesize collagen so that the skin contains typically from 80 to 85% type I collagen and from 10 to 15% type III collagen. Chronologically aged skin reduces collagen types I and III due to skin photoaging (23). Radiation activates cellular mechanisms which cause clinical manifestations of skin photoaging, such as wrinkles, pigmentation, telangiectasias and neoplasm (39, 40). Nitrous proteins and Cytochrome C oxidase are always considered the main targets of light (41–43). However, recent studies have shown that the cryptochromes and opsins (44, 45)

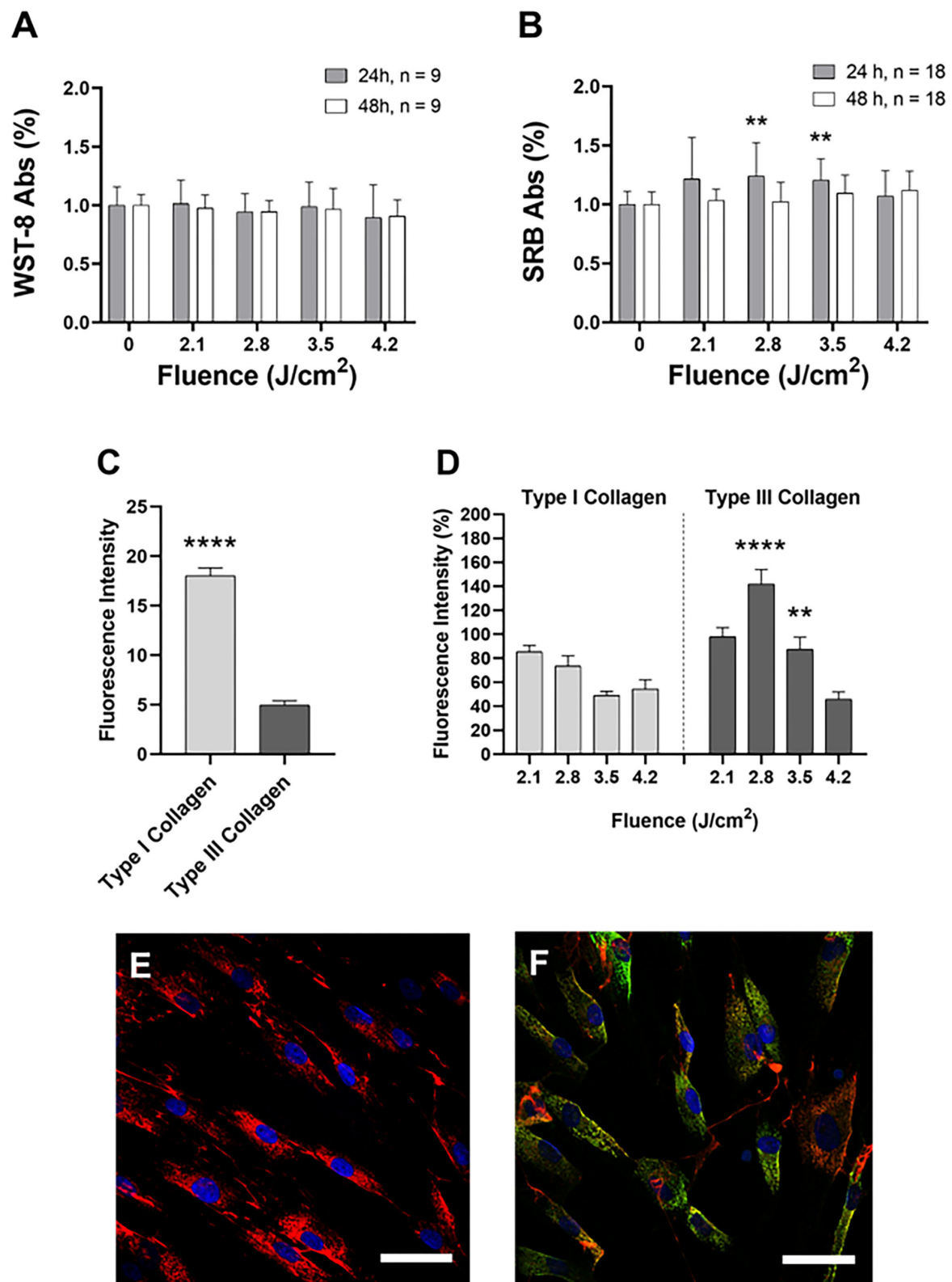


FIGURE 1

Cell viability (A) and proliferation (B) after 24 h (gray) and 48 h (white) after the irradiation. Data are expressed as mean \pm SD, $n = 9$ (A) and $n = 18$ (B). Statistical analysis: $**p < 0.01$ (vs. 0 fluence). The one-way ANOVA, Kruskal-Wallis test followed by Dunn's test of multiple comparisons

(Continued)

FIGURE 1 (Continued)

post-hoc. (C) Fluorescence intensity of type I and type III collagen in untreated cells: collagen was reported in light gray, type III collagen in dark gray. Data are expressed as mean \pm SEM, $n = 20$. Statistical analysis: Mann-Whitney two-tailed test, **** $p < 0.0001$. (D) Fluorescence intensity of type I collagen (light gray) and type III collagen (dark gray) compared at the same applied dose. Data are expressed as mean \pm SD, $n = 20$. Statistical analysis: Mann-Whitney two-tailed test, ** $p < 0.01$; **** $p < 0.0001$ (vs. the same fluence). Example of confocal images of untreated (E) and treated (F) HDFa cells. Type I collagen: red; type III collagen: green; cell nuclei: blue. Representative images were acquired with a 63x oil objective (NA 1.4). Scalebar: 100 μ m.

are responsible for the cellular response to visible and UV light. The hypothesis therefore could be that a photon of light could hit several molecular targets by activating molecular targets such as reactive oxygen species (ROS), adenosine triphosphate (ATP) and ionized channels (44, 46) thus activating multiple signaling cascades. It is already well established that NIR light, as well as the visible spectrum, can induce a versatile and a significant range of changes in the expression pathways of several genes, leading to modifications in cell differentiation and proliferation, as well as collagen synthesis (47–49). Indeed, a positive effect on the induction of type I collagen production with 1,320 nm wavelength was also observed during the wound healing process (50).

The results obtained in this study are in line with the scientific literature concerning the rearrangement of types I and III collagen after laser therapy, suggesting a neocollagenesis activation (51, 52). Indeed, our results revealed a significant increase in type III collagen expression improvement, confirming the laser-induced neocollagenesis effect. Furthermore, our data demonstrate that irradiation with medium fluences of 1540 nm modulates cell proliferation. Concerning this evidence, even if there is no evidence in the literature of the possible effects of the laser in the various phases of the fibroblasts cell cycle, our findings indicate an increase in the cellular activity of the mitochondrial electrical potential following laser treatment.

References

- Farage MA, Miller KW, Elsner P, Maibach HI. Intrinsic and extrinsic factors in skin ageing: a review. *Int J Cosmet.* (2008) 30:87–95. doi: 10.1111/j.1468-2494.2007.00415.x
- Rittié L, Fisher G.J. UV-light-induced signal cascades and skin aging. *Ageing Res Rev.* (2002) 1:705–20. doi: 10.1016/S1568-1637(02)00024-7
- Manstein D, Herron GS, Sink RK, Tanner H, Anderson RR. Fractional photothermolysis: a new concept for cutaneous remodeling using microscopic patterns of thermal injury. *Lasers Surg Med.* (2004) 34:426–38. doi: 10.1002/lsm.20048
- Laubach HJ, Tannous Z, Anderson RR, Manstein D. Skin responses to fractional photothermolysis. *Lasers Surg Med.* (2006) 38:142–9. doi: 10.1002/lsm.20254
- Alexiades-Armenakas MR, Dover JS, Arndt KA. The spectrum of laser skin resurfacing: Nonablative, fractional, and ablative laser resurfacing. *J Am Acad Dermatol.* (2008) 58:719–37. doi: 10.1016/j.jaad.2008.01.003
- Hantash BM, Bedi VP, Kapadia B, Rahman Z, Jiang K, Tanner H, et al. *In vivo* histological evaluation of a novel ablative fractional resurfacing device. *Lasers Surg Med.* (2007) 39, 96–107. doi: 10.1002/lsm.20468
- Anderson RR, Donelan MB, Hivnor C, Greeson E, Ross EV, Shumaker PR, et al. Laser treatment of traumatic scars with an emphasis on ablative fractional laser resurfacing: consensus report. *JAMA Dermatol.* (2014) 150:187–93. doi: 10.1001/jamadermatol.2013.7761
- Solomon-Cohen E, Lapidoth M, Mimouni D, Akerman L, Slodownik D, Hodak E, et al. 1540-nm fractional erbium: glass laser is a safe and effective modality for non-ablative facial rejuvenation. *J Cosmet Dermatol.* (2021) 20:1679–83. doi: 10.1111/jocd.13958
- Modena DAO, Miranda ACG, Grecco C, Liebano RE, Cordeiro RCT, Guidi RM. Efficacy, safety, and guidelines of application of the fractional ablative laser erbium YAG 2940 nm and non-ablative laser erbium glass in rejuvenation, skin spots, and acne in different skin phototypes: a systematic review. *Lasers Med Sci.* (2020) 35:1877–88. doi: 10.1007/s10103-020-03046-7
- Alhattab MK, Al Abdullah MJ, Al-janabi MH, Aljanaby WA, Alwakeel HA. The effect of 1540-nm fractional erbium-glass laser in the treatment of androgenic alopecia. *J Cosmet Dermatol.* (2020) 19:878–83. doi: 10.1111/jocd.13122
- Tarjian AL, Goldberg DJ. Fractional ablative laser skin resurfacing: a review. *J Cosmet Laser Ther.* (2011) 13:262–4. doi: 10.3109/14764172.2011.630083

Author contributions

Conceptualization: FR and LP. Methodology and data curation: GM. Validation: GM, LP, DP, PB, CC, GC, and FR. Formal analysis and writing—original draft preparation: GM and LP. Investigation: GM, LP, and IF. Writing—review and editing: FR and IF. Supervision and funding acquisition: FR. All authors have read and agreed to the published version of the manuscript.

Conflict of interest

LP and IF are employed at El.En. Group.

The remaining authors declare that the research was conducted in the absence of any commercial or financial relationships that could be construed as a potential conflict of interest.

The handling editor GT declared a shared affiliation with the author CC at the time of review.

Publisher's note

All claims expressed in this article are solely those of the authors and do not necessarily represent those of their affiliated organizations, or those of the publisher, the editors and the reviewers. Any product that may be evaluated in this article, or claim that may be made by its manufacturer, is not guaranteed or endorsed by the publisher.

12. Cannarozzo G, Sannino M, Tamburi F, Chiricozzi A, Saraceno R, Morini C, et al. Deep pulse fractional CO₂ laser combined with a radiofrequency system: results of a case series. *Photomed Laser Surg.* (2014) 32:409–12. doi: 10.1089/pho.2014.3733
13. Chen SX, Cheng J, Watchmaker J, Dover JS, Chung HJ. Review of lasers and energy-based devices for skin rejuvenation and scar treatment with histologic correlations. *Dermatol Surg.* (2022) 48:441–8. doi: 10.1097/DSS.0000000000003397
14. Neaman KC, Baca ME, Piazza RC, VanderWoude DL, Renucci JD. Outcomes of fractional CO₂ laser application in aesthetic surgery: a retrospective review. *Aesthetic Surg J.* (2010) 30:845–52. doi: 10.1177/1090820X10386930
15. Bedi VP, Chan KF, Sink RK, Hantash BH, Herron GS, Rahman Z, et al. The effects of pulse energy variations on the dimensions of microscopic thermal treatment zones in non-ablative fractional resurfacing. *Lasers Surg Med.* (2007) 39:145–55. doi: 10.1002/lsm.20406
16. Shumaker PR, Kwan JM, Landers JT, Uebelhoefer NS. Functional improvements in traumatic scars and scar contractures using an ablative fractional laser protocol. *J Trauma Acute Care Surg.* (2012) 73:S116–21. doi: 10.1097/TA.0b013e318260634b
17. Waibel JS, Gianatasio C, Rudnick A, Siegel A. Use of lasers in wound healing: how to best utilize laser technology to prevent scar formation. *Curr Dermatol Rep.* (2018) 7:303–10. doi: 10.1007/s13671-018-0240-y
18. Fournier N, Dahan A, Mordon G, Diridollou S, Lagarde JM, Gall Y, et al. Nonablative remodeling: clinical, histologic, ultrasound imaging, and profilometric evaluation of a 1540 nm Er:glass laser. *Dermatol Surg.* (2001) 27:799–806. doi: 10.1046/j.1524-4725.2001.00355.x
19. Souil E, Capon A, Mordon S, Dinh-Xuan AT, Polla BS, Bachelet M. Treatment with 815-nm diode laser induces long-lasting expression of 72-kDa heat shock protein in normal rat skin. *Br J Dermatol.* (2001) 144, 260–6. doi: 10.1046/j.1365-2133.2001.04010.x
20. Ayuk SM, Abrahamse H, Hourel NN. The role of matrix metalloproteinases in diabetic wound healing in relation to photobiomodulation. *J Diabetes Res.* (2016) 2016. doi: 10.1155/2016/2897656
21. Haedersdal M, Moreau KER, Beyer DM, Nymann P, Alsjoern B. Fractional non-ablative 1540 nm laser resurfacing for thermal burn scars: a randomized controlled trial. *Lasers Surg Med.* (2009) 41:189–195. doi: 10.1002/lsm.20756
22. De Angelis F, Franco R. Fractional nonablative 1540-nm laser treatment of striae distensae in Fitzpatrick skin types II to IV: clinical and histological results. *Aesthet Surg J.* (2011) 31:411–9. doi: 10.1177/1090820X11402493
23. El-Domyati M, Attia S, Saleh F, Brown D, Birk DE, Gasparro F, et al. Intrinsic aging vs. photoaging: a comparative histopathological, immunohistochemical, and ultrastructural study of skin. *Exp Dermatol.* (2002) 11:398–405. doi: 10.1034/j.1600-0625.2002.110502.x
24. Cameli N, Mariano M, Serio M, Ardigò M. Preliminary comparison of fractional laser with fractional laser plus radiofrequency for the treatment of acne scars and photoaging. *Dermatol Surg.* (2014) 40:553–561. doi: 10.1111/dsu.12470
25. Tenna, S, Cogliandro, A, Piombino, L, Filoni, A, Persichetti, P. Combined use of fractional CO₂ laser and radiofrequency waves to treat acne scars: a pilot study on 15 patients. *J Cosmet Laser Ther.* (2012) 87:166–171. doi: 10.3109/14764172.2012.699678
26. Kisilevitz M, Lu KB, Wamsley C, Hoopman J, Kenkel J, Akgul Y. Novel use of non-invasive devices and microbipops to assess facial skin rejuvenation following laser treatment. *Lasers Surg Med.* (2020) 52:822–830. doi: 10.1002/lsm.23233
27. Mezzana P, Valeriani M, Valeriani R. Combined fractional resurfacing (10600 nm/1540 nm): tridimensional imaging evaluation of a new device for skin rejuvenation. *J Cosmet Laser Ther.* (2016) 18:397–402. doi: 10.1080/14764172.2016.1202417
28. Hopps E, Lo Presti R, Montana M, Noto D, Averna MR, Caimi G. Gelatinases and their tissue inhibitors in a group of subjects with metabolic syndrome. *J Investig Med.* (2013) 61:978–83. doi: 10.2310/JIM.0b013e318294e9da
29. Menghini R, Uccioli L, Vainieri E, Pecchioli C, Casagrande V, Stoehr R, et al. Expression of tissue inhibitor of metalloproteinase 3 is reduced in ischemic but not neuropathic ulcers from patients with type 2 diabetes mellitus. *Acta Diabetol.* (2013) 50:907–10. doi: 10.1007/s00592-013-0478-6
30. Ayuk SM, Abrahamse H, Hourel NN. Photobiomodulation alters matrix protein activity in stressed fibroblast cells *in vitro*. *J Biophotonics.* (2018) 11:e201700127. doi: 10.1002/jbio.201700127
31. Jo HY, Kim Y, Park HW, Moon HE, Bae S, Kim J, et al. The unreliability of MTT assay in the cytotoxic test of primary cultured glioblastoma cells. *Exp Neurobiol.* (2015) 24:235–245. doi: 10.5607/en.2015.24.3.235
32. Krassovska J, Borgschulze A, Sahlender B, Lögters T, Windolf J, Grotheer V. Blue light irradiation and its beneficial effect on Dupuytren's fibroblasts. *PLoS ONE.* (2019) 14:e0209833. doi: 10.1371/journal.pone.0209833
33. Orellana E, Kasinski A. Sulforhodamine B (SRB) assay in cell culture to investigate cell proliferation. *Bio-protocol.* (2016) 21:e1984. doi: 10.21769/BioProtoc.1984
34. Vichai V, Kirtikara K. Sulforhodamine B colorimetric assay for cytotoxicity screening. *Nat Protoc.* (2006) 1:1112–6. doi: 10.1038/nprot.2006.179
35. Skehan P, Storeng R, Scudiero D, Monks A, McMahon J, Vistica D, et al. New colorimetric cytotoxicity assay for anticancer-drug screening. *JNCI J Natl Cancer Inst.* (1990) 82:1107–12. doi: 10.1093/jnci/82.13.1107
36. Magni G, Banchelli M, Cherchi F, Coppi E, Fraccalvieri M, Rossi M, et al. Experimental study on blue light interaction with human keloid-derived fibroblasts. *Biomedicines.* (2020) :573. doi: 10.3390/biomedicines8120573
37. Schindelin J, Arganda-Carreras I, Frise E, Kaynig V, Longair M, Pietzsch T, et al. Fiji: an open-source platform for biological-image analysis. *Nat Methods.* (2012) 9:676–82. doi: 10.1038/nmeth.2019
38. Zerbinati N, Calligaro A. Calcium hydroxylapatite treatment of human skin: evidence of collagen turnover through picrosirius red staining and circularly polarized microscopy. *Clin Cosmet Investig Dermatol.* (2018) 11:29. doi: 10.2147/CCID.S143015
39. Kraft DC, Deocaris CC, Rattan SIS. Proteasomal oscillation during mild heat shock in aging human skin fibroblasts. *Ann N Y Acad Sci.* (2006) 1067:224–7. doi: 10.1196/annals.1354.028
40. Manela-Azulay M, Cuzzi T, Pinheiro JCA, Azulay DR, Rangel G.B. Objective methods for analyzing outcomes in research studies on cosmetic dermatology. *An Bras Dermatol.* (2010) 85:65–71. doi: 10.1590/S0365-05962010000100009
41. Mignon C, Botchkareva NV, Uzunbajakava NE, Tobin DJ. Photobiomodulation devices for hair regrowth and wound healing: a therapy full of promise but a literature full of confusion. *Exp Dermatol.* (2016) 25:745–9. doi: 10.1111/exd.13035
42. Karu TI. Cellular and molecular mechanisms of photobiomodulation (low-power laser therapy). *IEEE J Sel Top Quantum Electron.* (2014) 20. doi: 10.1109/JSTQE.2013.2273411
43. Chung H, Dai T, Sharma SK, Huang YY, Carroll JD, Hamblin MR. The nuts and bolts of low-level laser (Light) therapy. *Ann Biomed Eng.* (2012) 40:516–33. doi: 10.1007/s10439-011-0454-7
44. Hamblin MR, Hamblin MR. Mechanisms and applications of the anti-inflammatory effects of photobiomodulation. *AIMS Biophys.* (2017) 4:337–61. doi: 10.3934/biophy.2017.3.337
45. Garza ZCF, Born M, Hilbers PAJ, van Riel NAW, Liebmann J. Visible blue light therapy: molecular mechanisms and therapeutic opportunities. *Curr Med Chem.* (2017) 25:5564–77. doi: 10.2174/0929867324666170727112206
46. Wang Y, Huang YY, Wang Y, Lyu, P, Hamblin MR. Red (660 nm) or near-infrared (810 nm) photobiomodulation stimulates, while blue (415 nm), green (540 nm) light inhibits proliferation in human adipose-derived stem cells. *Sci Rep.* (2017) 7:1–10. doi: 10.1038/s41598-017-07525-w
47. Kim JE, Woo YJ, Sohn KM, Jeong KH, Kang H. Wnt/ β -catenin and ERK pathway activation: a possible mechanism of photobiomodulation therapy with light-emitting diodes that regulate the proliferation of human outer root sheath cells. *Lasers Surg Med.* (2017) 49:940–7. doi: 10.1002/lsm.22736
48. Sassoli C, Chellini F, Squecco R, Tani A, Idrizaj E, Nosi D, et al. Low intensity 635 nm diode laser irradiation inhibits fibroblast-myofibroblast transition reducing TRPC1 channel expression/activity: new perspectives for tissue fibrosis treatment. *Lasers Surg Med.* (2016) 48:318–332. doi: 10.1002/lsm.22441
49. Mamalis A, Garcha, M, Jagdeo J. Light emitting diode-generated blue light modulates fibrosis characteristics: fibroblast proliferation, migration speed, and reactive oxygen species generation. *Lasers Surg Med.* (2015) 47:210–5. doi: 10.1002/lsm.22293
50. Nelson BR, Majmudar G, Griffiths CEM, Gillard MO, Dixon AE, Tavakkol A, et al. Clinical improvement following dermabrasion of photoaged skin correlates with synthesis of collagen I. *Arch Dermatol.* (1994) 130:1136–42. doi: 10.1001/archderm.1994.01690090060008
51. El-Domyati M, Abd-El-Raheem T, Abdel-Wahab H, Medhat W, Hosam W, et al. Fractional versus ablative erbium:yttrium-aluminum-garnet laser resurfacing for facial rejuvenation: an objective evaluation. *J Am Acad Dermatol.* (2013) 68:103–12. doi: 10.1016/j.jaad.2012.09.014
52. Fitzpatrick RE, Rostan EF, Marchell N, El N. Collagen tightening induced by carbon dioxide laser versus erbium:YAG laser. *Lasers Surg Med.* (2000) 27:395–403. doi: 10.1002/1096-9101(2000)27:5<395::AID-LSM1000>3.0.CO;2-4



OPEN ACCESS

EDITED BY
Claudio Conforti,
University of Trieste, Italy

REVIEWED BY
David Dolivo,
Northwestern University, United States
Holly Nicola Wilkinson,
University of Hull, United Kingdom

*CORRESPONDENCE
Zhong Wen
wenzhong60@163.com
Qijun Zheng
zhengqj@szhospital.com
Chang Zou
zouchang@cuhk.edu.cn

†These authors have contributed
equally to this work and share first
authorship

SPECIALTY SECTION
This article was submitted to
Dermatology,
a section of the journal
Frontiers in Medicine

RECEIVED 21 August 2022
ACCEPTED 28 September 2022
PUBLISHED 26 October 2022

CITATION
Gong T, Wang Y, Dong S, Ma X, Du D,
Zou C, Zheng Q and Wen Z (2022)
Single-cell RNA-seq reveals
the communications between
extracellular matrix-related
components and Schwann cells
contributing to the earlobe keloid
formation.
Front. Med. 9:1000324.
doi: 10.3389/fmed.2022.1000324

COPYRIGHT
© 2022 Gong, Wang, Dong, Ma, Du,
Zou, Zheng and Wen. This is an
open-access article distributed under
the terms of the [Creative Commons
Attribution License \(CC BY\)](#). The use,
distribution or reproduction in other
forums is permitted, provided the
original author(s) and the copyright
owner(s) are credited and that the
original publication in this journal is
cited, in accordance with accepted
academic practice. No use, distribution
or reproduction is permitted which
does not comply with these terms.

Single-cell RNA-seq reveals the communications between extracellular matrix-related components and Schwann cells contributing to the earlobe keloid formation

Taogen Gong^{1,2†}, Yayu Wang^{3†}, Shaowei Dong^{4†}, Xiaoshi Ma⁵,
Danfeng Du⁵, Chang Zou^{4*}, Qijun Zheng^{3*} and Zhong Wen^{1*}

¹Otolaryngology-Head and Neck Surgery Center, Zhujiang Hospital, Southern Medical University, Guangzhou, China, ²Department of Otolaryngology-Head and Neck Surgery, The Second Clinical Medical College, Jinan University (Shenzhen People's Hospital), Shenzhen, China, ³Department of Cardiovascular Surgery, The Second Clinical Medical College, Jinan University (Shenzhen People's Hospital), Shenzhen, China, ⁴School of Medicine, Life and Health Sciences, The Chinese University of Hong Kong, Shenzhen, China, ⁵Department of Pathology, The Second Clinical Medical College, Jinan University (Shenzhen People's Hospital), Shenzhen, China

Keloid is a major type of skin fibrotic disease, with one prominent feature of extensive accumulation of extracellular matrix (ECM) components, and another feature of pain/itching, which is closely related to the peripheral nervous system (PNS). However, the molecular pathogenesis of these two prominent features still needs to be further explored. In the present study, we performed single-cell RNA sequencing (scRNA-seq) on clinical earlobe keloid samples and adjacent normal skin samples and constructed a keloid atlas of 31,379 cells. All cells were clustered into 13 major cell types using cell-type-specific markers. Among them, fibroblast, vascular endothelial cells, and smooth muscle cells were defined as the ECM-related populations according to their ECM-associated functions. Also, we found that Schwann cells (SCs) were the main neuron cells of PNS in the skin. Interestingly, the cell proportions of ECM-related populations, as well as SC were increased significantly in the earlobe keloid compared to the adjacent normal tissues, suggesting an important role of these cell types in the development of the earlobe keloid. Comprehensive cell-cell interaction analysis at the single-cell level revealed a strong interaction between SC and ECM-related subgroups which might be mediated by SEMA3C signaling pathways and MK/PTN gene family, which are found to be mainly involved in promoting cell proliferation and migration. Moreover, further exploration of the interactions of ECM-related populations and SC in different keloids, including earlobe keloid, back keloid, and chest keloid revealed an increasing amount of TGFβ-TGFβ receptor interactions in chest/back keloids as compared to earlobe keloid,

which suggested the anatomic site-specific pathogenesis in different keloids. Altogether, these findings suggested the interactions between ECM-related populations and SC contributing to the earlobe keloid formation and helped us to better understand the pathogenesis of keloids.

KEYWORDS

scRNA-seq, earlobe keloid, Schwann cells, ECM-related populations, cell interactions, site-specific pathogenesis

Introduction

Keloids are benign fibroproliferative tumors in the dermis, but they are unable to metastasize. After skin wounding, the self-healing mechanism of the skin will be triggered and produced scars during the wound healing process. However, when this wound healing process has been disturbed, it can result in excessive scar formation ranging from hypertrophic scars to keloids (1). As keloid pathogenesis is still unclear, keloid treatments are commonly through surgical resection, radiotherapy, and local injection of glucocorticoid, etc. However, these treatments still have a high recurrence rate and tend to aggravate the disease after recurrence, making it more difficult to treat keloid (2–4). Therefore, a thorough understanding of keloid pathogenesis would facilitate the development of clinical treatments for this disease.

Keloids tend to occur in areas of high mobility and tension, such as the chest, scapular region, earlobes, and upper arm (5). Keloids from different anatomical sites have site-specific morphology. For example, the single back keloids are grape-shaped, chest keloids are butterfly or non-butterfly shaped, and earlobe keloids have reniform to bulbous shapes (5). Due to different body surface areas suffering kinds of influences, such as UV radiation, trauma, and mechanical forces (6, 7), the occurrence and pathogenesis of keloids are also site-specific, including the difference between extracellular matrix (ECM) components and immune system (7).

The most prominent features of keloids are fibroblast proliferation and an extensive accumulation of ECM components, such as collagen (8). Now, a lot of studies mainly focus on the role of fibroblast in keloid pathogenesis (8–10). However, another prominent clinical feature of keloids is pain and itching, which leads to patients feeling very painful and increases their psychological pressure. This feature is closely related to the abundance of the peripheral nervous system (PNS) in the skin tissue. Skin as the largest organ of the human body contains an intricate PNS. The main cellular component of PNS is remarkable plastic glia, Schwann cells (SCs). In healthy skin, SC performs functions through differentiated (myelinating) or undifferentiated (non-myelinating) states (11). However, the wound microenvironment could reprogram SC to

invasive mesenchymal-like cells to drive axonal regrowth, cell proliferation, and inflammatory response to promote wound healing (12). Furthermore, in mice skin wound models, SC has been shown to dedifferentiate and regulate myofibroblast differentiation via TGF- β to promote skin wound healing (13). However, there is a lack of direct studies on the role of SC in earlobe keloid formation, and most studies are mainly based on mice models, lacking direct clinical samples.

In our study, we used scRNA-seq to characterize the transcriptomic profiles of single cells in earlobe keloid samples and adjacent normal skin samples. We further studied the interactions between ECM-related populations and SC in the development of keloids. In addition, we found that different kinds of keloids contribute to ECM accumulation by different mechanisms. These results suggested that the specific interactions between ECM-related subpopulations and Schwann cells could contribute to earlobe keloid formation.

Materials and methods

Patient specimens and tissue dissociation

This study was approved by the Medical and Ethics Committees of Shenzhen People's Hospital and each patient signed informed consent before enrolling in this study. We had a total of five patients, and we collected the keloid tissue and corresponding normal skin tissue of each patient. Normal skin tissue is adjacent to relatively normal tissue to keloid tissue. However, we only collected single-cell transcriptome data from a control sample for a technical reason. Detailed information is shown in [Supplementary Table 1](#). No patient received chemotherapy, radiotherapy, or intralesional steroid treatment before surgery. The skin tissues were washed two times in PBS and cut into small pieces to further dissociate in the lyase cocktail at 37°C for 30 min. Single-cell suspension was obtained by filtration through a 40- μ m filter. Red blood cells were removed with lysis buffer (Thermo Fisher Scientific, cat. no. 1966634). Cell viability was detected by trypan blue staining (Thermo Fisher Scientific, Waltham, MA, USA, cat. no.

T10282). If the cell viability is less than 80%, live cells would be further purified by a Dead Cell Removal Kit (Miltenyi Biotec, GER, cat. no. 130-090-101).

Single-cell library preparation and sequencing

Single-cell gel beads-in-Emulsion (GEM) generation, barcoding, sample cleanup, cDNA amplification, and cDNA library construction were performed using Chromium Next GEM Single Cell 3' Reagent Kits v3.1 (PN-1000121). After single-cell library preparation, the final library was quality-tested by Agilent 2100 bioanalyzer and sequenced on a HiSeq-PE150 platform (Novogene Bioinformatics Technology Co. Ltd, Beijing, China).

Single-cell RNA sequencing data preprocessing

The raw FASTQ sequence reads were preprocessed by Cell Ranger software (Version 5.0.1, V5.0.1). Reads were aligned to prebuilt GRCh38 reference assembly (V3.0.0, 10 × Genomics) and unique molecular identifier (UMI) counting was identified by cellranger count for each sample, and then UMI counting matrices were outputted and processed by R package Seurat (V4.0.5) (14) for downstream analysis. In order to filter low-quality cells and cell doublets, we performed a stringent quality control for each sample based on violin plots (Supplementary Figure 1), such as excluded cells with >15% mitochondrial UMIs and >1% red blood cells, detailed filtering parameters are shown in Supplementary Table 2. And then we used the Seurat function `NormalizeData` (parameters: `normalization.method = "LogNormalize," scale.factor = 10,000`) to normalize UMI counts for each cell by total expression, which can reduce batch effect between samples. We then used Seurat function `FindVariableFeatures` to define the top 2,000 highly variable genes (HVGs) and integrated all samples with a standard Seurat V5 integration algorithm based on 2,000 HVGs for batch effect correction.

Dimensional reduction and clustering

We ran a principal component analysis (PCA) dimensionality reduction using Seurat function `RunPCA` and used Seurat function `ElbowPlot` to identify the significant dimensions. In our study, we selected 30 PCs for clustering. Before clustering the cells, we constructed a shared nearest neighbor (SNN) graph based on the Euclidean distance in PCA space using Seurat function `FindNeighbors`. Cells were then clustered using Seurat function `FindClusters` based

on the Louvain algorithm, with a resolution of 1.5. Cells were displayed on the Unsupervised Uniform Manifold Approximation and Projection (UMAP) plot. Marker genes for each cluster were selected using Seurat function `FindAllMarkers` (`logfc.threshold = 0.25`, `test.use = "wilcox"`) and included canonical marker genes that had been reported before.

Phylogenetic analysis

We used Seurat function `BuildClusterTree` to construct a phylogenetic tree relating the "average" cell from each cell lineage. In addition to setting `dim = 1:30`, we used the default parameters.

Subpopulation analysis

After defining the major cell types, we selected some for further annotation, including fibroblast (FB), endothelial cells (ECs), and smooth muscle cells (SMCs). As we clustered all cells at a high resolution (`resolution = 1.5`), we directly split a UMI count matrix of cells in each major cell population from the whole matrix and performed the analysis to identify cell subpopulations. The steps of subpopulation analysis were similar to those of the whole dataset.

Functional analysis

Gene ontology (GO) functional enrichment (15) of differentially expressed genes (DEGs) was performed on R package `clusterProfiler` V4.2.0 (16) and a cutoff *P*-value < 0.05 was used to filter the significant enrichment results.

Trajectory and cell cycle analysis

We used the R package `monocle` (V2.21.1) (17) to infer the pseudotime trajectories of cells in specific subpopulations. The UMI matrix, gene information, and phenotype information were extracted from Seurat objects directly for building traces. Branches in the cell trajectory represent cells in different states with alternative gene expression patterns.

Cell–cell interaction network analysis

We used the R package `CellChat` (V1.1.3) (18) to identify the potential interactions between different cell populations. The `CellChatDB` human database was imported to construct the ligand–receptor interactions and secreted signaling was used for cell–cell communication analysis.

Statistical analysis

All statistical analyses were performed in R (V4.1.2). Student's *t*-test or Wilcoxon rank-sum test were used for the comparison of the two groups. *P* were adjusted for multiple hypothesis testing using the Benjamini–Hochberg method. A *P*-value < 0.05 was considered statistically significant.

Results

Single-cell transcriptomic map and cellular alterations in earlobe keloid

In this study, we first created a single-cell landscape of human normal skin and keloid samples by scRNA-seq. We collected five keloid tissues and one normal skin tissue from five female patients' ears. Next, we isolated skin tissues by enzymatic digestion, detected by trypan blue staining for viability, and performed scRNA-seq on the 10× Genomics Chromium platform (Figure 1A). After preprocessing raw sequence reads and stringent quality control (Supplementary Figure 1), we used the Seurat integration algorithm to remove potential technical bias to further correct batch effect across different samples (Supplementary Figure 3A). After then, we obtained 31,379 cells (normal skin: 2,514, keloid: 28,865, Supplementary Table 3) and merged them. All cells were clustered by UMAP-clustering and were divided into 35 cell clusters (Figure 1B), which were partitioned into 13 major cell types (Figure 1C) by classic markers and particular transcriptional signatures (Figure 1D and Supplementary Figure 3B), including COL1A1 and DCN for fibroblast (FB), ENG, and PECAM1 for vascular endothelial cells (VECs), VWF, and LYVE1 for lymphatic endothelial cell (LEC), ACTA2, and TAGLN for smooth muscle cells (SMCs), CD3D for T cells (IMMT), TPSB2, and TPSAB1 for mast cells (Mast), CD79A for B cells (IMMB), CD83 and HLA-DRA for monocyte (Mono), CD163 and CD68 for macrophage (Mø), KRT14 and KRT15 for keratinocyte (KRT), TOP2A and CENPF for cycling cells (Cyc), PMEL for melanocytes (MELs), and NRXN1 and S100B for Schwann cells (SCs) (19–21).

Next, we sought to determine the major cellular changes upon the onset of keloid by calculating the proportion of each cell type in normal skin and earlobe keloid samples (Figure 1E). We found that the cell proportions of FB, VEC, and SMC were increased in keloid samples when compared to normal skin, which was consistent with previous reports (20, 22). Gene functions of these populations were associated with the ECM organization and extracellular structure organization (Figure 1F), so we defined them as ECM-related populations. Besides, it was worth mentioning that the cell proportion of SC was also increased in keloid samples (Figure 1E), and this cell

type may be strongly associated with pain and itching of the keloid (23, 24).

Therefore, we further studied ECM-related populations and Schwann cells to reveal their roles in the formation of earlobe keloid.

Characteristics of extracellular matrix-related populations and Schwann cells in earlobe keloid

As ECM-related populations showed high heterogeneity in earlobe keloid, we further divided them into different subpopulations by distinct signatures, including FB (FB#1, FB#2, FB#3, FB#4), VEC (VEC#1, VEC#2, VEC#3), and SMC (SMC#1, SMC#2, SMC#3) (Figures 2A,B). Eight features were evaluated in each ECM-related subpopulation to further understand their gene functions (Figure 2C).

According to previously identified fibroblast subpopulation markers (20, 21, 25) and specific gene expressions of each subpopulation (Figure 2B), we could also annotate our fibroblasts into four subgroups. The dot plot of gene expression showed that FB#1: pro-inflammatory had higher cytokine gene expression (CXCL14) but lower expression of collagens (COL1A1 and COL1A2), and FB#1: pro-inflammatory had the highest module score in chemokine (Figure 2C). FB#2: mesenchymal highly expressed the three known markers, such as POSTN, COL11A1, ASPN of mesenchymal fibroblasts (20, 21, 25). Module scores also showed that FB#2: mesenchymal played well in collagens and proteinase (Figure 2C). The high expression of WISP2 and MFAP5 in FB#3: secretory-reticular and the high expression of PTGDS in FB#4: secretory-papillary, respectively, were also classic markers of each subpopulation (20, 21, 25). Next, we compared the cell proportion of each fibroblast subpopulation between keloid and normal skin samples. Results showed that FB#2: mesenchymal increased largely in keloid samples (Figure 2D) and had relatively large numbers of DEGs (Figure 2E) among the four subpopulations. Besides, the GO term of FB#2: mesenchymal showed that it was mainly related to ECM organization, ossification, and skeletal system development (Figure 2F), which could promote keloid formation. These results suggested that mesenchymal fibroblasts (FB#2) played an important role in the process of keloid by changing the cell proportion and gene function. And mesenchymal fibroblasts (FB#2) had a stronger mesenchymal component than other subpopulations.

Vascular endothelial cells were divided into three subpopulations by specific markers (Figure 2B) and gene functions (Figures 2C,G). We found that VEC#1 cluster highly expressed major histocompatibility complex (MHC) genes compared with other subpopulations, such as HLA-DRA and HLA-DRB. And it got the highest score of the MHC module among all ECM-related subpopulations (Figure 2C). According

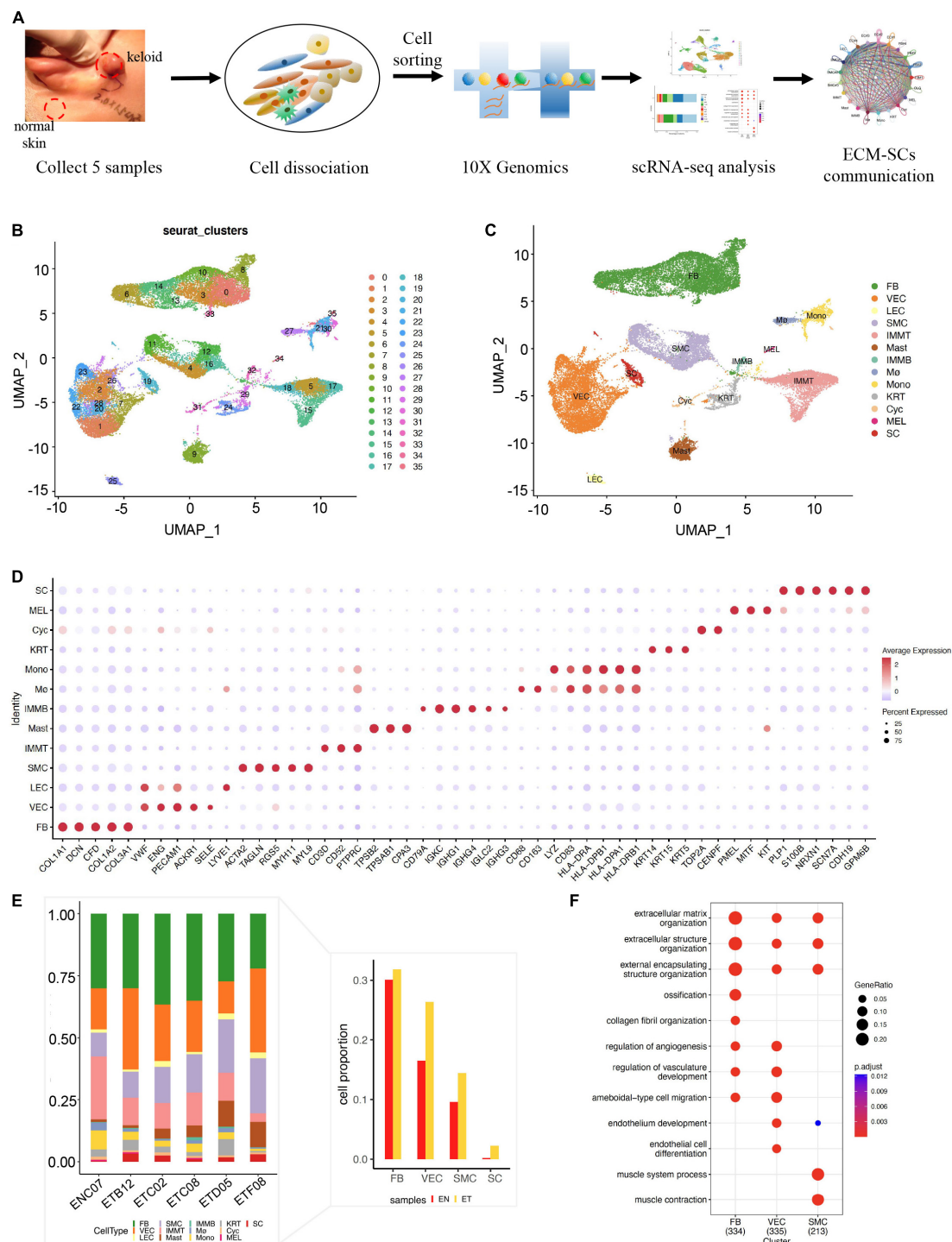


FIGURE 1

Single-cell RNA-seq revealed the cell landscape of normal skin and earlobe keloid samples. **(A)** The workflow of scRNA-seq in human normal skin (EN) and earlobe keloid samples (ET). **(B)** All cells were merged and clustered by UMAP-clustering and were divided into 35 clusters. **(C)** All cells were annotated into 13 major cell types, including: fibroblast (FB), endothelial cell (EC), smooth muscle cell (SMC), T cell (IMMT), B cell (IMMB), monocyte (Mono), macrophage (Mø), mast cell (Mast), keratinocyte (KRT), cycling cell (Cyc), melanocytes (MELs), and Schwann cells (SCs). **(D)** Dot plot shows the classical markers of 13 major cell types. Dot size presents the proportion of cells within the group expressing each gene, and dot color is related to its expression level. **(E)** Bar plot showed the cell proportions of different cell types in each sample. The right bar plot showed the cell proportions of ECM-related populations and SC between normal skin sample (EN) and earlobe keloid samples (ET). **(F)** Gene ontology (GO) biological process enrichment analysis of upregulated genes in each ECM-related population (Wilcoxon rank-sum test, Bonferroni correction, log2 fold change (log2FC) cutoff of 0.25, and adjusted P -value of < 0.05).

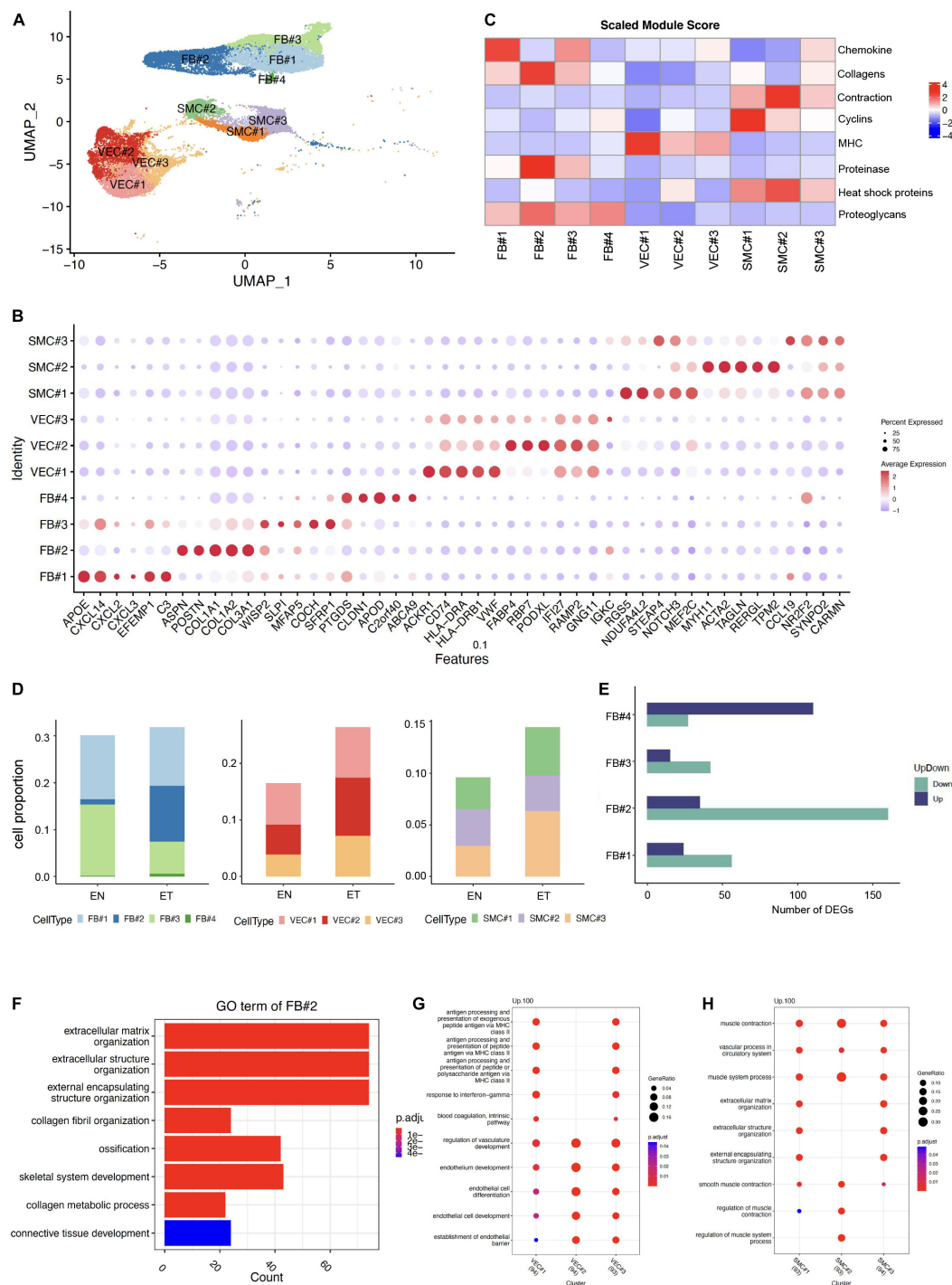


FIGURE 2

Characteristics of extracellular matrix (ECM)-related populations in earlobe keloid. (A) ECM-related populations were further divided into different subpopulations, including FB (FB#1, FB#2, FB#3, FB#4), VEC (VEC#1, VEC#2, VEC#3), and SMC (SMC#1, SMC#2, SMC#3). (B) Module scores of eight features (or functions) in each ECM-related subpopulation. (C) Dot plot shows the classical markers of each ECM-related subpopulation. Dot size presents the proportion of cells within the group expressing each gene, and dot color is related to its expression level. (D) The cell proportions of ECM-related subpopulation between normal skin sample (EN) and earlobe keloid samples (ET) (Wilcoxon rank-sum test, Bonferroni correction, log2 fold change (log2FC) cutoff of 0.25, and P -value of < 0.05). Purple bars indicate upregulated genes, and green bars indicate downregulated genes in earlobe keloid. (E) Number of DEGs in each fibroblast subpopulations between normal skin (EN) and earlobe keloid samples (ET) (Wilcoxon rank-sum test, Bonferroni correction, log2 fold change (log2FC) cutoff of 0.25, and P -value of < 0.05). Purple bars indicate upregulated genes, and green bars indicate downregulated genes in earlobe keloid. (F) Gene ontology (GO) biological process enrichment analysis of upregulated DEGs in mesenchymal fibroblast (FB#2) between earlobe keloid and normal skins. Its gene functions were mainly related to ECM organization, ossification, and skeletal system development. (G) GO biological process enrichment analysis of each VEC subpopulation. (H) GO biological process enrichment analysis of each SMC subpopulation.

to the GO enrichment analysis, VEC#1 cluster may perform immune functions at a condition, like actively involved with antigen processing and presentation and response to interferon-gamma (Figure 2G). VEC#2 cluster mainly performed the function of endothelial cell differentiation and endothelium development, and it had the largest expansion in the earlobe keloid compared with normal skin. VEC#3 cluster contained the above two characteristics. This cluster may stay in a transitional state.

We also identified three subpopulations of SMC, which were also defined by specific markers (Figure 2B) and gene functions (Figures 2C,H). SMC#1 highly expressed RGS5, which is a specific marker of myofibroblast (26), and it got a higher cyclin module score but a lower contractile score than SMC#2 cluster. SMC#2 cluster highly and specifically expressed ACTA2 and MYH11, which are involved in smooth muscle actin and myosin (27). However, the SMC#3 cluster showed both lower cyclin gene expression and contraction gene expression and expressed higher levels of cytokine genes, such as CCL19 and IL32, which suggested it was at a stressed state (28).

Schwann cells were defined by canonical neuron markers NRXN1, S100B, SCN7A, and GPM6B (29–31) (Figures 3A,B). We noticed that the cell proportion of SC was more than 10 times larger in earlobe keloid than in normal skin, indicating a potential role of SC in the formation of earlobe keloid (Figure 3C). GO enrichment results showed that the functions of SC were mainly concentrated in two chunks. One was related to the differentiation of neurons and involved in the signal transduction of the nervous system, which was the essential function of SC. At the same time, SC was involved in the ECM structure organization (Figure 3D).

We then explored differentially expressed genes of SC between earlobe keloid and normal skin. We found that the top 10 upregulated DEGs were main collagen genes, like COL11A1 (Figure 3E), which were associated with the ECM organization and ECM structure constituent, etc. (Figure 3F).

These results suggested that Schwann cells not only participated in signal transduction but also may promote the formation of earlobe keloid by acting on changes in ECM structure.

Intercellular communication between normal skin and earlobe keloid samples

Next, we explored the cell–cell communication landscape between each cell type and subpopulation, especially the interactions between ECM-related populations and SC in earlobe keloid and normal skin. To better study cell–cell communication mediated by ligand–receptor interactions, we used the R package Cellchat (18).

As detailed in Circos plots and bar plots, we found that a denser interaction network in keloid samples compared to

that in the normal sample, and the number of intercellular interactions in keloid samples was about 10 times more abundant than that in normal skin (ET: 2203, EN: 208, Figures 4A,B). As previously reported (1, 20, 22, 32), our results also showed that fibroblasts, endothelial cells, and smooth muscle cells are relatively active in the formation of keloids. However, we observed that the interaction of SC with other cells was obviously enhanced in the earlobe keloid, which had not been reported in previous studies (Figure 4A and Supplementary Figure 4), and further suggested that SC may also play an important role during the process of earlobe keloid.

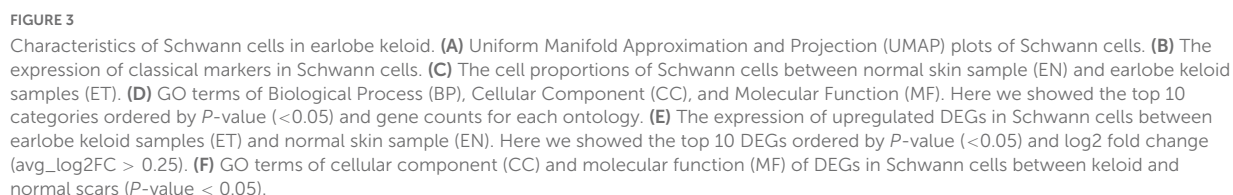
Then, using scatter plots (Figure 4C) to compare the outgoing and incoming interaction strength in 2D space, we observed that fibroblasts and endothelial cells emerge as one of the major sources and targets in earlobe keloid compared to normal skin. FB#1 and FB#2 were the major sources (ligands) in the earlobe keloid, and VEC#1 and VEC#2 were the major targets (receptors) in the earlobe keloid. Compared with signals in normal skin, SC had significant changes in both sending and receiving signals in the earlobe keloid, and mainly interacted with ECM-related subpopulations (Supplementary Figure 4).

To further reveal the outgoing (or incoming) signaling associated with each cell type in keloid and normal skin, respectively, we showed the signaling strength in specific cell populations by heatmap. Overall, the significant signal patterns related to keloid included, but were not limited to MK, MIF, and VEGF (Figure 4D). We observed that the specific and significant outgoing signal patterns of SC in the earlobe keloid were PTN, SEMA3, PDGF, and EGF (Supplementary Figure 5A).

Identify pathways between extracellular matrix-related subpopulations and Schwann cells contributed to the earlobe keloid

Next, we further identified signaling ligand–receptor pairs related to the process of earlobe keloid, we compared the communication probabilities mediated by ligand–receptor pairs between ECM-related subpopulations and SC (Figure 4E). We found that SC interacted strongly with fibroblast cells and vascular endothelial cells, especially with FB#2 and VEC#2. We observed that the SEMA3 pathway was significant and specific when SCs were the source cells and ECM-related subpopulations were the target cells in a keloid environment (Figure 4E). The signal was further amplified when we identified dysfunctional signaling by comparing DEGs analysis between keloid and normal samples (Supplementary Table 4) and SEMA3C was the main ligand.

SEMA3C protein is a member of the Class 3 semaphorin proteins family, which can interact with neuropilin isoforms (NRP1 and NRP2) and plexin receptors (PLXNA2 and PLXND1) (33, 34), and plays an important role in several



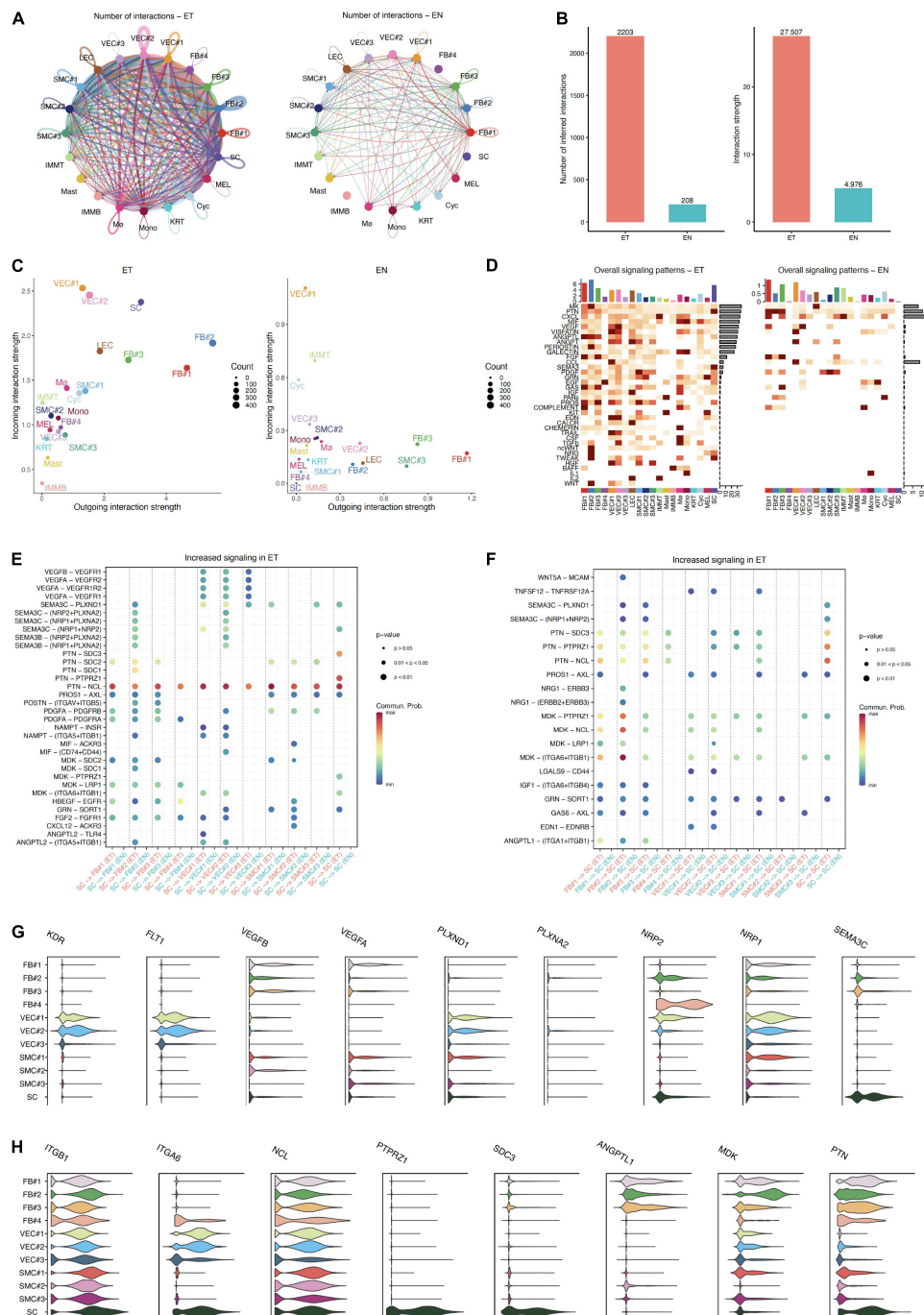


FIGURE 4

Intercellular communication in normal skin and keloid samples. **(A)** Circos plots show the interactions density between any two cell types in earlobe keloid samples (ET) and normal skin (EN), respectively. **(B)** Bar plots show the number of intercellular communication (left) and interaction strength (right) in earlobe keloid samples (ET) and normal skin (EN), respectively. **(C)** Comparing the outgoing and incoming interaction strength in 2D space by scatter plots to allow identifying the cell populations with significant changes in sending or receiving signals in earlobe keloid samples (ET) and normal skin (EN), respectively. **(D)** The heatmap showed all signaling patterns and the strength of each cell type and subpopulation in earlobe keloid samples (ET) and normal skin (EN), respectively. **(E)** The significant ligand–receptor pairs between ECM-related subpopulations and SC in earlobe keloid samples (ET) and normal skin (EN). Here, SC were as sources and ECM-related subpopulations were as targets. P -value < 0.05 was considered significant interactions. **(F)** The significant ligand–receptor pairs between ECM-related subpopulations and SC in earlobe keloid samples (ET) and normal skin (EN). Here, ECM subpopulations were as sources and SC were as targets. P -value < 0.05 was considered significant interactions. **(G)** Violin plots showed gene expression level of specific genes in ligand–receptor pairs in ECM-related subpopulations and SC, including SEMA3C and its consistent receptors. **(H)** Violin plots showed gene expression level of specific genes in ligand–receptor pairs in ECM-related subpopulations and SC, including PTN, MDK, and their consistent receptors.

respects, such as the neurogenesis (35), cardiac development (36), and promote or inhibit tumor progression (37). SEMA3C can also interact with the VEGF signaling pathways in endothelial cells to regulate cell proliferation and migration and so on (38). SEMA3C was found to be highly and specifically expressed in SC, according to our findings. Its consistent receptors, such as NRP1, NRP2, PLXND1, and VEGFR, were also highly and specially expressed in ECM-related populations, particularly fibroblasts and vascular endothelial cells (Figure 4G and Supplementary Figure 5B). Thus, we inferred that Schwann cells could interact with fibroblasts and vascular endothelial cells primarily via SEMA3C signaling pathways (SEMA3C_NRP1_PLXNA2, SEMA3C_NRP1_NRP2, SEMA3C_NRP2_PLXNA2, and SEMA3C_PLXND1), which could affect the cells proliferation of fibroblasts and vascular endothelial cells and lead to an increase in their proportion. Besides, Schwann cells could also release VEGF signaling to act on VEC#2, which can also help the cell proliferation of vascular endothelial cells.

Conversely, our results showed that ECM-related subpopulations can promote neurite outgrowth and migration through MK/PTN family (Figure 4F). MK and PTN are a two-member family of heparin-binding neurite outgrowth-promoting factors (39, 40), both of them can ligate with many receptors, such as syndecans (SDC3) (41, 42), integrins (ITGA6) (43), and nucleolin (NCL) (44), which help to promote neurite outgrowth and cell migration in a lot of inflammatory diseases and cancer. Our results showed that PTN was expressed in almost all ECM-related subpopulations, and its consistent receptors SDC3 and ANGPTL1 were highly expressed in SC, but MK was expressed mainly in fibroblasts, especially in FB#2 (Figure 4H and Supplementary Figure 5C). This further confirmed the fibroblast heterogeneity and the importance of FB#2 in earlobe keloid. Thus, we thought that ECM-related subpopulations, mainly the mesenchymal fibroblasts (FB#2), can promote Schwann cell proliferation and migration by the MK/PTN family, which contributed to the development of earlobe keloid.

Discussion

With the development of single-cell transcriptome technology, it has been gradually applied to the research of human skin diseases (20–22). It can help us understand keloid pathogenesis at the single-cell level and develop more precise therapeutic strategies. Current studies on keloid pathogenesis mainly focus on the mechanisms of fibroblast heterogeneity and hyperproliferation in the skin fibrotic process, as well as related inflammatory responses (20–22). However, the role of SC in keloid pathogenesis has been ignored, especially the relationship between SC and ECM structure.

Therefore, in our study, we performed the scRNA-seq data analysis on earlobe keloid samples and adjacent normal skin samples from the human ear region. We clustered 31,379 cells by UMAP-clustering and partitioned them into 13 major cell types (Figures 1C,D). We defined fibroblasts, vascular endothelial cells, and smooth muscle cells as the ECM populations, as we found these cells were closely related to the structure of ECM (Figure 1G). We further divided ECM-related populations into different subpopulations by distinct signatures, such as specific markers, gene functions, and gene module scores (Figures 2B,C). Referred to previous research (20, 21), we divided fibroblasts into four subpopulations: FB#1: pro-inflammatory fibroblasts, FB#2: mesenchymal fibroblasts, FB#3: secretory-reticular fibroblasts, and FB#4: secretory-papillary fibroblasts (Figure 2A).

We also found that part of vascular endothelial cells, especially VEC#1, could highly express major histocompatibility complex (MHC) genes, such as HLA-DRA and HLA-DRB (Figure 2D). Previous research had reported that vascular endothelial cells can function as immune/inflammation effectors and immune cell mobilizers under a condition (45–47). Therefore, we inferred that during the formation of the earlobe keloid, the expansion of vascular endothelial cells was not only related to the ECM structure but also played an immune role under certain stimulation. However, the specific transformation mechanism of vascular endothelial cells remains to be further studied.

Our results also verified that Schwann cells were increased significantly in the earlobe keloid (Figure 2A), and actively interacted with ECM-related subpopulations by both sending and receiving signals in the earlobe keloid (Figure 4C and Supplementary Figure 4). Signaling ligand–receptor pairs revealed that SC could influence cell proliferation of ECM-related subpopulations via SEMA3C signaling pathways and VEGF signaling pathways. Conversely, ECM-related subpopulations could also promote SC proliferation and migration by MK/PTN family, especially by the mesenchymal fibroblasts (Figures 5A–D). We noticed that Matrin et al. (48) also found that keloidal Schwann cells contribute to the formation of the extracellular matrix, which could also further support our results. However, they did not further propose the relevant pathways of Schwann cells affecting ECM. Our results could supplement the role of Schwann cells in keloid formation and contribute to comprehensively studying the pathogenesis of keloids.

In addition, in order to explore whether the pathogenesis of different kinds of keloids is site-specific, we compared the difference in interactions between ECM-related subpopulations and SC in different kinds of keloids, including earlobe keloid, back keloid, and chest keloid. The scRNA-seq data of other keloids were downloaded from the GEO database under accession codes “GSE163973” (20). The downloaded data were processed using the above methods. All cells were clustered

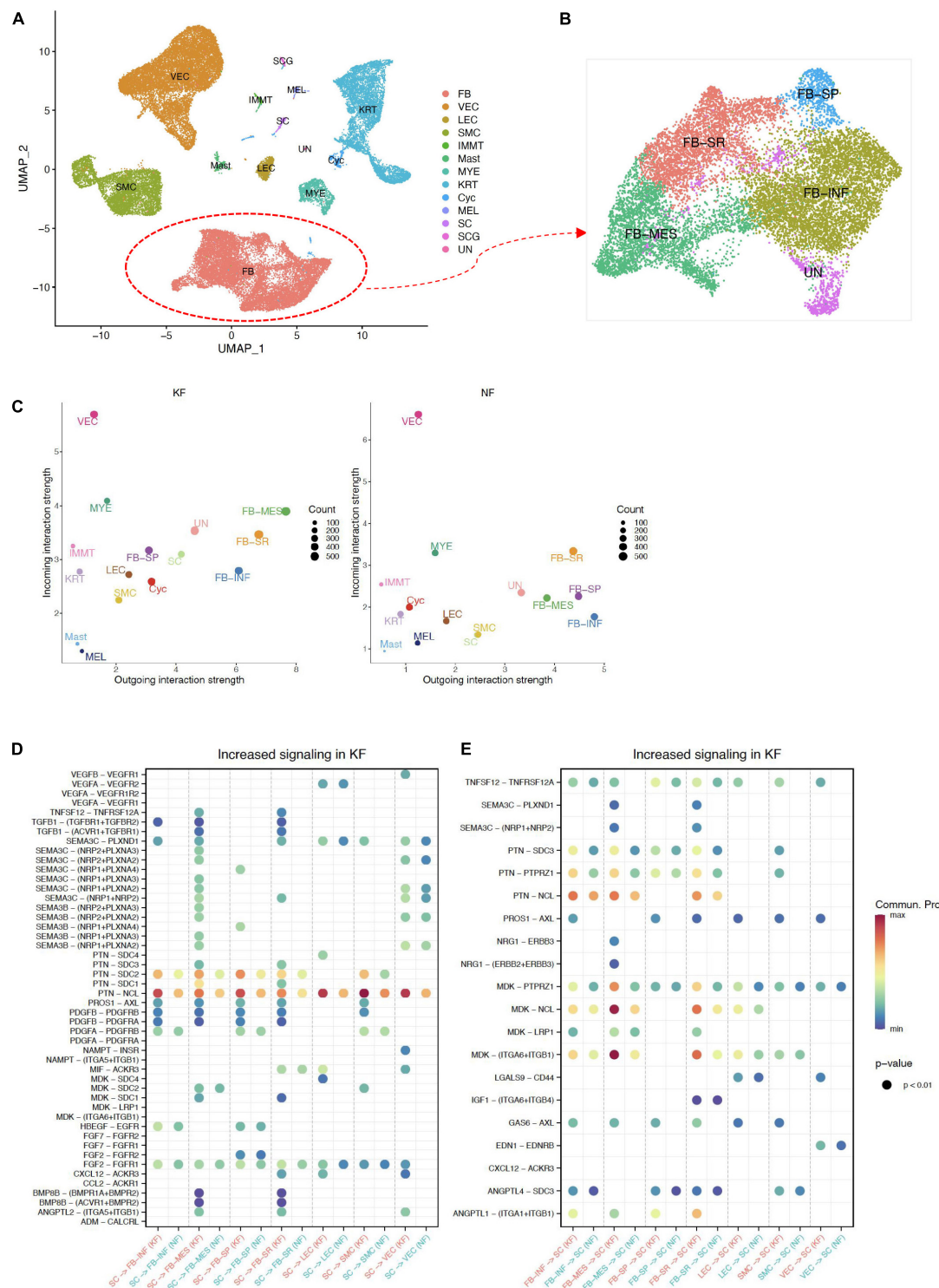


FIGURE 5

Interactions between ECM-related populations and SC in chest/back keloids. **(A)** UMAP plots of all cells in chest/back keloids, the clustering resolution was 1.5. **(B)** UMAP plots of fibroblasts in chest/back keloids, the clustering resolution was 1.0. **(C)** Comparing the outgoing and incoming interaction strength in 2D space by scatter plots to allow identify the cell populations with significant changes in sending or receiving signals in chest/back keloids (KF) and normal skin (NK), respectively. **(D)** The significant ligand–receptor pairs between ECM-related subpopulations and SC in chest/back keloids (KF) vs. normal skin (NK). Here, SC were as sources. P -value < 0.05 was considered significant interactions. **(E)** The significant ligand–receptor pairs between ECM-related subpopulations and SC in chest/back keloids (KF) vs. normal skin (NK). Here, SC were as targets. P -value < 0.05 was considered significant interactions.

and partitioned into 13 major cell types by classic markers (Figure 5A and Supplementary Figure 6A). Fibroblasts could also be divided into four main subpopulations: FB-INF: pro-inflammatory fibroblasts, FB-MES: mesenchymal fibroblasts, FB-SR: secretory-reticular fibroblasts, and FB-SP: secretory-papillary fibroblasts (Figure 5B and Supplementary Figure 6B). We found that mesenchymal fibroblasts played an important role in any keloids (Figure 5D). And interactions between SC and ECM-related subpopulations were mainly through SEMA3C signaling pathways and MK/PTN family in both earlobe keloids and chest/back keloids. However, the VEGF signaling pathways were not the main ligand of SC in chest/back keloids. Besides, we found an increase in TGF β –TGF β receptor interactions in chest/back keloids compared to earlobe keloid (Figures 5E,F). Our results indicated that the interactions between SC and ECM-related subpopulations had different signaling pathways in different kinds of keloids, which also indicated that the keloid pathogenesis was site-specific.

However, there were still some limitations in our study. First, we lacked sufficient control samples. Therefore, in order to test the accuracy of our data, we verified our data by comparing them with other published single-cell transcriptome data. Second, we will need to further verify the reliability of our results through experiments in future. For example, we can regulate the SEMA3C pathway to observe the development of earlobe keloid formation and help us to better understand the pathogenesis of keloids.

In a word, based on the single-cell transcriptomic map of earlobe keloid, we characterized ECM-related populations and Schwann cells at the single-cell level. We first revealed the role of interactions between ECM-related populations and Schwann cells in the process of earlobe keloid by some main signal pathways. We also revealed that the pathogenesis of different kinds of keloids was site-specific. These findings may help us better understand the pathogenesis of keloids and provide more targeted treatment strategies for different kinds of keloids.

Data availability statement

The data presented in this study are deposited in the Genome Sequence Archive (GSA) for Human database, accession number: HRA002631. All other relevant data can also be visualized within the article and its **Supplementary material** or from the corresponding author upon reasonable request.

Ethics statement

The studies involving human participants were reviewed and approved by the Medical and Ethics Committees of

Shenzhen People's Hospital. The patients/participants provided their written informed consent to participate in this study.

Author contributions

ZW, QZ, and CZ contributed to the conception and design of the study. YW and SD organized the database and performed the statistical analysis. TG, XM, and DD did the experiment and constructed the single-cell library. YW wrote the first draft of the manuscript. TG and SD revised the manuscript. ZW, QZ, and CZ contributed to the edit and review the manuscript. All authors approved the submitted version.

Funding

This study was supported by the Shenzhen Science and Technology Innovation Commission (JCY20190807150403655), the Health, Population, and Family Planning Commission of Shenzhen Municipality (SZXJ2018023), the Guangdong Basic and Applied Basic Research Foundation (2020B1515120032 and 2019B1515120033), the Science and Technology Foundation of Shenzhen (JCYJ20210324115800001), the Shenzhen Key Medical Discipline Construction Fund (SZXK053 and SZXK01), and the Guangdong Provincial Natural Science Foundation (2021A1515010919).

Conflict of interest

The authors declare that the research was conducted in the absence of any commercial or financial relationships that could be construed as a potential conflict of interest.

Publisher's note

All claims expressed in this article are solely those of the authors and do not necessarily represent those of their affiliated organizations, or those of the publisher, the editors and the reviewers. Any product that may be evaluated in this article, or claim that may be made by its manufacturer, is not guaranteed or endorsed by the publisher.

Supplementary material

The Supplementary Material for this article can be found online at: <https://www.frontiersin.org/articles/10.3389/fmed.2022.1000324/full#supplementary-material>

SUPPLEMENTARY FIGURE 1

Quality control for each sample is based on violin plots. nFuture_RNA: the number of genes whose expression is greater than 0 detected in one cell, nCount_RNA: the total gene expression in one cell, percent.mt: percentage of mitochondrial gene expression in one cell, percent.HB: percentage of red blood gene expression in one cell.

SUPPLEMENTARY FIGURE 2

Two thousand HVGs of merged samples. Top 10 HVGs were labeled on the scatter plot (right).

SUPPLEMENTARY FIGURE 3

(A) UMAP plots of all cells in normal skin sample (ENC07) and earlobe keloid samples (ETB12, ETC02, ETC08, ETD05, and ETF06). (B) Dot plot showed the classical markers of all cell types, including subpopulations. Dot size presents the proportion of cells within the group expressing each gene, and dot color is related to its expression level.

SUPPLEMENTARY FIGURE 4

Network interactions of each cell type in earlobe keloid. Interactions between SC and other cell types were amplified.

SUPPLEMENTARY FIGURE 5

(A) The heatmap showed outgoing and incoming signaling patterns and the strength of each cell type and subpopulation in earlobe keloid samples (ET) and normal skin (EN). (B) Violin plots showed gene expression level of specific genes in ligand–receptor pairs in all cell types, including SEMA3C and its consistent receptors. (C) Violin plots showed gene expression level of specific genes in ligand–receptor pairs in all cell types, including PTN, MDK, and their consistent receptors.

SUPPLEMENTARY FIGURE 6

(A) Heatmap showed the expression of specific genes in each cell type in chest/back keloids. (B) Dot plot showed the classical markers of each fibroblast subpopulations.

References

- Bran GM, Goessler UR, Hormann K, Riedel F, Sadick H. Keloids: current concepts of pathogenesis (review). *Int J Mol Med*. (2009) 24:283–93. doi: 10.3892/ijmm.00000231
- Fanous A, Bezdjian A, Caglar D, Mlynarek A, Fanous N, Lenhart SF, et al. Treatment of keloid scars with botulinum toxin type a versus triamcinolone in an athymic nude mouse model. *Plast Reconstr Surg*. (2019) 143:760–7. doi: 10.1097/PRS.00000000000005323
- Trisliana Perdanasari A, Lazzeri D, Su W, Xi W, Zheng Z, Ke L, et al. Recent developments in the use of intralesional injections keloid treatment. *Arch Plast Surg*. (2014) 41:620–9. doi: 10.5999/aps.2014.41.6.620
- Ojeh N, Bharatha A, Gaur U, Forde AL. Keloids: current and emerging therapies. *Scars Burn Heal*. (2020) 6:2059513120940499. doi: 10.1177/2059513120940499
- Bayat A, Arscott G, Ollier WE, Ferguson MW, Mc Grouther DA. Description of site-specific morphology of keloid phenotypes in an afrocaribbean population. *Br J Plast Surg*. (2004) 57:122–33. doi: 10.1016/j.bjps.2003.11.009
- OGawa R, Okai K, Tokumura F, Mori K, Ohmori Y, Huang C, et al. The relationship between skin stretching/contraction and pathologic scarring: the important role of mechanical forces in keloid generation. *Wound Repair Regen*. (2012) 20:149–57. doi: 10.1111/j.1524-475X.2012.00766.x
- Butzelaar L, Niessen FB, Talhout W, Schooneman DPM, Ulrich MM, Beelen RHJ, et al. Different properties of skin of different body sites: the root of keloid formation? *Wound Repair Regen*. (2017) 25:758–66. doi: 10.1111/wrr.12574
- Andrews JP, Marttala J, Macarak E, Rosenbloom J, Uitto J. Keloids: the paradigm of skin fibrosis - pathomechanisms and treatment. *Matrix Biol*. (2016) 51:37–46. doi: 10.1016/j.matbio.2016.01.013
- Griffin MF, desJardins-Park HE, Mascharak S, Borrelli MR, Longaker MT. Understanding the impact of fibroblast heterogeneity on skin fibrosis. *Dis Model Mech*. (2020) 13:dmm044164. doi: 10.1242/dmm.044164
- Wynn TA, Ramalingam TR. Mechanisms of fibrosis: therapeutic translation for fibrotic disease. *Nat Med*. (2012) 18:1028–40. doi: 10.1038/nm.2807
- Nocera G, Jacob C. Mechanisms of schwann cell plasticity involved in peripheral nerve repair after injury. *Cell Mol Life Sci*. (2020) 77:3977–89. doi: 10.1007/s00018-020-03516-9
- Clements MP, Byrne E, Camarillo Guerrero LF, Cattin AL, Zakka L, Ashraf A, et al. The wound microenvironment reprograms schwann cells to invasive mesenchymal-like cells to drive peripheral nerve regeneration. *Neuron*. (2017) 96:98–114.e7. doi: 10.1016/j.neuron.2017.09.008
- Parfejevs V, Debbache J, Shakhova O, Schaefer SM, Glausch M, Wegner M, et al. Injury-activated glial cells promote wound healing of the adult skin in mice. *Nat Commun*. (2018) 9:236. doi: 10.1038/s41467-017-01488-2
- Hao Y, Hao S, Andersen-Nissen E, Mauck WM III, Zheng S, Butler A, et al. Integrated analysis of multimodal single-cell data. *Cell*. (2021) 184:3573–87.e29. doi: 10.1016/j.cell.2021.04.048
- Ashburner M, Ball CA, Blake JA, Botstein D, Butler H, Cherry JM, et al. Gene ontology: tool for the unification of biology. the gene ontology consortium. *Nat Genet*. (2000) 25:25–9. doi: 10.1038/75556
- Wu T, Hu E, Xu S, Chen M, Guo P, Dai Z, et al. Clusterprofiler 4.0: a universal enrichment tool for interpreting omics data. *Innovation*. (2021) 2:100141. doi: 10.1016/j.xinn.2021.100141
- Qiu X, Hill A, Packer J, Lin D, Ma YA, Trapnell C. Single-cell RNA quantification and differential analysis with census. *Nat Methods*. (2017) 14:309–15. doi: 10.1038/nmeth.4150
- Jin S, Guerrero-Juarez CF, Zhang L, Chang I, Ramos R, Kuan CH, et al. Inference and analysis of cell-cell communication using cellchat. *Nat Commun*. (2021) 12:1088. doi: 10.1038/s41467-021-21246-9
- Guerrero-Juarez CF, Dedhia PH, Jin S, Ruiz-Vega R, Ma D, Liu Y, et al. Single-cell analysis reveals fibroblast heterogeneity and myeloid-derived adipocyte progenitors in murine skin wounds. *Nat Commun*. (2019) 10:650. doi: 10.1038/s41467-018-08247-x
- Deng CC, Hu YF, Zhu DH, Cheng Q, Gu JJ, Feng QL, et al. Single-cell RNA-seq reveals fibroblast heterogeneity and increased mesenchymal fibroblasts in human fibrotic skin diseases. *Nat Commun*. (2021) 12:3709. doi: 10.1038/s41467-021-24110-y
- Sole-Boldo L, Raddatz G, Schutz S, Mallm JP, Rippe K, Lonsdorf AS, et al. Single-cell transcriptomes of the human skin reveal age-related loss of fibroblast priming. *Commun Biol*. (2020) 3:188. doi: 10.1038/s42003-020-0922-4
- Liu X, Chen W, Zeng Q, Ma B, Li Z, Meng T, et al. Single-cell RNA-sequencing reveals lineage-specific regulatory changes of fibroblasts and vascular endothelial cells in keloids. *J Invest Dermatol*. (2022) 142:124–35.e11. doi: 10.1016/j.jid.2021.06.010
- Ashrafi M, Baguneid M, Bayat A. The role of neuromediators and innervation in cutaneous wound healing. *Acta Derm Venereol*. (2016) 96:587–94. doi: 10.2340/00015555-2321
- Bray ER, Cheret J, Yosipovitch G, Paus R. Schwann cells as underestimated, major players in human skin physiology and pathology. *Exp Dermatol*. (2020) 29:93–101. doi: 10.1111/exd.14060
- Philippeos C, Telerman SB, Oules B, Pisco AO, Shaw TJ, Elgueta R, et al. Spatial and single-cell transcriptional profiling identifies functionally distinct human dermal fibroblast subpopulations. *J Invest Dermatol*. (2018) 138:811–25. doi: 10.1016/j.jid.2018.01.016
- Mahoney WM Jr., Fleming JN, Schwartz SM. A unifying hypothesis for scleroderma: identifying a target cell for scleroderma. *Curr Rheumatol Rep*. (2011) 13:28–36. doi: 10.1007/s11926-010-0152-8
- Burger J, Bogunovic N, de Wagenaar NP, Liu H, van Vliet N, Ijama A, et al. Molecular phenotyping and functional assessment of smooth muscle-like cells with pathogenic variants in aneurysm genes Acta2, Myh11, Smad3 and Fbn1. *Hum Mol Genet*. (2021) 30:2286–99. doi: 10.1093/hmg/ddab190
- Li Y, Ren P, Dawson A, Vasquez HG, Ageedi W, Zhang C, et al. Single-cell transcriptome analysis reveals dynamic cell populations and differential gene expression patterns in control and aneurysmal human aortic tissue. *Circulation*. (2020) 142:1374–88. doi: 10.1161/CIRCULATIONAHA.120.046528
- Deloulme JC, Raponi E, Gentil BJ, Bertacchi N, Marks A, Labourette G, et al. Nuclear expression of S100b in oligodendrocyte progenitor cells correlates with differentiation toward the oligodendroglial lineage and modulates oligodendrocytes maturation. *Mol Cell Neurosci*. (2004) 27:453–65. doi: 10.1016/j.mcn.2004.07.008

30. Seaberg BL, Purao S, Rimer M. Validation of terminal schwann cell gene marker expression by fluorescent in situ hybridization using Rnascope. *Neurosci Lett.* (2022) 771:136468. doi: 10.1016/j.neulet.2022.136468
31. Bang ML, Vainshtein A, Yang HJ, Eshed-Eisenbach Y, Devaux J, Werner HB, et al. Glial M6b stabilizes the axonal membrane at peripheral nodes of ranvier. *Glia.* (2018) 66:801–12. doi: 10.1002/glia.23285
32. Macarak EJ, Wermuth PJ, Rosenbloom J, Uitto J. Keloid disorder: fibroblast differentiation and gene expression profile in fibrotic skin diseases. *Exp Dermatol.* (2021) 30:132–45. doi: 10.1111/exd.14243
33. Valiulyte I, Steponaitis G, Kardonaite D, Tamasauskas A, Kazlauskas A. A sema3 signaling pathway-based multi-biomarker for prediction of glioma patient survival. *Int J Mol Sci.* (2020) 21:7396. doi: 10.3390/ijms21197396
34. Alto LT, Terman JR. Semaphorins and their signaling mechanisms. *Methods Mol Biol.* (2017) 1493:1–25. doi: 10.1007/978-1-4939-6448-2_1
35. Kolodkin AL, Matthes DJ, Goodman CS. The semaphorin genes encode a family of transmembrane and secreted growth cone guidance molecules. *Cell.* (1993) 75:1389–99. doi: 10.1016/0092-8674(93)90625-z
36. Gitler AD, Lu MM, Epstein JA. Plexind1 and semaphorin signaling are required in endothelial cells for cardiovascular development. *Dev Cell.* (2004) 7:107–16. doi: 10.1016/j.devcel.2004.06.002
37. Rehman M, Tamagnone L. Semaphorins in cancer: biological mechanisms and therapeutic approaches. *Semin Cell Dev Biol.* (2013) 24:179–89. doi: 10.1016/j.semcdb.2012.10.005
38. Banu N, Teichman J, Dunlap-Brown M, Villegas G, Tufro A. Semaphorin 3c regulates endothelial cell function by increasing integrin activity. *FASEB J.* (2006) 20:2150–2. doi: 10.1096/fj.05-5698fje
39. Xu C, Zhu S, Wu M, Han W, Yu Y. Functional receptors and intracellular signal pathways of midkine (Mk) and pleiotrophin (Ptn). *Biol Pharm Bull.* (2014) 37:511–20. doi: 10.1248/bpb.b13-00845
40. Sorrelle N, Dominguez ATA, Brekken RA. From top to bottom: midkine and pleiotrophin as emerging players in immune regulation. *J Leukoc Biol.* (2017) 102:277–86. doi: 10.1189/jlb.3MR1116-475R
41. Raulo E, Chernousov MA, Carey DJ, Nolo R, Rauvala H. Isolation of a neuronal cell surface receptor of heparin binding growth-associated molecule (Hb-Gam). identification as N-syndecan (Syndecan-3). *J Biol Chem.* (1994) 269:12999–3004.
42. Imai S, Kaksonen M, Raulo E, Kinnunen T, Fages C, Meng X, et al. Osteoblast recruitment and bone formation enhanced by cell matrix-associated heparin-binding growth-associated molecule (Hb-Gam). *J Cell Biol.* (1998) 143:1113–28. doi: 10.1083/jcb.143.4.1113
43. Koutsoumpa M, Polyarchou C, Courty J, Zhang Y, Kieffer N, Mikelis C, et al. Interplay between Alpha5beta3 integrin and nucleolin regulates human endothelial and glioma cell migration. *J Biol Chem.* (2013) 288:343–54. doi: 10.1074/jbc.M112.387076
44. Lamprou M, Koutsoumpa M, Kaspis A, Zompra K, Tselios T, Papadimitriou E. Binding of pleiotrophin to cell surface nucleolin mediates prostate cancer cell adhesion to osteoblasts. *Tissue Cell.* (2022) 76:101801. doi: 10.1016/j.tice.2022.101801
45. Shao Y, Saredy J, Yang WY, Sun Y, Lu Y, Saaoud F, et al. Vascular endothelial cells and innate immunity. *Arterioscler Thromb Vasc Biol.* (2020) 40:e138–52. doi: 10.1161/ATVBAHA.120.314330
46. Drummer CT, Saaoud F, Shao Y, Sun Y, Xu K, Lu Y, et al. Trained immunity and reactivity of macrophages and endothelial cells. *Arterioscler Thromb Vasc Biol.* (2021) 41:1032–46. doi: 10.1161/ATVBAHA.120.315452
47. Mai J, Virtue A, Shen J, Wang H, Yang XF. An evolving new paradigm: endothelial cells—conditional innate immune cells. *J Hematol Oncol.* (2013) 6:61. doi: 10.1186/1756-8722-6-61
48. Direder M, Weiss T, Copic D, Vorstandlechner V, Laggner M, Pfisterer K, et al. Schwann cells contribute to keloid formation. *Matrix Biol.* (2022) 108:55–76. doi: 10.1016/j.matbio.2022.03.001



OPEN ACCESS

EDITED BY

Paolo Romita,
University of Bari Aldo Moro, Italy

REVIEWED BY

Yosep Chong,
Uijeongbu St. Mary's Hospital,
South Korea
Manuel Valdebran Canales,
Medical University of South Carolina,
United States

*CORRESPONDENCE

Zhang Yu
zhangyu19940419@163.com

SPECIALTY SECTION

This article was submitted to
Dermatology,
a section of the journal
Frontiers in Medicine

RECEIVED 09 June 2022

ACCEPTED 17 October 2022

PUBLISHED 03 November 2022

CITATION

Yu Z, Kaizhi S, Jianwen H, Guanyu Y
and Yonggang W (2022) A deep
learning-based approach toward
differentiating scalp psoriasis and
seborrheic dermatitis from
dermoscopic images.
Front. Med. 9:965423.
doi: 10.3389/fmed.2022.965423

COPYRIGHT

© 2022 Yu, Kaizhi, Jianwen, Guanyu
and Yonggang. This is an open-access
article distributed under the terms of
the [Creative Commons Attribution
License \(CC BY\)](#). The use, distribution
or reproduction in other forums is
permitted, provided the original
author(s) and the copyright owner(s)
are credited and that the original
publication in this journal is cited, in
accordance with accepted academic
practice. No use, distribution or
reproduction is permitted which does
not comply with these terms.

A deep learning-based approach toward differentiating scalp psoriasis and seborrheic dermatitis from dermoscopic images

Zhang Yu*, Shen Kaizhi, Han Jianwen, Yu Guanyu and
Wang Yonggang

Inner Mongolia Medical University, Hohhot, China

Objectives: This study aims to develop a new diagnostic method for discriminating scalp psoriasis and seborrheic dermatitis based on a deep learning (DL) model, which uses the dermoscopic image as input and achieved higher accuracy than dermatologists trained with dermoscopy.

Methods: A total of 1,358 pictures (obtained from 617 patients) with pathological and diagnostic confirmed skin diseases (508 psoriasis, 850 seborrheic dermatitis) were randomly allocated into the training, validation, and testing datasets (1,088/134/136) in this study. A DL model concerning dermoscopic images was established using the transfer learning technique and trained for diagnosing two diseases.

Results: The developed DL model exhibits good sensitivity, specificity, and Area Under Curve (AUC) (96.1, 88.2, and 0.922%, respectively), it outperformed all dermatologists in the diagnosis of scalp psoriasis and seborrheic dermatitis when compared to five dermatologists with various levels of experience. Furthermore, non-proficient doctors with the assistance of the DL model can achieve comparable diagnostic performance to dermatologists proficient in dermoscopy. One dermatology graduate student and two general practitioners significantly improved their diagnostic performance, where their AUC values increased from 0.600, 0.537, and 0.575 to 0.849, 0.778, and 0.788, respectively, and their diagnosis consistency was also improved as the kappa values went from 0.191, 0.071, and 0.143 to 0.679, 0.550, and 0.568, respectively. DL enjoys favorable computational efficiency and requires few computational resources, making it easy to deploy in hospitals.

Conclusions: The developed DL model has favorable performance in discriminating two skin diseases and can improve the diagnosis, clinical decision-making, and treatment of dermatologists in primary hospitals.

KEYWORDS

deep learning, scalp psoriasis, seborrheic dermatitis, dermoscopy, artificial intelligence (AI)

Introduction

As a common and recurring chronic inflammatory skin disease, psoriasis has been an affliction of over 125 million people worldwide (1). It manifests high incidence, easy recurrence, and long course, which makes a significant impact on the physical and mental health of patients. In China, more than six million diagnoses of psoriasis have been reported, and the prevalence is increasing year by year, which poses a challenge to public health. The problem is exacerbated by insufficient and unevenly distributed medical resources. It is known that the diagnosis of psoriasis relies on doctors' skills and auxiliary measures. However, most experienced dermatologists and medical devices are deployed in big cities, whereas dermatologists and general practitioners in remote areas exhibit low diagnostic accuracy for skin disease. Consequently, many patients are misdiagnosed or under delayed treatment. In this context, we aim to develop an automatic diagnosis technology for addressing the above problem.

An appropriate auxiliary diagnostic measure should be determined as the input of the automatic diagnosis technology. Histopathology is not regarded as the primary examination in many hospitals due to the requirement for traumatic samples and skin pathology experts, and RCM (reflectance confocal microscopy) is also unfavorable in practice owing to its high costs (2). The dermoscopy instrument, as a low-cost and noninvasive device, takes the enlarged view of lesions with simple backgrounds, few interference factors, and obvious structure, and therefore enjoys high accuracy and specificity in psoriasis lesions diagnosis. Thus, dermoscopy is adopted in this study. The characteristics of typical scalp psoriasis and seborrheic dermatitis under dermoscopy are shown in Figure 1.

Based on dermoscopic images, we develop a deep learning (DL)-based classification model for the diagnosis of skin diseases. The DL technique eliminates tedious preprocessing and complicated intermediate design by achieving data-driven end-to-end classification, which greatly simplifies method design. The representative DL technique, namely convolutional neural networks (CNNs) exhibit remarkable capability in feature extraction and thus has been widely employed for image classification (3–5). Over the past few years, a variety of DL-based medical applications have been reported, such as the assisted diagnosis of digestive tract tumors with pathology, MRI, and ultrasound images (6–9), the diagnosis of dysphagia with photographs of the anterior neck (10), and the precise location and identification of cells in microscopic images (11). In the dermatology field, DL uses trunk or longitudinal skin stratification images of patients' lesions to diagnose skin tumors, atopic dermatitis, psoriasis, and fungal infections (12–15). However, rare studies focus on scalp skin disease, since it is challenging to be accurately diagnosed due to hair interference, unobvious vascular features, and coverage of thick white scales. In particular, scalp psoriasis is one of the most

affected conditions since it is hard to distinguish from seborrheic dermatitis. Motivated by this, we propose a DL-based classification model for psoriasis and seborrheic dermatitis on the scalp in this paper to give diagnostic suggestions in a variety of complex situations.

The contributions of this study are summarized as follow, First, we propose a new dataset including various scalp psoriasis and scalp seborrheic dermatitis samples to train the DL model. Then, the well-trained DL model is compared with those of 5 Chinese certified dermatologists proficient in diagnosing using dermoscopy with respect to diagnostic accuracy, and we validate the DL model can benefit non-proficient doctors by improving their performance. Finally, we evaluate the feasibility of the model by assessing its computational load. Overall, the developed DL model can be used as a pre-screening tool to help the general practitioners make recommendations when faced with scalp psoriasis and scalp seborrheic dermatitis, assist dermatologists to prioritize their diagnoses, and lay the foundation for precision medicine and telemedicine consultation.

Materials and methods

Design and settings

In this diagnostic study, all the dermoscopic images were obtained from the Department of Dermatology, Affiliated Hospital of Inner Mongolia Medical University. The trial was reviewed and approved by the institutional ethics committee. From December 2019 to January 31, 2022, we selected a total of 1,624 dermoscopic images (obtained from 735 patients) of scalp parts preliminarily diagnosed with psoriasis and seborrheic dermatitis. The model of dermoscopy is BN-PFMF-8001, the magnification is 20–220x, and the imaging resolution is $2,592 \times 1,944$ pixel. During the dermoscopic image acquisition, we selected different magnifications of the 20–40x interval according to the patient's lesion size. In order to enhance the generalization ability of the developed DL model, image samples for training were processed by data augmentation methods. The images were rotated randomly at $[-90, 90]$ degrees and scaled randomly at $[1, 2]$. These image rotations and flips were performed in MATLAB using the deep learning toolbox. And the dataset was also standardized into a Gaussian distribution. Two senior dermatologists interpreted the images. Two sixty six images were removed due to ambiguous diagnosis. They combined the pathological results and diagnostic treatment effects, and re-diagnosed and classified the dermoscopic images. When there are different opinions between the two dermatologists, another dermatologist with 7 years of experience in dermatology is introduced to make a decision. The experience of 3 dermatologists in reading the test set ranged from 5 to 7 years. A total of 1,358 pictures (obtained from 617 patients)

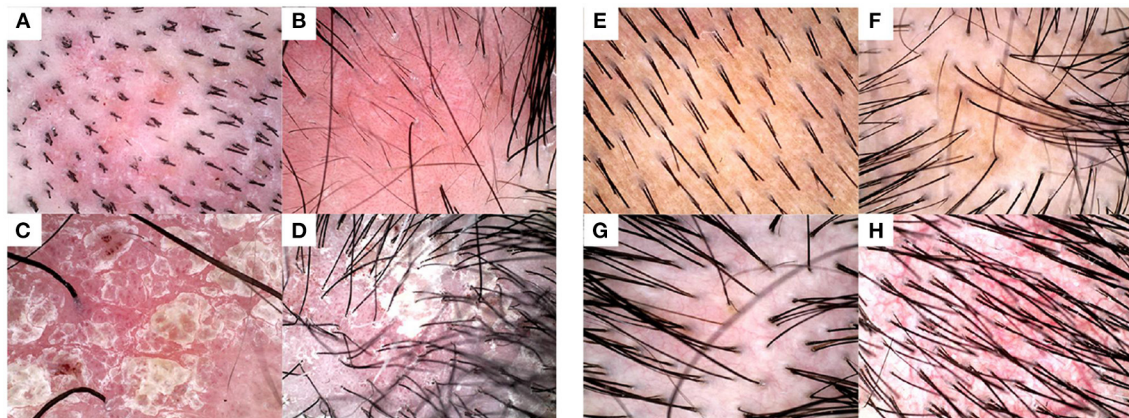


FIGURE 1

Examples of typical dermoscopic images. Typical images from (A–D) psoriasis lesions, wherein annular and hairpin blood vessels that have high specificity for the diagnosis can be seen under dermoscopy, and (E–H) seborrheic dermatitis lesions, wherein branching and atypical vessels show distinct unstructured white areas and honeycombed pigmentation networks.

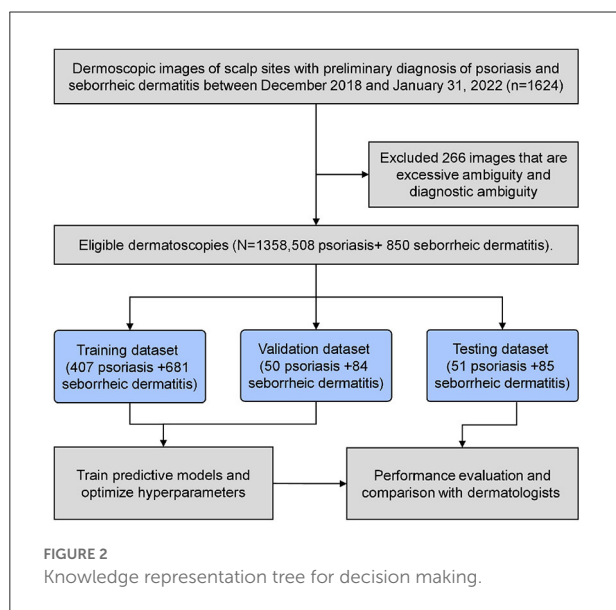


FIGURE 2

Knowledge representation tree for decision making.

with clinically proven scalp psoriasis (508 cases) and seborrhea dermatitis (850 cases) were randomly assigned to training, validation, and test datasets (1,088/134/136 lesions). 650 of the 1,358 photos (from 331 patients) had been confirmed by pathological biopsy. The above described is shown in the workflow chart in Figure 2.

We developed a DL model based on the above 1,358 dermoscopic images of scalp sites, wherein the training and validation datasets were used for the model training, and the testing dataset was employed for the model evaluation. Owing to the powerful information extraction performance of the convolution-based deep learning model, in our methodology,

image titling or subsetting operations were not involved. An image interpolation method was adopted to remap the original dermatoscopy image to the specified input size (224×224 pixel). To evaluate the developed DL model, we compare its diagnostic accuracy against dermatologists with various dermatoscopy experience levels, namely five dermatologists, a dermatology graduate student, and two general practitioners. Five dermatologists and one dermatology graduate student were from two hospitals affiliated with Inner Mongolia Medical University, and two general practitioners were from township hospitals in Inner Mongolia Province. Among the five dermatologists, three (60%) were male and two (40%) were female. One dermatology graduate student and two general practitioners were female. Additionally, two dermatologists have <3 years of experience in dermatoscopy, two between 3 and 5 years and one more than 5 years.

Development of the DL diagnosis model

The developed DL model was established based on the transfer learning technique. We employed the far-reaching deep neural network, namely GoogLeNet as the backbone of the developed model. GoogLeNet is a 22-layer deep convolutional network that is pre-trained using the ImageNet dataset for image classification. To establish the DL model, we tweaked the last convolutional layer of the GoogleNet and used the transfer learning technique to retrain the parameters of the deep network for achieving the diagnosis of psoriasis and seborrheic dermatitis. The schematic diagram of the model is shown in Figure 3. As for the learning configuration, we adopted an Adam optimizer with an initial learning rate of $1e-4$ and the mean square error (MSE) loss function with L2

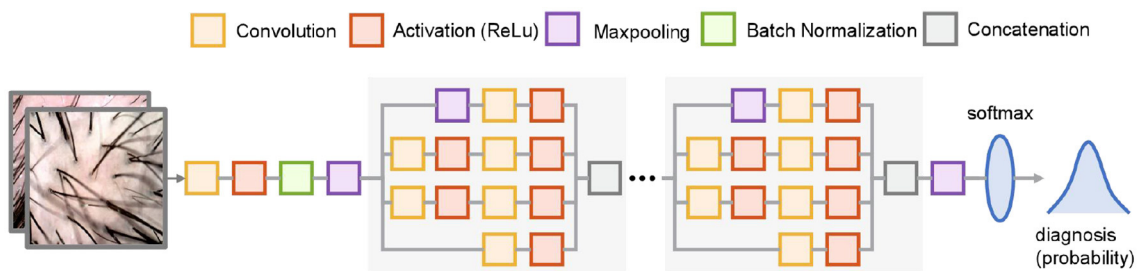


FIGURE 3

Schematic diagram of the architecture of the developed DL model. The gray boxed parts are repeated nine times and partially omitted for brevity. The model receives 224×224 pixel images and outputs the probability of two diseases.

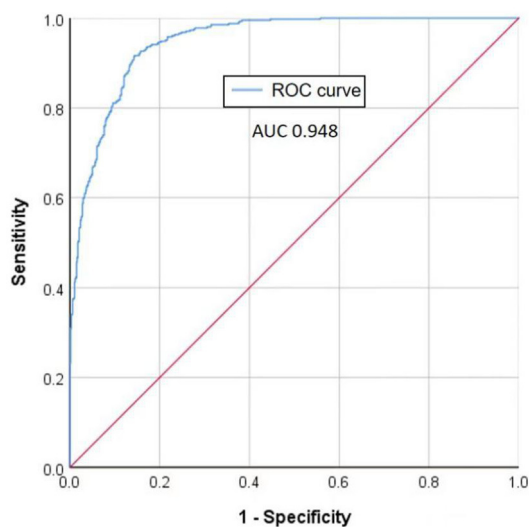


FIGURE 4

ROC curve of the training set of the developed DL model.

regularization. The training dataset was for model learning and the validation dataset was to eliminate the overfitting problem in the training process. The model training was performed on a PC with a GPU of Nvidia RTX 3070, and the scripts were written using MATLAB. More training details can be found in [Supplementary materials](#).

Statistical analysis

Analysis of the data was completed using SPSS (Version 25.0; Chicago, IL), with a two-sided P -value of <0.05 being considered statistically significant. The performance of the diagnosis of the developed model was assessed by the receiver operating characteristic (ROC) curve analysis and the area under

curve (AUC). Z test was used to compare the differences of AUCs for different predictive results.

Results

Patient characteristics

A total of 1,358 patients were enrolled in the training, validation, and testing cohort. In the training (psoriasis accounted for 30.0% [407/1,088]), validation (psoriasis accounted for 37.3% [50/134]) and test (psoriasis accounted for 37.5% [51/136]) data sets, there was no significant difference in the prevalence of scalp psoriasis and seborrheic dermatitis ($\chi^2 = 2.933$, $P = 0.231$). There were 508 patients with psoriasis, aged 35.4 ± 11.2 . Men account for 265/508 and women for 243/508. There were 850 patients with seborrheic dermatitis, aged 32.6 ± 9.9 . Men account for 476/850 and women account for 374/850.

Diagnostic performance comparison between the DL model and dermatologists

To evaluate the training performance of the developed DL model, the ROC curve performed using the training dataset is illustrated in [Figure 4](#), where a 0.948 AUC indicates our model achieves a favorable accuracy.

In the test data set, when comparing the diagnostic performance of the prediction model and dermatologists with different years of experience in the diagnosis of seborrheic dermatitis and psoriasis on the scalp, the results showed that the diagnostic ability of the DL model was better than those of five dermatologists. [Figure 5](#) summarizes the sensitivity, specificity and AUC of the combined model and dermatologist. As shown in [Figure 5](#), the AUC values reflect the level of diagnostic accuracy. As a result of limited medical resources in practice, it is common for general practitioners and dermatology

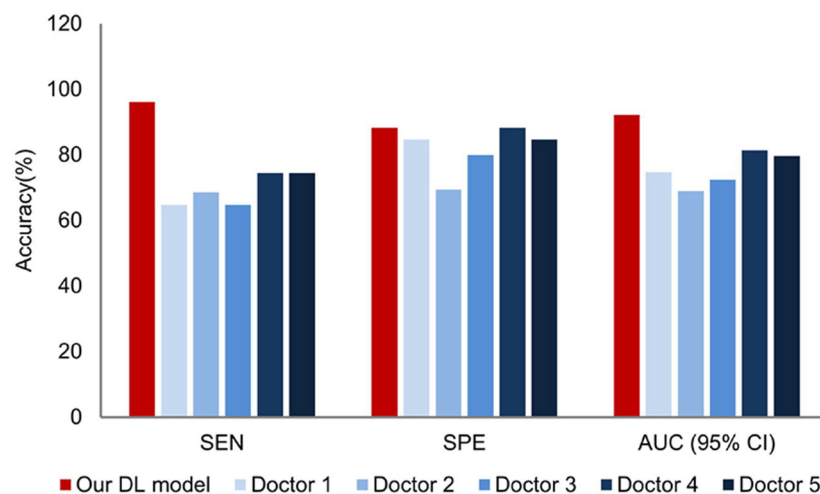


FIGURE 5
Comparison of the DL model and dermatologist in the testing dataset.

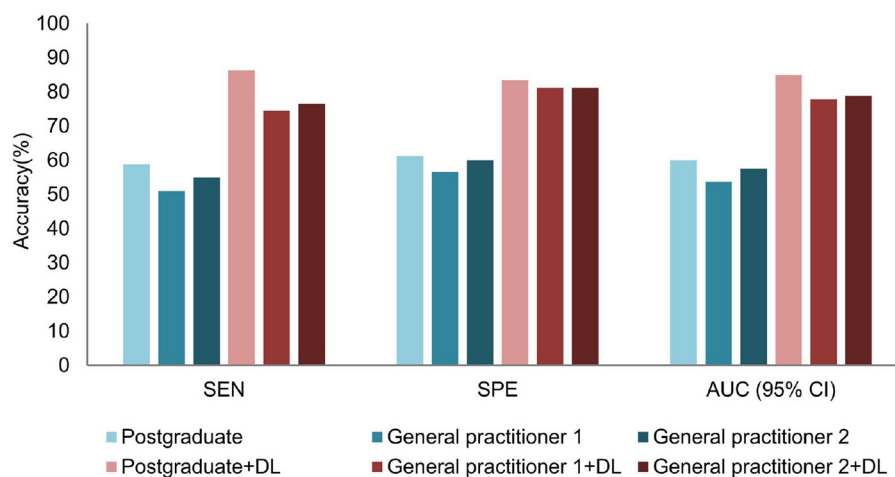


FIGURE 6
Comparison before and after DL model assistance for graduate students and general practitioners in the test dataset.

students to diagnose and treat skin conditions, and their performance in dermoscopy and dermatology diagnosis is inferior to dermatologists. Thus, it is necessary to investigate the effect of the proposed DL model on the diagnostic performance of general practitioners and dermatology students. As shown in Figure 6, the dermatology graduate student and two general practitioners were able to improve the accuracy of dermoscopy identification with the assistance of the DL model. The AUCs of the dermatology graduate student, general practitioner 1, and general practitioner 2 increased from 0.600, 0.537, 0.575 to 0.849, 0.778, 0.788, respectively. Assisted by the DL model, their diagnostic ability was even comparable to that of dermatologists.

Furthermore, the consistency of the dermatology graduate student and two general practitioners significantly improved as shown in Figure 7. In the absence of the DL help, their kappa values were 0.191, 0.071, and 0.143, respectively. When assisted by the DL model, kappa values were raised to 0.679, 0.550, and 0.568, respectively, which were equivalent to dermatologists who have studied dermatology.

Furthermore, the developed DL model can achieve accurate diagnosis regarding lesion images with few typical features. Six lesion images with vague diagnoses are demonstrated in Figure 8, where no obvious signs of typical psoriasis or seborrheic dermatitis were found, such as round vessels, hairpin

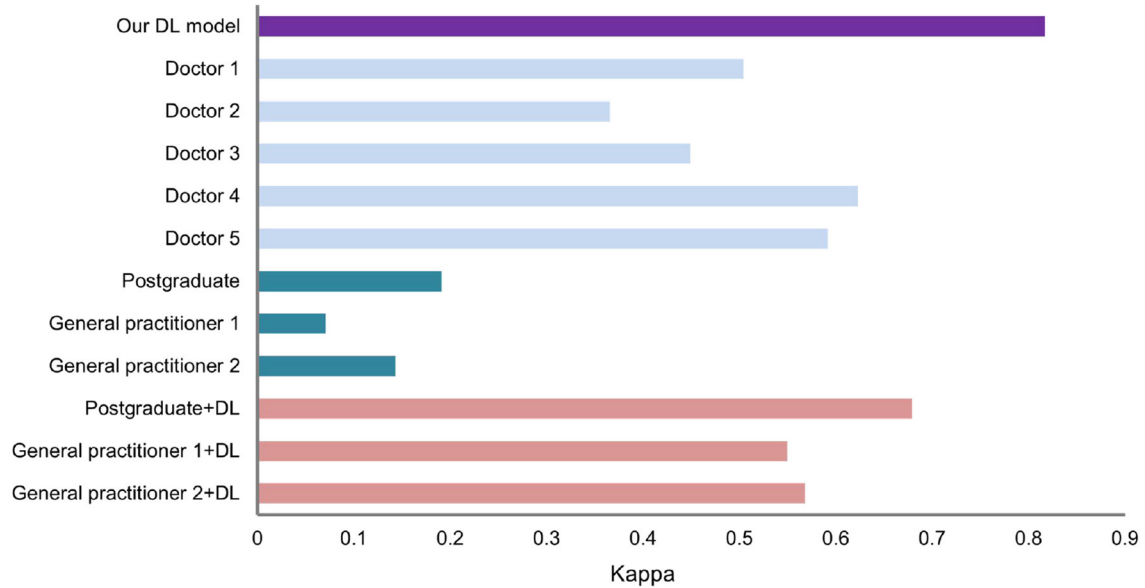


FIGURE 7
Kappa value of the DL model and dermatologist.

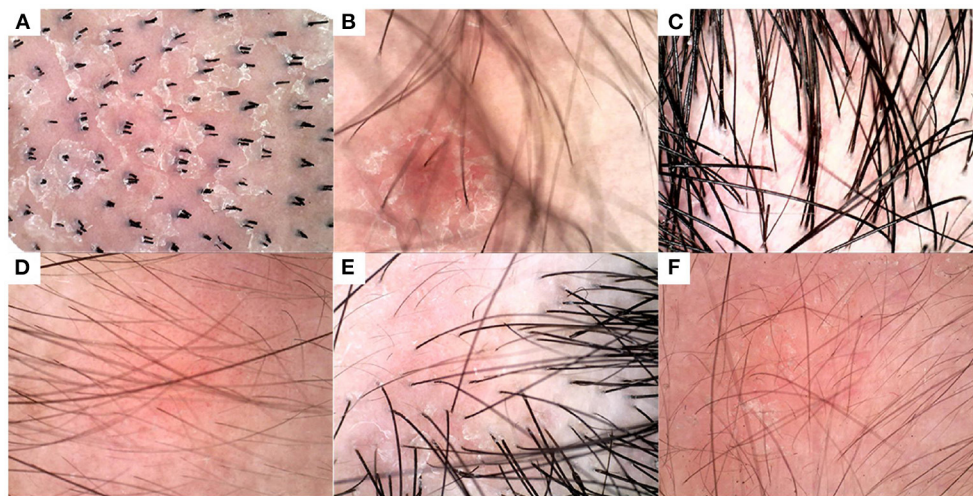


FIGURE 8
Diagnosis results of DL model and humans (five physicians) on some indistinguishable lesion images. The below figures are represented in ground truth disease type and correctly diagnosis rate of humans: (A) seborrheic dermatitis, 40%, (B) seborrheic dermatitis, 60%, (C) seborrheic dermatitis, 0%, (D) psoriasis, 20%, (E) psoriasis, 40%, and (F) psoriasis, 40%. For comparison, the DL model correctly diagnosed all six images.

vessels, branch vessels, or atypical vessels. For these images, the probabilities of correct diagnosis by five dermatologists were 40, 60, 0, 20, 40, and 40%, respectively, whereas the DL model achieved the correct diagnosis in all lesions. It is probably because DL can eliminate dandruff, hair, and other influencing factors based on other information in lesions.

Nonetheless, it is significant to analyze the failure cases of the DL model. As shown in Figure 9, the weights of the

last intermediate layer of the DL model were extracted and plotted to visualize the attention of the model, where a red area indicates higher attention whereas a blue area indicates lower attention. Figures 9B,D show that the DL model paid the most attention to the blood scab and non-vascular area, respectively. However, in a human expert's opinion, vascular characteristics should be the preferred diagnosis mark. To some extent, these attention distributions explain the DL model's misdiagnosis.

TABLE 1 Clock time consumption of the DL model.

Inputs	Device	Mean (s)	Standard deviation (s)
One sample (1 image)	GPU	0.0246	0.0061
Total test set (136 images)	GPU	0.5501	0.0150
One sample (1 image)	CPU	0.0488	0.0014
Total test set (136 images)	CPU	2.2209	0.2380

Means and standard deviations are obtained based on 30 runs.

Comparing the correctly diagnosed and incorrectly diagnosed images in Figures 8, 9, it is indicated that a better cleanup of the affected scalp area could potentially improve the DL model's accuracy.

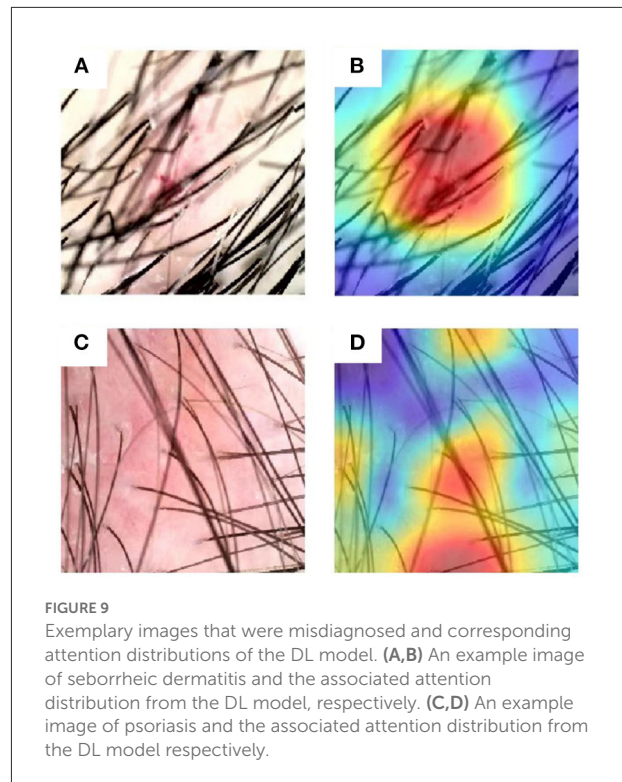
Overall, the diagnostic accuracy of the DL model is still higher than that of 5 dermatologists trained in dermoscopy with respect to dermoscopic images with less obvious typical characteristics.

Computational performance evaluation of the DL model

The computation performance of the developed DL model is of great importance to evaluate its applicability in practice. The DL model has higher computational efficiency on a GPU in general, but it can also be deployed on CPU-only devices when considering the hospital setting. A GPU of Nvidia RTX 3070 and a CPU of Intel i3 8100, respectively served as the computing device of the DL model to simulate the real-world deployment environment. Then we calculated the clock time consumption of two devices in completing the diagnosis and provided the results in Table 1. Our results suggest that the GPU is indeed faster at executing models. However, the computational cost of single dermoscopic images in the CPU environment is also very low. In this way, we validated that the developed DL model exhibits favorable real-time computational efficiency and can be employed in real-world hospitals for diagnosis.

Discussion

Accurate identification of psoriasis and seborrheic dermatitis on the scalp is of great significance to numerous patients in China. An accurate and rapid examination will greatly reduce patients' anxiety by cutting out biopsy and pathological confirmations and avoiding incorrect treatment. In this study, we developed a deep learning model to diagnose scalp psoriasis and seborrheic dermatitis under dermoscopy. The DL model exhibits better diagnostic performance than most dermatologists. In the diagnosis of psoriasis on scalp sites,



DL models have higher sensitivity and specificity compared with dermatologists, thus meeting the clinical requirements for accurate diagnosis. Furthermore, the DL model can benefit dermatologists with varying levels of training and experience: one dermatology graduate student and general practitioners can greatly improve their diagnosis accuracy by using the DL model.

The results show the superiority of our DL model in the diagnostic accuracy of scalp psoriasis and seborrheic dermatitis, which could potentially benefit dermatologists. Based on the diagnosis results of 51 pictures of psoriasis cases in the test set, the model reached 96.1% sensitivity. Therefore, the DL model can prevent the delay of patients' treatment, tackle the development of the disease course, and improve the prognosis when encountering patients with ambiguous diagnoses. In addition, we can see from Figures 5, 6 that the DL model not only outperformed the diagnostic accuracy of the five dermatologists, but also assists graduate students and general practitioners to significantly improve the diagnostic accuracy.

Despite the resource consumption of the training process, the well-trained model can easily be implemented in simple digital skin examination systems, such as personal computers. The developed model can identify the basic characteristics of the two diseases, eliminate hair interference, and enable remote diagnosis. The global pandemic of COVID-19 has strained medical resources and made it hard for patients to access hospitals (especially those that offer higher-level treatments).

In this context, increasing numbers of dermatological patients seek online advice due to the visibility of most skin diseases. However, for online treatment, patients must provide images of their lesions. The image quality of the scalp surface and the difficulty of removing scales complicate medical judgment. The DL model developed in this paper process 224×224 pixel images and can achieve accurate and rapid diagnosis with low image resolution.

Limitations

This study selected dermoscopic images from the dermatology department of the dermatology hospital of the Inner Mongolia Medical University. It is not excluded that the results of this study may not fully represent all manifestations of scalp psoriasis and seborrheic dermatitis, and there may be the problem of generalization. By collecting images from the same well-trained dermatologist, we eliminate the variance caused by the proficiency of different dermatologists in the operation of dermatoscopy. Nevertheless, it should be considered to reduce the requirements for photo quality and the photography process, so that the algorithm can be more easily applied to practical situations. In addition, the diagnosis of dermatologists generally needs to start with the patient's medical history. This study focuses on visual information and does not consider the influencing factors of skin lesions such as the family history of the disease, the degree of activity, and obesity. A total of 650 of the 1,358 photos in this study (from 331 patients) have been confirmed by pathological biopsy; however, there may be diagnostic bias in the samples that have not been confirmed by pathological biopsy. Dermoscopy selection, hair coverage, and other factors can also affect diagnosis accuracy. The images we selected in the training, validation, and test sets were all from fair-skinned people, all of whom were Chinese. In the future, these factors will be integrated into the DL model to further improve diagnostic accuracy.

Conclusions

The DL model has high specificity (88.2%), sensitivity (96.1%), and AUC (0.922) in differentiating scalp psoriasis and seborrheic dermatitis. In terms of the AUC values, the accuracy of the DL model is higher than that of dermatologists who have undergone dermoscopy training. The DL model can also help the dermatology graduate students and general practitioners to improve the diagnostic accuracy of scalp psoriasis and seborrheic dermatitis. With the assistance of the DL model, the AUCs of one dermatology graduate student and two general practitioners have been increased by 0.249, 0.241, 0.213, respectively.

Data availability statement

The raw data supporting the conclusions of this article will be made available by the authors, without undue reservation.

Ethics statement

The studies involving human participants were reviewed and approved by Inner Mongolia Medical University. Written informed consent for participation was not required for this study in accordance with the national legislation and the institutional requirements. Written informed consent was not obtained from the individual(s) for the publication of any potentially identifiable images or data included in this article.

Author contributions

ZY: conceptualization, methodology, software, validation, formal analysis, writing, and funding acquisition. HJ, SK, WY, and YG: resources, data curation, and investigation. All authors contributed to the article and approved the submitted version.

Conflict of interest

The authors declare that the research was conducted in the absence of any commercial or financial relationships that could be construed as a potential conflict of interest.

Publisher's note

All claims expressed in this article are solely those of the authors and do not necessarily represent those of their affiliated organizations, or those of the publisher, the editors and the reviewers. Any product that may be evaluated in this article, or claim that may be made by its manufacturer, is not guaranteed or endorsed by the publisher.

Supplementary material

The Supplementary Material for this article can be found online at: <https://www.frontiersin.org/articles/10.3389/fmed.2022.965423/full#supplementary-material>

References

1. National Psoriasis Foundation Data. Available online at: www.psoriasis.org (accessed October 2017).
2. Lian-Sheng ZH, Zhi-Ping WE, Yan-Qun LI. Sensitivity and specificity of Munro microabscess detected by reflectance confocal microscopy in the diagnosis of psoriasis vulgaris. *J Dermatol.* (2012) 39:282–3. doi: 10.1111/j.1346-8138.2011.01366.x
3. He K, Zhang X, Ren S, Sun J. Deep residual learning for image recognition. In: *Proceedings of the IEEE Conference on Computer Vision and Pattern Recognition*. Las Vegas, NV: IEEE (2016). doi: 10.1109/CVPR.2016.90
4. Krizhevsky A, Sutskever I, Hinton GE. Imagenet classification with deep convolutional neural networks. *Adv Neural Inform Process Syst.* (2012) 60:84–90. doi: 10.1145/3065386
5. Chandra SS, Bran Lorenzana M, Liu X, Liu S, Bollmann S, Crozier S. Deep learning in magnetic resonance image reconstruction. *J Med Imag Radiat Oncol.* (2021) 65:564–77. doi: 10.1111/1754-9485.13276
6. Wang J, Liu X. Medical image recognition and segmentation of pathological slices of gastric cancer based on Deeplab v3+ neural network. *Comput Methods Programs Biomed.* (2021) 207:106210. doi: 10.1016/j.cmpb.2021.106210
7. Wang P, Liu X, Berzin TM, Brown JR, Liu P, Zhou C, et al. Effect of a deep-learning computer-aided detection system on adenoma detection during colonoscopy (CAdE-DB trial): a double-blind randomised study. *Lancet Gastroenterol Hepatol.* (2020) 5:343–51. doi: 10.1016/S2468-1253(19)30411-X
8. Zhang W, Yin H, Huang Z, Zhao J, Zheng H, He D, et al. Development and validation of MRI-based deep learning models for prediction of microsatellite instability in rectal cancer. *Cancer Med.* (2021) 10:4164–73. doi: 10.1002/cam4.3957
9. Wang L, Song H, Wang M, Wang H, Ge R, Shen Y, et al. Utilization of ultrasonic image characteristics combined with endoscopic detection on the basis of artificial intelligence algorithm in diagnosis of early upper gastrointestinal cancer. *J Healthcare Eng.* (2021). doi: 10.1155/2021/2773022
10. Sakai K, Gilmour S, Hoshino E, Nakayama E, Momosaki R, Sakata N, et al. A machine learning-based screening test for sarcopenic dysphagia using image recognition. *Nutrients.* (2021) 13:4009. doi: 10.3390/nu1314009
11. Gol S, Pena RN, Rothschild ME, Tor M, Estany J. A polymorphism in the fatty acid desaturase-2 gene is associated with the arachidonic acid metabolism in pigs. *Sci Rep.* (2018) 8:1–9. doi: 10.1038/s41598-018-32710-w
12. Haenssle HA, Fink C, Schneiderbauer R, Toberer F, Buhl T, Blum A, et al. Man against machine: diagnostic performance of a deep learning convolutional neural network for dermoscopic melanoma recognition in comparison to 58 dermatologists. *Ann Oncol.* (2018) 29:1836–42. doi: 10.1093/annonc/mdy166
13. Esteva A, Kuprel B, Novoa RA, Ko J, Swetter SM, Blau HM, et al. Dermatologist-level classification of skin cancer with deep neural networks. *Nature.* (2017) 542:115–8. doi: 10.1038/nature21056
14. Czajkowska J, Badura P, Korzekwa S, Płatkowska-Szczerek A. Deep learning approach to skin layers segmentation in inflammatory dermatoses. *Ultrasonics.* (2021) 114:106412. doi: 10.1016/j.ultras.2021.106412
15. Tognetti L, Bonechi S, Andreini P, Bianchini M, Scarselli F, Cevenini G, et al. A new deep learning approach integrated with clinical data for the dermoscopic differentiation of early melanomas from atypical nevi. *J Dermatol Sci.* (2021) 101:115–22. doi: 10.1016/j.jdermsci.2020.11.009



OPEN ACCESS

EDITED BY
Robert Gniadecki,
University of Alberta, Canada

REVIEWED BY
Carmen Dell'Aquila,
University of Trieste, Italy
Roberta Giuffrida,
University of Messina, Italy

*CORRESPONDENCE
Irene Fusco
i.fusco@deka.it

SPECIALTY SECTION
This article was submitted to
Dermatology,
a section of the journal
Frontiers in Medicine

RECEIVED 04 August 2022
ACCEPTED 04 November 2022
PUBLISHED 21 November 2022

CITATION
Piccolo D, Mutlag MH, Pieri L, Fusco I,
Conforti C, Crisman G and Bonan P
(2022) Lipoma management with
a minimally invasive 1,444 nm Nd:YAG
laser technique.
Front. Med. 9:1011468.
doi: 10.3389/fmed.2022.1011468

COPYRIGHT
© 2022 Piccolo, Mutlag, Pieri, Fusco,
Conforti, Crisman and Bonan. This is
an open-access article distributed
under the terms of the [Creative
Commons Attribution License \(CC BY\)](#).
The use, distribution or reproduction in
other forums is permitted, provided
the original author(s) and the copyright
owner(s) are credited and that the
original publication in this journal is
cited, in accordance with accepted
academic practice. No use, distribution
or reproduction is permitted which
does not comply with these terms.

Lipoma management with a minimally invasive 1,444 nm Nd:YAG laser technique

Domenico Piccolo¹, Mohammed Hussein Mutlag²,
Laura Pieri³, Irene Fusco ^{3*}, Claudio Conforti⁴,
Giuliana Crisman¹ and Paolo Bonan⁵

¹Skin Centers, Avezzano, Italy, ²Roma Clinic, Baghdad, Iraq, ³El.En. Group, Calenzano, Italy,
⁴Department of Dermatology and Venereology, Dermatology Clinic, Maggiore Hospital, University
of Trieste, Trieste, Italy, ⁵Laser Cutaneous Cosmetic and Plastic Surgery Unit, Villa Donatello Clinic,
Florence, Italy

Background: Lipoma is the most common benign mesenchymal tumor that is composed of mature fat cells. Subdermal laser lipoma treatment may be recommended as an alternative to surgery for its removal.

Purpose: The purpose of the study was to investigate the efficacy of the 1,444 nm Nd:YAG laser subcutaneous intralesional application as a treatment option for lipoma.

Materials and methods: On 60 patients (37 women and 23 men) with lipomas localized above the muscle and lipomatosis in various regions, a subcutaneous, micro-pulsed 1,444 nm Nd:YAG laser procedure was executed. Before treatment, an ultrasound was performed and the lipomas were measured. The same lighting setup and photographic tools were used to take pictures of each patient.

Results: The lipoma reduced or completely disappeared in all cases at the last follow-up, and no infections, burns, skin lesions, episodes of severe bleeding, or other serious adverse effects were reported. The most common transient side effects were ecchymosis and edema. Partial lesion reduction refers to rare cases of lipomatosis in which the lipomas were so small that suction and accurate positioning of the capsular membrane contours were impossible.

Conclusion: Lipoma treatment with a 1,444 nm Nd:YAG laser is a safe and effective minimally invasive procedure without risk of scarring. For cellular disruption, laser treatment is an effective and safe option.

KEYWORDS

lipoma, 1,444 nm Nd:YAG laser, subcutaneous intralesional application, liposuction, cellular disruption

Introduction

Lipomas are non-cancerous, fatty tissue growths that slowly develop under the skin. A round or oval-shaped mass of fat tissue that is easily moved when touched is referred to as a lipoma and usually does not cause pain. Lipomas are very common; approximately one in every 1,000 people has one, and they most commonly appear between the ages of 40 and 60, but can develop at any age. People of all genders can be affected, and they can even be present at birth; however, women are significantly more likely to be impacted than men. Lipomas can show anywhere in the body, although they are most frequently found in the back, torso, arms, legs, shoulders, neck, and forehead areas. If they press against a nerve or appear near a joint, they can be uncomfortable (1). Lipomas are all composed of white fat. Some lipomas contain blood vessels (angiolipoma, a painful lipoma) as well as other tissues such as fibrous tissue (fibrolipoma), brown fat (hibernoma), or tissue that produces blood cells (myelolipoma). To rule out dangerous disorders such as liposarcoma (a type of cancer), imaging tests like ultrasound, magnetic resonance imaging (MRI) scan, or a computed tomography (CT) scan must be used to analyze lipomas. The symptoms of liposarcoma are similar to those of lipoma. These benign soft tissue tumors can be removed with an outpatient procedure if they cause pain, grow to a large size, or grow in an uncomfortable area; Patients typically leave the hospital the same day after undergoing surgical lipoma excision; in fact, it is an effective and safe procedure. Liposuction may be recommended as an alternative to lipoma surgery to remove the lipoma; liposuction was actually introduced to achieve superior aesthetic results through the use of small incisions (2, 3). The first description of micropulsed Nd:YAG laser lipolysis with optical fiber was in 1994, and it is now one of the most widely used laser assisted lipoplasty methods in the world (4). Previous studies have demonstrated that pulsed Nd:YAG laser has lipolytic effects, causes the coagulation of small vessels and the reticular dermis, and the formation of neocollagen in the subcutaneous layer and dermal tissue. In the treatment of lipoma, Nd:YAG laser acts in two ways: As an optomechanical effect against the lipoma membrane and fat cells, and as thermal heating (thermal effect). The laser action fragments the capsular membrane of a lipoma in the same way that it fragments adipocyte membranes (5). Several interstitial laser systems have been developed over the years, with harmonic Nd:YAG wavelengths such as 1,064, 1,320, and 1,444 nm; additionally, the use of the Nd:YAG laser at 1,444 nm for the treatment of lipomas has been described in the literature. The 1,444 nm wavelength is very safe in laser-assisted lipolytic treatments because the energy is absorbed twice by both water and fat, keeping the tissue adjacent to the target area safe and protected. For laser-assisted lipolysis, it is even asserted that 1,444 nm wavelength is more efficient, because its affinity for fat is ten times that of an equivalent of 1,064 nm wavelength (6).

Laser lipolysis is usually performed using a cannula containing a laser fiber and a minimally invasive approach; the small cannula used for laser irradiation is applied subcutaneously and moved back and forth to allow the laser energy to be adsorbed by the adipocytes. As a result, pores are formed in the adipocyte cell membranes, allowing dissolved fat to migrate into the extracellular space. Compared to traditional liposuction procedures, laser lipolysis causes less bleeding, bruising, and swelling, resulting in a faster recovery (4, 7, 8).

Based on literature findings, this study was conducted in order to assess the efficacy and safety of 1,444 nm Nd:YAG laser for lipoma management.

Materials and methods

Study device and patient population

A subcutaneous, micro-pulsed, 1,444 nm Nd:YAG laser procedure was used on sixty patients (median age, 39 years; range, 24–69 years; 37 women and 23 men) with lipomas localized above the muscle, and lipomatosis in various regions (LipoAI, Deka, Florence, Italy). The study device is intended for soft tissue surgical incision, excision, vaporization, ablation, and coagulation. Skin, cutaneous tissue, subcutaneous tissue, striated and smooth tissue, muscle, cartilage meniscus, mucous membrane, lymph vessels and nodes, organs, and glands are all included. The study device is also approved for laser-assisted lipolysis. Patients who were pregnant or lactating, as well as those with a history of keloid formation were excluded from the study.

Study protocol

Before treatment, an ultrasound was performed and the lipomas were measured (max diameter 15 cm). Lesions were found on the face, neck, torso, and extremities. All patients were photographed in the same lighting setup for documentation. All subjects gave their informed consent. Before beginning the surgery, each lesion was identified and marked. Every process was carried out in an outpatient setting, under aseptic conditions, and subsequently an adequate subcutaneous local anaesthetic/tumescent solution was injected. To make the benign tumor stand out for easier removal, the anaesthetic solution was infiltrated into the tumor rather than the surrounding tissue. A cannula with a 600-m optical fiber was introduced through a 1 mm incision after making sure that the patient and the entire team had appropriate eye protection. The fiber passed through the proximal end of the clamp, in order for the fiber to be a little longer than the cannula. The fiber extended no more than 2–3 mm beyond the end of the cannula. When the laser emission was activated, the fiber tip

had to be outside the cannula. At the end of the treatment, the handpiece was removed from the treatment area. To see the subcutaneous laser action while it was in use, the therapy beam and the targeting beam were coupled into the optical cable from the laser head. The risk of cutaneous burns and perforations was reduced by this trans-illumination effect, which gave the surgeon accurate knowledge of where and at what level the Nd:YAG laser was working. The more intense the aiming light, the more superficial (subdermal) the laser treatment. The following parameters were used to treat subjects in a single session of micropulsed (max 100 μ s) subdermal 1,444 nm Nd:YAG laser energy: the pulse rate is 30 Hz, and the power was 6 W. The lipoma size and endpoint determined the total accumulated energy used in each case. The clinical endpoint was determined by palpation, the creation of the optimal contour and shape, and the elimination of cannula resistance, which triggered lipolysis and the subsequent transformation of the fatty tissue into an oily, less dense solution. The laser was applied to three layers in large lesions (more than 5 cm in largest diameter): deep, medium, and finally subdermal.

Using a 2-mm-diameter cannula and a negative pressure of 0.5 atm (50 kPa or 350–400 mmHg), an oily solution containing fat cell debris and membrane dissolved lipid was aspirated from the area after treatment. The incision site was closed with sutures or covered with sterile-strips; at the end of the procedure, it was covered with a smooth, non-adherent antimicrobial dressing, such as compression bandages, for 1-week post procedure. Following surgery, the patients were checked on a regular basis. The follow-up period ranged from 1 week to 6 months, with 1- and 3-month interim visits.

Adverse events

During the study all possible adverse effects at the treatment site were monitored.

Results

All patients were pleased with the small 1 mm wounds from the cannula entry point well, which were no longer visible a few months after laser treatment. Patients returned for follow-up exams on a regular basis following laser surgery. At the last follow-up, the lipoma had reduced or completely disappeared in all cases, and no infections, burns, skin lesions, episodes of severe bleeding, or other serious adverse effects were reported. Two cases representing the aesthetic improvement of the lipoma after treatment are clearly shown in **Figures 1–3**. The transient side effects were mostly ecchymosis and edema. All subjects tolerated the postsurgical period well. Patients generally reported a “prickling” sensation for a couple of days without severe pain. Cases of partial lesion reduction refer to rare cases

of lipomatosis in which the dimensions of the lipomas were so small that suction and accurate positioning of the contours of the capsular membrane were impossible.

Discussion

A lipoma is a benign soft tissue tumor composed of fat cells that grows and often requires removal as the benign tumor grows because it can become not only an aesthetic problem but can also cause nerve compression. Although the exact mechanism of lipoma formation is uncertain, it has been suggested that following blunt trauma, rupture of the fibrous septum may result in adipose tissue proliferation (9). Surgery and liposuction have been the typical treatments for this condition, allowing for histopathological analysis of the tissue removed. The main disadvantage of surgical excision is the possibility of large and visible scars that will be permanent due to the size of the tumor and the possible recovery time. Liposuction has been suggested as a less invasive and more aesthetically pleasing treatment option (10, 11). Although liposuction is widely used, the presence of fibrous structures in lipomas and the small dimensions of benign tumors can be a limitation in some cases; in fact, relapse rates are higher in these cases because the remains of the capsule can be left in place. Liposuction therapy is not appropriate for the rare CD34-positive spindle cell lipoma, which can be “fat-free” (12). It has been reported in the literature that up to 10% of lipomas are not completely removed (11). The use of laser therapy for the treatment of lipomas is already validated in the literature (**Table 1**).

A subdermal Nd:YAG laser method was used to treat 83.3% of lesions in a single session. The side effects were minor and transient, and the small 1–2 mm wound was well tolerated by all patients (1). The recurrence rate in giant lipomas was higher, approaching 18% in surgically removed tumors (13). Indeed, giant lipomas are therapeutically challenging (14, 15), and in these cases, the ability to prevent lipoma relapse using the same minimally invasive 1,444 nm device and technique, while avoiding large scars, is advantageous. The use of the pulsed 1,444 nm Nd:YAG laser as a treatment option for lipomas overcomes the limitations of traditional tumescent liposuction with minimal invasiveness. Due to the excellent aesthetic results, the need for multiple treatments does not appear to be a major disadvantage in some patients. Compared to the 1,064 nm wavelength, the 1,444 nm wavelength has a substantially higher duality of absorption in both water and fat (16). The high fat absorption ensures efficient lipolysis, and the high-water absorption confines the thermal reaction to the tissues surrounding the optical fiber tip. In *in vivo* minipig and *in vitro* human fat experiments, the 1,444 nm Nd:YAG laser demonstrated a greater lipolytic effect than the 1,064 nm Nd:YAG laser (6). Since its initial description in 1994, Nd:YAG laser lipolysis has mostly been



FIGURE 1

Image of giant lipoma placed on patient's back acquired using the 3D Photography System LifeViz® Mini (QuantifiCare) before (A) and 6 months after laser treatment (B). A complete removal of the lipoma is observed without any aesthetic damage.

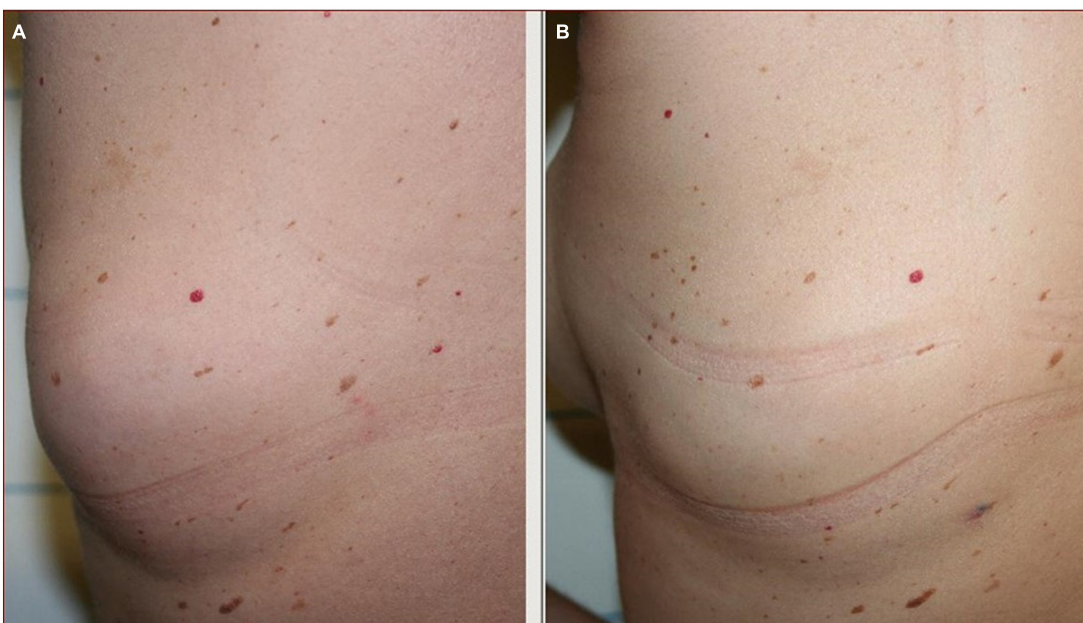


FIGURE 2

Lipoma on patient's back (A). Photographic evaluation shows a complete lipoma removal after laser treatment (B).

used in Europe and South America (4). It is now one of the most widely used laser lipoplasty techniques worldwide. Laser lipolysis is usually performed with a cannula containing a laser fiber that is inserted into the treatment area. To allow the laser energy to dissolve excess fat, the cannula is moved back and forth. The photoacoustic effect mechanically disrupts adipocytes, whereas the photothermal effect converts

laser light into heat energy in fat, collagenous tissue, and hemoglobin. Heat causes increased liquefaction and disruption of the cell membrane, allowing for extracellular drainage. The heat causes coagulation of small vessels in the fat tissues, which makes the procedure easier by reducing trauma and bleeding and allowing for faster recovery. The heating of the deep dermis and conjunctive septa of subcutaneous tissues



FIGURE 3

Frontal (A) and lateral (C) view of the lipoma located on the left side of the patient's back. A complete removal of the lipoma is observed 1 month after laser treatment without leaving visible aesthetic marks (B,D).

TABLE 1 Clinical studies using non-ablative and ablative lasers for lipomas.

References	Laser	Patient number	Lipoma type	Methods	Findings
Stebbins et al. (20)	980 nm diode laser	1	Back lipoma	Laser lipolysis was performed using a continuous wave. Laser energy was delivered to the lipoma <i>via</i> a 600-mm fiberoptic ensheathed in a 1.2-mm diameter stainless steel cannula, with the distal 2 mm of the fiber extending beyond the distal tip of the cannula. The power was set at 20 W, and a total of 7,000 J were administered to the lipoma. Total treatment time was approximately 20 min.	No evidence of lipoma on U/S at 2-months follow-up. 90% reduction on U/S at 1-month follow-up.
Min Lee et al. (21)	1,444-nm neodymium-doped yttrium aluminum garnet (Nd:YAG)	3	Back lipoma	Subjects were treated in a single session of micropulsed subdermal 1,444-nm Nd:YAG laser energy using the following parameters: pulse rate 30 Hz, pulse energy 200 mJ, pulse width 100 ms, power 6 W. The total accumulated energy used in each case ranged from 1,100 to 4,200 J/cm ² and was determined by the lipoma size.	In all cases, reduction or complete disappearance of the lipoma was observed at 6-month follow-up, and no infections, episodes of severe bleeding, or any other serious adverse effects were reported.
Goldman and Wollina (1)	1,064-nm Nd:YAG	20 patients (11 women and 9 men)	Subdermal lipoma	The laser energy was delivered to the subcutaneous tissue in direct contact with the lipoma through a 300-lm fiberoptic with a 1-mm-diameter stainless steel microcannula of variable length connected to the tip of the fiber. In large lipomas (more than 5 cm in diameter), a 600-μm fiberoptic with a 1.2-mm-diameter cannula was used. The total accumulated energy used in each lesion ranged from 5,000 to 32,000 J/cm ² .	Subdermal lipoma treatment using a 1,064-nm Nd:YAG laser resulted in complete or almost complete removal of the tumor in 100% of patients. Four partial relapses were observed that were treated successfully by the same procedure. Adverse effects were mild and temporary.
Sergey et al. (22)	960 nm diode laser	1	Nasopharyngeal lipoma	Neoplasm was removed by using an 8 W contact diode laser with 0° rigid endoscope, under topical anesthesia with 2 ml of 10% lidocaine solution.	The endoscopic endonasal approach with the use of a 960 nm diode laser and topical anesthesia was implemented to remove the neoplasm non-invasively and thus achieve a good long-term result.
Lombardo et al. (23)	CO ₂ laser	1	Laryngeal lipoma	The dimension of the lesion with its well-defined capsule edging allowed us to perform an excisional biopsy using TLM with CO ₂ laser; in addition, we made a continuous wave laser treatment on the excisional margins and to the wound bed to avoid relapses.	The use of transoral laser CO ₂ micro-laryngoscopy (TLM) provided good management of a small intrinsic lipomas of the larynx, minimizing the potential for relapses.

causes collagen denaturation, which is followed by vascular proliferation and collagen neosynthesis. According to a recent study, 1,064 and 1,320 nm have collagen as the primary tissue target, with adipocyte damage occurring secondarily (8). Furthermore, when compared to the other two wavelengths for laser-assisted lipolysis, 1,320 and 1,064 nm, 1,444 nm have the highest ablation efficiency with the least amount of heat localization over the depth (17). Since its introduction, numerous publications have claimed that laser-assisted lipolysis is significantly better than conventional liposuction. Katz et al. suggested that conventional liposuction may worsen skin laxity (18), but Min et al. propose that, in addition to its well-known

indications for liposculpture of the face and body, therapy with the 1,444-nm Nd:YAG laser may also be utilized for skin tightening. As a result, the 1,444 nm laser may enhance the beneficial effects of laser lipolysis, such as dermal tightening, less bleeding and pain, minimal tissue damage, and faster recovery (19).

Study limitations

One of the limitations of the study is the absence of a patient's satisfaction assessment. Our future goal

investigate the indicative times and the patient satisfaction index, in order to better validate our scientific findings.

Conclusion

Our findings showed that lipoma treatment with a 1,444 nm Nd:YAG laser is a minimally invasive, scar-free, safe, and effective procedure.

Data availability statement

The original contributions presented in the study are included in the article, further inquiries can be directed to the corresponding author.

Ethics statement

Ethical review and approval was not required for the study on human participants in accordance with the local legislation and institutional requirements. Written informed consent was obtained from the individual(s) for the publication of any identifiable images or data included in this article.

References

- Goldman A, Wollina U. Lipoma treatment with a subdermal Nd:YAG laser technique. *Int J Dermatol*. (2009) 48:1228–32. doi: 10.1111/j.1365-4632.2008.04007.x
- Nichter LS, Gupta BR. Liposuction of giant lipoma. *Ann Plast Surg*. (1990) 24:362–5. doi: 10.1097/0000637-199004000-00011
- Berenguer B, de la Cruz L, de la Plaza R. Liposuction in atypical cases. *Aesth Plast Surg*. (2000) 24:13–21. doi: 10.1007/s002669910003
- Apfelberg DB, Rosenthal S, Hunstad JP, Achauer B, Fodor PB. Progress report on multicenter study of laser-assisted liposuction. *Aesthet Plast Surg*. (1994) 18:259–64. doi: 10.1007/BF00449791
- Badin A, Moraes L, Godek L, Chiaratti MG, Canta L. Laser lipolysis: flaccidity under control. *Aesth Plast Surg*. (2002) 26:335–9. doi: 10.1007/s00266-002-1510-3
- Tark KC, Jung JE, Song SY. Superior lipolytic effect of the 1,444 nm Nd:YAG laser: comparison with the 1,064 nm Nd:YAG laser. *Lasers Surg Med*. (2009) 41:721–7. doi: 10.1002/lsm.20786
- Anderson RR, Farinelli W, Laubach H, Manstein D, Yaroslavsky AN, Gubeli J, et al. Selective photothermolysis of lipid-rich tissues: a free electron laser study. *Lasers Surg Med*. (2006) 38:913–9. doi: 10.1002/lsm.20393
- Khoury JG, Saluja R, Keel D, Detwiler S, Goldman MP. Histologic evaluation of interstitial lipolysis comparing a 1064, 1320 and 2100nm laser in an *ex vivo* model. *Lasers Surg Med*. (2008) 40:402–6. doi: 10.1002/lsm.20683
- Aust MC, Spies M, Kall S, Gohritz A, Boorboor P, Kolokythas P, et al. Lipomas after blunt soft tissue trauma: are they real? Analysis of 31 cases. *Br J Dermatol*. (2007) 157:92–9. doi: 10.1111/j.13652133.2007.07970.x
- Al-basti HA, El-Khatib HA. The use of suction-assisted surgical extraction of moderate to large lipomas: long term follow-up. *Aesth Plast Surg*. (2002) 26:114–7. doi: 10.1007/s00266-002-1492-1
- Choi CW, Kim BJ, Moon SE, Youn SW, Park KC, Huh CH. Treatment of lipomas assisted with tumescent liposuction. *J Eur Acad Dermatol Venerol*. (2006) 21:243–6. doi: 10.1111/j.1468-3083.2006.02037.x
- Billings SD, Folpe AL. Diagnostically challenging spindle cell lipomas: a report of 34 “low-fat” and “fat-free” variants. *Am J Dermatopathol*. (2007) 29:437–42. doi: 10.1097/DAD.0b013e31813735df
- Serpell JW, Chen RY. Review of large deep lipomatous tumours. *ANZ J Surg*. (2007) 77:524–9. doi: 10.1111/j.1445-2197.2007.04042.x
- Sanchez MR, Golomb FM, Moy JA, Potozkin JR. Giant lipoma: case report and review of the literature. *J Am Acad Dermatol*. (1993) 28:266–8. doi: 10.1016/s0190-9622(08)81151-6
- Terzioglu A, Tuncali D, Yuksel A, Bingul F, Aslan G. Giant lipomas: a series of 12 consecutive cases and a giant liposarcoma of the thigh. *Dermatol Surg*. (2004) 30:463–7. doi: 10.1111/j.1524-4725.2004.30022.x
- Jung YC. Preliminary experience in facial and body contouring with 1444 nm micropulsed Nd:YAG laser-assisted lipolysis: a review of 24 cases. *Laser Ther*. (2011) 20:39–46. doi: 10.5978/islsm.20.39
- Youn JIA. Comparison of wavelength dependence for laser-assisted lipolysis effect using monte carlo simulation. *J Opt Soc Korea*. (2009) 13:267–71. doi: 10.3807/JOSK.2009.13.2.267
- Katz B, McBean J, Cheung JS. The new laser liposuction for men. *Dermatol Ther*. (2007) 20:448–51. doi: 10.1111/j.1529-8019.2007.00160.x
- Min KH, Kim JH, Park HJ, Chung HS, Heo CY. The skin-tightening effects of 1,444-nm Nd:YAG laser on human skin: an *in vivo* study. *Aesthetic Plast Surg*. (2014) 38:585–91. doi: 10.1007/s00266-014-0316-4

Author contributions

DP, MM, LP, CC, GC, and PB: conceptualization, methodology, validation, supervision, and funding acquisition. LP: formal analysis and writing—original draft preparation. LP, MM, and IF: investigation. DP, MM, LP, CC, and GC: data curation. LP and IF: writing—review and editing. All authors have read and agreed to the published version of the manuscript.

Conflict of interest

Authors LP and IF were employed by El.En. Group.

The remaining authors declare that the research was conducted in the absence of any commercial or financial relationships that could be construed as a potential conflict of interest.

Publisher's note

All claims expressed in this article are solely those of the authors and do not necessarily represent those of their affiliated organizations, or those of the publisher, the editors and the reviewers. Any product that may be evaluated in this article, or claim that may be made by its manufacturer, is not guaranteed or endorsed by the publisher.

20. Stebbins WG, Hanke CW, Petersen J. Novel method of minimally invasive removal of large lipoma after laser lipolysis with 980 nm diode laser. Case report. *Dermatol Ther.* (2011) 24:125–30. doi: 10.1111/j.1529-8019.2010.01385.x
21. Min Lee H, Won CH, Lee MW, Choi JH, Chang S. Letter: treatment of lipomas using a subdermal 1,444-nm micropulsed neodymium-doped yttrium aluminum garnet laser. *Dermatol Surg.* (2011) 37:1375–6 doi: 10.1111/j.1524-4725.2011.02084.x
22. Sergey K, Baranskaya SV. Nasopharyngeal lipoma: clinical case. *Rev Laryngosc.* (2021) 131:E1099–102. doi: 10.1002/lary.28990
23. Lombardo N, Lobello N, Piazzetta G, Ciriolo M, Pelaia C, Testa D, et al. Intrinsic laryngeal lipoma treated with transoral CO2 Laser microsurgery: an unusual case report. *Am J Case Rep.* (2020) 3:e920528. doi: 10.12659/AJCR.920528



OPEN ACCESS

EDITED BY

Stefania Guida,
Vita-Salute San Raffaele University, Italy

REVIEWED BY

Claudio Conforti,
University of Trieste, Italy
Roberta Giuffrida,
The University of Messina, Italy
Giorgio Stabile,
Vita-Salute San Raffaele University, Italy

*CORRESPONDENCE

Ayman Grada
ayman.grada@case.edu
Christopher G. Bunick
christopher.bunick@yale.edu

SPECIALTY SECTION

This article was submitted to
Dermatology,
a section of the journal
Frontiers in Medicine

RECEIVED 01 September 2022

ACCEPTED 22 November 2022

PUBLISHED 08 December 2022

CITATION

Grada A, Del Rosso JQ, Moore AY,
Stein Gold L, Harper J, Damiani G,
Shaw K, Obagi S, Salem RJ, Tanaka SK
and Bunick CG (2022) Reduced
blood-brain barrier penetration
of acne vulgaris antibiotic sarecycline
compared to minocycline
corresponds with lower lipophilicity.
Front. Med. 9:1033980.
doi: 10.3389/fmed.2022.1033980

COPYRIGHT

© 2022 Grada, Del Rosso, Moore,
Stein Gold, Harper, Damiani, Shaw,
Obagi, Salem, Tanaka and Bunick. This
is an open-access article distributed
under the terms of the [Creative
Commons Attribution License \(CC BY\)](#).
The use, distribution or reproduction in
other forums is permitted, provided
the original author(s) and the copyright
owner(s) are credited and that the
original publication in this journal is
cited, in accordance with accepted
academic practice. No use, distribution
or reproduction is permitted which
does not comply with these terms.

Reduced blood-brain barrier penetration of acne vulgaris antibiotic sarecycline compared to minocycline corresponds with lower lipophilicity

Ayman Grada^{1*}, James Q. Del Rosso^{2,3}, Angela Y. Moore^{4,5},
Linda Stein Gold⁶, Julie Harper⁷, Giovanni Damiani^{8,9,10},
Katharina Shaw¹¹, Sabine Obagi¹², Raidah J. Salem¹³,
S. Ken Tanaka¹⁴ and Christopher G. Bunick^{15,16*}

¹Case Western Reserve University School of Medicine, Cleveland, OH, United States, ²JDR Dermatology Research, Las Vegas, NV, United States, ³Advanced Dermatology and Cosmetic Surgery, Maitland, FL, United States, ⁴Baylor University Medical Center, Dallas, TX, United States, ⁵Arlington Research Center, Arlington, TX, United States, ⁶Henry Ford Health System, Detroit, MI, United States, ⁷The Dermatology and Skin Care Center of Birmingham, Birmingham, AL, United States, ⁸Clinical Dermatology, Istituto di Ricovero e Cura a Carattere Scientifico (IRCCS) Istituto Ortopedico Galeazzi, Milan, Italy, ⁹Department of Biomedical, Surgical and Dental Sciences, University of Milan, Milan, Italy, ¹⁰Ph.D. Program in Pharmacological Sciences, Department of Pharmaceutical and Pharmacological Sciences, University of Padua, Padua, Italy, ¹¹NYU Langone Health, New York, NY, United States, ¹²USC Neurorestoration Center, Los Angeles, CA, United States, ¹³Medical Affairs, Almirall, LLC, Malvern, PA, United States, ¹⁴Paratek Pharmaceuticals, Inc., King of Prussia, PA, United States, ¹⁵Department of Dermatology, Yale School of Medicine, New Haven, CT, United States, ¹⁶Program in Translational Biomedicine, Yale School of Medicine, New Haven, CT, United States

Background: Vestibular side effects such as dizziness and vertigo can be a limitation for some antibiotics commonly used to treat acne, rosacea, and other dermatology indications.

Objective: Unlike minocycline, which is a second-generation tetracycline, sarecycline, a narrow-spectrum third-generation tetracycline-class agent approved to treat acne vulgaris, has demonstrated low rates of vestibular-related adverse events in clinical trials. In this work, we evaluate the brain-penetrative and lipophilic attributes of sarecycline in 2 non-clinical studies and discuss potential associations with vestibular adverse events.

Methods: Rats received either intravenous sarecycline or minocycline (1.0 mg/kg). Blood-brain penetrance was measured at 1, 3, and 6 h postdosing. In another analysis, the lipophilicity of sarecycline, minocycline, and doxycycline was measured *via* octanol/water and chloroform/water distribution coefficients (logD) at pH 3.5, 5.5, and 7.4.

Results: Unlike minocycline, sarecycline was not detected in brain samples postdosing. In the octanol/water solvent system, sarecycline had a

numerically lower lipophilicity profile than minocycline and doxycycline at pH 5.5 and 7.4.

Conclusion: The reduced blood-brain penetrance and lipophilicity of sarecycline compared with other tetracyclines may explain low rates of vestibular-related adverse events seen in clinical trials.

KEYWORDS

acne vulgaris, sarecycline, minocycline, dizziness, blood-brain barrier, lipophilicity, antibiotic

Introduction

Second-generation tetracycline-class antibiotics such as doxycycline and minocycline have been the mainstay treatment of moderate-to-severe acne vulgaris for over 50 years (1–3); however, the use of minocycline is often limited by vestibular side effects such as dizziness and tinnitus, leading to the inclusion of a warning for central nervous system side effects in the minocycline package insert (4). These side effects can impair an individual's ability to perform daily tasks such as driving (4), thus contributing to the overall burden of managing acne vulgaris. In contrast, vestibular side effects are not typically associated with use of doxycycline (2). The higher lipophilicity of minocycline compared with doxycycline [e.g., distribution coefficient (logD) values of 1.11 (minocycline) vs. 0.95 (doxycycline) (5)] allows for greater penetration of the blood-brain barrier, thereby potentiating vestibular infiltration and by extension, dizziness and vertigo (2).

Sarecycline is a narrow-spectrum, 3rd generation tetracycline-class oral antibiotic approved by the US Food and Drug Administration (FDA) in 2018 for the treatment of moderate-to-severe acne vulgaris (6, 7). The efficacy and safety of sarecycline have been reported in two phase 3 randomized controlled trials [SC1401 (ClinicalTrials.gov identifier NCT02320149; $N = 968$) and SC1402 (ClinicalTrials.gov identifier NCT02322866; $N = 1034$), and its long-term safety was examined in a 40-week open-label extension study (ClinicalTrials.gov identifier NCT02413346; $N = 490$) (8, 9). Notably, low rates of vestibular-related adverse events (e.g., dizziness, motion sickness) were observed in these studies, and no events of vertigo or tinnitus were reported in patients receiving sarecycline (Figure 1). However, no clinical trials to date have compared sarecycline head-to-head with other tetracycline-class drugs (10), limiting the ability to make direct comparisons for safety and tolerability across therapies. Further, it remains unclear whether the biochemical properties of sarecycline (e.g., blood-brain barrier penetrance, lipophilicity) could be contributing to the low rates of vestibular adverse events in clinical trials.

Here, we investigated the potential relationship between the brain-penetrative and lipophilic attributes of sarecycline from 2 preclinical *in vivo* and *in vitro* analyses. In the first analysis, we examined the ability of sarecycline to penetrate the blood-brain barrier relative to minocycline in a rat model study. In the second analysis, we determined the lipophilicity of sarecycline compared with minocycline and doxycycline.

Materials and methods

Blood-brain barrier penetration study

Ethics statement

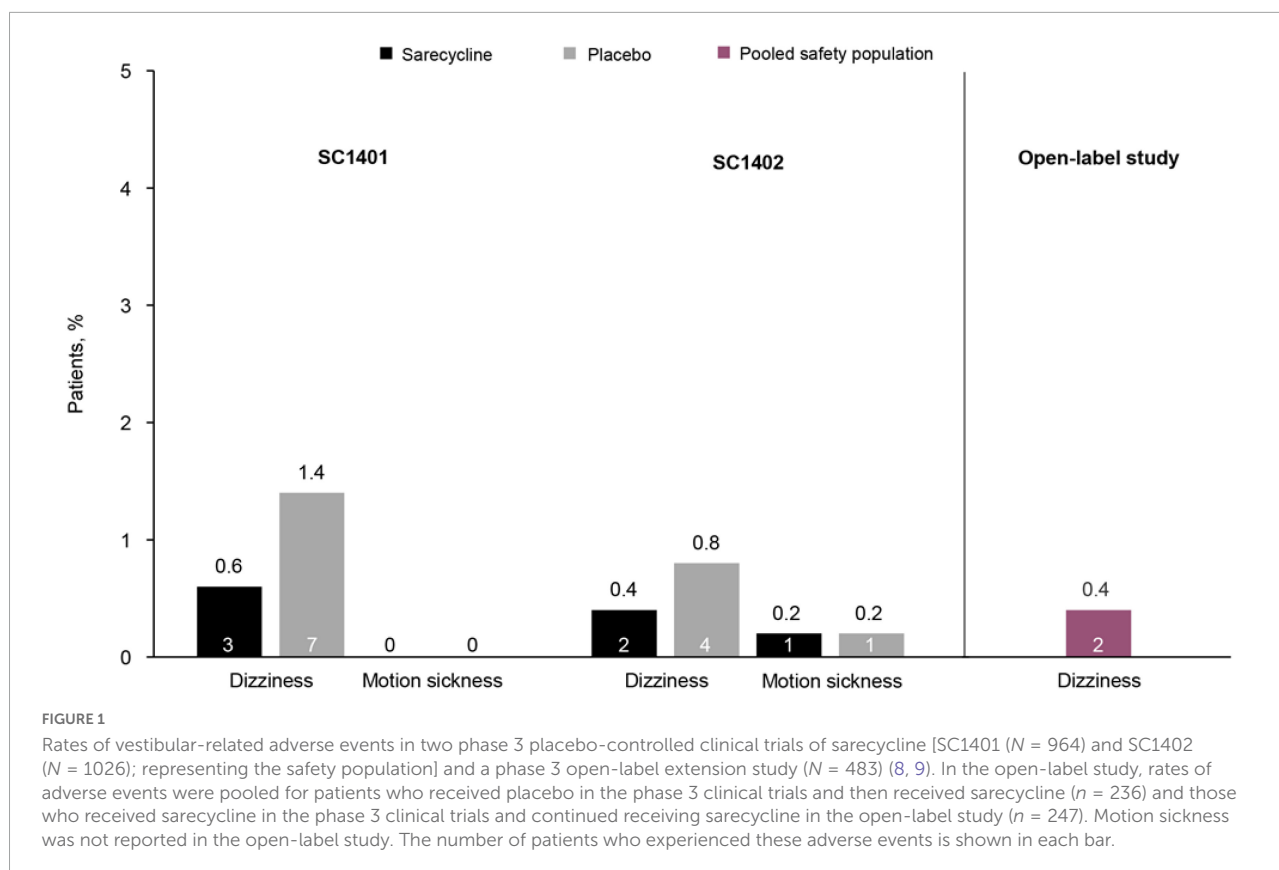
All protocols involving animals were approved by the Institutional Animal Care and Use Committee (IACUC).

Procedures

Six male Wistar rats (150–200 g; Charles River Laboratories, Wilmington, MA, USA) were used in this study. Each rat was pre-cannulated in the jugular vein. Rats were kept in individual cages, with water and feed *ad libitum*, and alternating 12 h light cycles. Before dosing, rats underwent an overnight fast (~16 h) in metabolic cages and were weighed to determine dose volume (1.0 ml/kg). The rats were then intravenously (IV) dosed with either sarecycline ($N = 3$) or minocycline ($N = 3$) at a total dose of 1.0 mg/kg, and access to food was restored 2 h after dosing. Subsequently, rats were euthanized *via* CO₂ and brain samples and whole blood, collected *via* heart puncture, were harvested from 2 rats at each of the following time points: 1, 3, and 6 h postdosing.

Analysis

The endpoint of this analysis was concentration of sarecycline or minocycline in plasma ($\mu\text{g/ml}$) and in brain



samples ($\mu\text{g/g}$) at 1, 3, and 6 h postdosing. Plasma and brain homogenate samples were prepared by protein precipitation with acetonitrile, followed by centrifugation. The samples were injected on an API 2000 mass spectrometer (Applied Biosystems, Foster City, CA, USA) and analyzed in positive ion mode using doxycycline as an internal standard. Values were calculated using Analyst 1.2 quantitation software (SciEx, Framingham, MA, USA). Linear through zero regression analysis with no weighting factor was used to determine the calculated concentrations of the injected samples.

Lipophilicity study

Procedure

Sarecycline, minocycline, and doxycycline were each prepared as 1.0 mg/ml stock solutions (4/8 ml) in 3 separate aqueous phase pH buffers (pH 3.5, 5.5, and 7.4). The pH of aqueous phase stock solutions was adjusted to within 0.1 of the desired pH before analysis; stock solutions had a further equilibration period of 2 h before pH adjustment as needed.

Aqueous phase stock solutions were quantified by high performance liquid chromatography (HPLC) before mixing with the organic phase to avoid any potential degradation effects. Next, 2 ml each of aqueous saturated octanol/chloroform

and aqueous stock solution were combined and vortex-mixed to encourage interaction between phases. Each experimental condition was conducted in triplicate.

The mixtures were equilibrated at 25°C for 24 h at 750 rotations per minute to allow partitioning. At 2 intervals, the mixtures were vortex-mixed to ensure that an emulsion formed. Following equilibration, the mixtures were allowed to settle before aqueous and organic layers were separated into discrete HPLC vials.

Following 24-h equilibration and phase separation, final pH values of the aqueous phases were recorded. Sarecycline and doxycycline octanol and chloroform phases were diluted as needed with acetonitrile, and minocycline octanol and chloroform phases were diluted as needed with dimethyl sulfoxide. Phases were analyzed by HPLC.

Lipophilicity and data analysis

The endpoint of this analysis was the calculation of logD values for each compound at pH 3.5, 5.5, and 7.4. LogD values were calculated by the ratio of the peaks found in the aqueous phase vs. the organic layer, with lower values indicating less lipophilicity and higher values indicating greater lipophilicity. Confirmation of recovery was calculated by determining the concentration of the aqueous stock solution.

Results

Blood-brain barrier penetration study

Brief results of this study have been reported previously (10). Concentrations of sarecycline and minocycline in rat blood plasma and brain are included in [Table 1](#) and illustrated in [Figure 2](#). Concentrations of sarecycline and minocycline in rat plasma were similar to each other at each measured time point following IV administration [0.460, 0.217, 0.049 $\mu\text{g/ml}$ (sarecycline) versus 0.333, 0.174 and 0.077 $\mu\text{g/ml}$ (minocycline) at hours 1, 3, and 6, respectively]. However, while detectable concentrations of minocycline in the brain were observed at each measured time point (0.074, 0.139, and 0.068 $\mu\text{g/g}$ at hours 1, 3, and 6, respectively), the level of sarecycline remained below the lower limit of quantitation (0.05 $\mu\text{g/g}$) in all brain samples at each measured time point.

Lipophilicity study

The logD values of sarecycline, minocycline, and doxycycline in octanol/water and chloroform/water solvent systems at 25°C are reported in [Table 2](#). In the octanol/water system, sarecycline was numerically less lipophilic than minocycline at pH 5.5 and 7.4 (−0.16 vs. 0.09 and −0.26 vs. 0.12, respectively) and numerically more lipophilic at pH 3.5 (−0.30 vs. −1.07, respectively). The lipophilicity of doxycycline was between that of sarecycline and minocycline at pH 5.5 and 7.4.

In the chloroform/water system, sarecycline was also numerically less lipophilic than minocycline at pH 7.4, was similarly lipophilic at pH 5.5, and was more lipophilic at pH 3.5. Overall, absolute values of logD were higher in the chloroform/water system than in the octanol/water system for sarecycline (pH 3.5, 1.14 vs. −0.30; pH 5.5, 1.48 vs. −0.16; and pH 7.4, 1.46 vs. −0.26, respectively) and minocycline (pH 3.5, 0.07 vs. −1.07; pH 5.5, 1.49 vs. 0.09; and pH 7.4, 1.65

vs. 0.12, respectively), whereas there was little difference in doxycycline logD values between the 2 solvent systems for each pH solution. Differences in logD values observed between the 2 solvent systems may be attributed to the unique hydrogen bonding capabilities of each system (11).

Discussion

To explore potential mechanisms of action associated with the development of vestibular adverse events with certain oral tetracyclines, preclinical *in vitro* and *in vivo* analyses were performed to examine the biochemical properties of sarecycline relative to minocycline and doxycycline. In the analysis of *in vivo* blood-brain barrier penetrance, IV administered minocycline was detectable in the brain in rats, whereas sarecycline was not (10). In the analysis of *in vitro* lipophilicity, sarecycline had slightly lower logD values compared with doxycycline and minocycline at pH 5.5 and 7.4 in the octanol/water system. Taken together, these results suggest that the lower lipophilicity and reduced brain penetrance of sarecycline relative to minocycline could explain the lower incidence of vestibular adverse events (dizziness, tinnitus, vertigo) seen in sarecycline clinical trials vs. minocycline clinical trials.

In phase 3 clinical trials of sarecycline, overall rates of vestibular adverse events were low ([Figure 1](#)) (8, 9). In two identical, randomized, double-blind, placebo-controlled, phase 3 studies of sarecycline (SC1401 and SC1402), rates of the vestibular-related adverse events dizziness and motion sickness were low ($\leq 1\%$) in 994 patients treated with sarecycline (SC1401 = 481; SC1402 = 513) over 12 weeks (8). Additionally, rates of dizziness were lower in patients receiving sarecycline (0.6 and 0.4%) compared with those receiving placebo (1.4 and 0.8%). In both studies, no events of vertigo or tinnitus were reported in either treatment group. Further, in a phase 3 open-label extension study of 483 patients who completed one of the two phase 3 placebo-controlled 12-week trials, dizziness occurred in 0.4% of patients during up to 40 additional weeks of sarecycline treatment (9). Similarly, no events of vertigo or tinnitus were reported in the extension study. Comparatively, in a placebo-controlled, dose-ranging, 12-week trial of extended-release minocycline in 233 patients with moderate to severe facial acne vulgaris, rates of acute vestibular adverse events (dizziness, vertigo, and ringing in the ears) were most commonly reported during the first 5 days of treatment (12, 13). Incidence of acute vestibular adverse events was dose dependent, occurring in 10.2, 23.7, and 28.3% of patients receiving extended-release minocycline 1, 2, or 3 mg/kg, respectively, versus 16.4% in the placebo group during the first 5 days of treatment. Similarly, in a pooled analysis of phase 3 trials of extended-release 1 mg/kg minocycline, rates of acute vestibular adverse events were

TABLE 1 Concentration of minocycline and sarecycline in plasma ($\mu\text{g/ml}$) and brain ($\mu\text{g/g}$) after intravenous administration.

Concentration	Time point (hours)		
	1	3	6
Minocycline			
Plasma ($\mu\text{g/ml}$)	0.333	0.174	0.077
Brain ($\mu\text{g/g}$)	0.074	0.139	0.068
Sarecycline			
Plasma ($\mu\text{g/ml}$)	0.460	0.217	0.049
Brain ($\mu\text{g/g}$)	BLQ	BLQ	BLQ

LOQ (plasma) = 0.025 $\mu\text{g/ml}$, LOQ (brain) = 0.05 $\mu\text{g/g}$. BLQ, below the limit of quantification; LOQ, limit of quantification.

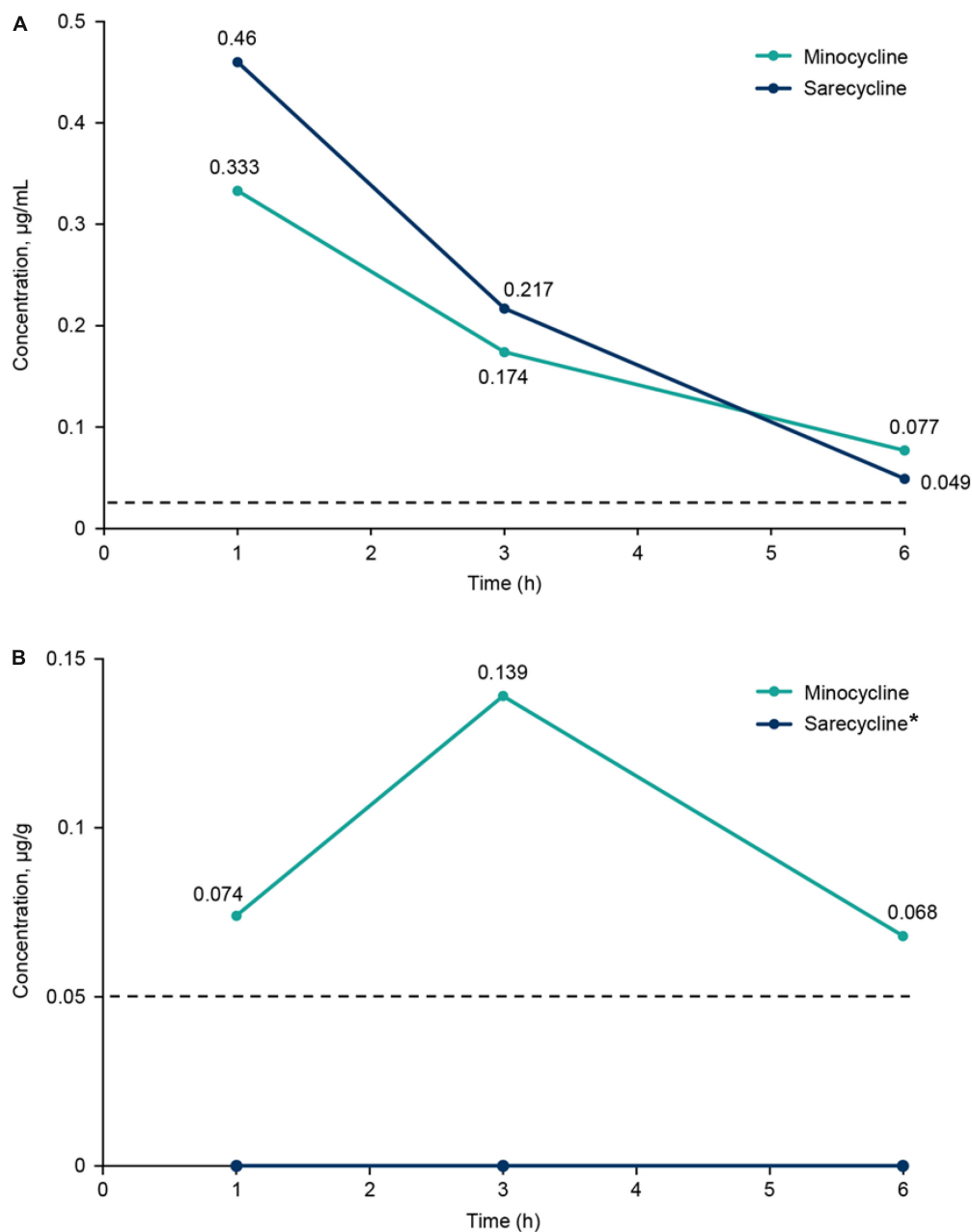


FIGURE 2

(A) Plasma concentrations of sarecycline and minocycline following intravenous administration in rats. (B) Brain concentrations of sarecycline and minocycline following intravenous administration in rats. Dashed line indicates limit of quantitation for plasma (0.025 µg/mL) and brain (0.05 µg/g). *Concentration of sarecycline in the brain was below the limit of quantitation at all time points.

9–10.5% during the first 5 days of treatment (13). In a systematic review representing 226,019 pediatric and adult acne patients, Armstrong et al. reported adverse events associated with sarecycline, minocycline, doxycycline and tetracycline, and showed higher rates of acute vestibular events associated with minocycline (~10%) (14).

In the current analysis, sarecycline was not detected in rat brain samples up to 6 h following IV dosing (10). In contrast,

levels of minocycline were detected in rat brain up to 6 h after IV dosing. A limitation of this animal study is the small sample size, which may make it difficult to generalize. However, the trend seen in the results support previous reports that minocycline has high lipid solubility and, thus, may more readily cross the blood-brain barrier compared with other tetracyclines (15). For instance, a previous report in a canine model indicated that the blood-brain penetrance of minocycline was almost

TABLE 2 Distribution coefficients (SD) of sarecycline HCl, doxycycline HCl, and minocycline HCl.

Solvent system	Compound	pH 3.5	pH 5.5	pH 7.4
Octanol/Water at 25°C	Sarecycline HCl	−0.30 (0.03)	−0.16 (0.01)	−0.26 (0.01)
	Doxycycline HCl	−0.01 (0.02)	0.00 (0.02)	−0.08 (0.03)
	Minocycline HCl	−1.07 (0.01)	0.09 (0.02)	0.12 (0.02)
Chloroform/Water at 25°C	Sarecycline HCl	1.14 (0.01)	1.48 (0.01)	1.46 (0.00)
	Doxycycline HCl	−0.15 (0.01)	−0.07 (0.01)	−0.15 (0.01)
	Minocycline HCl	0.07 (0.02)	1.49 (0.02)	1.65 (0.02)

HCl, hydrochloride; SD, standard deviation.

threefold higher than that of doxycycline after IV dosing (16). Although no human studies have definitively confirmed this association, the higher brain penetrance of minocycline is suspected to contribute to its higher rates of associated vestibular-related side effects relative to other tetracyclines (10, 16). Minocycline is considered unacceptable for military aviators and is completely restricted for use because of the risk for central nervous system side effects including vestibular side effects such as light-headedness, dizziness and vertigo (17). Conversely, the low rates of vestibular and phototoxic events seen with narrow-spectrum sarecycline make it an acceptable treatment option for the military population and individuals whose lifestyles and careers would suffer because of vestibular side effects.

Previously published logD values of tetracyclines, especially that of minocycline, are variable and inconsistencies permeate in the dermatology literature. For instance, it was previously reported that minocycline was fourfold more lipophilic than doxycycline and 10-fold more lipophilic than tetracycline at a pH of 5.5 (18, 19). Another analysis found that the logD values for minocycline and doxycycline at pH 5.6 were similar (1.11 and 0.95, respectively) (5). The current analysis indicates that in the octanol/water solvent system at pH 5.5 and 7.4, sarecycline (−0.16 and −0.26, respectively) was slightly less lipophilic than both minocycline (0.09 and 0.12, respectively) and doxycycline (0.00 and −0.08, respectively).

A limitation of this analysis is the interpretation of the lipophilicity results. Because octanol/water solvent systems are the most utilized format for lipophilicity analyses (20), this output was determined to provide the more meaningful result in the current analysis rather than the chloroform/water solvent system. However, caution has been advised for basing pharmacological behavior on partition coefficients, limiting the scope of these results (16). Nevertheless, a strength of the current analysis is that the low lipophilicity of sarecycline is supported by data demonstrating a lack of detectable brain penetrance in rats, which further validates the pharmacological profile of sarecycline.

The lower lipophilicity and decreased blood-brain barrier penetration observed for sarecycline ultimately must be explained by chemical structure differences between it

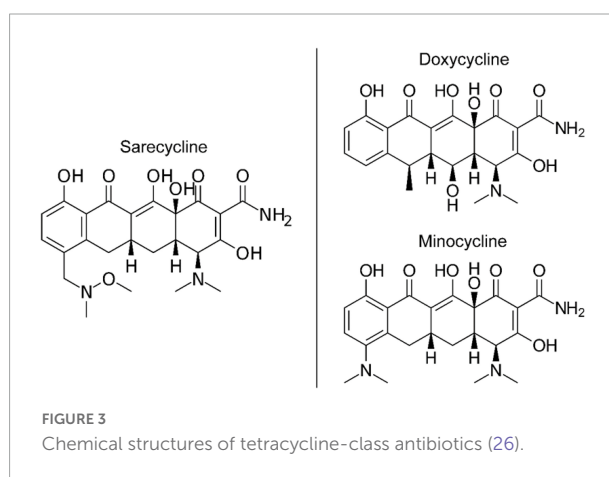


FIGURE 3
Chemical structures of tetracycline-class antibiotics (26).

and minocycline and doxycycline (21–23). While all three drugs share a common naphthacene four-ring core (21, 22), sarecycline is distinguished by a long C7 extension (7-[[methoxy(methyl)amino]methyl]) that provides unique and enhanced ribosomal binding through mRNA contact (Figure 3) (21). The C7 moiety contains an oxygen atom (21), which functions as an acceptor of hydrogen bonds, thereby reducing lipophilicity (24, 25). Additional studies are warranted to investigate the mechanism by which sarecycline is associated with lower rates of vestibular adverse events relative to other tetracyclines, but the chemical structure points toward the C7 moiety oxygen. Thus, the new frontier in this work is specific alterations in the chemical properties of dermatologic drugs have potential to make a major impact on reducing real-world adverse events experienced by patients.

While high drug lipophilicity in the skin is a desired attribute as it helps in penetrating and accumulating in the lipid-rich pilosebaceous unit—where acne vulgaris therapeutic target, *Cutibacterium acnes*, resides and proliferates (19)—the increased potential of minocycline to cross the blood-brain barrier compared with other tetracycline-class drugs has served as a purported explanation for the higher rates of vestibular side effects associated with systemic minocycline use in acne treatment, which typically requires a prolonged treatment duration (27–30). Although no confirmatory link has been

established, the lack of detectable brain penetrance of sarecycline and its relatively low lipophilicity compared with minocycline as reported in these preclinical studies may correspond with the lower rates of vestibular adverse events observed in clinical trials of sarecycline.

Data availability statement

The raw data supporting the conclusions of this article will be made available by the authors, without undue reservation.

Ethics statement

The animal study was reviewed and approved by the Institutional Animal Care and Use Committee (IACUC).

Author contributions

AG, CB, and ST: conceptualization. AG and ST: methodology. CB: validation. AG: formal analysis. AG and ST: investigation. AG, RS, and ST: resources. AG and LSG: writing—original draft preparation. AG, AM, LSG, CB, JH, GD, KS, RS, and ST: writing—review and editing. CB, SO, and RS: visualization. AG, RS, and ST: supervision. RS: project administration. All authors have read and agreed to the published version of the manuscript.

Funding

This study received funding from Almirall, LLC. The funder was involved in the study design, collection, analysis, interpretation of data, the writing of this article, and the decision to submit it for publication.

References

1. Zaenglein AL, Pathy AL, Schlosser BJ, Alikhan A, Baldwin HE, Berson DS, et al. Guidelines of care for the management of acne vulgaris. *J Am Acad Dermatol*. (2016) 74:945–73.e33. doi: 10.1016/j.jaad.2015.12.037
2. Del Rosso JQ. Oral doxycycline in the management of acne vulgaris: current perspectives on clinical use and recent findings with a new double-scored small tablet formulation. *J Clin Aesthet Dermatol*. (2015) 8:19–26.
3. Graber EM. Treating acne with the tetracycline class of antibiotics: a review. *Dermatol Rev*. (2021) 2:321–30. doi: 10.1002/der2.49
4. SOLODYN. *SOLODYN [package insert]*. Scottsdale, AZ: Medicis pharmaceutical corporation (2011).
5. Colaizzi JL, Klink PR. pH-Partition behavior of tetracyclines. *J Pharm Sci*. (1969) 58:1184–9. doi: 10.1002/jps.2600581003
6. SEYSARA. *SEYSARA [package insert]*. Exton, PA: Almirall, LLC (2020).
7. Del Rosso JQ, Stein Gold L, Baldwin H, Harper JC, Zeichner J, Obagi S, et al. Management of truncal acne with oral sarecycline: pooled results from two phase-3 clinical trials. *J Drugs Dermatol*. (2021) 20:634–40.
8. Moore A, Green LJ, Bruce S, Sadick N, Tischen E, Werschler P, et al. Once-daily oral sarecycline 1.5 mg/kg/day is effective for moderate to severe acne vulgaris: results from two identically designed, phase 3, randomized, double-blind clinical trials. *J Drugs Dermatol*. (2018) 17:987–96.
9. Pariser DM, Green LJ, Lain EL, Schmitz C, Chinigo AS, McNamee B, et al. Safety and tolerability of sarecycline for the treatment of acne vulgaris: results from a phase III, multicenter, open-label study and a phase I phototoxicity study. *J Clin Aesthet Dermatol*. (2019) 12:E53–62.
10. Moore AY, Del Rosso J, Johnson JL, Grada A. Sarecycline: a review of preclinical and clinical evidence. *Clin Cosmet Investig Dermatol*. (2020) 13:553–60. doi: 10.2147/CCID.S190473

Acknowledgments

Editorial assistance was provided under the direction of the authors by Deirdre Rodeberg, Ph.D., CMPP, and Chris Lawrence, Ph.D., ELS, at MedThink SciCom.

Conflict of interest

AG was a former employee of Almirall, LLC. RS is an employee of Almirall, LLC. ST was an employee of Paratek Pharmaceuticals, Inc. AM has received research funds and honoraria from Almirall, Galderma, Mayne, and Vyne. JH has served as an advisor, investigator, speaker for Almirall, Cutera, EPI, Galderma, Sun, and Vyne. GD has received research funds and honoraria from Almirall, Galderma, Novartis, Amgen, and UCB. LSG has served as an advisor, investigator, and speaker for Almirall, Sun, Galderma, Ortho Derm, Cutera, and EPI Health. CB has served as an investigator for Almirall, a consultant for Abbvie, Almirall, LEO Pharma, Sanofi-Regeneron, UCB, a speaker for and received honoraria from Allergan, Almirall, LEO Pharma, and UCB.

The remaining authors declare that the research was conducted in the absence of any commercial or financial relationships that could be construed as a potential conflict of interest.

Publisher's note

All claims expressed in this article are solely those of the authors and do not necessarily represent those of their affiliated organizations, or those of the publisher, the editors and the reviewers. Any product that may be evaluated in this article, or claim that may be made by its manufacturer, is not guaranteed or endorsed by the publisher.

11. el Tayar N, Tsai RS, Testa B, Carrupt PA, Leo A. Partitioning of solutes in different solvent systems: the contribution of hydrogen-bonding capacity and polarity. *J Pharm Sci.* (1991) 80:590–8. doi: 10.1002/jps.2600800619
12. Stewart DM, Torok HM, Weiss JS, Plott RT, Solodyn Phase 2 Study Group. Dose-ranging efficacy of new once-daily extended-release minocycline for acne vulgaris. *Cutis.* (2006) 78(Suppl.):11–20.
13. Fleischer AB Jr., Dinehart S, Stough D, Plott RT, Solodyn Phase 2 Study Group, Solodyn Phase 3 Study Group. Safety and efficacy of a new extended-release formulation of minocycline. *Cutis.* (2006) 78(Suppl.):21–31.
14. Armstrong AW, Hekmatjah J, Kircik LH. Oral tetracyclines and acne: a systematic review for dermatologists. *J Drugs Dermatol JDD.* (2020) 19:s6–13.
15. Cunha BA, Baron J, Cunha CB. Similarities and differences between doxycycline and minocycline: clinical and antimicrobial stewardship considerations. *Eur J Clin Microbiol Infect Dis.* (2018) 37:15–20. doi: 10.1007/s10096-017-3081-x
16. Barza M, Brown RB, Shanks C, Gamble C, Weinstein L. Relation between lipophilicity and pharmacological behavior of minocycline, doxycycline, tetracycline, and oxytetracycline in dogs. *Antimicrob Agents Chemother.* (1975) 8:713–20. doi: 10.1128/AAC.8.6.713
17. Brahe C, Peters K. Fighting acne for the fighting forces. *Cutis.* (2020) 106:18–20. doi: 10.12788/cutis.0057
18. Cunha BA, Garabedian-Ruffalo SM. Tetracyclines in urology: current concepts. *Urology.* (1990) 36:548–56. doi: 10.1016/0090-4295(90)80201-W
19. Leyden JJ, Del Rosso JQ. Oral antibiotic therapy for acne vulgaris: pharmacokinetic and pharmacodynamic perspectives. *J Clin Aesthet Dermatol.* (2011) 4:40–7.
20. Giaginis C, Tsantili-Kakoulidou A. Alternative measures of lipophilicity: from octanol-water partitioning to IAM retention. *J Pharm Sci.* (2008) 97:2984–3004. doi: 10.1002/jps.21244
21. Batool Z, Lomakin IB, Polikanov YS, Bunick CG. Sarecycline interferes with tRNA accommodation and tethers mRNA to the 70S ribosome. *Proc Natl Acad Sci U S A.* (2020) 117:20530–7. doi: 10.1073/pnas.2008671117
22. Nguyen F, Starosta AL, Arenz S, Sohmen D, Donhofer A, Wilson DN. Tetracycline antibiotics and resistance mechanisms. *Biol Chem.* (2014) 395:559–75. doi: 10.1515/hsz-2013-0292
23. Dufès C. Chapter 6: Brain delivery of peptides and proteins. In: Walle CVD editor. *Peptide and Protein Delivery.* Cambridge, MA: Academic Press (2011). p. 105–22. doi: 10.1016/B978-0-12-384935-9.10006-9
24. Chikhale EG, Ng KY, Burton PS, Borchardt RT. Hydrogen bonding potential as a determinant of the in vitro and in situ blood-brain barrier permeability of peptides. *Pharm Res.* (1994) 11:412–9. doi: 10.1023/A:1018969222130
25. Czyrski A. Determination of the lipophilicity of ibuprofen, naproxen, ketoprofen, and flurbiprofen with thin-layer chromatography. *J Chem.* (2019) 2019:1–6. doi: 10.1155/2019/3407091
26. Bunick CG, Keri J, Tanaka SK, Furey N, Damiani G, Johnson JL, et al. Antibacterial mechanisms and efficacy of sarecycline in animal models of infection and inflammation. *Antibiotics (Basel).* (2021) 10:439. doi: 10.3390/antibiotics10040439
27. Brogden R, Speight T, Avery G. Minocycline: a review of its antibacterial and pharmacokinetic properties and therapeutic use. *Drugs.* (1975) 9:251–91. doi: 10.2165/00003495-197509040-00005
28. Zarzuelo A, Galvez J, Garrido-Mesa N, Garrido-Mesa N. Minocycline: far beyond an antibiotic. *Br J Pharmacol.* (2013) 169:337–52. doi: 10.1111/bph.12139
29. Somech R, Arav-Boger R, Assia A, Spier Z, Jurgenson U. Complications of minocycline therapy for acne vulgaris: case reports and review of the literature. *Pediatric Dermatol.* (1999) 16:469–72. doi: 10.1046/j.1525-1470.1999.00106.x
30. Ochsendorf F. Minocycline in acne vulgaris. *Am J Clin Dermatol.* (2010) 11:327–41. doi: 10.2165/11319280-000000000-00000



OPEN ACCESS

EDITED BY

Stefania Guida,
Vita-Salute San Raffaele University, Italy

REVIEWED BY

Fazil Ahmad,
Imam Abdulrahman Bin Faisal
University, Saudi Arabia
Annalisa Saltari,
University Hospital Zurich, Switzerland

*CORRESPONDENCE

Xin Li
13661956326@163.com

†These authors have contributed
equally to this work and share first
authorship

SPECIALTY SECTION

This article was submitted to
Dermatology,
a section of the journal
Frontiers in Medicine

RECEIVED 11 August 2022

ACCEPTED 28 November 2022

PUBLISHED 15 December 2022

CITATION

Zhang M, Hong S, Sun X, Zhou Y,
Luo Y, Liu L, Wang J, Wang C, Lin N
and Li X (2022) Exploration of and
insights into advanced topical
nanocarrier systems for the treatment
of psoriasis.
Front. Med. 9:1017126.
doi: 10.3389/fmed.2022.1017126

COPYRIGHT

© 2022 Zhang, Hong, Sun, Zhou, Luo,
Liu, Wang, Wang, Lin and Li. This is an
open-access article distributed under
the terms of the [Creative Commons
Attribution License \(CC BY\)](#). The use,
distribution or reproduction in other
forums is permitted, provided the
original author(s) and the copyright
owner(s) are credited and that the
original publication in this journal is
cited, in accordance with accepted
academic practice. No use, distribution
or reproduction is permitted which
does not comply with these terms.

Exploration of and insights into advanced topical nanocarrier systems for the treatment of psoriasis

Miao Zhang^{1,2†}, Seokgyeong Hong^{1,2†}, Xiaoying Sun²,
Yaqiong Zhou², Ying Luo², Liu Liu^{1,2}, Jiao Wang^{1,2},
Chunxiao Wang^{1,2}, Naixuan Lin^{1,2} and Xin Li^{1,2*}

¹Department of Dermatology, Yueyang Hospital of Integrated Traditional Chinese and Western Medicine, Shanghai University of Traditional Chinese Medicine, Shanghai, China, ²Institute of Dermatology, Shanghai Academy of Traditional Chinese Medicine, Shanghai, China

Psoriasis is a chronic inflammatory skin disease with an underlying autoimmune pathogenesis that has brought great distress to patients. Current treatment options include topical therapy, systemic therapy, and phototherapy. By disrupting the stratum corneum, nanocarriers have unique advantages in allowing drug carriers to be tailored to achieve targeted drug delivery, improve efficacy, and minimize adverse effects. Furthermore, despite their limited success in market translatability, nanocarriers have been extensively studied for psoriasis, owing to their excellent preclinical results. As topical formulations are the first line of treatment, utilize the safest route, and facilitate a targeted approach, this study, we specifically describes the management of psoriasis using topical agents in conjunction with novel drug delivery systems. The characteristics, advantages, weaknesses, and mechanisms of individual nanocarriers, when applied as topical anti-psoriatic agents, were reviewed to distinguish each nanocarrier.

KEYWORDS

novel drug delivery systems, psoriasis, topical therapy, transdermal, nanocarriers

1 Introduction

Psoriasis is a recurrent inflammatory autoimmune skin disorder that ranges in severity from highly inflammatory red erythema patches supported by silvery scales to the entire skin surface, exacerbating itching, irritation, and body pain (1). The etiology of psoriasis involves a combination of hereditary and environmental factors that lead

Abbreviations: DC, dendritic cell; SC, stratum corneum; MTX, methotrexate; CYC, cyclosporine; NEs, nano-emulsions; SLNs, solid lipid nanoparticles; NLCs, nanostructured lipid carriers; BD, betamethasone dipropionate; CT, calcipotriol; SA, salicylic acid; ACT, acitretin; DIT, Dithranol; PPI, polypropylene imine; TAC, tacrolimus; PAMAM, polyamidoamine; 8-MOP, 8-methoxyp-soralen; DOTAP, dioleoyl-3-trimethylammonium propane; BP, betamethasone disodium 21-phosphate; AuNPs, gold nanoparticle; AgNPs, silver nanoparticle.

to histological changes in the skin (2, 3). At present, the treatment and management of psoriasis mainly involve topical agents, phototherapy, and systemic therapy. Topical agents are generally recommended as first-line treatment for mild psoriasis. However, for more severe conditions, phototherapy or systemic therapy is more suitable than topical agents (4). Although these methods can lessen the symptoms and signs of psoriasis, they all have limitations and are unable to completely cure the disease (5–7).

Therefore, recent research has attempted to design and develop a novel drug delivery system to compensate for the deficiencies of traditional drug delivery systems. The nanotechnology-based delivery systems have shown great advantages in increasing drug concentration at the targeted site, drug encapsulation efficiency, and skin penetration, thereby providing better efficiency, reduced side effects, and improved patient compliance. This review examines the various challenges in treating psoriasis, contemporary research into new drug delivery systems, and future potential for therapy.

2 Core pathogenesis: Massive proliferation of keratinocytes

The main clinical manifestation of psoriasis is evident in the outermost layer of the skin, which comprises keratinocytes. Keratinocytes were initially thought to be the primary cause of infection, with the immune system resulting in an excessive proliferation of skin cells, leading to immune-mediated disorders (8). Psoriasis occurs when skin cells accumulate in the epidermis instead of shedding, causing visible lesions (9). Additionally, the recognition of antimicrobial peptides is closely related to dendritic cell (DC) activation. LL-37, the most studied psoriasis-associated antimicrobial peptide, binds to DNA and stimulates toll-like receptors in plasmacytoid DC (10). Subsequently, plasmacytoid DC activation produces type I IFN (IFN- α and IFN- β), which further promotes the phenotypic maturation of myeloid DC. Th1 cells then differentiate and together with Th1 cytokines secrete a mass of inflammatory cytokines, of which the most pivotal are IL-12 and IL-23 in psoriasis. Subsequently, IL12 stimulates Th1 to produce IFN and TNF- α and IL23 stimulates Th17 to produce IL17 and IL22 (11–13).

The maintenance stage of psoriatic inflammation is the proliferation of keratinocytes, mainly involved in four aspects. The most important is the activation of adaptive immune responses by T-cell subsets, represented here by the involvement of Th17 cytokines, such as IL-23, IL-22, and IL-17 (14), followed by the inflammatory milieu activating keratinocyte proliferation through IL-17, TNF- α , and IFN- γ (10). However, LL37 and DNA greatly increase the type I IFN production. Moreover, with the help of cytokine (IL-1, IL-6, and TNF- α), chemokine, and

AMP secretion, keratinocytes can also participate actively in the inflammatory cascade.

Previous studies have shown that the TNF- α and IL-23/IL-17A axis is the main driver of psoriasis, and the interaction between IL-17A and keratinocytes is a key issue in developing psoriasis. This review aimed to highlight the important role of keratinocytes in the pathogenesis of psoriasis because patients with psoriasis are typically characterized by epidermal hyperproliferation, which aggravates the burden of traditional drug administration. Furthermore, we will present the unique advantages of the novel drug delivery system by breaking through the thick stratum corneum to explore the treatment of psoriasis patients (Figure 1).

3 Treatment challenges: Difficulties in penetrating the horny psoriatic layer

The function of the skin in psoriasis and how the pathological condition of the skin minimizes or exceeds the barrier function of the cuticle and epidermis have been a concern for researchers for many years. An experimental study in Japan reported that psoriatic skin has lower water content, free fatty acids, and natural moisturizing factors than normal skin, while the sebum content remains unaffected (15). The main concern regarding an effective response to dermatological agents is their need to reach the targeted site and remain at effective concentrations for a period. Abnormal thickening of the stratum corneum (SC) results from the hyperproliferation of keratinocytes and as a direct result of hindered penetration of the skin; topical drug delivery to psoriatic skin presents a difficult challenge for conventional formulations.

4 Conventional management for psoriasis: The multi-organ pitfalls remains

Treatment choices for psoriasis management comprise three main approaches: topical treatment, systemic treatment, and phototherapy (Figure 2A). Topical therapy is generally considered the first-line treatment for mild-to-moderate localized psoriasis and can be used with phototherapy or systemic therapy for moderate-to-severe psoriasis. Topical agents used include coal tar, dithranol (DIT), and retinoids, as well as tacrolimus (TAC), corticosteroids, salicylic acid (SA), tazarotene, and vitamin D analogs. However, owing to the lack of continuous elimination of the lesion, this may relapse and increase the psychological burden of the patient (16, 17).

Oral retinoids, methotrexate (MTX), cyclosporine (CYC), and fumaric acid esters are utilized in the treatment of psoriasis.

Organ toxicity may occur after systematic treatment with these drugs, such as the fact that MTX is toxic to the liver and cyclosporine is nephrotoxic (18, 19). Biological agents, specifically anti-IL-17A, anti-IL-23, and anti p-40 agents, have been shown to be effective against psoriasis in recent years. However, as anti-IL17A agents are associated with mycosis and neutropenia, anti-TNF- α treatments are not recommended for patients with heart problems (20, 21).

Compared with biological agents, apremilast (a small-molecule inhibitor of phosphodiesterase 4) acts at an earlier point in the inflammatory cascade, resulting in broad regulation of multiple inflammatory mediators (22). As for the conventional phototherapies, narrow-band UVB and photochemotherapy, such as PUVA (psoralen plus UVA), are used to a lower extent. Therefore, current research aims to apply novel nanocarriers to safely and effectively delivery anti-psoriatic drugs. Thus, we decided to restrict this study to topical approaches.

5 Promising strategies: Advanced topical nanocarrier systems

Nanoparticles offer advantageous properties as alternatives to conventional formulations. Therefore, by adding a targeting moiety, controlling the size of the vector, and combining hydrophobic drugs in hydrophilic carriers, the carrier can be customized. An ideal drug carrier should cross the thick stratum corneum and selectively recognize target cells by surface ligands, and most importantly, the drug-ligand complex must be stable in the biological environment and the drug carrier must be biodegradable and non-toxic (23). Novel drug delivery systems can be classified into three broad categories based on their main components: polymer-based, lipid-based, and metallic nanocarriers (Figure 2B). In this review, we discuss the above-mentioned nanocarriers, which have been proven effective in clinical and experimental studies in the past few years. The advantages and disadvantages of nanocarriers for psoriasis treatment are summarized in Table 1.

5.1 Mechanism of action of nanostructures

Lipid-based nanocarriers improve skin surface adhesion, contact with SC, and boost the penetration efficiency of biologically active ingredients into the skin (24). Polymer-based nanocarriers provide the facility of enhanced concentration gradient at the skin surface and offer tunable physical or chemical properties that can achieve sustained or controlled release of the incorporated drug at the delivery site (25). Metallic nanocarriers are conjugated to diverse targeted peptides for functional nanoparticles to penetrate biological tissues

successfully (26). The potential penetration routes of the novel drug delivery system are shown in Figure 1.

5.2 Lipid based nanocarriers

Lipid-based nanocarriers comprise physiological lipids whose structures are safe and non-toxic. These mainly include the following six types: liposomes, ethosomes, niosomes, nanoemulsions (NEs), solid lipid nanoparticles (SLNs), and nanostructured lipidic carriers (NLCs).

5.2.1 Liposomes

Liposomes are simple, self-assembling spherical vesicles consisting of one or more lipid bilayers arranged in concentric circles and enclosing equal volumes of aqueous compartments, similar to bilayer membranes of living cells (27). Liposomes are widely used as drug transporters for lipophilic and hydrophilic molecules because of their amphiphilic nature and bilayer structure (28). To evaluate the anti-psoriasis effects of cationic liposomes, dioleoyl-3-trimethylammonium propane (DOTAP) was used to prepare the CYC-loaded liposomes. The results demonstrated a strong affinity for anionic skin membranes, resulting in improved efficacy in an imiquimod-induced psoriatic plaque model (29). Another study showed that peptide-modified curcumin-loaded liposomes assisted in skin permeation and drug retention of liposomes. Consequently, peptide-modified curcumin-loaded liposomes significantly improved psoriatic lesions and decreased epidermal thickness (30). These findings proved that various modifications of liposomes could improve skin permeability. However, there is no definitive evidence of its effectiveness in patients with psoriasis, as it seems to accumulate a majority of drugs in the upper layers of the SC. One study addressed this deficiency by designing capsaicin and anti-TNF- α small interfering RNA-encapsulated cyclic cationic head lipid-polymer hybrid nanocarriers. Based on *in vitro* skin distribution studies, this complex effectively delivered FITC-siRNA up to 360 μ m skin depth, suggesting that anti-TNF- α small interfering RNA and capsaicin can be delivered into the deeper dermal milieu with the cooperation of novel cationic lipid-polymer hybrid nanoparticles (31).

5.2.2 Ethosomes

Ethosomes are novel ultra-deformable nanovesicles with high-quality alcohol in water, comprising phospholipids that are generally used at a concentration of 0.5–10% (32). Interactions with the polar head group of lipids enable fluidity of the skin tissue structure lipid bilayer, which triggers drug release into deeper layers of the epidermis. One study compared the safety and clinical efficacy of liposomes and ethosomes in psoriasis patients. After treatment, the mean psoriasis area and severity index change for liposomes and ethosomes were –68.66% and

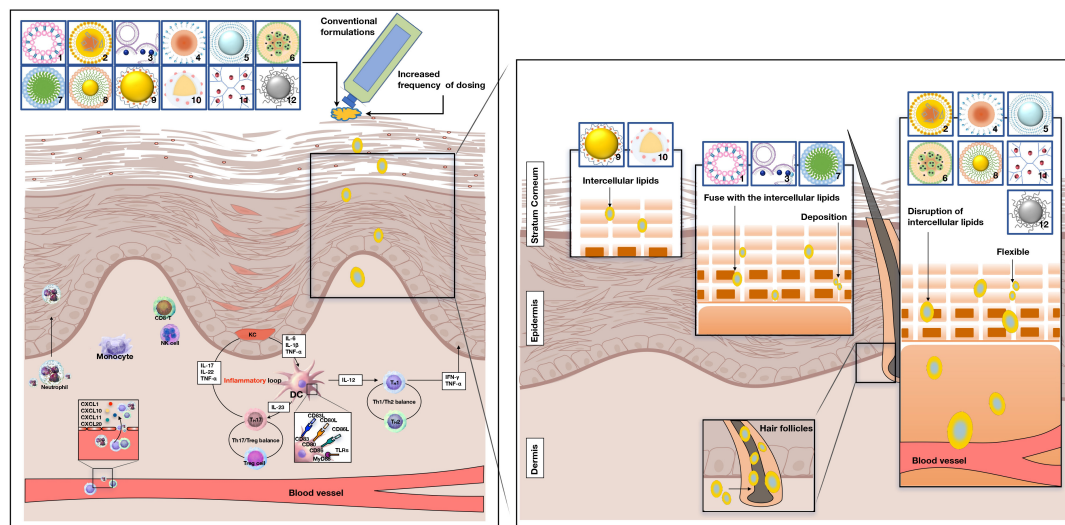


FIGURE 1

Potential penetration routes of novel drug systems and conventional formulations. Pathogenesis of psoriasis is related to the KC/DC/T loop. 1: liposomes, 2: nanostructured lipid carriers, 3: niosomes, 4: nanoemulsions, 5: ethosomes, 6: solid lipid nanoparticles, 7: micelles, 8: gold particle, 9: nanocapsules, 10: nanosphere, 11: dendrimers, 12: silver particle. pDC, plasmacytoid dendritic cells; DC, dendritic cells; KC, keratinocyte. NK -cell, natural killer cell; IL-17A, interleukin-17A; IL-17 F, interleukin-17 F; IL-12, interleukin-12. TNF- α , tumor necrosis factor- α ; IL-6, interleukin-6; IL-1 β , interleukin-1 β ; IFN- γ , interferon- γ ; Th1 cell, T helper 1 cells; Th2 cell, T helper 2 cell; Treg cell, T regulatory cells.

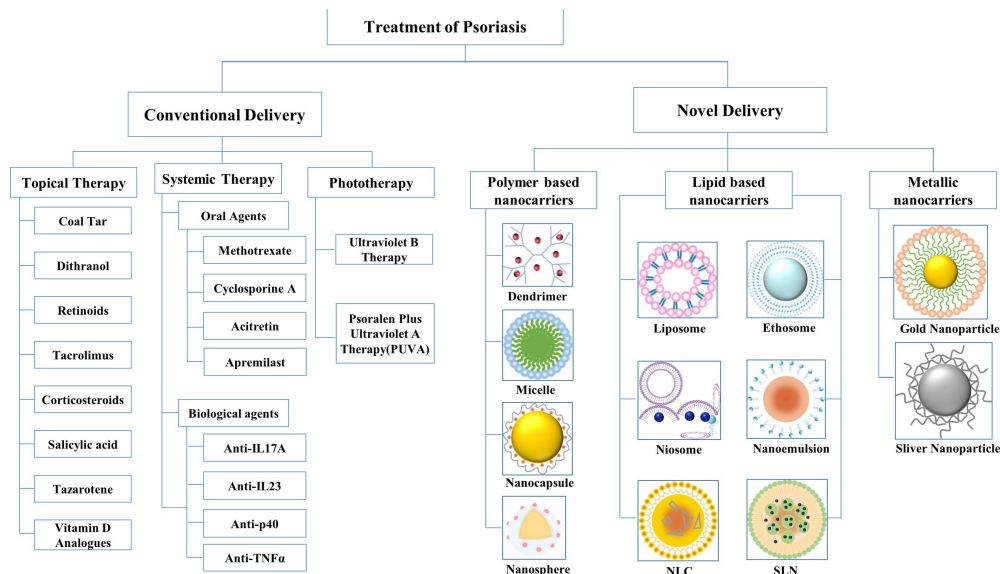


FIGURE 2

Conventional drug delivery systems and novel drug delivery systems for the treatment of psoriasis. NLC, nanostructured lipid carriers; SLN, solid lipid nanoparticles.

–81.84%, respectively, indicating that ethosomal preparations were more effective than liposomes (33). In another study, ethosomal gel loaded with MTX-incorporated SA was assessed for its anti-psoriatic potential in imiquimod-induced mice. Based on the results obtained from continuous monitoring for 24 h, MTX-SA-ethosome gel releases MTX slowly over

an extended period, with >30% drug retention detected in the skin (34). These studies have confirmed the synergistic effect of incorporating alcohol into liposomes. However, the risk of allergies may concomitantly increase with an increase in the amount of ethanol. Along with safety concerns, the ethanolic core of ethosomes may evaporate at relatively high

TABLE 1 The advantages/disadvantages of nanocarriers for the treatment of psoriasis.

Nanoformulation	Advantages	Disadvantages
Liposomes	Biocompatible, ease of surface alteration and amphiphilic nature	Weak loading capacity, rapid drug leakage, limited physical and chemical stability during storage
Ethosomes	The ability of targeting deep skin layers, showing excellent flexibility, and deformability	Risk of organic solvent residue, poor yield
Niosomes	Improving the bioavailability of insufficiently absorbed drugs and possessing more penetration power of drugs through skin	Less skin penetration, do not reach up to deeper skin layer
Nanoemulsions	Elastic properties and fluid performance	Usage of expensive instruments
Solid lipid nanoparticles	Higher efficacy, biocompatible, biodegradable, flexibility of size, and surface manipulation	Poor stability, poor batch to batch reproducibility, sterilization difficulties, low drug loading
Nanostructured lipidic carriers	Biodegradable, increasing the drug payload and reducing drug leakage during storage	Sterilization difficulties
Micelles	Thermodynamic stability, self-assembling, and targeting potential	Not good for hydrophilic drugs
Dendrimers	Ease of preparation and modification; better skin penetration	Polymer dependent biocompatibility
Nanocapsule	Sustained release, incremental drug selectivity and effectiveness, improvement of drug bioavailability, and alleviation of drug toxicity	Physical and chemical instability
Nanosphere	Lower polymer content and a high loading capacity, significant drug accumulation	Low stability
Gold nanoparticle	Ease of functionalization, large surface area compared to volume and small particle size	Cytotoxicity to epidermal keratinocytes and hair follicles' stem cells, causing skin irritation
Sliver nanoparticle	Targeting, improving solubility and stability, hindering side effects	Whether it passes the skin barrier or remains retained in the skin layers was controversial

temperatures in the local inflammatory area of psoriatic skin. Both issues require further pharmacodynamic investigation and clarification of their clinical efficacy.

5.2.3 Niosomes

Niosomes self-assemble from amphiphilic non-ionic surfactants with cholesterol and are oriented into a bilayer structure with a neutral total charge (35). The presence of non-ionic surfactants modifies the horny layer of psoriasis into looser, more permeable tissue; therefore, the residence time and local concentration of the drug in the SC and epidermis can be improved (36). Niosomes containing MTX in chitosan gels had maximum penetrability, with a significantly reduced total score, from 6.2378 ± 1.4857 to 2.0023 ± 0.1371 , compared with commercially available gels (37). This study was combined with other experimental results, which demonstrated that MTX-encapsulated niosomes exhibited noticeable changes

in ameliorating skin lesions, decreasing spleen index and epidermal thickness, and downregulating the mRNA expression of proinflammatory cytokines (38). In addition, celastrol niosomes offer an enhanced *ex vivo* osmotic profile of drug deposition in viable skin layers, and a significantly higher degree of keratosis, reduction in drug activity, and epidermal thickness were achieved (39). In the literature review, we noted that the composition, size, and surface charge of niosomes play important roles in determining the permeability, stability, and retention of drugs in the skin layer.

5.2.4 Nanoemulsions

Nanoemulsions are formed by dispersing two immiscible liquids (frequently water and oil) with droplet sizes ranging from 20 to 500 nm (40). Three types of NEs have been well-studied for particular applications: oil-in-water (o/w) emulsions, water-in-oil (w/o) emulsions, and bicontinuous NEs. The

effectiveness of transdermal drug absorption of w/o NEs is promoted *via* skin appendages by increasing the solubility of drugs and producing a larger concentration gradient between NEs and the skin (41). Similarly, to promote the permeation of CYC into the SC, one study introduced a nanoemulsion for transporting cyclosporine as an anti-inflammatory drug with the addition of nutmeg and virgin coconut oil mixture. The emulsified CYC confirmed not only an increase in drug loading but also increased skin hydration in wholesome volunteers due to the greater content of fatty acids in the combined oil solution (42). Moreover, some specifically designed NE systems have been recommended as moisturizers for daily skin care of patients with psoriasis. Therefore, scholars developed o/w NEs using rice bran oil, and the results confirmed that elevated NEs maintained normal skin pH and hydration (43). However, the low viscosity of NEs may also be overcome through a hydrogel thickening process, limiting its topical application.

5.2.5 Solid lipid nanoparticles

Unlike conventional liposomes, SLNs are solid lipids with an average diameter of 10–1000 nm that remain solid at room and body temperatures (44). There are two main factors that affect drug release characteristics: drug deposition patterns and the melting points of lipids. The beneficial effects of SLNs can be summarized as the “occlusion effect,” which occurs because of the formation of an occlusive hydrophobic film on top of the SC, resulting in better hydration and transcutaneous penetration (35). One study verified that betamethasone dipropionate (BD)-calcipotriol (CT)-loaded SLNs extensively increased the dermal absorption of BD/CT and delayed the abrupt growth of keratinocytes. Consistently, an *in vivo* mouse tail model demonstrated that the administration of BD-CT-SLNs reduced epidermal thickness and increased melanocyte count without side effects compared to Daivobet™, which can verify the anti-psoriatic activity of BD-CT-loaded SLNs (45). Similar observations were reported when SLNs were applied as a topical solution containing a combination of MTX and etanercept (46). These results show that SLNs have great potential to limit dose-dependent toxicity by reducing the systemic exposure of the encapsulated drug.

5.2.6 Nanostructured lipidic carriers

Nanostructured lipidic carriers were designed to fill in the gap between SLNs regarding drug solubility and leakage by replacing up to 30% of the solid lipid mass of SLNs with liquid lipids. Although a certain amount of liquid lipids is replenished, the output of NLCs by mixing remains in a solid form at room or body temperature (47). When incorporating liquid lipids (an imperfect and less-ordered crystalline structure of NLCs) was created, displaying a considerable “occlusion effect,” which is appropriate for topical

administration. A comparative study evaluated the potential use of carbomer gel-bearing methotrexate-loaded NLC carriers for topical application of methotrexate in contrast to SLNs. The skin drug deposition study indicated the greatest deposition of drug-enriched NLC5 hydrogel (28.8%), in contrast to plain drug-enriched hydrogel (11.4%) and drug-enriched SLN hydrogel (18.6%) (48). Fluorescence microscopy showed that these lipid-based systems have a localization effect in deeper skin regions. Another randomized controlled trial further confirmed the anti-psoriasis effects of NLCs by formulating and characterizing acitretin (ACT) NLCs. A notably higher deposition of acitretin was discovered in human cadaver skin from ACTNLC gel ($81.38 \pm 1.23\%$) than from ACT plain gel ($47.28 \pm 1.02\%$) (49).

5.3 Polymer-based nanocarriers

Polymer-based nanocarriers are colloidal structures composed of macromolecules that contain natural or synthetic polymers as the chief excipients. Compared with lipid-based nanocarriers, polymers tend to accumulate in the dermis layer, suggesting that the former is suitable for topical treatment, whereas the latter is more appropriate for transdermal treatment (50). Four types of polymer-based nanocarriers, namely, micelles, dendrimers, nanospheres, and nanocapsules, are discussed in the next section.

5.3.1 Micelles

Micelles are spherical structures with diameters less than 100 nm, formed by the self-assembly of amphiphilic molecules in an aqueous system through a hydrophobic effect (51). In the micelle structure, the hydrophobic core carries lipophilic drugs and the hydrophilic shell carries hydrophilic drugs, which are suitable for drug administration. To enhance the cutaneous bioavailability of TAC, TAC-loaded polymeric micelles were formulated using biodegradable and biocompatible methoxy-poly (ethylene glycol)-dihexyl-substituted polylactide diblock copolymer. The results showed that compared with Protopic, TAC deposition in skin was significantly increased by this formula (0.1% W/W; TAC ointment, 1.50 ± 0.59 and 0.47 ± 0.20 $\mu\text{g}/\text{cm}$, respectively) (52). In a similar way, silibinin-loaded polymeric micelles were prepared in another study. The average particle size of the optimized samples was 18.3 ± 2.1 nm, the encapsulation efficiency was $75.8 \pm 5.8\%$, and the release time of silybin was prolonged. Moreover, silibinin permeation through psoriatic skin after 48 h of treatment with polymeric micelles and the aqueous control was 80.35 and 92.6, respectively (53). These micelles have been designed for targeted drug delivery because of their easy structural deformation under the influence of pH, temperature, or reduction-oxidation reactions *in vivo*. Therefore, micelles are more suitable for local administration or in combination with other polymer materials when controlled drug release is required (54).

TABLE 2 Topical applications of nanocarriers in drug delivery for psoriasis treatment.

Nanocarriers	Typical components	Carried drug	Preparation technique	Excipients	Size (nm) Zeta potential (mV)	Encapsulation efficiency (%)	Drug release (%)	Skin permeability	Stability	Experimental studies	Transdermal delivery mechanism	References
Liposomes	phospholipids	Cyclosporine	Ethanol injection, thin film hydration, reverse phase evaporation	N-(1-(2,3-dioleoyloxy) propyl)-cholesterol, chloroform, ethanol	111 ± 1.62 41.12 ± 3.56	93 ± 2.12	120 h:43.86 ± 4.85	NN/A	4 (4°)	IMQ rats	(1) Improve the hydration degree of the SC. (2) Change the structure of the epidermis by fusion with the SC and disrupt its lipid arrangement. (3) Permeate into the intercellular spaces <i>via</i> diffusion and capillary action	(19)
		Curcumin	Thin film hydration	Peptide	94–100 –22.0	97	96 h:>80	Permeate into the dermis	1 (4°)	IMQ rats		(20)
		Capsaicin SiRNA	Double emulsion solvent evapo-ration	Ethanol	163 ± 9 35.14 ± 8.23	92	N/A	Permeate into deep dermis	N/A	IMQ rats		(21)
Ethosomes	Phospholipids (0.5–10%), ethanol (20–45%)	Anthralin	Thin film hydration	Cholesterol/PL-90G, chloroform and methanol	146–381 N/A	85.0 ± 0.6	27.1 ± 0.4	Permeate through the upper layers of the SC	N/A	Psoriasis patients	The flexibility and deformability of ethosomes facilitate drugs passing through SC and target deep skin layers	(23)
		Methotrexate Salicylic Acid	Cold method	Soya phosphatidyl-choline, chloroform, methanol,hydro-ethanolic solution	376.04 ± 3.47 ~20	91.77 ± 0.02	26.13 ± 1.61	8 h:5.87 ± 0.01% Permeate through the SC	N/A	IMQ rice		(24)
Niosomes	Non-ionic surfactants cholesterol	Methotrexate	Lipid layer hydration	Glycerin, propylene glycol	N/A	N/A	N/A	N/A	N/A	Psoriasis patients	(1) The bilayer membrane made of non-ionic surfactant containing cholesterol has strong permeability. (2) High chemical stability	(27)
		Methotrexate Nicotinamide	Ethanol injection	Absolute ethanol	181.27 ± 1.44 –24.53 ± 1.37	71.05 ± 0.8	N/A	Permeate into the dermis, mainly in the SC	N/A	BALB/c mice		(28)
		Celastrol	Thin film hydration	Cholesterol, carbopol 934, span 20, span 60	147.4 ± 5.6 textbf –48.9 ± 1.1	N/A	N/A	N/A	N/A	IMQ rice		(28)

(Continued)

TABLE 2 (Continued)

Nanocarriers	Typical components	Carried drug	Preparation technique	Excipients	Size (nm)	Encapsulation efficiency (%)	Drug release (%)	Skin permeability	Stability	Experimental studies	Transdermal delivery mechanism	References
					Zeta potential (mV)							
Nano-emulsions	Oil phase, surfactant and cosurfactant	Cyclosporine	Emulsification	Tween 80	159.9 –	N/A	3 h:81.49	N/A	>3 months (4°/RT)	Healthy volunteers	(1) Increase the solubility and diffusivity of SC. (2) Extract and swell skin lipids to enhance penetration through the pores. (3) Permeate the scaly keratinized psoriatic skin through the hydrophilic pathways and pores	(32)
		Rice bran oil	Emulsion phase inversion	N/A	69 ± 17 –	N/A	N/A	N/A	>90 days (4°/RT)	Healthy volunteers, psoriasis patients		(33)
SLNs	Solid lipids	Psoralen	Solvent injection	Precirol ATO 5, oleic acid, tween 80, soybean phospholipids	296.6 ± 49.5 –40.0 ± 5.9	N/A	~70	Low permeation in hyperproliferative skin	N/A	Nude mice		(35)
		Betamethasone Calcipotriol	Hot melt high shear homogenization	Compritol 888 ATO, glyceryl monostearate and precirol ATO 5	188 ± 16 N/A	85.10 ± 2.02 (BD) 97.87 ± 0.08 (CT)	48 h:45–56 (BD), 25–31 (CT)	4 h: Permeate into the dermis through appendageal pathway and intercellular route	12 (RT)	HacaT, mouse tail model	(1) Fusion with membrane. (2) Lipid-fluidizing property. (3) Occlusive effect. (4) Utilizing the skin transport pathways, including transcellular route, intercellular route and trans-appendageal route	(36)
		Methotrexate Etanercept	Hot ultrasonication	Cetyl palmitate, Polysorbate	356 ± 2 –27 ± 4	88 ± 2	52 ± 4	8 h:75–80%, Permeate into the dermis	8 (RT)	Psoriatic skin		(37)
NLCs	Solid and liquid Lipids	Methotrexate	Solvent diffusion	Glyceryl monostearate, ethanol, acetone, PBS	221 ± 14 –33.6 ± 1.2	62.72 ± 0.94	N/A	24 h: 24.7% ± 2.3%, Permeate through the dermis	16 (RT)	Albino rats		(39)
		Acitretin	Solvent diffusion	Oleic acid, precirol ATO 5, tween 80, acetone	223 ± 8.92 –26.4 ± 0.86	63.0 ± 1.54	30 h:80.22 ± 3.40	N/A	N/A	Psoriatic patients	(1) Occlusive effect of solid matrix. (2) Liquid lipids increase skin hydration	(40)

(Continued)

TABLE 2 (Continued)

Nanocarriers	Typical components	Carried drug	Preparation technique	Excipients	Size (nm)	Encapsulation efficiency (%)	Drug release (%)	Skin permeability	Stability	Experimental studies	Transdermal delivery mechanism	References
					Zeta potential (mV)							
Micelles	Surfactant, macromolecule polymer	Tacrolimus	Solvent evaporation	Acetone, phosphate, acetic acid	52.9	88.14 ± 0.20	1.5	Permeate into upper dermis	7 months (4°)	Human skin	Preferentially deposited in skin wrinkles, between the corneocyte clusters, where there is a more permeable zone, which could increase drug delivery	(45)
		Silibinin	N/A	Cholesterol, lecithin, oleic acid, polox-amer	18.3 ± 2.1	75.8 ± 5.8	4 h:21.8	48 h: 80.35 ± 3.37%, Permeate through the full-thickness psoriatic skin	> 3 months (RT)	IMQmice		(46)
Dendrimer	Core, repeating units, terminal surface groups	Dithranol	Divergent method	Ethylenediamine	8 ± 0.04 12.0 ± 0.42	57.1 ± 1.32	N/A	24 h: 95.33%, Permeate through skin	N/A	Rats	(1) <i>In vivo</i> degradation of covalent bond between drugs dendrimer by suitable enzymes. (2) Releasing of the drug from dendrimer due to physical changes or stimulus like pH, temperature, etc	(48)
		8-methoxy-psoralen	Convergent method	Polyamidoamine (PAMAM) dendrimers G3 and G4	N/A	N/A	N/A	29 h: 0.6 mol h ⁻¹ cm ⁻²	N/A	Wistar rats		(49)
		TNF- α siRNA	N/A	PAMAM dendrimer (P-G3), triton X-100, diethyl pyro carbonate water	99.80 ± 1.80 13.40 ± 4.84	98.72 ± 2.02	N/A	N/A	N/A	Wistar rats		(50)
Nanocapsule	Active materials (core) and a protective matrix (shell)	Tretinoin	Interfacial deposition of the preformed polymer method	Sorbitan monooleate, polymer, acetone	228 ± 08 -7.27 ± 0.66	>99.9%	N/A	N/A	1 h:56-57%	Photo-degradation studies	(1) The initial burst effect: either to surface adsorbed drug either to surface adsorbed drug. (2) The second slow phase: the diffusion of the drug molecules and the reservoir core. (3) Polymer erosion.	(52)
		Dithranol	Interfacial deposition	Ethylene-diaminetetraacetic acid, sorbitan monostearate, Tween 80	241 ± 4, -7.6 ± 0.6	N/A	24 h:96	N/A	15 days: 52%	Photo-degradation studies		(53)
		Dexamethasone	Interfacial deposition	Sorbitan mono-oleate, polysorbate 80	201 ± 06 -5.73 ± 0.42	N/A	N/A	N/A	N/A	Allium cepa root meristem model		(54)

(Continued)

TABLE 2 (Continued)

Nanocarriers	Typical components	Carried drug	Preparation technique	Excipients	Size (nm)	Encapsulation efficiency (%)	Drug release (%)	Skin permeability	Stability	Experimental studies	Transdermal delivery mechanism	References
					Zeta potential (mV)							
Nanosphere	Spherical shape polymeric matrix	Paclitaxel	Ultra-centrifugation and resuspension	Suberic acid, poly (ethylene glycol) monomethyl ether, Tween-80	N/A	68 ± 90 (BE) 65 ± 78 (LE)	72 h: 8.4–58%	Significant amounts of paclitaxel into the epidermal layer of skin	8 days (4°C)	Human cadaver skin	(1) The erosion of polymer matrix. (2) enzymatic degradation of polymeric bonds. (3) Diffusion of the drug entrapped physically	(56)
		Betamethasone disodium 21-phosphate	Oil-in-water solvent diffusion	Poly (d, l-lactic acid), poly (d, l-lactic/glycolic acid)	178 ± 18	11.7 ± 0.8	1 h: 63	N/A	24 h: 45%	N/A		(57)
Gold nanoparticles (AuNPs)	Gold precursor	Methotrexate	Chemical synthesis	Deionized water	4 ± 1 –32 ± 1	N/A	1 h: 80% 24 h: 95%	Observed both in the epidermis and, at less intensity, also in the dermis	6 months (4°C)	Wild-type mice Healthy human	Conjugated to various cellular targeting peptides to provide functional nanoparticles	(60)
		Cornusmas	Green synthesis	N/A	N/A	N/A	N/A	N/A	N/A	Psoriatic patients		(61)
		Woodfordia fruticosa	Biogenic synthesis	Milli-Q water	10~20 –26.2	N/A	N/A	N/A	N/A	Healthy albino mice		(62)
Silver particles (AgNPs)	Silver precursor	Black elderberry fruits	Green synthesis	Resin, absolute ethanol	20~80 –20.9	N/A	N/A	N/A	1 month	HaCaT cells Wistar rats	AgNPs are up taken by the cells by active mechanisms e.g., endocytosis or by passive mechanisms e.g., by diffusion	(64)
		Selaginella myosurus plant	Biological synthesis (centrifugation)	N/A	N/A	N/A	N/A	N/A	N/A	Wistar albinos rats		(65)

N/A, not available; IMQ, imiquimod; siRNA, small interfering RNA; SC, stratum corneum; RT, refrigeration ton; BD, betamethasone; CT, calcipotriol; TNF- α , tumor necrosis factor- α ; PAMAM, polyamidoamine; PBS, phosphate buffered saline.

5.3.2 Dendrimers

Dendrimers are highly-branched and nano-sized micromolecules with a controlled, globular, reactive three-dimensional structure. Drug molecules form drug-dendritic molecular conjugates through non-covalent interactions or covalently linked functional groups (55). The three dendrimer types were peptide dendrimers, glycodendrimers, and lysine-core dendrimers. One study explored the potential of DIT-loaded polypropylene imine (PPI) dendrimers and their characterization was performed using spectroscopy and transmission electron microscopy. Confocal laser scanning-microscopy images and skin penetration studies demonstrated that PPI can be utilized to enhance the local bioavailability of molecules in a controlled manner. PPI enhances transdermal absorption in a controlled manner, while DIT accumulation in the skin *via* dendritic molecular vectors may help optimize drug targeting to the epidermis and dermis (56). Another study focused on the enhancement of transdermal delivery of 8-methoxyp-soralen (8-MOP) DOTAP by the dendritic molecules G3 and G4 of polyamidoamine (PAMAM). Another study focused on the enhancement effect of PAMAM dendrimers G3 and G4 on transdermal delivery of 8-MOP. Enhanced *in vivo* 8-MOP skin penetration into the deeper layers of the skin was obtained, and G4 PAMAM dendrimers provided a better penetration enhancement effect for 8-MOP compared to G3 PAMAM (57). Moreover, one study compared the PAMAM dendrimers' suitability with DOTAP liposomes for topical delivery of siRNA against TNF- α . The results showed that phenotypic and histopathological features were improved, and IL-6, TNF- α , IL-17, and IL-22 levels decreased in the dendritic plexus and liposome treatment groups compared to the imiquimod group (58).

5.3.3 Nanocapsule

Nanocapsule is a type of nanoparticle that consists of one or more active components (core) and a protective matrix (shell), with the core consisting of a liquid suspension containing the medicine and the polymer constituting the shell (59). One study created tretinoin-loaded nanocapsules and assessed the influence of nanoencapsulation on the photostability of tretinoin from different perspectives. Inferring that nanocapsules are a suitable carrier for tretinoin to treat psoriasis, photodegradation experiments showed a 2-fold increase in drug stability in a methanolic solution, with an increased half-life between 85 and 100 min (60). In another experimental investigation, the stability of DIT-loaded lipid-core nanocapsules was compared to that of medication-free solutions by photodegradation against UVA light. It showed greater stability (half-life times of approximately 4 and 1 h for the DIT-loaded lipid-core nanocapsules), and an irritation test was conducted to evaluate the safety of the formulations; it was proved that the drug's toxicity was reduced due to nanoencapsulation (IS = 0) compared to the effects observed

with DIT dispersion (10.43 ± 0.67) (61). Vertical Franz diffusion cells were used to study and test the dexamethasone-loaded polymeric nanocapsules. The results of the *in vitro* release showed that there was minor drug release per cm² after 2 and 24 h (62).

5.3.4 Nanosphere

Nanospheres are matrix systems in which medicine is either disseminated inside the polymer matrix or adsorbed on the surface of the sphere. The polymer matrix constituents and capacity to absorb fluid affect the speed of drug release (63). Nanospheres have received considerable attention recently, owing to their protective shell and ability to oxidize easily. Previous study created polymeric betamethasone disodium 21-phosphate (BP) nanoparticles and PEG-block-PLA/PLGA copolymers and homopolymers from poly (D, L-lactic acid) and poly (D, L-lactic/glycolic acid). Small nanoparticles released more BP than larger ones, whereas PLGA homopolymers released BP more quickly than PLA homopolymers (64). Tyrosine-derived nanospheres (TyroSpheres) encapsulated in anti-proliferative paclitaxel were further developed. The findings demonstrated that TyroSpheres increased [approximately 4,000 times better than that of phosphate-buffered saline (PBS)] and permitted sustained, dose-controlled release over a 72 h period under conditions simulating skin permeation. By enabling paclitaxel to be delivered into the epidermis at concentrations of >100 ng/cm² of skin surface area and by increasing the cytotoxicity of loaded paclitaxel to human keratinocytes, tyrospheroids may effectively treat psoriasis (65).

5.4 Metallic nanocarriers

Metallic nanomaterials have been of significant interest to the scientific community for many decades. These particles have antibacterial, antifungal, and anti-skin cancer effects, and therefore, are promising for the management of dermatological diseases. Types of metallic nanoparticles have been synthesized using different elements, such as gold nanoparticles (AuNPs) and silver nanoparticles (AgNPs).

5.4.1 Gold nanoparticles

Solid colloidal particles, called AuNPs, with sizes ranging from 1 to 100 nm, are created from metal precursors. Nanoparticles and their contents can also pass through biological barriers that are difficult to access and penetrate, owing to their small size. Using different chemistries or because of their high affinity for thiolated molecules, they can function easily with all types of electron-donating compounds (26, 66). The ease of functionalization, increased surface area to

volume ratio, small particle size, and the anti-inflammatory action they perform provide a synergistic effect when loaded with anti-inflammatory drugs (67). Combining topical AuNPs and AgNPs with cornus mas inhibits proliferation in human plaque psoriasis by downregulating the activity of nuclear factor-3B, as well as decreasing cluster of differentiation 68-positive macrophages and IL-12 and TNF- α production (68). In another study, woodfordia fruticosa (flower extract)-enriched AuNPs were used to reduce hyperplasia, parakeratosis, and serum concentrations of TNF- α , IL-22, and IL-23 and showed that 1% AuNPs (ointment) mixed with Swiss albino mice showed the lowest energy level and had a significant therapeutic value (69).

5.4.2 Silver nanoparticles

Silver nanoparticles are one of the most promising metal nanoparticles and have been widely used in nanomedicine, especially for the diagnosis and treatment of cancer. In addition, the potential of AgNPs for the delivery of antimicrobial, antibacterial, antifungal, and anti-material agents has been explored. Moreover, AgNPs have been effectively used as delivery carriers for anti-psoriasis drugs (70). A team prepared biocompatible AgNPs containing fruit extracts of European blackberry and examined their anti-inflammatory effects. The synthesized nanoparticles have good anti-inflammatory effects and have been studied both *in vivo* and *in vitro*. *In vitro*, anti-inflammatory effects were shown by a reduction in cytokine production and maintenance of low levels after UVB irradiation. *In vivo*, AgNPs pre-administration reduced cytokine levels in the foot tissue and had a long-term protective effect. AuNPs are considered promising anti-psoriasis treatments (71). Another study evaluated the anti-inflammatory capability of nanoparticles created in rats using carrageenan-induced hind foot edema models and albumin denaturation and suggested that silver nanoparticles may reduce or prevent the release of acute inflammatory mediators. This study unequivocally demonstrated that *Selaginella myosurus* mediated by AgNPs might be a source of anti-inflammatory medications (72).

In addition to the above-mentioned nanocarriers, diverse novel carriers have been developed for the effective delivery of various anti-psoriatic drugs. Table 2 lists the topical applications of nanocarriers in drug delivery for psoriasis therapy, which collectively constitutes a large category of human conditions. Novel delivery systems have gained a unique position for safe and effective drug delivery to other dermatological diseases, including atopic dermatitis, melanoma, and acne. Considering the unique features of each nanocarriers, we suggest that a proper combination should be considered based on the physicochemical properties of the loaded drugs and the clinical characteristics of patients with psoriasis.

6 Conclusion and future perspective

Although psoriasis cannot be permanently treated, controlling its clinical manifestations can significantly improve the quality of life of patients and eliminate their psychological burden. Drug delivery for skin disorders has always been a clinical challenge given that it is essential to achieve maximum possible epidermal penetration and retention with minimum drug absorption into the bloodstream to avoid side effects. Hyper-keratinized skin thickens the cuticle, making it difficult for different active ingredients to circumvent, which directly affects drug delivery and retention. Accordingly, novel drug delivery systems, such as liposomes, niosomes, SLNs, and NLCs hold promise in preclinical and experimental studies, owing to their ability to overcome key formulation challenges.

Many studies have explored this, but further research should be performed. Contemporary research focuses more on polymer and lipid nanoparticles, while metal nanoparticles may attract more interest in future work because of their small size and outstanding performance. Additionally, hybrid nanosystems can combine the advantages of different types of nanoparticles to obtain the most appropriate drug delivery system for patients. This approach has not been thoroughly studied in the local treatment of psoriasis but may greatly improve the management of these psoriatic plaques.

In conclusion, we noted that published data on nanodermatology appear to be successful at different stages of the healthcare process, offering a personalized approach to immune-mediated inflammatory dermatosis. In the future, high-prognosis psoriasis models (*in vivo* and *in vitro* models) are needed to improve the adoption rates, which may be a key approach in the fight against psoriasis.

Author contributions

MZ and SH contributed to manuscript writing, editing, and data collection. XS, YZ, YL, LL, JW, CW, and NL contributed to data analysis. XL contributed to conceptualization and supervision. All authors have read and approved the final manuscript.

Funding

This work was sponsored by the National Natural Science Foundation of China (Nos. 82074427 and 81874470), the Xinglin Scholar, Shanghai University of Traditional Chinese Medicine (No. RY411.14.12), Science and Technology Commission of Shanghai Municipality (Nos. 22Y11922200

and 21Y21920102), and Shanghai Health Care Commission (No. 20224Z0019).

Conflict of interest

The authors declare that the research was conducted in the absence of any commercial or financial relationships that could be construed as a potential conflict of interest.

References

- Sala M, Elaissari A, Fessi H. Advances in psoriasis physiopathology and treatments: up to date of mechanistic insights and perspectives of novel therapies based on innovative skin drug delivery systems (ISDDS). *J Control Release*. (2016) 239:182–202. doi: 10.1016/j.jconrel.2016.07.003
- Mabuchi T, Chang TW, Quinter S, Hwang ST. Chemokine receptors in the pathogenesis and therapy of psoriasis. *J Dermatol Sci*. (2012) 65:4–11. doi: 10.1016/j.jdermsci.2011.11.007
- Pradhan M, Singh D, Singh MR. Novel colloidal carriers for psoriasis: current issues, mechanistic insight and novel delivery approaches. *J Control Release*. (2013) 170:380–95. doi: 10.1016/j.jconrel.2013.05.020
- Gungor S, Rezigue M. Nanocarriers mediated topical drug delivery for psoriasis treatment. *Curr Drug Metab*. (2017) 18:454–68. doi: 10.2174/1389200218666170222145240
- Cai XC, Ru Y, Liu L, Sun XY, Zhou YQ, Luo Y, et al. Efficacy and safety of biological agents for the treatment of pediatric patients with psoriasis: a bayesian analysis of six high-quality randomized controlled trials. *Front Immunol*. (2022) 13:896550. doi: 10.3389/fimmu.2022.896550
- Liu L, Wang J, Li HJ, Zhang S, Jin MZ, Chen ST, et al. Sphingosine-1-phosphate and its signal modulators alleviate psoriasis-like dermatitis: preclinical and clinical evidence and possible mechanisms. *Front Immunol*. (2021) 12:759276. doi: 10.3389/fimmu.2021.759276
- Wang J, Zhang S, Xing M, Hong S, Liu L, Ding XJ, et al. Current evidence on the role of lipid lowering drugs in the treatment of psoriasis. *Front Med*. (2022) 9:900916.
- Traub M, Marshall K. Psoriasis–pathophysiology, conventional, and alternative approaches to treatment. *Altern Med Rev*. (2007) 12:319–30.
- Armstrong AW, Read C. Pathophysiology, clinical presentation, and treatment of psoriasis: a review. *JAMA*. (2020) 323:1945–60. doi: 10.1001/jama.2020.4006
- Morizane S, Yamasaki K, Mühleisen B, Kotol PF, Murakami M, Aoyama Y, et al. Cathelicidin antimicrobial peptide LL-37 in psoriasis enables keratinocyte reactivity against TLR9 ligands. *J Invest Dermatol*. (2012) 132:135–43. doi: 10.1038/jid.2011.259
- Nestle FO, Conrad C, Tun-Kyi A, Homey B, Gombert M, Boyman O, et al. Plasmacytoid dendritic cells initiate psoriasis through interferon- α production. *J Exp Med*. (2005) 202:135–43. doi: 10.1084/jem.20050500
- Gregorio J, Meller S, Conrad C, Di Nardo A, Homey B, Lauerma A, et al. Plasmacytoid dendritic cells sense skin injury and promote wound healing through type I interferons. *J Exp Med*. (2010) 207:2921–30. doi: 10.1084/jem.20101102
- Santini SM, Lapenta C, Donati S, Spadaro F, Belardelli F, Ferrantini M. Interferon- α -conditioned human monocytes combine a Th1-orienting attitude with the induction of autologous Th17 responses: role of IL-23 and IL-12. *PLoS One*. (2011) 6:e17364. doi: 10.1371/journal.pone.0017364
- Nestle FO, Turka LA, Nickoloff BJ. Characterization of dermal dendritic cells in psoriasis. Autostimulation of T lymphocytes and induction of Th1 type cytokines. *J Clin Invest*. (1994) 94:202–9. doi: 10.1172/JCI117308
- Takahashi H, Tsuji H, Minami-Hori M, Miyauchi Y, Iizuka H. Defective barrier function accompanied by structural changes of psoriatic stratum corneum. *J Dermatol*. (2014) 41:144–8. doi: 10.1111/1346-8138.12393
- Torsekar R, Gautam MM. Topical therapies in psoriasis. *Indian Dermatol Online J*. (2017) 8:235–45. doi: 10.4103/2229-5178.209622
- Bos JD, Spuls PI. Topical treatments in psoriasis: today and tomorrow. *Clin Dermatol*. (2008) 26:432–7. doi: 10.1016/j.clindermatol.2007.10.025
- Lindqvist T, Salah LA, Gillstedt M, Wennberg AM, Osmancevic A. Methotrexate management in psoriasis: are we following the guidelines? *Acta Derm Venereol*. (2018) 98:449–51. doi: 10.2340/00015555-2857
- Ho VC, Griffiths CE, Berth-Jones J, Papp KA, Vanaclocha F, Dauden E, et al. Intermittent short courses of cyclosporine microemulsion for the long-term management of psoriasis: a 2-year cohort study. *J Am Acad Dermatol*. (2001) 44:643–51. doi: 10.1067/mjd.2001.112400
- Bai F, Li GG, Liu Q, Niu X, Li R, Ma H. Short-Term Efficacy and Safety of IL-17, IL-12/23, and IL-23 Inhibitors Brodalumab, Secukinumab, Ixekizumab, Ustekinumab, Guselkumab, Tildrakizumab, and Risankizumab for the Treatment of Moderate to Severe Plaque Psoriasis: a systematic review and network meta-analysis of randomized controlled trials. *J Immunol Res*. (2019) 2019:2546161. doi: 10.1155/2019/2546161
- Ten Bergen LL, Petrovic A, Krogh Aarebrot A, Appel S, The TNF- α /IL-23/IL-17 axis-Head-to-head trials comparing different biologics in psoriasis treatment. *Scand J Immunol*. (2020) 92:e12946. doi: 10.1111/sji.12946
- Haber SL, Hamilton S, Bank M, Leong SY, Pierce E. Apremilast: a novel drug for treatment of psoriasis and psoriatic arthritis. *Ann Pharmacother*. (2016) 50:282–90. doi: 10.1177/1060028015627467
- Barratt G. Colloidal drug carriers: achievements and perspectives. *Cell Mol Life Sci*. (2003) 60:21–37. doi: 10.1007/s000180300002
- Zhang Z, Tsai PC, Ramezanli T, Michniak-Kohn BB. Polymeric nanoparticles-based topical delivery systems for the treatment of dermatological diseases. *Wiley Interdiscip Rev Nanomed Nanobiotechnol*. (2013) 5:205–18. doi: 10.1002/wnan.1211
- Kim ST, Jang DJ, Kim JH, Park JY, Lim JS, Lee SY, et al. Topical administration of cyclosporin A in a solid lipid nanoparticle formulation. *Pharmazie*. (2009) 64:510–4.
- Daraee H, Eatemadi A, Abbasi E, Fekri Aval S, Kouhi M, Akbarzadeh A, et al. Application of gold nanoparticles in biomedical and drug delivery. *Artif Cells Nanomed Biotechnol*. (2016) 44:410–22. doi: 10.3109/21691401.2014.955107
- Akbarzadeh A, Rezaei-Sadabady R, Davaran S, Joo SW, Zarghami N, Hanifehpour Y, et al. Liposome: classification, preparation, and applications. *Nanoscale Res Lett*. (2013) 8:102. doi: 10.1186/1556-276X-8-102
- Allen TM, Cullis PR. Liposomal drug delivery systems: from concept to clinical applications. *Adv Drug Deliv Rev*. (2013) 65:36–48. doi: 10.1016/j.addr.2012.09.037
- Walunj M, Doppalapudi S, Bulbake U, Khan W. Preparation, characterization, and *in vivo* evaluation of cyclosporine cationic liposomes for the treatment of psoriasis. *J Liposome Res*. (2020) 30:68–79. doi: 10.1080/08982104.2019.1593449
- Yu F, Zhang Y, Yang C, Li F, Qiu B, Ding W. Enhanced transdermal efficiency of curcumin-loaded peptide-modified liposomes for highly effective antipsoriatic therapy. *J Mater Chem B*. (2021) 9:4846–56. doi: 10.1039/D1TB00557J
- Desai PR, Marepally S, Patel AR, Voshavar C, Chaudhuri A, Singh M. Topical delivery of anti-TNF α siRNA and capsaicin via novel lipid-polymer hybrid nanoparticles efficiently inhibits skin inflammation *in vivo*. *J Control Release*. (2013) 170:51–63. doi: 10.1016/j.jconrel.2013.04.021
- Toutou E, Dayan N, Bergelson L, Godin B, Eliaz M. Ethosomes – novel vesicular carriers for enhanced delivery: characterization and skin penetration properties. *J Control Release*. (2000) 65:403–18. doi: 10.1016/S0168-3659(99)00222-9

Publisher's note

All claims expressed in this article are solely those of the authors and do not necessarily represent those of their affiliated organizations, or those of the publisher, the editors and the reviewers. Any product that may be evaluated in this article, or claim that may be made by its manufacturer, is not guaranteed or endorsed by the publisher.

33. Fathalla D, Youssef EMK, Soliman GM. Liposomal and ethosomal gels for the topical delivery of anthralin: preparation, comparative evaluation and clinical assessment in psoriatic patients. *Pharmaceutics*. (2020) 12:446. doi: 10.3390/pharmaceutics12050446
34. Chandra A, Aggarwal G, Manchanda S, Narula A. Development of topical gel of methotrexate incorporated ethosomes and salicylic acid for the treatment of psoriasis. *Pharm Nanotechnol*. (2019) 7:362–74. doi: 10.2174/2211738507666190906123643
35. Fang JY, Fang CL, Liu CH, Su YH. Lipid nanoparticles as vehicles for topical psoralen delivery: solid lipid nanoparticles (SLN) versus nanostructured lipid carriers (NLC). *Eur J Pharm Biopharm*. (2008) 70:633–40. doi: 10.1016/j.ejpb.2008.05.008
36. Sinico C, Fadda AM. Vesicular carriers for dermal drug delivery. *Expert Opin Drug Deliv*. (2009) 6:813–25. doi: 10.1517/17425240903071029
37. Lakshmi PK, Devi GS, Bhaskaran S, Sacchidanand S. Niosomal methotrexate gel in the treatment of localized psoriasis: phase I and phase II studies. *Indian J Dermatol Venereol Leprol*. (2007) 73:157–61. doi: 10.4103/0378-6323.32709
38. Yang X, Tang Y, Wang M, Wang Y, Wang W, Pang M, et al. Co-delivery of methotrexate and nicotinamide by cerosomes for topical psoriasis treatment with enhanced efficacy. *Int J Pharm*. (2021) 605:120826. doi: 10.1016/j.ijpharm.2021.120826
39. Meng S, Sun L, Wang L, Lin Z, Liu Z, Xi L, et al. Loading of water-insoluble celastrol into niosome hydrogels for improved topical permeation and anti-psoriasis activity. *Colloids Surf B Biointerfaces*. (2019) 182:110352. doi: 10.1016/j.colsurfb.2019.110352
40. Singh Y, Meher JG, Raval K, Khan FA, Chaurasia M, Jain NK, et al. Nanoemulsion: concepts, development and applications in drug delivery. *J Control Release*. (2017) 252:28–49. doi: 10.1016/j.jconrel.2017.03.008
41. Wu H, Ramachandran C, Weiner ND, Roessler BJ. Topical transport of hydrophilic compounds using water-in-oil nanoemulsions. *Int J Pharm*. (2001) 220:63–75. doi: 10.1016/S0378-5173(01)00671-8
42. Musa SH, Basri M, Fard Masoumi HR, Shamsudin N, Salim N. Enhancement of physicochemical properties of nanocolloidal carrier loaded with cyclosporine for topical treatment of psoriasis: *in vitro* diffusion and *in vivo* hydrating action. *Int J Nanomed*. (2017) 12:2427–41. doi: 10.2147/IJN.S125302
43. Bernardi DS, Pereira TA, Maciel NR, Bortoloto J, Viera GS, Oliveira GC, et al. Formation and stability of oil-in-water nanoemulsions containing rice bran oil: *in vitro* and *in vivo* assessments. *J Nanobiotechnol*. (2011) 9:44. doi: 10.1186/1477-3155-9-44
44. Woo JO, Misran M, Lee PF, Tan LP. Development of a controlled release of salicylic acid loaded stearic acid-oleic acid nanoparticles in cream for topical delivery. *ScientificWorldJournal*. (2014) 2014:205703. doi: 10.1155/2014/205703
45. Sonawane R, Harde H, Katariya M, Agrawal S, Jain S. Solid lipid nanoparticles-loaded topical gel containing combination drugs: an approach to offset psoriasis. *Expert Opin Drug Deliv*. (2014) 11:1833–47. doi: 10.1517/17425247.2014.938634
46. Ferreira M, Barreiros L, Segundo MA, Torres T, Selores M, Costa Lima SA, et al. Topical co-delivery of methotrexate and etanercept using lipid nanoparticles: a targeted approach for psoriasis management. *Colloids Surf B Biointerfaces*. (2017) 159:23–9. doi: 10.1016/j.colsurfb.2017.07.080
47. Haider M, Abdin SM, Kamal L, Orive G. Nanostructured lipid carriers for delivery of chemotherapeutics: a review. *Pharmaceutics*. (2020) 12:288. doi: 10.3390/pharmaceutics12030288
48. Tripathi P, Kumar A, Jain PK, Patel JR. Carbomer gel bearing methotrexate loaded lipid nanoparticles shows improved topical delivery intended for effective management of psoriasis. *Int J Biol Macromol*. (2018) 120:1322–34. doi: 10.1016/j.ijbiomac.2018.08.136
49. Agrawal Y, Petkar KC, Sawant KK. Development, evaluation and clinical studies of Acitretin loaded nanostructured lipid carriers for topical treatment of psoriasis. *Int J Pharm*. (2010) 401:93–102. doi: 10.1016/j.ijpharm.2010.09.007
50. Abdel-Mottaleb MM, Neumann D, Lamprecht A. Lipid nanocapsules for dermal application: a comparative study of lipid-based versus polymer-based nanocarriers. *Eur J Pharm Biopharm*. (2011) 79:36–42. doi: 10.1016/j.ejpb.2011.04.009
51. Larsson J, Sanchez-Fernandez A, Leung AE, Schweins R, Wu B, Nylander T, et al. Molecular structure of maltoside surfactants controls micelle formation and rheological behavior. *J Colloid Interface Sci*. (2021) 581:895–904. doi: 10.1016/j.jcis.2020.08.116
52. Lapteva M, Mondon K, Möller M, Gurny R, Kalia YN. Polymeric micelle nanocarriers for the cutaneous delivery of tacrolimus: a targeted approach for the treatment of psoriasis. *Mol Pharm*. (2014) 11:2989–3001. doi: 10.1021/mp400639e
53. Chavoshy F, Zadeh BSM, Tamaddon AM, Anbardar MH. Delivery and anti-psoriatic effect of silibinin-loaded polymeric micelles: an experimental study in the psoriatic skin model. *Curr Drug Deliv*. (2020) 17:787–98. doi: 10.2174/1567201817666200722141807
54. Li N, Qin Y, Dai D, Wang P, Shi M, Gao J, et al. Transdermal delivery of therapeutic compounds with nanotechnological approaches in psoriasis. *Front Bioeng Biotechnol*. (2021) 9:804415. doi: 10.3389/fbioe.2021.804415
55. Liu M, Fréchet JM. Designing dendrimers for drug delivery. *Pharm Sci Technol Today*. (1999) 2:393–401. doi: 10.1016/S1461-5347(99)00203-5
56. Agrawal U, Mehra NK, Gupta U, Jain NK. Hyperbranched dendritic nanocarriers for topical delivery of dithranol. *J Drug Target*. (2013) 21:497–506. doi: 10.3109/1061186X.2013.771778
57. Borowska K, Laskowska B, Magoń A, Mysliwiec B, Pyda M, Wołowicz S. PAMAM dendrimers as solubilizers and hosts for 8-methoxypsoralene enabling transdermal diffusion of the guest. *Int J Pharm*. (2010) 398:185–9. doi: 10.1016/j.ijpharm.2010.07.019
58. Kojima C. Preclinical studies of dendrimer prodrugs. *Expert Opin Drug Metab Toxicol*. (2015) 11:1303–15. doi: 10.1517/17425255.2015.1052404
59. Mora-Huertas CE, Fessi H, Elaissari A. Polymer-based nanocapsules for drug delivery. *Int J Pharm*. (2010) 385:113–42. doi: 10.1016/j.ijpharm.2009.10.018
60. Ourique AF, Pohlmann AR, Guterres SS, Beck RC. Tretinoin-loaded nanocapsules: Preparation, physicochemical characterization, and photostability study. *Int J Pharm*. (2008) 352:1–4. doi: 10.1016/j.ijpharm.2007.12.035
61. Savian AL, Rodrigues D, Weber J, Ribeiro RF, Motta MH, Schaffazick SR, et al. Dithranol-loaded lipid-core nanocapsules improve the photostability and reduce the *in vitro* irritation potential of this drug. *Mater Sci Eng C Mater Biol Appl*. (2015) 46:69–76. doi: 10.1016/j.msec.2014.10.011
62. Marchiori ML, Lubini G, Dalla Nora G, Friedrich RB, Fontana MC, Ourique AF, et al. Hydrogel containing dexamethasone-loaded nanocapsules for cutaneous administration: preparation, characterization, and *in vitro* drug release study. *Drug Dev Ind Pharm*. (2010) 36:962–71. doi: 10.3109/03639041003598960
63. Carino GP, Jacob JS, Mathiowitz E. Nanosphere based oral insulin delivery. *J Control Release*. (2000) 65:261–9. doi: 10.1016/S0168-3659(99)00247-3
64. Ishihara T, Kubota T, Choi T, Takahashi M, Ayano E, Kanazawa H, et al. Polymeric nanoparticles encapsulating betamethasone phosphate with different release profiles and stealthiness. *Int J Pharm*. (2009) 375:148–54. doi: 10.1016/j.ijpharm.2009.04.001
65. Sheihet L, Dubin RA, Devore D, Kohn J. Hydrophobic drug delivery by self-assembling triblock copolymer-derived nanospheres. *Biomacromolecules*. (2005) 6:2726–31. doi: 10.1021/bm050212u
66. Sibuyi NRS, Moabelo KL, Fadaka AO, Meyer S, Onani MO, Madiehe AM, et al. Multifunctional gold nanoparticles for improved diagnostic and therapeutic applications: a review. *Nanoscale Res Lett*. (2021) 16:174. doi: 10.1186/s11671-021-03632-w
67. Bessar H, Venditti I, Benassi L, Vaschieri C, Azzoni P, Pellacani G, et al. Functionalized gold nanoparticles for topical delivery of methotrexate for the possible treatment of psoriasis. *Colloids Surf B Biointerfaces*. (2016) 141:141–7. doi: 10.1016/j.colsurfb.2016.01.021
68. Crisan D, Scharffetter-Kochanek K, Crisan M, Schatz S, Hainzl A, Olenic L, et al. Topical silver and gold nanoparticles complexed with Cornus mas suppress inflammation in human psoriasis plaques by inhibiting NF-κB activity. *Exp Dermatol*. (2018) 27:1166–9. doi: 10.1111/exd.13707
69. Raghuwanshi N, Yadav TC, Srivastava AK, Raj U, Varadwaj P, Pruthi V, et al. Structure-based drug designing and identification of *Woodfordia fruticosa* inhibitors targeted against heat shock protein (HSP70-1) as suppressor for Imiquimod-induced psoriasis like skin inflammation in mice model. *Mater Sci Eng C Mater Biol Appl*. (2019) 95:57–71. doi: 10.1016/j.msec.2018.10.061
70. Pradhan M, Alexander A, Singh MR, Singh D, Saraf S, Saraf S. Understanding the prospective of nano-formulations towards the treatment of psoriasis. *Biomed Pharmacother*. (2018) 107:447–63. doi: 10.1016/j.biopha.2018.07.156
71. David L, Moldovan B, Vulcu A, Olenic L, Perde-Schrepler M, Fischer-Fodor E, et al. Green synthesis, characterization and anti-inflammatory activity of silver nanoparticles using European black elderberry fruits extract. *Colloids Surf B Biointerfaces*. (2014) 122:767–77. doi: 10.1016/j.colsurfb.2014.08.018
72. Kedi PBE, Meva FE, Kotsedi L, Nguemfo EL, Zangueu CB, Ntumba AA, et al. Eco-friendly synthesis, characterization, *in vitro* and *in vivo* anti-inflammatory activity of silver nanoparticle-mediated *Selaginella myosurus* aqueous extract. *Int J Nanomed*. (2018) 13:8537–48. doi: 10.2147/IJN.S174530



OPEN ACCESS

EDITED BY
Robert Gniadecki,
University of Alberta, Canada

REVIEWED BY
Yanfei Zhang,
Xi'an Jiaotong University, China
Zhiqi Hu,
Southern Medical University, China

*CORRESPONDENCE
Irene Fusco
✉ i.fusco@deka.it

SPECIALTY SECTION
This article was submitted to
Dermatology,
a section of the journal
Frontiers in Medicine

RECEIVED 01 September 2022


ACCEPTED 10 January 2023

PUBLISHED 06 February 2023

CITATION
Piccolo D, Mutlag MH, Pieri L, Fusco I,
Conforti C, Crisman G and Bonan P (2023)
Minimally invasive 1,444-nm Nd:YAG laser
treatment for axillary bromhidrosis.
Front. Med. 10:1034122.
doi: 10.3389/fmed.2023.1034122

COPYRIGHT
© 2023 Piccolo, Mutlag, Pieri, Fusco, Conforti,
Crisman and Bonan. This is an open-access
article distributed under the terms of the
[Creative Commons Attribution License \(CC BY\)](https://creativecommons.org/licenses/by/4.0/).
The use, distribution or reproduction in other
forums is permitted, provided the original
author(s) and the copyright owner(s) are
credited and that the original publication in this
journal is cited, in accordance with accepted
academic practice. No use, distribution or
reproduction is permitted which does not
comply with these terms.

Minimally invasive 1,444-nm Nd:YAG laser treatment for axillary bromhidrosis

Domenico Piccolo¹, Mohammed Hussein Mutlag², Laura Pieri³,
Irene Fusco ^{3*}, Claudio Conforti⁴, Giuliana Crisman¹ and
Paolo Bonan⁵

¹Skin Centers, Avezzano, Italy, ²Roma Clinic, Baghdad, Iraq, ³EL.En. Group, Calenzano, Italy, ⁴Department of Dermatology and Venereology, Dermatology Clinic, Maggiore Hospital, University of Trieste, Trieste, Italy, ⁵Laser Cutaneous Cosmetic and Plastic Surgery Unit, Villa Donatello Clinic, Florence, Italy

Background: Axillary bromhidrosis is an apocrine glands hyperactivity disease.

Methods: A total of 24 patients (15 men and 9 women) with axillary bromhidrosis underwent a laser procedure with a 1,444-nm Nd:YAG laser. Parameters evaluated in this study were as follows: the degree of malodor (T0, baseline; T30, after 1 month; and T180, after 6 months), postoperative pain, short-term decreased mobility (T1, after 1 day; T7, after 7 days; and T30, after 1 month), and overall satisfaction (T30, after 1 month and T180, after 6 months). A visual analog scale (VAS), from 0 to 10, was used to assess pain and decreased mobility, with lower values denoting less severity.

Results: A total of 24 patients were followed up for 6 months after laser treatment. At baseline, all patients (100%) complained of a strong axillary malodor (mean degree of malodor at T0 = 2.0 ± 0.00). It decreased to 0.50 ± 0.64 at T30. At T180, the degree of malodor was 0.54 ± 0.57 . Both T30 and T180 degrees of malodor significantly decreased from the baseline value ($p < 0.01$). The mean degree of patient satisfaction at T30 was 1.75 ± 0.52 , and at T180, it was 1.67 ± 0.21 . Among the 24 patients, eight complained of moderated pain 1 day after treatment. The pain subsided on day 7, except for two patients, with VAS = 1. Pain and mobility restrictions were in any case resolved within T30.

Conclusion: Treatment with a 1,444-nm Nd:YAG laser for subdermal interstitial coagulation could be a less invasive and more effective option treatment for axillary bromhidrosis.

KEYWORDS

axillary bromhidrosis, axillary osmidrosis, axillary hyperhidrosis, Nd:YAG laser, subdermal coagulation, 1,444-nm laser

1. Introduction

Human sweat gland disorders are widespread and cause a considerable negative effect on social, psychological, and emotional wellbeing. It was found that the detrimental impacts of these ailments are equivalent to those of severe diseases such as rheumatoid arthritis, psoriasis, multiple sclerosis, and kidney failure (1). For this reason, it is essential to properly recognize and manage these disorders to guarantee the best patient care. While hyperhidrosis is caused by a sweat gland malfunctioning due to abnormally increased sweating (that greatly exceeds

the human body's thermoregulatory requirements), bromhidrosis (also known as osmidrosis, malodorous sweating, or body odor) is a chronic pathologic condition characterized by an excessive and extremely unpleasant body odor. Axillary bromhidrosis is a medical condition characterized by apocrine gland hyperactivity, and it is a common cause of consultation in dermatology. It is distinguished by a strong aggressive odor caused by the decomposition of bacteria in the apocrine secretions. Axillary odor control is a universal topic, and for this reason, the pathophysiology and etiology of axillary bromhidrosis have been extensively researched and described. The apocrine gland quantity, personal care, sex, age, emotions, hormonal level, ABCC11 genotype, concurrent hyperhidrosis, and disorders inducing bacterial overgrowth, such as intertrigo, diabetes, erythrasma, and obesity, all influence odor levels (2). Genetic histological examination of axillary tissue reveals that subjects with bromhidrosis have a greater number and dimensions of apocrine glands than control subjects (3). Skin surface bacteria decompose apocrine secretions into ammonia and short-chain fatty acids, which have distinct odors. Bacterial flora in the armpit area has been shown to convert non-odorous sweat precursors to more odorous volatile acids, resulting in a definite body odor (4). In most people with axillary bromhidrosis, familiarity was found due to the Mendelian traits of apocrine gland-related phenotypes (5). A variety of factors influence the level of intervention, including the severity of the symptoms, the patient's personal choice, side effect tolerability, and consent to repeat the treatment several times (6). Improved hygiene, antiperspirant and antibacterial substances, botox, lasers, and, finally, surgery can be proposed, considering the patients' expectations. Surgery has a great chance of success, but it also has an elevated complication rate, including skin necrosis, hematoma formation, and permanent scarring. Less invasive methods have frequently been linked to high recurrence rates. Recently, less invasive techniques improve the cure rate while avoiding the drawbacks of previous methods. In the present study, we illustrate our experience with the minimally invasive technique using a 1,444-nm Nd:YAG laser for subdermal coagulation treatment of axillary bromhidrosis.

2. Materials and methods

A total of 24 subjects (9 women and 15 men, 48 armpits) aged 19–57 (mean age, 35.4) years, with a BMI of $26.05 \pm 2.05 \text{ kg m}^{-2}$ and with axillary bromhidrosis, underwent a laser procedure with a 1,444-nm Nd:YAG laser (LipoAi; DEKA, Florence, Italy). Among them, 14 also had axillary hyperhidrosis. We excluded patients who were pregnant or lactating, as well as those who had a history of keloid formation. Based on the Helsinki Declaration, all subjects provided written informed consent to participate. The patients' suitability to participate in the study was assessed. All subjects' medical information was taken and recorded, a physical examination was carried out, and vital signs were controlled. Bromhidrosis was recognized when both the dermatologist and patient perceive the malodor. The preoperative degree of patient-assessed malodor was recorded for each subject. All treatments were done as outpatients with local anesthesia. To better define the hair-bearing area, which was delimited using a dermatological pen in the supine position with the arms abducted just before starting the procedure, all participants were instructed not to shave both axillae 1 week before the treatment. Following ordinary tumescent anesthesia, where an

anesthetic consisting of a 0.4% lidocaine solution was injected into each side of the axillary fossa, two/four small holes (depending on the treatment area dimension) were made at the anterior and distal borders of each axilla with an 18-gauge needle. The handpiece is equipped with a very useful clip blockage passing through the laser handpiece and cannula. Moreover, the fiber insertion is protected by a fiber-protecting option, which is activated by changing the clamp position. Throughout the incision site, the cannula was introduced into the target layer of the dermal–subdermal junction. The transcutaneous guidance laser aiming beam was used to control where the cannula tip is during the whole procedure, monitoring both depth and position. A wider transcutaneous illumination area revealed the deeper fiber tip positioning. This allowed us to continuously check the correct position of the fiber during the procedure, which was fundamental to avoid any possible damage in deeper structures such as blood vessels or the brachial plexus. The laser was applied in a crisscross pattern with repeated cannulation. A foot switch was used to control the laser emission. Apocrine glands in the subcutaneous and dermal layers were destroyed by irradiation with a 600- μm fiber passing through the laser handpiece and cannula. The laser setting was as follows: pulse energy = 175 mJ and pulse rate = 40 Hz (power 7 W). The delivered energy varied from 1,800 to 2,300 J (mean delivered energy 2,092 J). We irradiated the laser once per 0.5–1.0 cm^2 area within 1.5 s to avoid irreversible skin damage caused by excessive heat production after tissue–laser interaction. Cold packs were applied immediately after the laser treatment to the area to reduce the risk of skin heat injury. There was no need for sutures. The procedure took approximately 5 min on one side. After laser treatment, a compressive dressing was utilized for 24 h. We followed up with all patients on postoperative days 1, 7, 30, and 180 after the procedure.

Parameters evaluated during the study were as follows: the degree of malodor (T0, before treatment; T30, after 1 month; and T180, after 6 months), postoperative pain, short-term decreased mobility (T1, after 1 day; T7, after 7 days; and T30, after 1 month), and overall satisfaction (T30, after 1 month and T180 after 6 months). Malodor was graded as either absent (grade 0), fair (grade 1), or strong (grade 2). “Absent” means that nobody (neither the patient nor the physician, nor anyone nearby) was aware of the malodor. “Fair” indicates a not persistent malodor sometimes noticeable when the subject sweated. “Strong” implies that the patient and those around him or her were aware of the malodor. The satisfaction degree was classified into three scores: poor (grade 0), fair (grade 1), and good (grade 2) (7). The severity of malodor was the same on both sides of the axillary of the patient.

A visual analog scale (VAS) from 0 to 10 was used to assess the level of pain and decreased mobility, with lower scores indicating less severity. The occurrence of adverse reactions, such as burns, hematoma, infection, scarring, skin and fat tissue necrosis, sensory loss, seroma, allergic reaction, and anesthesia-related complications, was used to assess safety. In case symptoms of adverse reaction persisted, the patients were monitored until the healing was complete.

3. Results

A total of 24 patients were followed up for 6 months after laser treatment. At baseline, all patients (100%) complained of a strong axillary malodor. At T30 follow-up, malodor level was evaluated as

absent in 14 patients (58%), fair in eight patients (33%), and strong in two patients (8%). At T180 follow-up, malodor level was evaluated as absent in 14 patients (58%), fair in nine patients (37%), and strong in one patient (9%) (Figure 1). The mean degree of malodor at baseline (T0) was 2.0 ± 0.00 . It diminished to 0.50 ± 0.64 at 1 month (T30) after laser treatment. The level of malodor varied significantly at T0 and T30 ($p < 0.001$). Six months (T180) after the laser treatment, the malodor degree was marginally increased to 0.54 ± 0.57 . However, it continued to remain significantly lower than the baseline value ($p < 0.001$), and the difference between the mean degree at T30 and T180 was not significant. Subject's satisfaction was estimated (three-grade scale: 0 = poor, 1 = fair, and 2 = good). One month (T30) after the laser treatment, 19 patients (79%) reported good satisfaction, four patients (17%) reported fair satisfaction, and only one patient (4%) reported poor satisfaction. After 6 months (T180), 17 patients (71%) reported good satisfaction, six patients (25%) reported fair satisfaction, and one patient (4%) reported poor satisfaction (Figure 2). The mean degree of patient satisfaction 1 month after the laser surgery (T30) was 1.75 ± 0.52 and 6 months after laser surgery (T180) was 1.67 ± 0.21 . The difference between the mean degree of satisfaction at T30 and T180 was not significant. A VAS scale (0–10) was used for documenting pain and mobility limitations after the procedure on day 1 (T1), day 7 (T7), and 1 month (T30) after surgery. On T1, 8 of the 24 patients complained of pain, and their mean VAS score was 1.63 ± 0.70 . All of them no longer complained of any pain on day 7 except for two patients for whom the VAS score was, in any case, low (only 1). Pain and limitations in mobility were all resolved within 4 weeks of the treatment (T30). When compared to standard surgery, the side effects were mild. Twenty-eight of the 48 axillae treated (58%) had ecchymosis, which usually resolved within 1 or 2 weeks. Only one patient (4.2%) reported a shallow second-degree burn in one axilla only (2.1% of treated axillae). This burn was completely healed within 10 weeks using conservative methods with no scarring or contracture. The patient was followed up until the complete recovery. We noted no complications such as granuloma, seroma, dehiscence, or wound infection. During the clinical follow-up period, no skin necrosis or

recurrences occurred. The procedure was successful, with only minor postoperative restrictions on patients' social activities.

4. Discussion

For axillary bromhidrosis, numerous therapeutic approaches have been developed, including both surgical and non-surgical options. Among surgical approaches, subdermal excision of the apocrine glands, suction-curettage technique, and subcutaneous scissor with micropore or endoscopic surgical treatment was generally performed. However, all these techniques require repeated treatments, induration, pain, and scarring in the armpits. Non-surgical methods are thought to have a higher frequency of recurrence than surgical procedures. Nevertheless, these techniques do not carry the risks of complications that can be associated with traditional surgery, such as axillary nerve plexus damage, strong postoperative discomfort, bleeding, and severely restricted mobility (8). For all of these factors, no consensus on the best surgical approach has been reached for treating axillary bromhidrosis and more and more patients continue to prefer minimally invasive procedures for treating it. This is the reason why new techniques have been developed. Patients who underwent liposuction for axillary bromhidrosis reported high satisfaction and quick recovery (9); Indeed, the overall complication rate was significantly lower than the percent complication rate seen with open surgical treatment. To improve the efficiency of liposuction for bromhidrosis, curettage can be combined with liposuction (10); when this combination was made (curettage and liposuction), almost all patients were satisfied with their outcomes. The use of both focused ultrasound and microwave technologies has been introduced. The first one acts on sweat glands that have a high water content, inducing cavitation which is followed by apocrine glands disruption (11, 12). Microwave therapy instead heats the layer between the skin and subcutaneous fat, resulting in sweat glands destruction (13, 14); the most common side effects were edema, redness, altered sensation in the skin of the treatment limb, and swelling outside the axilla. Lasers have also been adopted for axillary bromhidrosis treatment,

Degree of Malodor

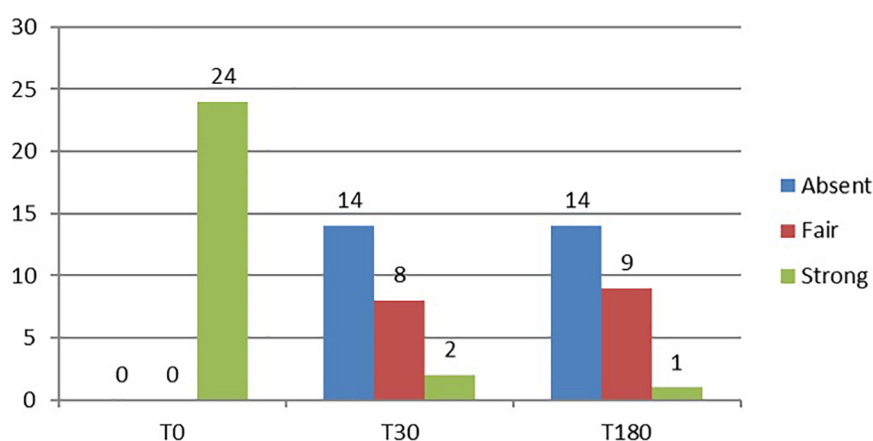


FIGURE 1

Histogram representation of the degree of malodor assessment results at baseline (T0) and study follow-up visits (T30 and T180).

Patient's Satisfaction

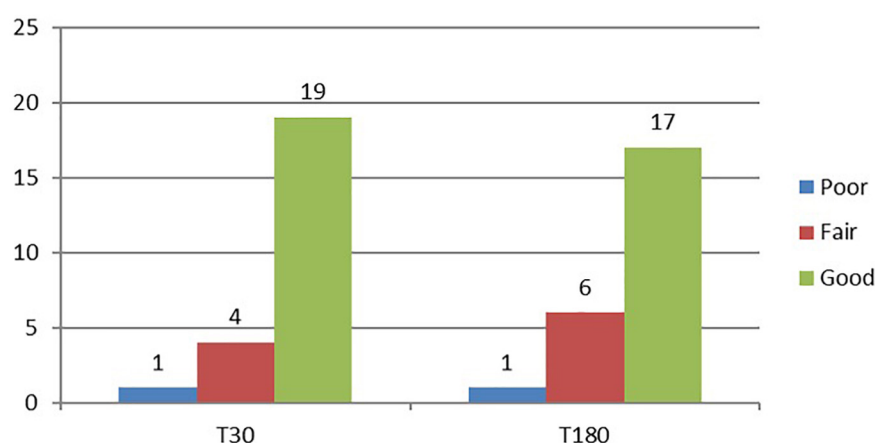


FIGURE 2

Histogram representation of patient satisfaction assessment results at study follow-up visits (T30 and T180).

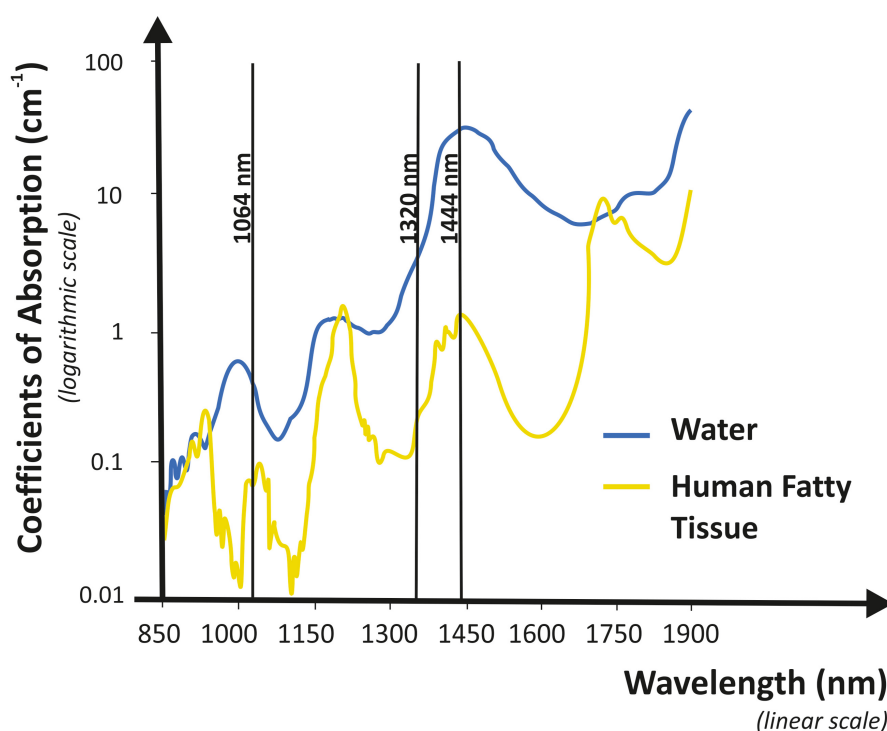


FIGURE 3

Graphical representation of absorption coefficient vs. wavelength for water and human fat. The 1,444-nm wavelength shows high selectivity characteristics and it is highly absorbed by human fat.

dissolving fat and destroying apocrine glands. Following laser treatment, histopathological examination showed reduced density and considerable alterations in the apocrine glands (15). Axillary bromhidrosis has been treated with a variety of lasers. With all of them, the recovery time is short as well as the risk of adverse reactions is low, but the relapse frequency is higher than with traditional surgery. The CO₂ laser was one of the first reported laser systems (16). Pulsed 1,064-nm Nd:YAG wavelength has achieved good results (17, 18). Unfortunately, its selective fat dissolution capability is quite low, so melting fat over a large area is difficult

and time-consuming. Furthermore, researchers found that, among several wavelengths, 1,444 nm provides the highest degree of efficacy for fat tissue selective ablation and thermal confinement, permitting, in a short time, fat removal in different areas. When compared to other wavelengths, 1,444 nm is absorbed more strongly by the fat than the water. This wavelength has been shown to have a greater lipolytic effect in comparison with 1,064-nm (19) and 1,320-nm wavelengths, which mean a higher efficiency together with heat confinement with limited diffusion to surrounding tissue. In other words, 1,064 and 1,320 nm lasers need a greater amount of energy,

three or two times, respectively, than that of the 1,444 nm laser to treat the same volume (20). The same study also observed that, because the fat is the main target, selective photothermolysis occurred at 1,444 nm because this wavelength matches up to a fat peak absorption, despite the fact that water absorption in the tissue is much higher (Figure 3). According to the scientific literature (8, 15, 21, 22), we believe that the 1,444-nm laser would specifically destroy apocrine glands in fatty tissues *via* a subdermal interstitial approach. After 6 months (T180), malodor was absent in 28 axillae (58%), fair in 18 axillae (33%), and poor in two axillae (4%). The majority of subjects treated (96%) were pleased with their outcomes for both efficacy and side effects. We also discovered that hyperhidrosis changes were related to bromhidrosis data. Although there are some differences between the present bromhidrosis study using a 1,444-nm laser and those mentioned previously, there was no significant difference in the clinical results among them. We tried to compare our findings to those of other treatment modalities such as ultrasound, microwave, and other Nd:YAG lasers (11–14, 17). The outcomes of most studies were evaluated in accordance with the patient satisfaction level, which ranged from 65 to 100%. It was challenging to compare these researches accurately because the majority of them employed various evaluation tools. To directly compare these modalities, more clinical research is required. We followed up on all patients on postoperative days 1, 7, 30, and 180, after the procedure and observed superficial second-degree burns on only one axilla (2.1%), which healed during conservative management. We found no complications, such as granuloma, seroma, wound infection, or dehiscence. During the clinical follow-up, no skin necrosis took place. The treatment using a 1,444-nm laser showed fewer significant adverse reactions in comparison with alternative approaches, such as liposuction or traditional surgery (9, 23). Main acute complications, such as postoperative pain and limited mobility, were less common in subjects undergoing laser therapy. According to our findings, except for mild ecchymosis and a skin crust induced by heat, laser treatment did not cause any long-term side effects. In any case, over-treatment and excessive heating can cause higher injury hazards or skin necrosis. Also, technical errors, such as skin injury produced by the fiber tip and incorrect target treatment, can cause necrosis of the epidermal layer. Therefore, laser operators should be properly trained to perform the procedure and must constantly monitor any changes in surface skin color. During the recovery process, the apocrine glands and fat tissue denatured by the laser were absorbed by surrounding tissues. As also assumed by Jeong et al. (8), the sweat glands that have not been completely denatured may re-engraft onto the tissue, potentially causing recurrence. In our experience, we did not record significant relapses during the study. This could be due to the limited follow-up of 6 months. Further investigations are necessary with a greater amount of patients and a longer follow-up to better clarify this aspect. Although not considered in our clinical study, liposuction and/or curettage can be combined with laser lipolysis (17), potentially resulting in greater effectiveness and better outcomes. Supplementary clinical trials are required to evaluate this possibility.

4.1. Study limitations

Further future studies will be required for long-term analyses with a larger patient sample size and the use of histological

examination to better assess apocrine glands density reduction and skin necrosis development.

5. Conclusion

Treatment with a 1,444-nm Nd:YAG laser for subdermal interstitial coagulation could be a less invasive and more effective alternative option treatment for axillary bromhidrosis with benefits such as treatment speed, small wound size, quick recovery, unnoticeable scars, and return to normal regular lives. Additional studies with a greater amount of patients, a sham control group, and a longer follow-up are necessary to clarify some aspects left open by the present trial.

Data availability statement

Data that support the study findings are available on request from the corresponding author (IF).

Ethics statement

Ethical review and approval was not required for the study on human participants, in accordance with the local legislation and institutional requirements.

Author contributions

DP, MM, LP, CC, GC, and PB: conceptualization, funding acquisition, methodology, and validation. LP: formal analysis. LP, MM, and IF: investigation. DP, MM, LP, CC, and GC: data curation. LP: writing—original draft preparation. LP and IF: writing—review and editing. DP, MM, LP, CC, GC, and PB: supervision. All authors read and agreed to the published version of the manuscript.

Conflict of interest

LP and IF were employed by El.En. Group.

The remaining authors declare that the research was conducted in the absence of any commercial or financial relationships that could be construed as a potential conflict of interest.

Publisher's note

All claims expressed in this article are solely those of the authors and do not necessarily represent those of their affiliated organizations, or those of the publisher, the editors and the reviewers. Any product that may be evaluated in this article, or claim that may be made by its manufacturer, is not guaranteed or endorsed by the publisher.

References

- Cinà C, Clase C. The Illness Intrusiveness Rating Scale: a measure of severity in individuals with hyperhidrosis. *Qual Life Res.* (1999) 8:693–8. doi: 10.1023/a:1008968401068
- Morioka D, Nomura M, Lan L, Tanaka R, Kadomatsu K. Axillary osmidrosis: Past, present, and future. *Ann Plast Surg.* (2020) 84:722–8. doi: 10.1097/SAP.0000000000002111
- Bang Y, Kim J, Paik S, Park S, Jackson I, Lebeda R. Histopathology of apocrine bromhidrosis. *Plast Reconstr Surg.* (1996) 98:288–92. doi: 10.1097/00006534-199608000-00012
- Sato T, Sonoda T, Itami S, Takayasu S. Predominance of type I 5alpha-reductase in apocrine sweat glands of patients with excessive or abnormal odour derived from apocrine sweat Osmidrosis. *Br J Dermatol.* (1998) 139:806–10. doi: 10.1046/j.1365-2133.1998.02504.x
- Morioka D, Ohkubo F, Amikura Y. Clinical features of axillary osmidrosis: a retrospective chart review of 723 Japanese patients. *J Dermatol.* (2013) 40:384–8. doi: 10.1111/1346-8138.12115
- Malik A, Porter C, Feldman S. Bromhidrosis treatment modalities: a literature review. *J Am Acad Dermatol.* (2021) 19:S0190–9622(21)00175-4. doi: 10.1016/j.jaad.2021.01.030
- Park Y, Shin M. What is the best method for treating osmidrosis? *Ann Plast Surg.* (2001) 47:303–9.
- Jeong J, Hong J, Pak C, Kim J, Heo C. Treatment of axillary osmidrosis using a laser with a 1,444-nm wavelength. *Dermatol Surg.* (2014) 40:851–7. doi: 10.1111/dsu.0000000000000027
- Perng C, Yeh F, Ma H, Lin J, Hwang C, Shen B, et al. Is the treatment of axillary osmidrosis with liposuction better than open surgery? *Plast Reconstr Surg.* (2004) 114:93–7. doi: 10.1097/01.prs.0000127801.15386.99
- Tsai R, Lin J. Experience of tumescent liposuction in the treatment of osmidrosis. *Dermatol Surg.* (2001) 27:446–8. doi: 10.1046/j.1524-4725.2001.00318.x
- Ozawa T, Nose K, Harada T, Muraoka M, Ishii M. Treatment of osmidrosis with the Cavitron ultrasonic surgical aspirator. *Dermatol Surg.* (2006) 32:1251–5. doi: 10.1111/j.1524-4725.2006.32285.x
- Niiyama S, Aiba S, Katsuoka K, Ito Y, Sumiya N. Treatment of osmidrosis using the ultrasonic surgical aspirator. *Acta Derm Venereol.* (2006) 86:238–40. doi: 10.2340/00015555-0078
- Hong H, Lupin M, O'Shaughnessy K. Clinical evaluation of a microwave device for treating axillary hyperhidrosis. *Dermatol Surg.* (2012) 38:728–35. doi: 10.1111/j.1524-4725.2012.02375.x
- Lee S, Chang K, Suh D, Song K, Ryu H. The efficacy of a microwave device for treating axillary hyperhidrosis and osmidrosis in Asians: a preliminary study. *J Cosmet Laser Ther.* (2013) 15:255–9. doi: 10.3109/14764172.2013.807114
- Jung S, Jang H, Kim H, Lee S, Lee K, Kim S, et al. A prospective, long-term Follow-Up Study of 1,444 nm Nd:YAG Laser: A new modality for treating axillary bromhidrosis. *Ann Dermatol.* (2014) 26:184–8. doi: 10.5021/ad.2014.26.2.184
- Park J, Cha S, Park S. Carbon dioxide laser treatment vs subcutaneous resection of axillary osmidrosis. *Dermatol Surg.* (1997) 23:247–51. doi: 10.1111/j.1524-4725.1997.tb00036.x
- Ichikawa K, Miyasaka M, Aikawa Y. Subcutaneous laser treatment of axillary osmidrosis: a new technique. *Plast Reconstr Surg.* (2006) 118:170–4. doi: 10.1097/01.prs.0000221005.86108.0d
- Kim D, Kim J, Yeo H, Kwon H, Son D, Han K. Treatment of axillary osmidrosis using a subcutaneous Pulsed Nd-YAG Laser. *Arch Plast Surg.* (2012) 39:143–9. doi: 10.5999/aps.2012.39.2.143
- Tark K, Jung J, Song S. Superior lipolytic effect of the 1,444 nm Nd:YAG laser: comparison with the 1,064 nm Nd:YAG laser. *Lasers Surg Med.* (2009) 41:721–7. doi: 10.1002/lsm.20786
- Youn J, Holcomb J. Ablation efficiency and relative thermal confinement measurements using wavelengths 1,064, 1,320, and 1,444 nm for laser-assisted lipolysis. *Lasers Med Sci.* (2013) 28:519–27. doi: 10.1007/s10103-012-1100-9
- Lee K, Kim S, Yi S, Kim J, Kim I. Subdermal coagulation treatment of axillary bromhidrosis by 1,444 nm Nd:YAG Laser: A comparison with surgical treatment. *Ann Dermatol.* (2014) 26:99–102. doi: 10.5021/ad.2014.26.1.99
- Lee S, Ryu H, Kim I. Minimally invasive surgery for axillary osmidrosis using a combination of subcutaneous tissue removal and a 1,444-nm Nd:YAG Laser. *Ann Dermatol.* (2014) 26:755–7. doi: 10.5021/ad.2014.26.6.755
- Qian J, Wang X. Effectiveness and complications of subdermal excision of apocrine glands in 206 cases with axillary osmidrosis. *J Plast Reconstr Aesthet Surg.* (2010) 63:1003–7. doi: 10.1016/j.bjps.2009.05.004



OPEN ACCESS

EDITED BY

Giusto Trevisan,
University of Trieste, Italy

REVIEWED BY

Alessandro Pileri,
University of Bologna, Italy
Diego Signoretti,
University of Trieste, Italy

*CORRESPONDENCE

Ping Wang
✉ dermwang@aliyun.com

SPECIALTY SECTION

This article was submitted to
Dermatology,
a section of the journal
Frontiers in Medicine

RECEIVED 30 August 2022

ACCEPTED 06 February 2023

PUBLISHED 17 February 2023

CITATION

Wang J, Wang Y, Zhou H, Wang P, Zhu M, Li L
and Shen H (2023) Clinicopathological
features, therapeutic options, and significance
of CD103 expression in 15 patients with
follicular mucinosis.
Front. Med. 10:1032072.
doi: 10.3389/fmed.2023.1032072

COPYRIGHT

© 2023 Wang, Wang, Zhou, Wang, Zhu, Li and
Shen. This is an open-access article distributed
under the terms of the [Creative Commons
Attribution License \(CC BY\)](#). The use,
distribution or reproduction in other forums is
permitted, provided the original author(s) and
the copyright owner(s) are credited and that
the original publication in this journal is cited,
in accordance with accepted academic
practice. No use, distribution or reproduction is
permitted which does not comply with
these terms.

Clinicopathological features, therapeutic options, and significance of CD103 expression in 15 patients with follicular mucinosis

Jiaqi Wang¹, Yanqing Wang², Hongyu Zhou², Ping Wang^{1*},
Mengyan Zhu¹, Liuyu Li¹ and Hong Shen¹

¹Department of Dermatology, Hangzhou Third People's Hospital, Affiliated Hangzhou Dermatology
Hospital of Zhejiang University School of Medicine, Hangzhou, China, ²Department of Dermatology,
Hangzhou Third People's Hospital, Zhejiang Chinese Medical University, Hangzhou, China

Background: Follicular mucinosis (FM) is generally divided into a primary benign
idiopathic form and a secondary form associated with mycosis fungoides.

Objective: To analyze the clinical and pathological features of FM and explore the
pathological significance of CD103 expression.

Methods: In this case series, we retrospective analysis the clinical, pathological,
treatment and follow-up treatment of 15 cases of FM. The expression of CD103
in all cases was detected by immunohistochemistry.

Result: A total of 15 patients were enrolled, 7 were primary follicular mucinosis
(P-FM) and 8 were mycosis fungoides-associated follicular mucinosis (MF-FM).
Lesions of both P-FM and MF-FM are difficult to distinguish, present with
red or dark red plaques and follicular papules. Pathologically, MF-FM showed
more significant infiltrates of folliculotropic lymphoid cells, and the amount
and proportion of CD103+ cells were significantly higher than that in P-FM.
Follow-up data were available for 13 patients. Three cases were resolved after
surgical resection, two patients were marked improved after oral administration
of hydroxychloroquine and three times ALA photodynamic therapy respectively.
The rest patients showed only modest efficacy.

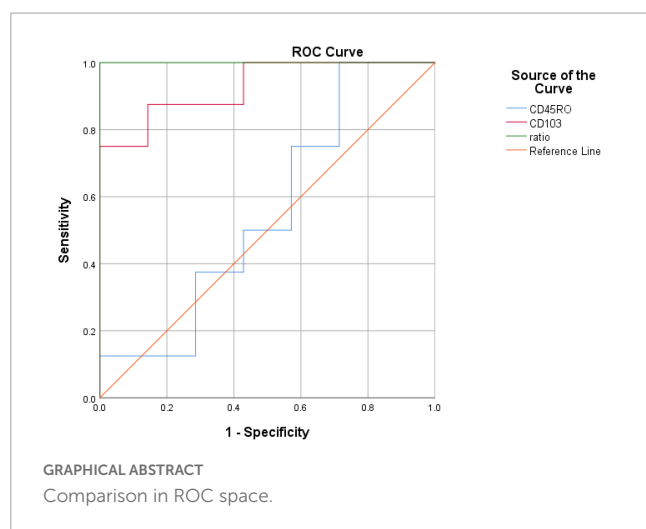
Conclusion: FM should be differentiated based on pathological characteristics
and treatment response, CD103 is helpful in differential diagnosis of FM.

KEYWORDS

follicular mucinosis, mycosis fungoides, tissue resident memory T cell, CD103, TRM cell

Introduction

Follicular mucinosis (FM), also known as Alopecia mucinosa, is an epithelial reaction
pattern characterized by mucin deposition in the outer root sheath and sebaceous gland.
The pathogenesis of FM is not completely understood. There are some controversies in FM



include nomenclature, biologic behavior, and treatment options. Firstly, it is not suitable to be named alopecia mucinosa, since most cases do not occur on the scalp. Secondly, some regard FM as an inflammatory process but with a tendency for clonal lymphocyte proliferation, but Ackerman proposed that FM was a form of cutaneous T-cell lymphoma (1). Therefore, it is of great clinical significance to distinguish the nature of FM. Finally, treatment options for FM are very difficult, and actually most treatment options are not effective in most cases. CD103 is the surface marker of Tissue resident memory T cell (TRM cell). MF is considered to be a TRM cell tumor (2). In this study, 15 cases of FM were collected to analyze the clinicopathological features and to explore the application value of CD103 expression in determining the nature of FM.

Materials and methods

All patients were collected in the dermatology department of the Affiliated 3rd Hospital of Hangzhou from 2014 to 2021. Diagnosis of FM was mainly depended on pathological findings, clinical follow-up and treatment effect, and other possible diseases are excluded. Hematoxylin and eosin stained tissue sections were analyzed. Immunohistochemical studies were performed with antibodies against CD3, CD4, CD5, CD7, CD8, CD20, CD30, CD45RO, CD56, TIA1 cytotoxic granule associated RNA binding protein, and Ki67. The expression of CD103 (Abcam, ab224202, 1:100 dilution) in all cases was detected by immunohistochemistry. Appropriate positive and negative controls were included for all antibodies tested. Immunohistochemical positive cells of 5 non-overlapping high-power fields of follicle ($\times 400$) were counted by Image Pro Plus 6.0 software. The ratio of CD103/CD45 in follicle was calculated, and the data were statistically processed by SPSS25.0 software. The Medical Ethics Committee of Hangzhou Third hospital, reviewed and approved the protocol (2021KA001), and all patients provided written informed consent.

Results

Clinical features

The patients included four children (age <18 years) and 11 adults (age ≥ 18 years), ranged from 9 to 86 years (mean age 33.8 year; median age 32 years). The duration of clinical symptoms before diagnosis ranged from 1 week to 10 years. Eleven cases were limited to the face and neck, and four cases involved the face, limbs and trunk simultaneously. The lesions may present as red or dark red plaques, follicular papules with irregular shape and infiltration, with a small amount of scales on the erythema in two patients. Four cases involved the scalp with alopecia. There was no atrophy in the skin lesions. One patient had mild pain, two patients had mild itching, and the rest had no obvious subjective symptoms. Among the 15 patients, 7 were primary follicular mucinosis (P-FM) (6 localized, 1 generalized) and 8 were mycosis fungoides-associated follicular mucinosis (MF-FM) (6 localized, 2 generalized). Routine laboratory examinations such as blood routine, urine routine, hepatic and renal function, and autoantibody series were within normal limits.

Histopathology

Most of the patients had mild to moderate hyperkeratosis and parakeratosis. Reticular degeneration of epithelial cells in the outer root sheath and sebaceous gland was observed with cystic fissure and mucin accumulation. Alcian blue staining was positive in all patients. There were different degree of lymphocytes infiltration in follicular epithelium, and eight cases of MF-FM showed prominent lymphocyte atypia and epidermotropism. All the 15 cases had dense or scattered eosinophils infiltrates.

Immunohistochemistry

All the cases showed CD3(+), CD4(+), CD5(+), CD20(−), CD79a(−), CD8(+)(3/15), CD30(+)(1/15), TIA-1(+)(2/15), granzyme B(+)(1/15). Table 1 illustrates the result of CD45RO count, CD103 count, and CD103/CD45RO ratio in both the follicle compartments of P-FM and MF-FM groups. There was no significant difference in CD45RO positive cells between the two groups ($p = 0.74$), while the ratio of CD103 and CD103/CD45RO in MF-FM group was significantly higher than that in PFM group ($p = 0.01$, $p < 0.01$, respectively).

TABLE 1 CD45RO, CD103, and CD103/CD45RO ratio in follicle compartments of P-FM and MF-FM.

	P-FM ($n = 7$)	MF-FM ($n = 8$)	p
CD45RO/5HPF	56.71 ± 36.07	62.50 ± 30.06	0.74
CD103/5HPF	10.43 ± 8.40	38.38 ± 15.92	0.01
CD103/CD45RO	0.22 ± 0.10	0.64 ± 0.15	<0.01

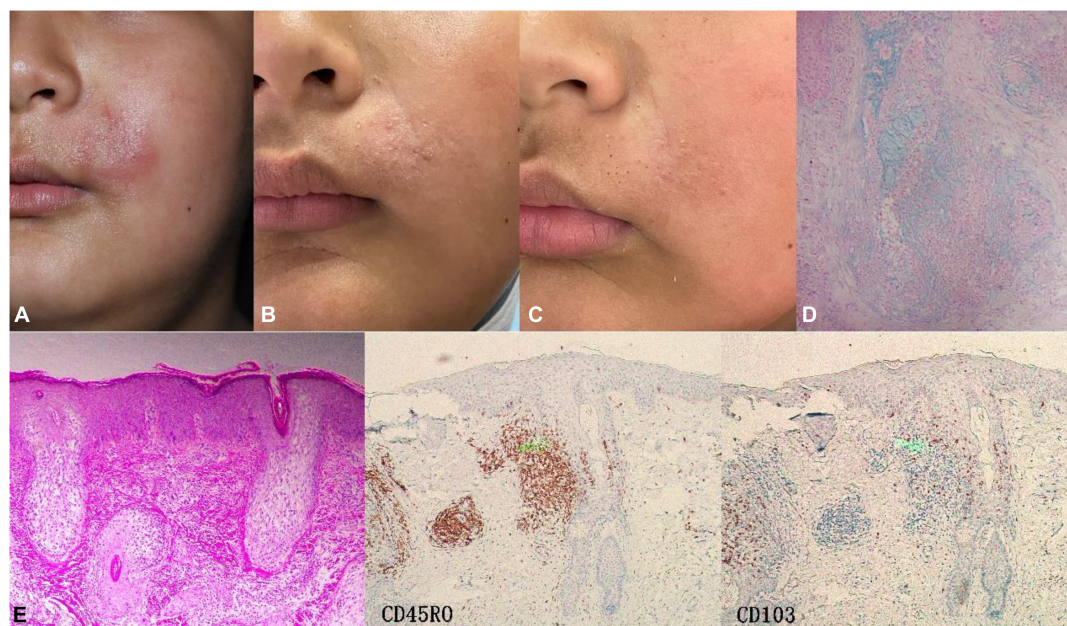


FIGURE 1

Case3 (P-FM). (A) The boy presented with perioral infiltrating red plaque on the left side at first visit. (B) After 2 months of oral hydroxychloroquine, most of the lesions subsided with a little scale. (C) After 5 months of oral hydroxychloroquine, the skin lesions basically regressed, leaving enlarged pores. (D) Alcian blue staining was positive. (E) Histopathology showed enlarged, distorted hair follicle expanded by pools of intrafollicular mucin deposition. IHC, CD45RO (++) CD103 (+–).

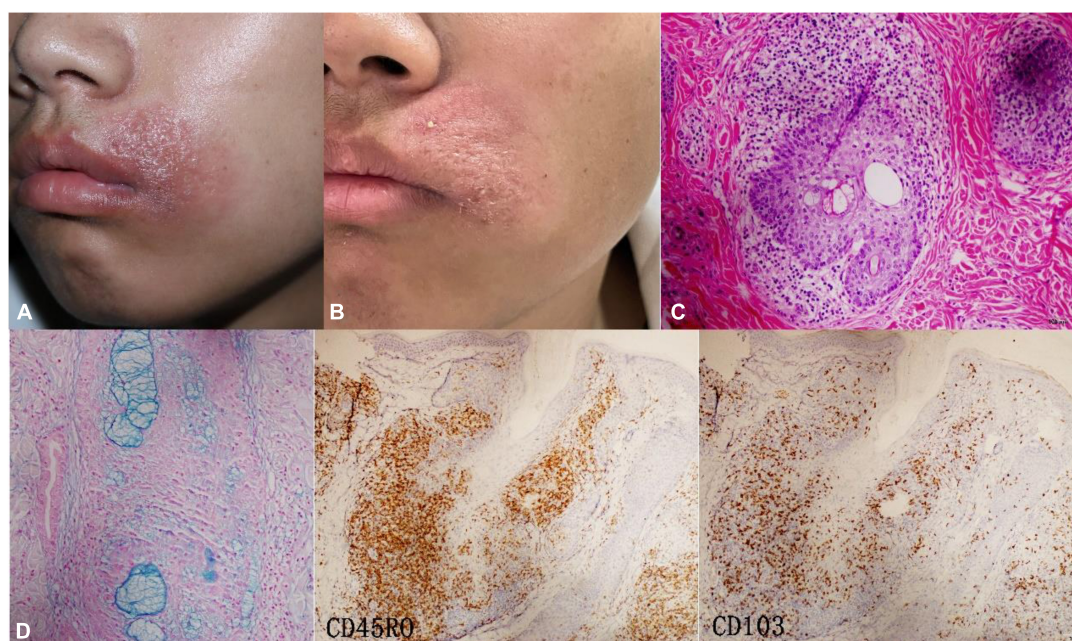


FIGURE 2

Case4 (localized MF-FM). (A) At first visit, the boy presented with perioral red plaque on the left side. (B) After three times ALA-PDT, the sense of infiltration significantly decreased. (C) Alcian blue staining was positive. (D) Histopathology showed a dense infiltration of lymphocytes around the follicle. IHC, CD45RO (+++) CD103 (++).

Treatment and follow-up

Follow-up data were available for 13 patients (6–42 months, mean 24.3 months), 6 patients were P-FM, and 7 patients were MF-FM. Of the six P-FM patients, two patients were

cured after surgical resection, and one patient was improved after oral administration of hydroxychloroquine (Figure 1). Of the seven MF-FM patients, one patient was cured after surgical resection, one patient was improved by ALA-PDT (Figure 2). The rest patients often had two or more treatments.

The main treatment including one systematic glucocorticoids, two NB-UVB phototherapy, three oral hydroxychloroquine, one oral thalidomide and one topical glucocorticoids all showed ineffective.

Discussion

Follicular mucinosis is a histologic pattern present in a multitude of benign, inflammatory, and neoplastic skin conditions. The clinical presentation of FM is variable, but the typical presentation is dark eczema-like plaques, follicular papules, with or without alopecia and pruritus. The most common lesions occur on the scalp, face and neck. Pathologically, different degrees of mucin deposition and lymphocyte infiltration were observed in the outer root sheath and sebaceous gland (1).

Since Hermann Pinkus first reported six cases of alopecia with mucin deposition in follicular in 1957, which now known as FM, there have been many controversy on the definition, classification, and pathogenesis of FM. The most accepted classification lists a primary form (PFM), which is benign and idiopathic mainly occurring in children and young adults, and a secondary form, typically affecting elderly patients, most commonly associated with MF. The chances of lymphoma appearing in follicular mucinosis patients vary greatly, ranging from 14 to 32% (3). In our study, it even reached more than half, which may be related to different evaluation criteria.

There is no uniform standard for the diagnosis and differentiation of P-FM and MF-FM, and the clinicopathological features of both of them overlap to some extent (4). It is not reliable to judge FM only according to age, lesion morphology and location. MF-FM confined in the head or face of adolescents is not uncommon in literature (5). Among the eight MF-FM collected in this study, six patients had lesions confined to the head and face, and two patients were younger than 18 years old.

Pathologically, Mehregan (6) noted that the dominant infiltration of eosinophils suggested primary benign FM, but different amounts of eosinophils could be observed in all our cases, and there were a considerable number of eosinophils in some MF-FM lesions. Monoclonal studies of T cell rearrangements have also failed to reliably distinguish between FM and MF. In a study with an average follow-up period of 10 years, TCR rearrangements were clonable in 5 out of 7 PFM patients, but none progressed to MF (5). The difficulty in the diagnosis of cutaneous lymphoma is well illustrated in FM, when a small percentage of neoplastic T cells is present among a larger population of reactive lymphocytes and other inflammatory cells. So, we try to find a molecular marker that could distinguish the properties of FM: CD103 staining was performed on all FM patients. The results showed that both localized MF-FM and generalized MF-FM presented more positive cells than PFM. This is easily explained. MF is considered a TRM cell tumor (7), and tumor cells often express the TRM cell markers CD103 and CD69 (2). CD103 interacts with the E-cadherin expressed by keratinocytes and is essential for TRM cell residency in the epithelium (8). CD103 specifically marked the folliculotropic/epidermotropic lymphocytes that resided in the epidermis for a long time, and the number of CD103-positive lymphocytes infiltrated by

MF-FM was higher than that of PFM under the background of CD45RO with similar infiltration degree. Therefore, we believe that CD103 is expected to be the basis of classification and diagnosis of FM. In addition, in a study of 203 cases of Folliculotropic Mycosis Fungoides, the morphology of the lesion and the degree of perifollicular lymphocyte infiltrates were also considered to be the basis for distinguishing indolent Folliculotropic Mycosis Fungoides with an aggressive form (9). Due to the limitation of sample size, we expect to confirm the results in a larger sample study. There may be more precise and scientific technical methods and judgment basis to distinguish the two subtypes in the future.

The course of FM is chronic, and spontaneous remission is rarely reported. None of the treatments has been shown to be consistently effective. Local resection may be the best choice for the treatment of localized FM. In this study, three patients with limited skin lesions had no recurrence after cosmetic surgery, so it is recommended to remove the lesions as completely as possible during pathological examination. The treatment of MF-FM should refer to classical MF, including topical drugs, phototherapy and various systemic drugs. However, like folliculotropic MF, NB-UVB and other methods commonly used to treat MF are often less effective due to the special location and depth of lymphocyte infiltration (10). In the case of poor response to phototherapy and oral medication, local radiotherapy or local ALA-PDT therapy is recommended for localized MF-FM, while systemic chemotherapy is recommended for generalized MF-FM. The treatment of MF-FM has a slow onset, difficult remission and poor prognosis. Therefore, early diagnosis, treatment and long-term follow-up of FM are very important.

In summary, we described the clinicopathological features and CD103 expression in 15 FM patients. The nature of FM is still unclear, and it is difficult to distinguish PFM with MF-FM based on its clinical, pathological and molecular results, but their biological behavior and therapies are different. The expression of CD103 is expected to play a useful role in the determination of FM properties.

Data availability statement

The original contributions presented in this study are included in the article/**Supplementary material**, further inquiries can be directed to the corresponding author.

Ethics statement

The studies involving human participants were reviewed and approved by the Medical Ethics Committee of Hangzhou Third hospital (2021KA001). Written informed consent to participate in this study was provided by the participants' legal guardian/next of kin. Written informed consent was obtained from the individual(s), and minor(s)' legal guardian/next of kin, for the publication of any potentially identifiable images or data included in this article.

Author contributions

PW, MZ, and HS contributed to conception and design of the study. YW, LL, and HZ collected the data. JW wrote the first draft of the manuscript. All authors contributed to manuscript revision, read, and approved the submitted version.

Funding

This work was supported by Medical and Health Science and Technology Planning Project of Zhejiang Province (2021455749); the Zhejiang Provincial Natural Science Foundation of China (Y2080112); and Zhejiang Natural Science Foundation of China (LBZ22H160001).

Acknowledgments

The patients in this manuscript have given written informed consent to publication of their case details.

References

1. Khalil J, Kurban M, Abbas O. Follicular mucinosis: a review. *Int J Dermatol.* (2021) 60:159–65. doi: 10.1111/ijd.15165
2. Adachi T, Kobayashi T, Sugihara E, Yamada T, Ikuta K, Pittaluga S, et al. Hair follicle-derived IL-7 and IL-15 mediate skin-resident memory T cell homeostasis and lymphoma. *Nat Med.* (2015) 21:1272–9. doi: 10.1038/nm.3962
3. Bauer F, Almeida J, Sementilli A, Mattos E, Dinato SL. Idiopathic follicular mucinosis in childhood. *Bras Dermatol.* (2020) 95:268–70. doi: 10.1016/j.abd.2019.06.010
4. Heymann W. Predicting the nature of follicular mucinosis: still a sticky situation. *J Am Acad Dermatol.* (2019) 80:1524–5. doi: 10.1016/j.jaad.2019.04.005
5. Brown H, Gibson L, Pujol R, Lust J, Pittelkow M. Primary follicular mucinosis: long-term follow-up of patients younger than 40 years with and without clonal T-cell receptor gene rearrangement. *J Am Acad Dermatol.* (2002) 47:856–62. doi: 10.1067/mjd.2002.124604
6. Mehregan D, Gibson L, Muller S. Follicular mucinosis: histopathologic review of 33 cases. *Mayo Clin Proc.* (1991) 66:387–90. doi: 10.1016/s0025-6196(12)60662-4
7. Campbell J, Clark R, Watanabe R, Kupper T. Sezary syndrome and mycosis fungoides arise from distinct T-cell subsets: a biologic rationale for their distinct clinical behaviors. *Blood.* (2010) 116:767–71. doi: 10.1182/blood-2009-11-251926
8. Masopust D, Soerens A. Tissue-Resident T cells and other resident leukocytes. *Annu Rev Immunol.* (2019) 37:521–46. doi: 10.1146/annurev-immunol-042617-053214
9. van Santen S, Roach RE, van Doorn R, Horváth B, Bruijn MS, Sanders CJ, et al. Clinical staging and prognostic factors in folliculotropic mycosis fungoides. *JAMA Dermatol.* (2016) 152:992–1000. doi: 10.1001/jamadermatol.2016.1597
10. Mitteldorf C, Stadler R, Sander C, Kempf W. Folliculotropic mycosis fungoides. *J Dtsch Dermatol Ges.* (2018) 16:543–57. doi: 10.1111/ddg.13514

Conflict of interest

The authors declare that the research was conducted in the absence of any commercial or financial relationships that could be construed as a potential conflict of interest.

Publisher's note

All claims expressed in this article are solely those of the authors and do not necessarily represent those of their affiliated organizations, or those of the publisher, the editors and the reviewers. Any product that may be evaluated in this article, or claim that may be made by its manufacturer, is not guaranteed or endorsed by the publisher.

Supplementary material

The Supplementary Material for this article can be found online at: <https://www.frontiersin.org/articles/10.3389/fmed.2023.1032072/full#supplementary-material>

Frontiers in Medicine

Translating medical research and innovation into
improved patient care

A multidisciplinary journal which advances our
medical knowledge. It supports the translation
of scientific advances into new therapies and
diagnostic tools that will improve patient care.

Discover the latest Research Topics

[See more →](#)

Frontiers

Avenue du Tribunal-Fédéral 34
1005 Lausanne, Switzerland
frontiersin.org

Contact us

+41 (0)21 510 17 00
frontiersin.org/about/contact



Frontiers in Medicine

